P-237

NASA Contractor Report 178166

Laminar Flow Control Perforated Wing Panel Development

J. E. Fischler et al

Douglas Aircraft Company
McDonnell Douglas Corporation
Long Beach, California

(NASA-CR-178166) LAMINAR FLOW CONTROL
PERFORATED WING PANEL DEVELOPMENT   N90-10187
(McDonnell-Douglas Corp.) 237 p   CSCL 11D
                                                        Unclas
                                              G3/24 0237128

NASA

National Aeronautics and
Space Administration

Langley Research Center
Hampton, Virginia 23665

NASA Contractor Report 178166

Laminar Flow Control Perforated Wing Panel Development

J. E. Fischler et al

Douglas Aircraft Company
McDonnell Douglas Corporation
Long Beach, California

NVSN
National Aeronautics and
Space Administration

Langley Research Center
Hampton Virginia 23665

Date for general release will
be three (3) years from date indicated on the document

FOREWARD

This document covers the contract work performed by the Douglas Aircraft Company of the McDonnell Douglas Corporation on the "Development of Laminar Flow Control Wing Porous Surface Structures (WSSD)" - NASA Contract NAS1-17506. The WSSD program is part of the NASA Laminar Flow Control (LFC) program supported by NASA through the Langley Research Center.

Acknowledgement for their support and guidance is given to the NASA Laminar Flow Control (LFC) Project Manager, Mr. R. D. Wagner, and the Project Technical Monitor Mr. D. V. Maddalon.

The Douglas personnel primarily responsible for this work were;

Max Klotzsche	Program Manager, CRAD and Cooperative Technology Development
Wil Pearce	LFC Project Manager
Jerry Fischler	WSSD Project Manager and Structural Analyses
Frank Gallimore	Materials and Processing
Laurie Davis	Electron Microscope Analyst
Steve Dunham	Mechanical Test Engineer

Acknowledgement for their support and guidance in helping Mr. Fischler to provide interactive computer programs for combining various materials and structural concepts is given to A. V. Hawley - Section Manager - Composites R.& D., and M. Ashizawa - Principal Engineer/Scientist.

i

TABLE OF CONTENTS

1.0 SUMMARY

During this wing porous surface structure development program, a panel designed to provide a suction surface suitable for hybrid laminar flow has been fabricated, structurally tested, and analyzed, and has successfully sustained the expected strain level of a commercial transport wing box that it will be attached to. In addition, it has met the aerodynamic waviness criteria so that transition to turbulence is not expected to result from the panel deflections chordwise and spanwise, and waviness between flutes up to a load factor of at least 1.5g.

The procedure used was to first optimize the design for strength only. The primary structural strength consideration is that the panel must withstand 4500 micro in./in. ultimate strain in the direction of spanwise stiffening. This is typical for the wing box of a commercial transport to which the hybrid leading edge would be attached. Initially, analytical computer codes were available. The computer codes for the all-metals allowed the analyst to select one of many metals. Also, the all-composites computer codes allowed the analyst to select one of many composites. From the computer data bank, the monolayer properties of only selected composites are obtained and printed out along with the panel geometry, see Table 1.1. Notice that only composite properties are described. The mixture of a titanium perforated sheet bonded to a composite substructure could not initially be handled with the available computer codes. Extension of these codes to combine composites and metals was needed. Using company funds, these computer codes were modified. However, in order to later make comparisons, the preliminary analyses were done using all composite hat-stiffened panels of fiberglass cloth and carbon/epoxy cloth. The hat-stiffener depth, rib spacing, and distribution of laminates in the skin, cap, base, and webs were varied to achieve 4500 micro in./in. ultimate strain with minimum weight. Preliminary panel weight estimates made before the new sandwich analyses programs for different material

1

combinations became available were relatively high. When the new design codes were run for panels with a titanium sheet bonded to various laminates of fiberglass cloth and carbon/epoxy cloth, the optimum design panel weights were significantly less.

Using computer programs, development panels have been analyzed for weight, strain, deflections, and thermal balance of the laminates. Lap shear tests of the adhesives were used for developing the cure cycle to yield high strength at room temperature, +160°F and -65°F. Compression tests of 3- by 3-inch panels followed by 4- by 10-inch panels, then 10- by 20-inch panels, and finally a two-bay flat panel 10 by 27 inches long were then used to determine overall panel strength. This gradual evolution of small to large panels allowed us to keep the costs down by improving the larger panels using the tests results on the smaller panels. The panels are composed of perforated titanium adhesively bonded to corrugated flutes of carbon/epoxy cloth and fiberglass cloth bonded to a lower composite skin to form a closed sandwich. This design provides a strong structure with alternate flutes used for suction of the boundary layer through the perforated titanium.

2.0   INTRODUCTION

The program objective was to further develop and test the Douglas
laminar flow control (LFC) suction panel design to ensure that
strength, strain and smoothness requirements are met for a subsonic
transport aircraft wing using a hybrid LFC system to reduce drag.
The parameters considered are divided into five major categories: 1.
optimum strength-weight considerations, 2. adhesive strength
development, 3. deflection considerations to meet the LFC surface
waviness tolerance, 4. fabrication processes, and 5. thermal
effects. All of the above mentioned categories interact. These
interactions sometimes dominated the design to the point that
analyses and development testing of the interaction effects were
needed before the optimum structural design could be finalized.

The panel surface waviness criteria for laminar flow were used as an
upper limit for panel deflections due to lateral pressure loadings.
It was desired that laminar flow would exist up to a 1.5g maneuver
load factor. Therefore, both the initial deflection, and its
magnification from the beam-column effects of loading up to 1.5g were
included to ensure that the total deflection would meet the panel
surface waviness requirements. The selection of the optimum panel
depth and rib spacing was mainly influenced by the beam-column
effects. Any theoretical bowing due to thermal expansion effects was
included in the analysis.

The LFC structural panels were originally cured at 265°F. The panels
then were cooled to either room temperature or -65°F to simulate
flight at altitude. As the panels shrink, bowing and waviness can
occur due to differences in the thermal coefficients of expansion.
Since the rigidity in the chordwise direction was less than that in
the spanwise direction due to spanwise flute stiffness, different
deflections occurred in these directions. This usually caused a
concave depression at room temperature. By stiffening the inner

surface skin of the sandwich panel, the initial surface bowing was reduced. This stiffening of the inner face also reduced the deflections between flutes (called flute waviness).

Curing at 300°F instead of 265°F improved the adhesive strength, but the higher cure temperature also increased the thermal contraction effects. The surface waviness and flute waviness were measured on the panels at room temperature using a special device invented for this purpose. The thermal deflections measured as the panel cooled to room temperature were then extrapolated to the -65°F condition. The room temperature test panels were therefore able to provide the deflection data used to predict the thermal deflections for the critical -65°F condition. These results were compared with theoretical results, using methods developed separately with company funds.

Perhaps the worst problem encountered in the development testing which caused schedule delays, was the need for further development of the AF31 adhesive bonds between the perforated titanium sheet and the composite pad, and the bond between the composite pad and the fiberglass flute cap. The adhesive supplier's reference data had indicated only a mild reduction of 27 percent cold, and 23 percent hot, from Table 1.17, in the strength properties of the adhesive at cold, 65°F, and hot, 160°F, conditions compared with room temperature conditions. Therefore, the initial design values for compression strain at room temperature were increased by about 25 percent to compensate for the expected reduction in adhesive strength under hot and cold conditions. The initial panel designs were tested successfully at room temperature using short column 3- by 3-inch panels and longer 4.5- by 10-inch panels. They provided the extra margin expected to be needed for hot and cold conditions. The room temperature compression strain values at failure were between 7,000 and 10,000 micro in./in. for the small panels as measured on the titanium side. This was about 50 percent more than the required 4500 micro in./in. For the longer 8- by 20-inch panels, mid-panel values

4

of 6600 micro in./in. and end panel values of 7800 micro in./in. were achieved at room temperature. However, the small compression 3- by 3-inch panels, when tested in the environmental chamber at cold and hot conditions, deteriorated to approximately half the strain capacity expected. This required an immediate halt in the fabrication of the larger panels for further design development to meet the hot and cold conditions.

Development tests were initiated immediately to obtain the combination of cure cycle and materials that would increase the adhesive strength at hot and cold conditions without any loss at room temperature. New materials, cure temperatures, time cycles, and applied pressures were varied for lap shear test specimens. Data at room temperature, cold, and hot conditions were gathered for fiberglass cloth bonded to perforated titanium, carbon/epoxy cloth bonded to titanium or fiberglass cloth, and fiberglass cloth bonded to fiberglass cloth. Seven different cure cycles (from Cure Cycles A to G) were investigated. Significantly improved lap shear strengths for the new combinations were obtained at room temperature and for cold and hot conditions.

As part of the improved adhesive development program, carbon/epoxy cloth bonded to perforated titanium, carbon/epoxy cloth bonded to fiberglass cloth, and carbon/epoxy cloth bonded to carbon/epoxy cloth, were tested with the AF31 adhesive at the new curing cycles. Some of these combinations showed increased strength, especially at the higher curing temperature of 300°F with increased pressures.

To better understand why the bond strengths with the "New" curing cycles were so much better than before at -65°F and +160°F, highly magnified photos of the failure surfaces were obtained. Previous experience under Contract NAS1-15527 had indicated that ductile failures and brittle failures can be distinguished with high magnification photos. The ductile failures have much higher shear

5

allowables while the powdered brittle bonds have lower shear allowables. Some of these same characteristics were found with the various materials when cured with the AF31 adhesive bond.

Since the final cure cycle for the adhesive was raised to 300°F (from 265°F), it was necessary to do analyses to verify that any additional panel waviness at -65°F would not significantly reduce the final mid-panel strain to less than 4500 micro in./in. due to beam-column effects. This was determined by analyses and was partially verified by test.

The new material combinations, and improved curing cycles, were then applied to 3- by 3-inch compression panels, 4.5- by 10-inch intermediate sized panels, and finally to 8- by 20-inch and 10- by 27-inch, two-bay, long compression panels. The final test panels survived the static test successfully with strain values that met the requirements at -65°F, room temperature, and +160°F.

Further testing of a larger two-bay panel with axial end loads and laterally loaded pressures at 1.5g with the thermal environments expected are suggested in the conclusions and recommendations section as the next phase of the laminar flow structures development to verify the panel waviness. Also, it is recommended that these panels should be developed and tested with the best chordwise and spanwise joints in place.

3.0   SYMBOLS AND ABBREVIATIONS

c   column end-fixity coefficient - non dimensional

SPF/DB   superplastic forming and co-diffusion bonding

h   wave height in inches

λ wave length in inches

n load factor

$D_{11}, D_{22}, D_{12}, D_{66}$ orthotropic plate flexural stiffnesses

E   modulus of elasticity

I   Moment of inertia for bending in the plane perpendicular to the corrugations

ν Poisson's ratio

w deflection in inches

W_{MAX} maximum mid-bay deflection in inches

a_{11} initial deflection in inches caused by lateral load bending. Used in the beam column analysis as an eccentricity (inches)

α magnification ratio of initial eccentricity from the axial beam column effect

a,b   effective panel length, $\frac{L}{\sqrt{c}}$, and effective panel width, b inches

L actual column length (inches)

7

N_{xx} axial loading in pounds per inch

A   area of panel in inches squared

ε strain in inches per inch

B dimensionless column form $L'/\rho \div \pi \sqrt{E/F_{MAX}}$

L'/ρ effective column length $= \dfrac{L}{\rho\sqrt{c}}$ in inches

F_{MAX} yield stress at a permanent strain of 0.002 inches/inch, in pounds per square inch

K   I/Ac

c   Distance in inches from neutral axis to the outside fiber

Fc   Compression stress at critical loading in pounds per square inch

K_s Shear-buckling load coefficient $\dfrac{b^2 N_{xy}}{\pi^2 \sqrt[4]{D_{11} D_{22}^3}}$

N_x, N_y, N_{xy} in-plane loads per inch
x = axial, y = transverse, xy = shear

w displacement of panel in positive Z direction

4.0   PRELIMINARY TEST RESULTS

4.1   STRENGTH-WEIGHT CONSIDERATIONS

4.1.1   Introduction: A survey of DC-9 reports showed that a maximum ultimate strain level of 4500 micro in./in. at the front spar cap was required. Since the hybrid LFC leading edge panel will be attached to a commercial transport's wing box at the front spar, it must withstand the same strain.

Mini-computers (PDP-11) and the RATFOR (Rational Fortran) language were used to develop user-oriented interactive computer programs to solve numerous composite and metal formulas in a simple and efficient way. These programs were written in such a way that the knowledge of computer language or special training was not required and a quick turnaround of input and output was possible. These Douglas proprietary interactive programs for determining the axial compression and shear load capabilities of "Blade", "J", and "Hat" stiffened panels were usable for advanced composites as well as metals. Since these programs are interactive, optimization of the stiffened panel can be achieved by changing the configuration and re-running the program immediately to determine the effects. The original programs were only usable for either one set of composite monolayer properties, using any combination of ply orientation, see Table 1.1, or one set of metal properties. Further development of these programs, using DAC development funds, enabled us later to combine different material laminates with large variation in monolayer material properties.

4.1.2   Composite Hat-Stiffened Sheet: Preliminary studies on the effect of composite material combinations and rib pitch were of the "Hat" stiffened concept as shown in Figure 1.1. This was used initially with a high quality carbon/epoxy cloth with the monolayer properties shown in Table 1.1. The thickness for one laminate is 0.013 inches for Case "A". The skin has two plys at the 0-degree direction of the

fibers and a +45-degree direction for two additional laminates in the skin. The cap has two 0-degree fiber laminates. The base, which is part of the skin, has two plys at 0-degrees and two plys at +45-degrees; the webs have only two laminates of +45-degrees. The "Hats", which are spaced every 1.3 inches, have a height of 0.6 inches, a cap width of 0.8 inches, and a base of 1.2 inches. The panel has a width of 20.00 inches and a length of 30.0 inches. From the general stability failure mode, the lowest buckling load was 680 lb/in. Dividing the loading per inch by the area per inch resulted in a stress of only 7288 psi. Table 1.1 corresponded to 1007 micro in./in. strain which is only 22.4 percent of the required strain. The carbon/epoxy cloth was much more expensive than fiberglass cloth, and the 45-degree ply orientation was more costly to layup. Therefore, fiberglass tape was considered. The tape was layed up with 0-degree monolayer properties in both the 0-degree and 90-degree directions to duplicate fiberglass cloth. The resulting weight was substantially higher at 2.54 psf, and the strain at failure was only 912 micro in./in. (see Table 1.2). The lower elastic modulus for fiberglass and its higher density reduced structural efficiency. However, in its favor, fiberglass cloth is only $16 per pound versus carbon/epoxy cloth at $150 per pound, its thermal coefficient is much closer to titanium, and its lower modulus reduces the panel and joint loads at the required strain level. Therefore, some combination of both materials for a composite substructure to attach to the titanium porous sheet was desirable.

By reducing the panel length, the general stability failure mode increased from 958 lb/in. for Case B, Table 1.2, to 2003 lb/in. for Case C, Table 1.3. The allowable compression stress (2003 lb/in. divided by 0.1918 sq. in./in.) was only 10,443 psi, and the strain was only 1908 micro in./in. Further reduction of the panel length to 15.0 inches increased the micro in./in. of strain to 3308, which was only 73.5 percent of the desired 4500 micro in./in., (see Case D, Table 1.4).

10

Using a 50 percent mixture of fiberglass cloth (with a modulus of 2.9 x 10^6) and a 50 percent carbon/epoxy cloth (with a modulus of 8.2 x 10^6), gave the hat-stiffened sheet concept an average modulus of $(2.9 + 8.2)/2 = 5.55$ x 10^6 in both directions and yielded a strain of 7114 micro in./in. for the general stability failure mode at 12,997 lb/in for a panel with the hat stiffener height increased to 1 inch, Table 1.5. The compression buckling loading divided by the area per inch of 0.3292 gives an average stress of 39,480 psi. With case 1's, Table 1.5, low stress level and high strain capacity that greatly exceeded the requirement, the combined mixture of fiberglass and carbon/epoxy cloth is a candidate concept. However, as shown in Table 1.5, its weight is 3.0147 psf even without the rib support weight. This is too heavy and was optimized further.

Ten additional cases were analyzed and the results are included in Figure 1.2. Rib spacings of 10 to 15 inches were used for the minimum panel height of 0.513 inches, 12.5 to 20 inches for the height of 0.75 inches, and 15 to 20 inches for the height of 1.0 inch. Figure 1.2 shows that a rib spacing of 10.5 inches would be required for a strain of 4500 micro in./in. with the 0.513-inch height, 14.5 inches for the 0.75-inch height and 19 inches for the 1.0-inch height. Rib weight was then added to the panel weights as shown in Figure 1.3. Check marks shown in Figure 1.3 and indicate those Cases 1, 2, 5, and 8, that can sustain over 4500 micro in./in. The values of strain for those cases can be obtained from Figure 1.2.

4.1.3 <u>LFC Panels With Titanium Outer Skin, Corrugated Composite Core And Composite Inner Sheet Sandwich Structure - General Development</u>: The new minicomputer (PDP-11) programs were used to optimize the LFC sandwich structure shown in Figure 1.5, and enabled the user to input different laminates of metals and/or composites for any of the elements of the sandwich. Table 1.6 is an example of the use of this code (named BUCKCORU) in which the three materials; Codes 2, 5, and 7 were used with their monolayer properties for the lamina input as shown. The fabricated panel is shown in figure 1.6. The Angle (A)

11

and Material Code (C) of each Ply (P) were input for each element. For example, in Table 1.6, five plies of 0.005-inch laminates of titanium, Code 7, were used for the upper surface skin, and three plies of 0.010-inch laminates of carbon/epoxy cloth, Code 2, were used as core sheet and two plies of fiberglass cloth, each 0.005 inches, Code 5, were used as the outer face laminates for the lower surface skin.

Figures 1.7 and 1.8 show the results from the 23 cases listed in Table 1.7. Figures 1.7 and 1.8 show that heights of 0.75 inches or more and rib spacings of 12.5 inches to 15 inches, for Cases I, XIV, X, IX, VIII, XV, and XVI in Figure 1.7, and Cases XVIII, XX, XXI, XXII, and XIX in Figure 1.8, all meet the 4500 micro in./in. strain criteria. Figure 1.4 showed the weights of these concepts with the rib weights included for Cases I, II, III, and IV. Notice that Case II, because of its 10-inch rib spacing, has higher weights than Cases I and IX. The results should be compared with those for the hat stiffened panel in Figure 1.3, which also includes rib weight. Again, check marks indicate greater than 4500 micro in./in. Notice how much more structurally efficient the sandwich is. Notice in Table 1.7 the cases with a check mark that went over 4500 micro in./in. Eight cases earned a check mark for sufficient strain, and an asterisk for lower panel weight. The panel weights were between 1.285 to 1.5396 psf. These cases looked promising if they could meet the surface waviness tolerances. Table 1.8, Case IX, was an example where five fiberglass cloth laminates were used for the web and a very balanced concept was designed. Notice that the web buckling was still the critical failure mode at 5598 lb/in. However, the general failure mode occurs soon after, at 6097 lb/in. The optimum structural weight is when as many modes of failure occur simultaneously. Two close modes of failure are usually all that one can expect for one geometry.

The upper skin theoretically buckles at 8989 lb/in. which was approximately 61 percent more than the critical web buckling mode. The design flute spacing of 1.02 that was used in Table 1.8 was actually fabricated to be 1.110 and the actual height of 0.767 was slightly more than the assumed height of 0.75 inches (see Figure 1.9). The upper skin buckling strength would normally be reduced by the increase in pitch. However, the porous titanium upper skin width was actually only 0.600 inch wide as shown in Figure 1.9. This was accomplished by increasing the cap width to 0.510 inches compared with 0.410 inch at the other surface. This increase in cap width not only reduces the upper skin titanium unsupported width, but also reduces the adhesive shear stresses (by increasing the available adhesion width). This width increase was one of the major reasons that the 3- by 3-inch compression panels increased in room temperature compression strength from an average of 17,217 pounds (for panels $A1$, $A1_1$, $A1_2P$), to an average of 29,250 pounds (for panels A1-1, A1-2, A1-3, and A1-4), an increase of 70 percent (see Table 1.9). In addition to the wider cap width, pads that were added to increase the suction pressure drop through the porous surface further widened the adhesive area interface with the titanium (see Figure 1.9). This pad also increases the titanium buckling load. The buckling of the titanium causes shear, tension, peel, and bending stresses on the adhesive and is to be avoided to prevent other modes of failure. The thermal effects on the adhesive were also an important consideration that are discussed later in this report.

The optimum inner panel composite facing sandwich was that which increased the chordwise bending stiffness and reduced bowing enough to meet the waviness criteria. The increased stiffness of the inner panel facing laminates also helped to reduce the chordwise panel warping (caused by the thermal contraction from the 300°F curing temperature to the minimum operating temperature of -65°F) and made possible a sandwich depth of 0.75 inches with a reasonable rib spacing (this resulted in the minimum weight). The use of carbon/epoxy cloth laminates for the outer face sheets of the inner

panel sandwich (see Figures 1.9, 1.10, and 1.11) increased its bending stiffness and thereby increased its buckling stress. The increased stiffness of the composite surface has helped the latest LA1-7, LA1-8, LA1-9, and LA1-10 panels to now often fail on the composite side first rather than, previously, on only the titanium side. To ensure that the titanium bond would have a high margin of safety, it was desirable that the porous titanium outer skin be the last component to fail.

4.1.4   Further Description of Theoretical Panel Computer Analyses: Tables 1.6 and 1.8 are typical computer outputs for the concept of Figure 1.5 which is a sandwich with the upper skin of perforated titanium attached to a substructure of carbon/epoxy cloth and fiberglass cloth. The first block of material codes in Table 1.6 defines the materials used for the laminations and allows for seven program defined materials and one additional material defined by the engineer. The three selected materials for this case are Code 2, carbon/epoxy cloth, Code 5, fiberglass cloth, and Code 7, titanium material. The second block defines the material properties. The panel geometry and stiffener geometry are in the next block. The rib spacing of 15 inches is the column length. It is assumed that sufficient rigidity is provided for a width of 20 inches. The spacing, called out in Tables 1.6 and 1.8, is the pitch between stiffeners of 1.020 inches. The cap width is 0.510 inches and the base width is 0.40; the height is 0.613 inch for Table 1.6 and 0.750 inch for Table 1.8. The titanium sheet, Code 7, has five plies, 0.005 inch per ply, for a total thickness of 0.025 inches, and its longitudinal properties listed are at an angle of zero degrees. The lower skin is a sandwich with one layer of fiberglass cloth on each of the two outer faces of the sandwich, and carbon/epoxy cloth layers for the core, a total of five plies in Table 1.6 and four in Table 1.8. For later cases, the carbon/epoxy cloth was put on the outer faces and fiberglass cloth was used for the core. This gave more axial load stability due to increased bending stiffness. The cap has four laminates of fiberglass bonded to the titanium, then one

14

laminate of carbon/epoxy cloth, and then four laminates of fiberglass which are a continuation of the corrugated core. The base has the four layers of fiberglass cloth, (a continuation of the corrugation), plus one laminate of carbon/epoxy cloth. The web has four laminations of fiberglass cloth, in Table 1.6, and five in Table 1.8.

The next group of data is the output of the program. The local and general compression and shear buckling of each element was obtained, assuming simply supported edges. These were the elastic buckling allowables. The critical failure mode was the general stability compression mode of 4747 lb/in. for Table 1.6, and the web compression buckling mode of 5598 lb/in. for Table 1.8. In both cases the maximum strain exceeds the 4,500 micro in./in. requirement. The upper skin shear buckling mode of 3531 lb/in. was the lowest amount in Table 1.6 and Table 1.8. However, very little shear flow occurs. If the panel had a maximum strain of 4500 micro in./in. (ultimate loading) for the DC-9, the maximum panel loading would be 4747 x 4500/5427 or 4500 x $(874,834 \times 10^{-6})$ = 3937 lb/in. for Table 1.6, and the margin of safety would be 4747/3937 - 1 = +0.206 or 20.6 percent. For Table 1.8, using 4500 x 827,018 x 10^{-6} = 3722 lb/in., results in a margin of safety of 5598/3722 - 1 = 0.504 or 50.4 percent. This was considered sufficient margin for the hot and cold allowable deteriorations, plus some allowance for the magnification from the eccentricity caused by warpage. The next step was to determine if the panels that meet the axial strains could also be within the laminar flow control waviness criteria. The governing differential equation for the buckling of laminated composite panel is given in the appendix.

4.2   Laminar Flow Control Surface Waviness Versus Structural Stiffness, Depth, and Rib Spacing: The laminar flow control surface waviness tolerance that was used to determine the optimum structural configuration was shown in Figure 1.12. The maximum allowable mid-panel deflection h from the graph, at a wave length of 20 inches, was 0.0314 inches for the wing root section for a single wave. This

results in a h/ of 0.00157. The effective wave length is dependent on the support width of the panel, especially in the chordwise direction, and this depends on the leading edge design. The corresponding criteria at the wing tip for a wavelength of 20 inches is an h = 0.0484 inches. This results in a h/λ = 0.00242 inches.

Since the load factor on commercial transports rarely exceeds 1.5, the amount of waviness can be exceeded at or above this level. Deflections from all causes, (beam-column axial and lateral loading plus thermal deflections) need to be included.

Panels deflections of Case Numbers I to XXIV from Table 1.7 are shown in Figure 1.13, for 0.75- and 1.0-inch panel heights, and 15-inch rib spacing. Figure 1.14 shows panel deflections for the 0.875-inch height, with a 15-inch rib spacing from Table 1.11. Figure 1.15 is for 0.75-inch height, with a 10-inch rib spacing from Table 1.12. Further optimization was done in Table 1.13 for a height of 0.75 inches.

Notice that Case XXII, in Figure 1.13, at a load factor of n = 1.5 and for a panel height of 1.0 inch meets the waviness criteria at the tip but not at the root, this case is for a column length of 15 inches. When the panel heights were 0.875 and 0.75 inches, the lateral bending stiffnesses were even less, and the resulting waviness h/λ values were above the requirements (see Figures 1.13 and 1.14). A reduction in rib spacing to 10 inches was necessary in order to reduce the lateral deflections at a load factor of n = 1.5 for a desirable panel height of 0.75 inches (see Figure 1.15). This height is desirable because its panel weights are less than the one inch height panel weights shown in Figure 1.13. Additional data in Tables 1.7 and 1.11 show the weight differences numerically.

Table 1.14 shows the mid panel theoretical deflection for a typical initial 0.75-inch height panel with a 15-inch column length, and a lower skin with two core laminates of carbon/epoxy cloth and two face

sheets of fiberglass cloth. There are five laminates of fiberglass cloth for the webs. Figure 1.4 illustrates the details. However, the theoretical webs only have four laminates and the lower skin has five laminates. The height is 0.71-inches instead of 0.75-inches for the theoretical value in Table 1.14. The longitudinal (axial) bending stiffness, D_{11} was calculated to be 88,737.5 in Table 1.14. This value was derived from the formula;

$$D_{11} = \frac{EI}{1-\nu^2} = \text{Stiffness in the longitudinal direction.}$$

Where;

    E = Modulus of elasticity.

    I = Moment of inertia for bending in the plane perpendicular to the corrugations.

    ν = Poisson's ratio.

The maximum deflection, w max, is from the formula;

$$w\text{ max} = \frac{a_{11}}{1-\alpha} - \text{from Page 328 of Reference 1.}$$

Where;

    a_{11} = Initial eccentricity from panel bending from lateral loading.

    α = Magnification of initial eccentricity from the axial compression beam column effect.

The α value is from the formula;

$$\alpha = \frac{N_{xx}}{\frac{\pi^2}{a^2} D_{11} \left(1 + \frac{a^2}{b^2}\right)^2}$$

Where;

Nxx = Axial loading in pounds per inch at the designated load factor.

a = Effective panel length = $\dfrac{L}{\sqrt{c}}$

Where L = length between ribs
c = fixity coefficient = two, for continuous panel across the rib support.

b = Effective panel width.

Since the magnification factor is a factor of many parameters; the loading N_{xx}, the stiffness D_{11}, the effective panel length a, and the effective panel width b, the computer code must account for these when solving for the beam column deflection. After reviewing a number of early panels, the range in α was found to be from 0.1 to 0.25. To be slightly conservative, and avoid the problem of obtaining all the required data for computing for each case, it was assumed that for these typical panels, α = 0.3.

Notice the results of the panel deflection at the center in Table 1.14 are for four conditions, two without any axial loading and two with "beam column" axial loading. All four conditions had lateral pressure loading of 8.0 psi. When the loadings are applied, the edge fixity of C=4 is assumed for clamped edges and C=1 for simply supported edges. To obtain an estimate of the continuous beam-column with simply supported supports, the average value of the clamped and simply supported mid-bay deflection are used. For example, from Table 1.14, the deflection with axial load was the average of 0.1313 inches plus 0.0656 inches which equals 0.0985 inches. This is the value for the panel deflection, h. Dividing by the panel wave length, assumed to be 20 inches, results in a h/λ = 0.0049. This is significantly higher than the previously mentioned 0.00157 value required for laminar flow.

Since this is unacceptable, the panel height was increased and the lower skin and web laminates were increased in Table 1.15.

18

Table 1.15 is also shown. This theoretical configuration weight is less than the actual measured weight of one of the later developed configurations, LA1-7, shown in Figure 1.10. Therefore, the resulting stiffness of the later configurations are approximately equivalent, and the use of the theoretical maximum deflection of 0.05085 inches (0.0694 plus 0.0323 divided by two) will more closely predict the final concepts. When divided by the panel wave length of 20-inches, this is an h/λ of 0.00254. Reducing the lateral pressure loading for a limit load factor of n = 1.5, directly reduces the lateral deflection to forty percent of the ultimate load deflection of 0.05085-inches, which then is 0.02034-inches, and therefore results in h/λ = 0.0017. This value is eight percent higher than the 0.00157 requirement for laminar flow at the root chord. The column length used in Table 1.15 was for a rib spacing of 15 inches. A small decrease in the rib spacing will eliminate the eight percent excess.

The panel waviness therefore was shown to be sensitive to the panel stiffness, the rib spacing, the flight load factor, the magnification from the beam-column effect and the effective column width. All the deflections were based on a flat panel. A slightly convex upper surface curvature will decrease the deflections and further stiffen the panel.

An additional initial bowing comes from thermal stress. The panel was cured during fabrication at 300°F. The temperature at 30,000 feet for a standard day is -48°F. This is a thermal gradient of [300 - (-48)] = 348°F. Using the cold design condition -65°F for design results in [300 - (-65)] which is 365°F. From Table 1.16 the h/λ negative deflection "Dish" is between 2×10^{-4} inches and 3.125×10^{-4} inches at room temperature. Multiplying by 365/(300 - 75)°F = 1.62 yields an initial bowing of $(3.125 \times 10^{-4}) \times 1.62 = 5.07 \times 10^{-4}$ inches for the -65°F condition. This compares to the eccentricity obtained by the lateral pressure and beam-column deflection of 203.4×10^{-4} inches. Therefore, the thermal bowing

19

effect was almost negligible, about 2.5 percent of the lateral loading and beam-column effect. Actually, the suction loads cause a "Pillow" type deflection outward, called a "Crown", and any thermal bowing is usually a "Dish", inward. The "Crown" from the beam-column deflection and the "Dish" from the thermal gradient usually oppose each other. The later panel constructions have the inner sandwich with outer laminates of carbon/epoxy cloth (see Figure 1.10). This stiff composite backing with a low thermal coefficient of expansion from the carbon/epoxy cloth laminates prevents the opposite face sheet of titanium from contracting chordwise and pulling the panel into a "dish" curvature chordwise when cold. The increase in stiffness of the inner sandwich with the high percent of carbon/epoxy cloth (which has bending strength, and a lower thermal expansion coefficient) resists the titanium "Dish" curvature when cold. Also, when hot, the expansion of the titanium (which would cause a "Crown") was prevented by the stiff inner sandwich.

4.3   Development Of Better Adhesive Characteristics: The suppliers of AF31 adhesive properties, shown in Table 1.17, indicated sufficient overlap shear strength for room temperature, -65°F, and +180°F. The room temperature value is 3700 psi, for a 1-inch wide, 1/2-inch overlap, for a 350°F cure temperature held for 60 minutes with a pressure of 150 psi. The -67°F shear value is 2700 psi, (which is 73 percent of the room temperature value), and the 180°F is 2850 psi, (which is 77 percent of the room temperature value). Therefore, for -65°F and +160°F, the maximum design temperatures for our panels, an approximately 25 percent reduction in strength could be expected for the cold and hot conditions, with the maximum cold condition slightly more critical than the maximum hot condition.

By reducing the cure temperature to 250°F for two hours, and using a pressure of 75 psi, the overlap shear strength for 2024T3 aluminum at 75°F is increased to 4285 psi. If the specimen is allowed to soak for 24 hours, the shear strength is further increased to 4375 psi. Since the flute webs are fiberglass cloth, and can bow if subjected

20

to high temperatures and high compression pressures, the selection of four hours at 265°F with a pressure of 37 psi for the original Cure Cycle "A", seemed a reasonable choice to avoid web bowing and to obtain sufficient shear strength.

A series of 3-by 3-inch compression panels were fabricated and tested. These panels are described in Tables 1.9 and 1.10. They were called the "Early" 3- by 3-inch compression panels because another series of 3- by 3-inch panels were tested later, after improving the cure cycle and selecting additional materials from further lap shear coupon development tests. The early Configurations A1, $A1_1$, and $A1_2P$ were tested and failed at a 17,217 pound average load. After further improvements, the room temperature results increased to an average of 29,250 pounds. These improvements were widening the cap width to 0.51 inches, increasing the height to 0.75 inches nominal, increasing the fiberglass cloth webs to five plies, improving the backing sandwich by adding carbon/epoxy cloth, and adding pads. These improvements resulted in a 70 percent increase in room temperature compression properties. The average titanium strain was 8193 micro in./in. (see Table 1.9). With the 25 percent reduction in strength expected from Table 1.17, a 6145 micro in./in. strain was anticipated for the hot and cold conditions. This value, even after further reduction for beam-column eccentricity from the combined axial and lateral loading plus thermal bowing, above the 4500 micro in./in. required. However, the next series of tests on Specimens A1-5, A1-6, A1-7, and A1-8, in Tables 1.9 and 1.10, gave lower results than expected. The A1-5 value of 17,200 pounds compression load at +160°F was only 58.8 percent of the average 29,250 pounds for the room temperature A1-1 to A1-4 specimens and the A1-6 specimen, also at +160°F, was only 59.1 percent. The A1-7 and A1-8 specimens, at -65°F, were only 41.0 percent of the room temperature values.

These large reductions from room temperature test values indicated that the shear strength values of AF31 (Table 1.17) were not dependable for titanium porous sheet bonded to composites. Therefore, additional single overlap shear test specimens were fabricated using a perforated 6AL-4V titanium tab, Layer #1 of Figure 1.16, then a primer, Layer #2, followed by an AF31 adhesive, Layer #3, then a primer, Layer #4, and finally a fiberglass cloth tab, Layer #5. The tabs were 1-inch wide and had a 1/2-inch overlap. The #1 layer and #5 layer were the loaded layers that were pulled apart to determine the single shear strength. The autoclave cure identifications, temperatures, times, and pressures, as shown in Table 1.18, were used. For each cure cycle, three specimens were tested. The results are shown in Figure 1.17 for Cure Cycles "A", "D", "E", "F", and "G".

The "B" and "C" cure cycle strengths were significantly lower than the most desirable "F" and "G" cure cycles; therefore, those cases were not plotted. However, the room temperature "B" cure cycle average strength value was 1052 psi and the "C" cure cycle average value was 1216 psi. At +180°F, the "B" cure cycle, average value was 964 psi, 92 percent of the room temperature value; for the "C" cure cycle at +160°F, the average value was 1453 psi which was 119.5 percent of the room temperature value. The strength at higher temperature was close to the room temperature values. However, for the cold condition (-67°F) for the "B" cure cycle, the average strength was 700 psi, only 67 percent of the room temperature value. For the "C" cure cycle at -65°F, the value was 753 psi, only 62 percent of the room temperature value. Therefore, the "B" and "C" cure cycles were rejected because of their poor performance, especially for the cold conditions.

As indicated by the 3M Corporation Data shown in Table 1.17, 350°F at 150 psi pressure was used for the cure cycle temperature for one hour, with a rapid heat rise of 200°F/minute for Cure Cycle "B"; but, the results were poor, especially for the cold (-67°F) condition.

22

The old standard, Cure Cycle "A" was restricted to only 37 psi pressure to avoid thermal bowing and possible web bowing. Therefore, the "D" cure cycle was tried with a reduction to 300°F and double the former "A" cure cycle value to 75 psi pressure. This resulted in an average value of 1754 psi for the 160°F case which was 98 percent of the average room temperature value of 1791 psi (Figure 1.17). At -65°F, however, the average value was 1095 psi which was only 61 percent of the average room temperature value. This was too great a loss, therefore, Cure Cycle "D" was not acceptable. Holding 300°F for two hours and increasing the pressure to 100 psi for Cure Cycle "E" does not help the room temperature, +160°F, or -65°F shear allowables (see Figure 1.17).

Going back to the one-hour soak time and holding the 100 psi pressure helped considerably for the "F" cure cycle (see Figure 1.17). The average room temperature value increased to 2080 psi, 23 percent better than the "A" cure cycle value. The +160°F average value was 1607 psi, 77 percent of the average room temperature value. Best of all, the -65°F average shear value increased to 1532 psi which was 1532/647 = 2.37 times the "Old" "A" cure cycle cold condition value. This improvement was very significant. A slight tradeoff was made for the "G" cure cycle compared to the "D" cure cycle by increasing the soak time to two hours rather than one hour. The 75 psi pressure was more acceptable for reducing the possibility of bowing the flute webs. This "G" cure cycle has the highest room temperature test value of 2242 psi, almost the highest +160°F value of 1731 psi, and almost the highest -65°F value of 1529 psi.

The test results for the "Ftc" cure cycle (similar to the "F" cycle mentioned above, but with perforated titanium bonded to carbon/epoxy cloth) are shown in Figure 1.18. Bonding the perforated titanium to the carbon/epoxy cloth substantially increased the room temperature values, 2744 psi for cure "Ftc" compared with 2242 psi for the "G" cure cycle (see Figure 1.17, for the titanium to fiberglass cloth). This was 22 percent more. At +160°F, the "Ftc" cure cycle was 2020

psi versus 1731 psi, 17 percent more than cure cycle "G". Also, for the -65°F cold condition, a 1859 psi value for the "Ftc" cure cycle was 21 percent higher than the 1532 psi for the "F" cure cycle.

The test results for carbon/epoxy cloth bonded to fiberglass cloth with Cure Cycle "Gcf" (Figure 1.19) show higher properties at +160°F but slightly lower properties at -65°F when compared to carbon/epoxy cloth bonded to carbon/epoxy cloth as in Figure 1.18.

The shear strengths of fiberglass cloth bonded to fiberglass cloth for the "Fff" and "Gff" cure cycles shown in Figure 1.20 are much lower than carbon/epoxy cloth bonded to fiberglass cloth. Therefore, the inclusion of carbon/epoxy cloth within the fiberglass cloth laminate, will increase the bond strength, the panel strength, and the stiffness. However, the carbon/epoxy cloth is expensive relative to fiberglass cloth ($150 per pound versus $16 per pound). Plus, fabrication is more difficult and the thermal expansion of carbon/epoxy is small compared to the fiberglass and/or titanium. Therefore, the laminates must be balanced to prevent warpage, and only enough carbon/epoxy cloth used because of cost. Table 1.19 is a convenient summary of the comparison of the average shear values of different material combinations at room temperature, +160°F, and -65°F.

In the configurations shown in Figure 1.10, notice that the pad outer lamina, next to the cap was a carbon/epoxy cloth bonded to the fiberglass cloth. This was done using the "Gcf" cure cycle (No. VIII in Table 1.19) to take advantage of the increased strength with the 75 psi lower pressure to prevent bowing of the web flutes when the titanium and pad were bonded to the composite substructure. The pad and the perforated titanium were bonded together before joining them to the composite substructure when the higher 100 psi pressure could be applied. The inner carbon/epoxy layer was therefore moved to the titanium face (see Figure 1.11) and the Cure Cycle "Ftc" was used for increased strength. This is the No. 1 combination in Table 1.19.

24

Notice that No. 1 has the highest shear strength at all temperatures. Also, notice that where carbon/epoxy cloth or fiberglass cloth could be used, the carbon/epoxy cloth was bonded to the fiberglass cloth (the outer flute cap laminate). Number VIII, has higher single lap shear values than V, VI, IX, and X, and only suffers a difference in shear of 2189 - 2106 = 83 psi, which is 3.8 percent lower for the +160°F condition for a desirable 25 percent reduction in bonding pressure.

4.4   Microscopic Examination Of Adhesive Bonding: Microscopic examination of the lap shear specimens at different cure cycles and temperatures was used to yield a better understanding of the failure mechanism for the bonding of the different materials.

Figure 1.16 shows laminations of the perforated titanium (Layer #1) bonded to the fiberglass (Layer #5). Notice that the primer (EC 2174), Layer #2, was coated on the titanium, Layer #4 was coated on the fiberglass cloth, and an adhesive AF31, Layer #3, was inserted in between and then they were bonded. Tables 1.20 through 1.24 describe the failure modes of the perforated titanium bonded to the fiberglass cloth; this will be discussed later in more detail. Some general observations will be made first.

High magnification photographs, Figure 1.21, with 4000X magnification show the titanium and primed titanium surfaces before cure cycling and bonding. Referring to figure 1.22, XES (X-ray electronic scope) photographs show that only 3.16 percent silicon is picked up when the titanium is cleaned and scraped. The silicon may come from the sand particles of the sandpaper when cleaning. If it is sanded and cleaned, 4.58 percent silicon is picked up. After sanding, cleaning, and being primed, Layer #1 of Figure 1.16 picks up as much as 23.77 percent silicon. Past experience has shown that this large amount of silicon may cause a brittle failure. This was explored in Figures 6.17 and 6.18 of Reference 6. Figure 1.23 shows the Al room

temperature 91 percent primer cohesive* failure, and the A9 specimen
tested at -65°F resulting in a 55 percent primer adhesive** failure
(see Tables 1.20 to 1.24). The smooth surface with small smooth
particles allows a brittle failure. A rougher, larger particle, with
fingers extending outward, intertwines the materials and results in a
ductile failure. Usually the ductile failure has a higher strength
than the brittle failure. Notice in Figure 1.23, and from the
results in Figure 1.17, that the particles for A1 are much larger
than for A9 resulting in a higher (probably ductile) shear failure of
1740 psi as shown in Figure 1.17 and Table 1.25. The smaller A9
particles resulted in a lower (probably brittle) shear failure of
only 724 psi, from Figure 1.17 and Table 1.25, at -65°F. For the
F9 specimen, at -65°F, the larger irregular particles that
intertwine the materials, Figure 1.24, yields a 48 percent primer
cohesive and 45 percent AF31 and primer adhesive failure. This looks
more like a ductile failure than the A9, at -65°F, (see Figure
1.23). Therefore, this results in a 1526 psi failure, Table 1.28 and
Figure 1.17, more than twice the A9 failure. Many more coupons and
tests are desirable to further verify the above conclusions.

*   Cohesive Failure = The external failure loadings exceed the
     internal forces by which the molecules of like substances are
     held together (usually tension forces).
**   Adhesive Failure = The external failure loadings exceed the
     joining forces between two bodily parts that are normally
     separate.

4.4.1   Additional Studies Of Lap Shear Failures To Establish The Modes Of
        Failures And The Best Cure Cycles And Material Combinations:
        Initially, the perforated titanium bond to fiberglass cloth was
        investigated thoroughly to determine the best cure cycles. After
        these tests, additional tests using perforated titanium bonded to
        carbon/epoxy cloth, carbon/epoxy cloth bonded to fiberglass cloth,
        carbon/epoxy cloth bonded to carbon/epoxy cloth, and fiberglass cloth
        bonded to fiberglass cloth were investigated. Tables 1.25 to 1.27

26

show the lap shear values for the A, B, C and D cure cycles of perforated titanium to fiberglass cloth. Tables 1.28 and 1.29 for perforated titanium to fiberglass cloth show the values for "E", "F" and "G" cure cycles.

Microscopic examinations were made of Cures "A", "D", "E", "F", and "G" to determine the failure modes (see Tables 1.20 to 1.24). The "F" and "G" cure cycles were then compared to the "A" cure cycle in more detail. Photograph locations and the pictures of Specimens A1 to A9, and F1 to F9, showing the bonding failures of the perforated titanium to the fiberglass cloth are shown in Figures 1.25 to 1.27, and sketches of the types of failure are shown in Figures 1.28 and 1.29. In addition, carbon cloth bonded to fiberglass cloth, carbon cloth bonded to carbon cloth, and fiberglass cloth bonded to fiberglass cloth failures were investigated. Figures 1.30 and 1.31 show the layer description of the lap shear test specimens. Table 1.30 shows the failure mode description for the carbon cloth bonded to fiberglass for Cure Cycle "F" and Table 1.31 shows the failure mode description for carbon cloth bonded to fiberglass cloth for Cure Cycle "G". Tables 1.32 and 1.33 describe the failure modes of carbon cloth bonded to carbon cloth for the "F" and "G" cure cycles, respectively. Tables 1.34 to 1.37 give the lap shear test values for the above materials. The following are some general observations on the failure modes described in Tables 1.20 to 1.24.

4.4.2   Detailed Comparisons Of The "A", "F" And "G" Cure Cycles With Perforated Titanium Bonded To Fiberglass Cloth: At room temperature, the failure mode was over 90 percent cohesive failure of the primer Layer #2 (Cases A1, A2, and A3, see Table 1.20 and Figure 1.16 for the description of each layer). The "A" cure cycle of only 265°F was insufficient for the strength of the primer.

Going to the "F" and "G" cure cycles for comparison, which was at 300°F with higher pressures, the Layer #2 primer cohesive failure mode was considerably improved, resulting in only a 4 percent primer

cohesive failure mode, see Tables 1.23 and 1.24. The new major failure mode, at a higher shear value, became failure of the fiberglass primer to fiberglass adhesive. The average shear strength at room temperature increased from 1694 psi, from Table 1.25 for Cure "A", to 2080 psi, for Cure "F", see Table 1.28, and to 2242 psi for Cure "G", see Table 1.29. At +160°F, the "A" cure, bonded at only 265°F for four hours at the low pressure of 37 psi, give strength values of A4, A5, and A6 which decrease to an average of 1369 psi, from Table 1.25, a 19 percent reduction in average strength. The cohesive primer strength was decreasing in value with increasing temperature with the "A" cure cycle.

For comparison, going to specimen results for F4, F5, and F6, the failure was now at the fiberglass primer to the fiberglass, an adhesive failure (which was a higher strength mode of failure). Evidently, the higher temperature of 300°F, and higher pressure of 100 psi, has increased the cohesive primer strength so that the average at 160°F is 1607 psi, from Table 1.28, for the "F" cure, and 1731 psi for the "G" cure, from Table 1.29. These values are almost as good as the room temperature "A" cure values which were found to yield very high strain values for small and large test panels.

The cold -65°F conditions were the most critical since the "A" cure average values decreased to 647 psi, (Table 1.25) from the room temperature average of 1694 psi (Table 1.25) a strength loss of 62 percent. The A7, A8, and A9 values have the cohesive primer mode failure in two of the three specimens over 65 percent and 55 percent of the failure face. The remaining failure surfaces showed adhesive failure between the AF31 and the primer over the fiberglass (35 percent and 45 percent of the failure face). Evidently the "A" cure cycle does not provide adequate strength for the cohesive primer, or adhesion of the primer to fiberglass and to the AF31 at -65°F (see Table 1.20 for the failure mode descriptions).

28

For the cold -65°F condition, when using the "F" and "G" cure cycles, there was an increase in the cohesive primer strength. Failure then occurred principally in the adhesion of the AF31 to the primer <u>at a much higher loading</u>. Tests F7, F8, and F9 failed primarily as an adhesive failure (AF31 to primer - 48 percent), see Table 1.23 and Figure 1.16. Tests G7, G8, and G9 have 80 percent, 55 percent, and 75 percent failures in this mode. These "F" and "G" cures provided higher average strengths of 1532 psi, see Table 1.28, for the "F" cure cycle, and 1529 psi, see Table 1.29, for the "G" cure cycle. This was only a 10 percent reduction from the original 1694 psi value for Cure Cycle "A" at room temperature. The original design allowed for approximately a 23 to 27 percent reduction in strength for hot and cold conditions, so there was a 13 to 17 percent excess strength.

4.4.3   <u>Further Details Of Specific Tests Have Been Included To Help Describe The Nature Of The Failures</u>: Case A1 was a 91 percent primer, 3 percent AF31, and 6 percent fiberglass primer failure, see Table 1.20. The primary failure at room temperature was the #2 layer which was the EC2174 primer. The shear loading was 1740 psi, from Table 1.25. The "A" cure was 265°F for 4 hours and 37 psi pressure.

Case A2 was a 95 percent primer, 3 percent AF31, and 2 percent fiberglass primer failure, see Table 1.20. Similar to Case A1, there was a high 95 percent cohesive primer failure with only a 2 percent fiberglass primer failure compared to 6 percent for Case A1, and 4 percent for Case A3. The lower percent fiberglass primer at the loading face helped reduce the shear loading at failure to be only 1209 psi, from Table 1.25. The "A" cure cycle was 265°F for 4 hours and 37 psi pressure.

Case A3 was a 93 percent primer, 3 percent AF31, and 4 percent fiberglass primer failure, see Table 1.20. The failure at room temperature was similar to the Case A1 failure. The 4 percent

fiberglass primer/fiberglass failure helped to obtain the best shear strength of 2134 psi, from Table 1.25. The "A" cure cycle was 265°F for 4 hours and 37 psi pressure. The "A" cure cycle cases are compared to the "F" Cure Cycle Cases F1, F2, and F3, below.

Case F1 was a 1 percent primer, 1 percent AF31, and 98 percent fiberglass primer/fiberglass adhesive failure, see Table 1.23. The primary failure at room temperature was the #4 layer which is the EC2174 primer between the #3 layer AF31 adhesive, and the fiberglass Layer #5. Failure as an adhesive was at a very high shear value of 2178 psi, see Table 1.28. The "F" cure cycle was 300°F for 1 hour at 100 psi pressure. At the high cure temperature of 300°F, the primer EC2174 must gain in strength cohesively, and then fails at a higher strength. The high pressure of 100 psi must also help. The early Cases A1, A2, and A3, which had the EC2174 primer, failed cohesively. At the higher cure temperatures, the primer now fails as an adhesive, not cohesively at the much higher loading of 2178 psi. The now higher strength of the primer causes the next weaker link, the adhesive strength of the primer to fiberglass, to fail (but at a much higher load).

Cases F2 and F3 - The F2 was 1 percent primer, 1 percent AF31, and 98 percent fiberglass primer failure, see Table 1.23. Case F3 was a 1 percent primer, 2 percent AF31 and 97 percent fiberglass primer failure. F2 and F3 have failure stresses of 1595 psi and 2103 psi, respectively, from Table 1.28, which was much higher than the average A1, A2, and A3 value of 1694 psi. The cure cycle of 300°F for 1 hour at 100 psi must have strengthened the EC2174 primer so that it does not fail cohesively, and shifts the hierarchy of failure to the next weakest link which was an adhesive failure of the primer to the fiberglass. However, this failure mode was at a higher stress level. This was a result of the higher temperature (300°F) cure cycle for the "F" cure versus the "A" cure, and the higher pressure of 100 psi versus 37 psi.

30

Case A4 was a 60 percent primer, 10 percent AF31, and 30 percent fiberglass primer failure, see Table 1.20. At +160°F, the major failure mode (60 percent), was still the cohesive failure of the EC2174 primer. In addition, because of the higher temperature of +160°F, the layer between the primer on the fiberglass and the fiberglass (Layers #4 and #5), fail adhesively (30 percent). See Figure 1.28 which shows the higher shear failure 30% fiberglass primer/fiberglass adhesive failure mode in the A4 sketch. Note that A1 to A3 have very little of this higher strength mode. This increased the strength above the pure cohesive failure (see Case A6). This lower strength shear of 1434 psi, from Table 1.25, reduced the value to 85 percent of the room temperature average of A1, A2, and A3.

Case A5, at +160°F, was a 95 percent fiberglass primer to fiberglass adhesive failure (Layers #4 to #5), see Table 1.20. The failure was at 1779 psi, from Table 1.25, which was a higher failure mode value than the cohesive primer failure average of 1694 psi room temperature value for A1, A2, and A3.

Case A6, at +160°F, the #2 layer primer, was again a cohesive failure (90 percent), see Table 1.20, of only 895 psi at +160°F, see Table 1.25, which was only 53 percent of the average room temperature 1694 psi primer cohesive failure. Therefore, the cohesive failure of the primer at +160°F was lower than the cohesive primer failure at room temperature. Cases A4 and A5 had a 30 percent and 95 percent adhesive failure. This resulted in higher failure strengths than Case A6. At +160°F, the primer cohesive failure strength dropped to a very low value (only 895 psi), for Case A6. It was similar to the "A" cure of 265°F for 4 hours, and had very little strength in the primer. This low value of 895 psi was unacceptable.

Case A7, at -65°F, the major failure mode (93 percent), see Table 1.20, was the lower adhesive strength between the adhesive AF31 and the primer at this low temperature. The shear value was only 659

psi, see Table 1.25, which was only 38.9 percent of the average room temperature shear stress of 1694 psi (average of A1, A2, and A3). This value was unacceptable.

Changing the Cure to F7, a 1531 psi shear stress was obtained, see Table 1.28, which is 232.3 percent higher than A7. The F7 failure at -65°F was a 45 percent AF31 to primer adhesive failure with a 40 percent cohesive primer failure. As mentioned in Cases F2 and F3, the "F" cure cycle has increased the cohesive strength of the primer. The next hierarchy of failure, at a higher shear strength, was the AF31 to primer adhesive failure.

The A7 shear value of 659 psi, which was only 38.9 percent of the average room temperature value of 1694 psi, was the primary reason for development of a new cure cycle. Both the cohesive and adhesive primer modes lose strength using the "A" cure cycle.

Case A8, at -65°F, had a major failure mode of 65 percent primer cohesive failure, see Table 1.20. This was followed by an adhesive failure of the AF31 adhesive and the primer (35 percent). Improving the cohesive strength of the primer by using the "F" or "G" cure cycle improved the strength in shear significantly. For example, A8 went from 558 psi shear strength, see Table 1.25, to F8 of 1538 psi, see Table 1.28, and G8 of 1694 psi, see Table 1.29, by changing the cure cycle. This was a 1532 psi average for F7, F8, and F9, compared to 674 psi average for A7, A8, and A9, which was a 236.8 percent increase. The F8 failure at -65°F was a 48 percent AF31 to primer adhesive failure with a 38 percent cohesive primer failure. The "F" cure cycle improved the strength significantly.

Case A9, at -65°F, was a 55 percent primer cohesive failure, and a 45 percent AF31 adhesive to primer adhesive failure, see Table 1.20. Since the cohesive primer had a lower failure strength than the

32

adhesive failure mode, Case A9 resulted in a slightly higher strength of 724 psi compared to 558 psi for A8. However, both failure modes at -65°F have a low strength. The improved "F" or "G" cure cycles substantially increased the strength, by at least a factor of 2.0.

4.4.4 Detailed Considerations for Carbon/Epoxy Cloth Bonded to Fiberglass Cloth and Carbon/Epoxy Cloth: Microscopic examinations of the carbon/epoxy cloth to fiberglass cloth and carbon/epoxy cloth to carbon/epoxy cloth lap shear specimens were done with different cure cycles to determine the failure mode distributions. From these distributions, and the actual lap shear values of the specimens, analyses were done to determine the cohesive and adhesive strength of the components. Based on these results for room temperature, hot (+160°F), and cold (-65°F) conditions, the selections of the materials and joining cure cycle were made.

Further detailed analyses have been made to try to predict the test failure lap shear stresses for the carbon/epoxy cloth bonded to the fiberglass cloth using the "F" and "G" cure cycles. Some comparisons, and use of the "A" cure cycle data were also considered. These analyses have given us a better understanding of the role of the primers, adhesive AF31, and the effects of the "A", "F", and "G" cure cycles at various temperatures.

4.4.4.1 Detail Analyses of Fcf and Gcf Cure Cycle Lap Shear Specimens: Tables 1.30, 1.31, 1.32, and 1.33 show the specimens and percentage of layers that failed for the Fcf, Gcf, Fcc, and Gcc specimens. Reviewing the lap shear strengths, Figures 1.17, 1.18, 1.19, and 1.20 and Tables 1.19, 1.28, 1.29, 1.30, and 1.37 plus the XES and high magnification photographs, Figures 1.25, 1.26, 1.27, 1.28, 1.29, and 1.30 the following analyses has been done to help understand the hierarchy of the modes of failure.

1. The Carbon/Fiberglass Bond, using the "F" Cure Cycle

Specimen Fcf1: The (100 percent) cohesive failure of the carbon layer was the weak link for this room temperature specimen, see Table 1.30, but the value at 2414 psi, Table 1.35, was only exceeded by the Gcf, Table 1.35, Table 1.36, Fcc and Gcc specimens at room temperature, and Figures 1.18 and 1.19. The carbon internal strength (for a cohesive failure), was much higher than the primer cohesive failure average strength of only 1694 psi, Table 1.25, for the "A" cure cycle. Therefore, the "F" and "G" cure cycles have significantly strengthened the primers (Layers #2 and #4 - since they did not fail first as a primer cohesive failure). A 42.5 percent (2414/1694 = 1.425) increase in strength over the original "A" cure primer strength at room temperature was required to fail the carbon cloth layer internally (called a cohesive failure).

Specimen Fcf2 failed during loading; therefore, Specimen Fcf10 was substituted. This room temperature specimen had a 70 percent carbon cohesive failure and a 20 percent fiberglass cohesive failure, Table 1.30. The specimen failed at 2570 psi, Table 1.35. This was 6.5 percent higher than the Fcf1 failure, which was a 100 percent carbon cohesive failure. If one assumes that one can multiply by 70 percent the carbon cohesive shear strength of 2414 psi, (from Fcf1), then $0.7 \times 2414 + 0.2X = 0.9 \times 2570$. Therefore, the value of X was 3118.5 psi and is the 100 percent fiberglass cohesive failure strength. This assumes that the No. 2 - 1 percent primer, No. 3 - 7 percent AF31, and No. 4 - 2 percent primer, account for the remaining 10 percent of shear. The fiberglass cohesive failure strength was approximately 29 percent stronger than the carbon cohesive strength with the "F" cure cycle at room temperature, 3118.5/2414 = 1.29.

Specimen Fcf3: This specimen failed at 2589 psi, Table 1.35.
It had a 60 percent carbon cohesive failure and a 35 percent
fiberglass cohesive failure, Table 1.30. Using the 60 percent
times 2414 psi (from Fcf1), plus 35 percent times 3118.5 psi
(from Fcf10), yields 1448.4 psi plus 1091.5 psi which equaled
2540 psi. This represents 95 percent of the value. Dividing by
0.95 yields 2674 psi. The actual value measured was 2589 psi
which is 97 percent of the above theoretical value of 2674.
Therefore, the larger percent of the failure, being the
fiberglass cohesive failure (35 percent versus 20 percent for
Fcf10), did result in a higher total shear strength. This
completed the room temperature tests with the Fcf cure cycle
cohesive failure mode, a significantly higher failure mode than
the average primer cohesive mode of Cure "A", followed by the
still higher failure mode of the fiberglass cohesive failure
mode using the Fcf cure cycle.

Specimen Fcf4: This specimen was tested at +160°F and had a 50
percent carbon cohesive failure, a 4 percent AF31 adhesive
failure, a 6 percent No. 4 primer cohesive failure, and a 30
percent fiberglass cohesive failure, Table 1.30. The total
shear failure was at 2182 psi, Table 1.35.

It was assumed that at 160°F, the No. 2 and No. 4 primers, the
carbon cohesive and fiberglass cohesive strengths were all
weakened due to the elevated temperature. The value of 2182 psi
compared to the Fcf1 specimen value of 2414 psi at room
temperature was 0.903, a reduction of approximately 10 percent.
By using the following equation (assuming a reduction to 0.903
for elevated temperature); 0.903 [50% x 2414 (from Fcf1) + 30% x
3118.5 (from Fcf10) + 16%X] = 0.903 x 2414 x 0.96, and solving
for the primer strength, X, reveals that the Primers 2 and 4
together would have an effective strength of 1101 psi in shear,
based on the total lap shear area.

Summing up, 96 percent of the components (neglecting the 4 percent AF31 failure), the carbon cohesive failure contribution was 50 percent x 2414 x 0.903 = 1090 psi, and the fiberglass cohesive failure = 30 percent x 3118.5 x 0.903 = 844 psi, and the primers only contributed 0.16 x 1101 x 0.903 = 159 psi, which was 159/2182 x 0.96 = 7.6 percent of the final shear strength. Therefore, at temperature, the weaker primers have only a small effect on the strength.

Specimen Fcf5: This specimen was also tested at 160°F and had a 45 percent cohesive fiberglass failure (this was a higher strength shear failure), calculated at 100 percent to be 3118.5 psi (from Fcf10), and a 30 percent carbon cohesive failure at 2414 psi for 100 percent at room temperature, (from Fcf1) Table 1.30. These two components add up to 0.45 x 3118.5 x 0.903 = 1267 psi plus 0.3 x 2414 x 0.903 = 654 psi, = 1921.2 psi which accounts for 86 percent of the actual total shear of 2240 psi, Table 1.35. The remaining 14 percent could be distributed by the No. 2 - 12 percent primer, the No. 3 - 10 percent AF31 adhesive, and the No. 4 - 3 percent primer. Using the effective primer shear strength of 1101 psi (from Fcf4), times 12 percent plus 3 percent for the No. 2 and No. 4 primers, the contribution was 1101 x 0.15 = 165 psi. This leaves 2240 x 0.14 = 313.6 psi - 165 psi, which was 148.6/0.10 = 1486 psi for the AF31 100 percent adhesive shear strength. This analysis now provided the contributing 100 percent values of each layer. These values will be used next for Specimen Fcf6 to predict the theoretical value and will then be compared to the actual value.

Specimen Fcf6: This specimen was also tested at +160°F. It has a 40 percent carbon cohesive failure, a No. 2 - 10 percent primer cohesive failure, a 10 percent AF31 failure, another No. 4 - 10 percent primer cohesive failure and a 30 percent

fiberglass cohesive failure, Table 1.30. The specimen failed at
2146 psi, Table 1.35. Adding up the components should sum to
the 2146 psi value. The component values are:

Layer No. 1 - 40% carbon cohesive failure = 0.4 x 2414
           (from Fcf1) x 0.903 =   872

Layer No. 2 - 10% primer cohesive failure = 0.1 x 1101
           (from Fcf4) =   110

Layer No. 3 - 10% AF31 adhesive failure = 0.1 x 1486
           (from Fcf5) =   149

Layer No. 4 - 10% primer cohesive failure = 0.1 x 1101
           (from Fcf4) =   110

Layer No. 5 - 30% fiberglass cohesive failure = 0.3 x
           3118.5 (from Fcf10) x 0.903 =   <u>845</u>

                            Sum = 2086 psi

This is 2086/2146 = 0.972, or 3 percent in error between theory
and test results, which is very close in agreement. Again, the
primers and adhesive AF31 were the weaker elements that do not
contribute much to the total strength but help to redistribute
the load almost equally between the 40 percent carbon cohesive
and 30 percent fiberglass cohesive failures.

Specimen Fcf7: This was the first of the cold (-65°F) specimens
tested with the "F" cure cycle. Specimen Fcf 9 was considered
first for ease of analyses.

Specimen Fcf9: This was the third of the cold (-65°F) specimens
tested with the "F" cure cycle. This test had an 80 percent
carbon cohesive failure for the No. 1 layer, a 2 percent primer
failure for the No. 2 layer, a 6 percent AF31 adhesive failure
for the No. 3 layer, a 2 percent primer failure for the No. 4

layer, and a 10 percent fiberglass cohesive failure, Table 1.30. The Fcf1 failure at room temperature was 2414 psi and was a 100 percent carbon cohesive failure. The Fcf9 failure was 1894 psi, Table 1.35, and was an 80 percent carbon cohesive failure. Using the room temperature Fcf1, Fcf10, and Fcf3 distributions, the 10 percent fiberglass cohesive failure was 311.9 psi (at room temperature), which is (for 10 percent fiberglass) 0.10 x 3118.5 = 311.9 psi, the 80 percent carbon (at room temperature) = 2414 x 0.8 = 1931.2 psi, and the 6 percent AF31 failure of 0.06 x 1486 (from Fcf5) = 89.2 psi, plus the No. 2 and No. 4 primer failures of 0.04 x 1101 (from Fcf4) = 44.0 psi. These all sum to 311.9 + 1931.2 + 89.2 + 44.0 = 2376.3. The (-65°F) cold test value of failure was actually 1894 psi; this was 79.7 percent of the theoretical room temperature value.

The actual Fcf9 value of 1894 psi compared to the average room temperature value of 2524 psi (average of Fcf1, Fcf10, and Fcf3) was 75.0 percent. Therefore, the calculated distribution of 79.7 percent was a ratio of 1.06, again very close in agreement. The carbon cohesive strength for 80 percent at (-65°F) cold was 0.797 x 1931.2 = 1539 psi. When this was compared to the Fcf1 value (for 100 percent carbon cohesive failure) of 2414 psi the ratio was 1539/0.8/2414 = 1924/2414 = 0.797 for the carbon cohesive failure (for 100 percent) at (-65°F) cold to the room temperature value. With this analysis it was possible to go back to Specimen Fcf7 and estimate the calculated values compared to the test values.

Specimen Fcf7: This was the first of the cold (-65°F) specimens tested with the "F" cure cycle. It had a 60 percent carbon cohesive failure, a No. 2 - 2 percent primer cohesive failure, a No. 3 - 5 percent AF31 adhesive failure, a No. 4 - 8 percent cohesive primer failure, and a 25 percent fiberglass cohesive failure, Table 1.30. Using the same technique as in Specimen No. 6, but reducing the room temperature value by 0.797 (from Fcf9), the component values for the (-65°F) cold conditions are:

Layer No. 1 - 60% carbon cohesive failure = 0.6 x 2414 x
0.797 =   1154.4

Layer No. 2 - 2% primer cohesive failure = 0.02 x 1101 x
0.797 =   17.5

Layer No. 3 - 5% AF31 adhesive failure = 0.05 x 1486 x
0.797 =   59.2

Layer No. 4 - 8% primer cohesive failure = 0.08 x 1101 x
0.797 =   70.2

Layer No. 5 - 25% fiberglass cohesive failure = 0.25 x
3118.5 x 0.797 =   621.4
                                             Sum = 1922.7 psi

The actual test result for Fcf7 was 1958 psi, Table 1.35. Therefore, the theoretical distribution above, of 1922.7 psi, is 2 percent below the test result. The 60 percent carbon cohesive failure and the 25 percent fiberglass cohesive failure accounted for 1154.4 + 621.4 = 1775.8, which is 90.7 percent of the test failure strength. The high fiberglass cohesive strength showed only 25 percent of the failure area but accounts for 31.7 percent of the failure strength (621.4/1958 = 31.7%).

Specimen Fcf8: This specimen was also tested at -65°F. It had a 70 percent carbon cohesive failure, a 4 percent primer cohesive failure for Layer No. 2, a 6 percent AF31 adhesive failure, a 2 percent primer cohesive failure for Layer No. 4, and a 10 percent fiberglass cohesive failure, Table 1.30. Using the component values from specimen Fcf7, and the reduction for temperature of 0.797 (from Fcf9), the values for -65°F are:

Layer No. 1 - 70% carbon cohesive failure = 0.7 x 2414 x
0.797 =   1346.8

Layer No. 2 - 4% primer cohesive failure = 0.04 x 1101 x
0.797 =   35.1

Layer No. 3 - 6% AF31 adhesive failure = 0.06 x 1486 x
0.797 =   71.1

Layer No. 4 - 2% primer cohesive failure = 0.02 x 1101 x
0.797 =   17.6

Layer No. 5 - 10% fiberglass cohesive failure = .10 x
3118.5 x 0.797 =   248.5
                                               Sum = 1719.1 psi

The actual test result for Fcf8 was 1882 psi, Table 1.35. This is 9.5 percent higher than the theoretical calculated value computed above. The difference is 1882 - 1719 = 163 psi. If the fiberglass cohesive failure was 6.5 percent higher than the estimated 10 percent, or if the carbon cohesive value percent failure area was 0.785 instead of 0.70, then the theoretical value would exactly match the test values.

Looking at Figures 1.28 and 1.29 indicate that it was difficult to measure the percent of the mode of failure. Therefore, a small change in these percentages can easily occur. The carbon cohesive strength was the most important ingredient since it is approximately 1346.8 divided by 1882 psi or 71.6 percent of the total strength at -65°F.

2. The Carbon/Fiberglass Bond, Using the "G" Cure Cycle

Specimen Gcf3: This room temperature specimen has a 90 percent cohesive carbon failure, a 2 percent primer cohesive failure, a 5 percent AF31 adhesive failure, and a 3 percent fiberglass cohesive failure, Table 1.30. The test shear was 2464 psi, Table 1.35, the "F" cure cycle primer cohesive room temperature

strength value was 1101 psi, the "F" cure cycle AF31 adhesive failure was 1486 psi, and the "F" cure cycle fiberglass cohesive failure strength was 3118.5. Now, assuming that the main contribution to the 2464 psi test shear was the cohesive carbon failure, the equation is (where X = strength of cohesive carbon failure for the "G" cure cycle);

$$0.90X + 0.02 \times 1101 + 0.05 \times 1486 + 0.03 \times 3118.5 = 2464$$
$$0.90X = 2464 - 22.0 - 74 - 93.6 = 2464 - 189.6 = 2274.4$$
$$X = 2527 \text{ psi}.$$

This was the estimated cohesive carbon shear failure strength of the first layer. Notice that it is higher than the 2414 psi value for the "F" cure cycle 100 percent cohesive failure of the carbon layer (see Specimen Fcf1).

Specimen Gcf2: Using the results of Specimen Gcf3, the fiberglass cohesive strength of Layer No. 5 will be solved. The test strength of Gcf2 was 2590 psi, Table 1.35. The X value of the fiberglass cohesive strength is the unknown in the equation;

$$2590 = 0.20X + 0.70 \times 2527 \text{ (from Specimen Gcf1)}$$
$$\qquad + 0.07 \times 1101 \text{ (5\% primer, Layer No. 2, plus 2\% primer,}$$
$$\qquad \text{Layer No. 4)} + 0.03 \times 3118.5 \text{ (3\% AF31 adhesive,}$$
$$\qquad \text{Layer No. 3)}$$
$$0.20X = 2590 - (0.70 \times 2527 = 1768.9) - (0.07 \times 1101 = 77) -$$
$$0.03 \times 3118.5 = 93.6)$$
$$X = 650.5/0.20 = 3252.5 \text{ psi for the fiberglass cohesive failure}$$
$$\qquad 100 \text{ percent strength at room temperature}$$

Please notice that for the primers and adhesive, the room temperature values for the "F" cure cycle were assumed. However, these represent only 10 percent of the failure face. The fiberglass cohesive failure strength for the "G" cure was estimated to be slightly higher than the "F" cure cycle fiberglass cohesive failure strength of 3118.5 psi.

Specimen Gcf1: The estimated carbon cohesive strength and fiberglass cohesive strength derived for Gcf3 and Gcf2 will be used to solve the theoretical Specimen Gcf1 strength and then compared to the test results of 3021 psi, Table 1.35. The Gcf1 area failure face percentages were:

Layer No. 1 - 65% carbon cohesive failure = 0.65 x 2527 = 1643

Layer No's. 2 & 4 - 10% primer cohesive failure = 0.10 x
1101 = 110

Layer No. 3 - 5% AF31 to primer Layer 2 = 0.05 x 3118.5 = 156

Layer No. 5 - 20% fiberglass cohesive failure = 0.20 x
3252.5 = 651
Sum = 2560 psi

The test results are 18 percent higher than the theoretical values calculated above. The 65 percent carbon and the 20 percent fiberglass would have to be increased by 7 percent each in order to obtain the test value. This seems too high an error in estimating the failure face area percent. Therefore, the "G" cure cycle must be that much better than the "F" cure cycle for the room temperature condition.

The Specimens Gcf4, Gcf5, and Gcf6 are at +160°F. Assuming a reduction for elevated temperature of 0.903, (see Specimen Fcf4), the values from Specimen Gcf1 were used for Gcf4.

Specimen Gcf4: The areas of the failure face percentages multiplied by the theoretical allowables were:

Layer No. 1 - 45% carbon cohesive failure = 0.45 x 2527 x
0.903 = 1026.9

Layer No's. 2 & 4 - 10% primer cohesive failure = 0.10 x
         1101 x 0.903 =   99.4

Layer No. 3 - 20% AF31 adhesive failure = 0.20 x 3118.5 x
         0.903 =   563.2

Layer No. 5 - 15% fiberglass cohesive failure = 0.15 x
         3252.5 x 0.903 =   <u>440.6</u>

Sum = 2130.1 psi

The test value for specimen Gcf4 is 2270 psi, Table 1.35. The theoretical value of 2130.1 psi was six percent lower than the test value. This correlation seems reasonable.

Specimen Gcf5: The areas of the failure face percentages multiplied by the theoretical allowables were;

Layer No. 1 - 40% carbon cohesive failure = 0.40 x 2527 x
         0.903 =   912.8

Layer No's. 2 & 4 - 20% primer cohesive failure = 0.20 x
         1101 x 0.903 =   198.8

Layer No. 3 - 15% AF31 adhesive failure = 0.15 x 3118.5 x
         0.903 =   422.4

Layer No. 5 - 25% fiberglass cohesive failure = 0.25 x
         3252.5 x 0.903 =   <u>734.3</u>

Sum = 2268.3 psi

The test value of 2006 psi, Table 1.35, was 12 percent less than the predicted, theoretical value. Specimen Gcf4's test value was 6 percent more than the theoretical value. (-12% + 6%)/2 = -3% average deviation from the test values for the two cases investigated so far. More test specimens are desired to have a higher confidence level.

Specimen Gcf6:   The areas of the failure face percentages multiplied by the theoretical allowables were;

Layer No. 1 - 25% carbon cohesive failure = 0.25 x 2527 x
         0.903 =   570.5

Layer No's. 2 & 4 - 30% primer cohesive failure = 0.30 x
         1101 x 0.903 =   298.3

Layer No. 3 - 25% AF31 adhesive failure = 0.25 x 3118.5 x
         0.903 =   704.0

Layer No. 5 - 20% fiberglass cohesive failure = 0.20 x
         3252.5 x 0.903 =   587.4

                                   Sum = 2160.2 psi

The test value of 2043 psi, Table 1.35, was 94.6 percent of the theoretical value.

The low (25 percent) carbon cohesive failure percentage accounts for the major reduction in the test value of 2043 psi compared to a test value of 2270 psi, for the Specimen Gcf4 (which has 45 percent carbon cohesive failure). A 20 percent variation with the average of (25 + 45)/2 = 35% was a very wide variation in the failure face percentage. This results in a ten percent variation in test shear value.

The coefficient of variance is the standard deviation divided by the average value. With only three specimens, the standard deviation cannot be determined accurately. Using, instead, the minimum to maximum variation in failure percent of the most important layer for strength (the carbon epoxy cloth cohesive failure), divided by the average, was 20% divided by 35% which equals 0.57 at +160°F, and was a much larger variation than the equivalent room temperature value of 65% to 90% = 25%, for the

44

minimum to maximum, divided by the average value of 73 percent which yields 25/.73 = 0.343. At -65°F, Gcf7 to Gcf9, the minimum to maximum is 20 percent divided by the average of 90, 80, and 70 = 80 percent, which is 0.25.

Therefore, for some reason which was not obvious, the high temperature tests have a wider failure face percent (divided by the average) variation than those tested at room temperature or cold temperature conditions. Also, the AF31 adhesive strength stays within 5 percent for room temperature and within 8 percent for cold conditions. However, at elevated temperature the failure of the adhesive, AF31, varies by 15 percent to 25 percent, which is more than three times the variation at the room temperature and cold conditions. More test specimens are required to yield a higher confidence level in these results. The elevated temperature tests should have even more specimens than the room temperature and cold tests.

The Gcf7, Gcf8, and Gcf9 results were at -65°F. Assuming a reduction factor for cold temperatures of 0.797 from Specimen Fcf9, the room temperature values were modified as shown in the following section.

Specimen Gcf7: This specimen, at -65°F, has areas of the failure face percentages multiplied by the theoretical allowables of;

Layer No. 1 - 90% carbon cohesive failure = 0.9 x 2527 x
                0.797=   1812.6

Layer No's. 2 & 4 - 1% primer cohesive failure = 0.01 x
                  1101 x 0.797 =   8.8

Layer No. 3 - 4% AF31 adhesive failure = 0.04 x 3118.5 x

0.797 =   99.4

Layer No. 5 - 5% fiberglass cohesive failure = 0.05 x

3252.5 x 0.797 =   129.6

                                        Sum =   2050.4 psi

The test value of 2033 psi, Table 1.35, is one percent lower than the estimated theoretical value of 2050.4 psi, shown above. Notice that for the cold condition, the carbon cohesive failure is 1812.6/2033 = 89% of the total strength. With the 5 percent fiberglass cohesive failure strength added of 129.6/2033 = 6.4%, the two components add up to 95.4 percent of the total strength.

4.4.5   Conclusions - From the Lap Shear Tests of "Fcf" and "Gcf" Cure Cycles and Using the Theoretical Analyses of the Microscopic Failure Face Percentages:

4.4.5.1   The carbon cohesive strength has a much higher failure strength using the "Fcf" cure cycle at room temperature, and is much higher than the average primer cohesive critical strength for the "A" cure cycle.

4.4.5.2   The fiberglass cohesive failure mode is higher in strength than the carbon cohesive strength at room temperature.

4.4.5.3   At elevated temperature (+160°F), the primers and AF31 adhesive help to distribute the load almost equally between the carbon cohesive and fiberglass cohesive failure modes that carry most of the load for the Fcf cure cycle.

4.4.5.4   For the cold conditions (-65°F), the carbon cohesive layer carries most of the load (70 to 80 percent) for the Fcf cure cycle.

46

4.4.5.5 The minimum to maximum variation of the failure face percent divided by the average failure percent of the material layer that contributed most to the strength was investigated. The high temperature tests showed a wider variation than at room temperature and cold temperature conditions. No firm conclusions can be drawn from this. However, future tests should be made to increase the confidence level. When these are made, the number of +160°F specimens should be even greater than the room temperature and cold tests.

4.4.5.6 For a great number of the cases, the high percent cohesive failure of the basic laminating materials shows that the maximum strength potential was reached.

4.4.6   Recommendations for Future Lap Shear Tests: The information obtained and the analyses performed from the small lap shear tests enabled the determination of the best cure cycle for strength for the various materials that have been bonded together. Test results with 3- by 3-inch panels, using these optimum lap shear materials and cure cycles, have justified the effort expended on the lap shear tests. However, some of the following recommendations might further increase the lap shear strengths.

4.4.6.1 The cure cycle temperature was increased from the "A" cycle, 265°F, to the "F" and "G" cycles, 300°F. This increased the room temperature critical strength significantly, especially the strength gain of the carbon/epoxy cloth cohesive failure. The "F" cure cycle has a 100 psi pressure. Using this pressure to press the pad to the titanium is not difficult. However, the "G" cure cycle was chosen when pressing the perforated titanium and pad to the composite substructure because this cure cycle had the lower 75 psi pressure, and at 300°F the webs of fiberglass might bow if too high a pressure was exerted at the 300°F, which was a temperature high enough to begin softening of the fiberglass. Further investigation of the fiberglass by compression testing and analyses of the webs at higher temperatures is suggested to determine the temperature, pressure, and

time tradeoff limits for web buckling and/or bowing. After this study, a tradeoff of lap shear strength versus higher temperatures than 300°F might result in still higher lap shear strengths than were obtained using the "F" and "G" cure cycles.

4.4.6.2 Double lap shear specimens (to obtain the "pure" shear values without the induced bending of single lap shear specimens) should be tested versus temperature.

4.4.6.3 The peel, tension, fatigue, and bending allowables of the primers and adhesives should also be determined versus temperature and cure cycle.

Low tension and bending properties of adhesives may cause premature failures. Pictures of failures of 3- by 3-inch panels that have been tested in compression show that a side load component may have developed that caused the bond of the titanium sheet to the composite substructure to fail in peel, tension, or bending and this is discussed in the next section on testing. Further testing of the peel, tension fatigue, and bending strength are necessary to evaluate completely the selected cure cycle for the expected temperature and loading conditions.

48

5.0 PANEL TEST RESULTS

5.1 Introduction: The purposes of the panel tests were;

1. To confirm the choice of materials, adhesives and bonding, and curing cycles.

2. To verify that the bonding of the titanium perforated sheet to the composite substructure can survive the ultimate wing strains and temperature conditions.

3. To verify that the optimum geometry, materials, number of plies, and rib spacing chosen can sustain the expected wing strains.

4. To measure any initial panel surface deviations arising from the bonding and curing cycles.

5. To provide structural test data, progressing from small to larger panels, that can be used to analyze the final configuration and show that a sufficient margin of safety exists, and that the combined deflections from lateral loading, thermal expansion, and compression loading will not exceed the LFC overall panel and flute waviness criteria and cause turbulent flow at load factors less than 1.5g. Also, at ultimate strain loading, with eccentricities from thermal bowing, lateral deflection, and beam-column effects, the panel will not fail.

6. To conserve materials and fabrication costs, the testing was done using the small specimens whenever appropriate in the development of the panel design. The sizes are listed below:

   A. Small overlap shear specimens, each 3.5 inches long, with an overlap of approximately one-half an inch on the ends of the one-inch wide strips of the two materials to be joined were

tested at room temperature, hot (+160°F), and cold (-65°F) conditions. The previous section describes the results of these tests. Figure 1.32 shows an example of the shear test Specimen D10, fiberglass bonded to porous titanium.

B. The compression panels were cured in an autoclave. A flat steel tool, 20 inches wide and 4 feet long, was reinforced to provide a flat surface. Allowing for bagging and sealing margins reduced the available panel size to 10 by 30 inches.

Various panel sizes were investigated, influenced by the theoretical rib spacing and by the perforated and non-perforated titanium sheet sizes available. Some of the variations in sizes used were:

(1) From the 10- by 30-inch panel, cut three 10- by 10-inch panels. From these, cut 4.5- to 5.5-inch wide panels which are 8.0 to 10.0 inches long. Allowing just enough material for squaring the panels and machining the panels properly, required some experience. The early panels left more allowance for machining.

(2) Split the 10- by 30-inch length in half and make 10- by 15-inch long panels.

(3) From the above 10- by 15-inch panels, cut a panel approximately 3 by 15 inches long, leaving approximately a 7- by 15-inch long panel. Cut the 3- by 15-inch long panel into four panels. Machine and square-off three of these four panels for testing.

(4) Fabricate a 10- by 20-inch long panel, leaving a 10- by 10-inch panel from the original 10- by 30-inch panel. Cut the 10- by 10-inch panel into nine 3- by 3-inch panels.

(5) With the remaining perforated material 10 by 28 inches
long, cut a 10- by 27-inch long panel and add a center
rib for a two-bay panel test.

5.2   Panel Test Results and Discussions: Throughout this program many
panels were tested. The failures were analyzed and the panels were
significantly improved with time. Rather than bunch all similar
tests together and report on them collectively, more understanding
can be gained by discussing the early failures, the improvements, and
the later verification by tests. Whenever changes were made, the
smallest sized specimen or panels were used first to minimize the
cost and the time spent.

5.2.1   One of the first panels tested was the compression specimen Panel
10E, shown in Figure 1.33. The analysis indicated the number of
laminations shown in Table 1.38. Code 2 in Table 1.38 was
carbon/epoxy cloth, Code 5 was fiberglass cloth and, Code 7 was the
6AL-4V titanium. The theoretical critical failure mode was the web
buckling at 5053 lb/in., and the strain of 6307 micro in./in. The
actual failure load was 28,800 pounds. Using the panel width of 4.4
inches resulted in a loading of 6545 pounds per inch which was 29.5
percent higher than the theoretical value.

Table 1.38 was based on simply support edges to be conservative.
Fixed edges yield unconservative values. In order to stabilize the
edges from local buckling and prevent peeling, a channel of
fiberglass was added to each edge. This can be seen in Figure 1.34.
When the area and modulus of the edge channels were accounted for,
then the critical failure load on the panel itself should be reduced
to 5660 lb/in. This is still 11 percent higher than the theoretical
value. For future tests, these edge stabilizers were cut into three
short columns that would not carry load across the cuts. It is
difficult to determine from Figures 1.34, 1.35, 1.36, and 1.37
exactly what caused the failure. It could have been the buckling of

51

the flute webs, the failure of the composite side "lower skin", or the failure of the titanium primer, the fiberglass cloth, the carbon/epoxy cloth, and/or the AF31 adhesive. The strain gages shown in Figure 1.38 show that the strain in the titanium and composite lower skins were linear almost all the way up to failure. Figures 1.35 and 1.37 show that the cap to the titanium failed at the titanium primer bond to the titanium, or as a cohesive failure of the primer at the first full cap to the titanium. At the other cap locations, Figures 1.35, 1.36, and 1.37 showed that the fiberglass cloth failed as a cohesive failure, and the failure also occurred at the adhesive to the fiberglass.

Strain gages and dial gages were used as shown in Figure 1.39. Later, panels were instrumented at the webs with strain gages to determine the web stresses and to verify the critical failure modes. The 5000 micro in./in. of strain at 25,000 pounds, from Figure 1.38, represents the last strain measurement recorded before the failure load of 28,000 pounds. Assuming linearity, 28,800/25,000 x 5,000 equals 5760 micro in./in. strain at the failure load of 28,800 pounds. Using a modulus for titanium of 16.1 x 10^6, the maximum titanium stress was 92,736 psi. This was lower (by 33 percent) than the compression strength of fully stabilized 6AL-4V titanium sheet. Later tests, with improved bond strength, came closer to the ultimate titanium strength. The composites, using 5325 micro in./in. at 25,000 pounds, when increased to 28,800 pounds, results in 6134 micro in./in. At this strain, carbon/epoxy cloth would have a 50,299 psi stress. This is lower (by 28 percent) than the maximum strength of carbon/epoxy cloth. Therefore, it was concluded that the bond or adhesive strength was the limiting factor and the most critical failure mode for the short compression panel $10E_1$.

The geometry of the cross-section of the $10E_1$ configuration was similar to the 13F configuration, which is shown in Figure 1.40. The only change for the $10E_1$ configuration was that only two carbon/epoxy cloth laminates were sandwiched between four fiberglass

cloth laminates (two on each face of the base lower skin). The 13F$_1$ configuration, in Figure 1.40, showed that three carbon/epoxy cloth and two fiberglass cloth laminates were used for the base lower skin.

5.2.2   The A1 and L1 configurations were cut from the 13F concept shown in Figure 1.40. The "A" is for axial loading and the "L" for lateral loading in Figures 1.41, 1.42, and 1.43 show tested specimens which were approximately 3- by 3-inches. The titanium sheet was opened 90 degrees in Figure 1.43 to show the exposed bond layer on the A1 and L1 panels. The smooth surface of the titanium indicates a failure of the titanium primer, except for the yellow areas on the left end of the bottom A1 that indicates a fiberglass cloth failure and/or the adhesive. Notice in Figure 1.42 that the lateral loading failed the composite face of the L1 specimen. From Figure 1.43, this could have happened after the debond of the primer. Then the composite lower skin sandwich was the only resistance to the lateral load and would fail in bending.

From Table 1.9, the lateral ultimate loading was 5625 pounds for L1 and 13,250 pounds for A1. The axial strain gage readings for A1 were -3669 micro in./in. for the titanium and -4296 micro in./in. for the composite side. When the L1 specimen was loaded laterally, it failed at a strain of -2948 micro in./in. for the titanium and -2440 micro in./in. for the composite side. Dividing the A1 loading of 13,250 pounds by the specimen width of 2.882 inches equals a 4598 pounds per inch. Dividing by the area per inch (from Table 1.38) of 0.1216 sq. in./in., and subtracting one fiberglass laminate (difference between Configurations 10E and 13F) leaves a 0.1216 - 0.010 = 0.1116 sq. in./in. The stress was, therefore, 4598 divided by 0.1116 which equals only 41,201 psi. Using the titanium strain of 3669 multiplied by a modulus of 16.1 x 10^6 for titanium yields 59,071 psi in the titanium. Using an average of 6.07 x 10^6 for the composite modulus, (3/5 x [8.2 x 10^6] for three laminates of carbon/epoxy cloth, and 2/5 x [2.9 x 10^6] for two laminates of fiberglass

cloth), see Table 1.38, times the strain of 4296 micro in./in., yields only 26,077 psi for the composite side. Therefore, the composite substructure and the titanium were not loaded to their allowable strength. Notice, however, in Table 1.38, that the web buckling was critical at 5053 lb/in. which was close to the 4598 pounds per inch failure. If the web began to buckle, (similar to Figure 1.34), then the titanium bond at the primer and/or adhesive could fail.

Therefore, the 0.352 dimension of the cap to the titanium was increased to 0.51 inches, a 36 percent increase, to reduce the bond stresses. In addition, to increase the pressure drop, by reducing the number of open electron beam holes in the titanium, a "pad" was added to the titanium to block some of the holes. This pad helps to carry the high loads in the titanium sheet to the flute caps and it also helps prevent the titanium sheet from buckling between the flutes. Also, the wide pad, see Figure 1.44, has an increased area of adhesive between the titanium and the pad which reduces the adhesive stresses between the titanium sheet and the pad compared to the "old" adhesive area of the titanium sheet between the titanium sheet and the flute cap.

5.2.3   Before the pads were introduced into the panel design, three 4.2- by 10-inch panels were tested. Panel $H1_1$, Figure 1.45, shows a cross-section of this panel. To develop better allowables, an additional web ply was added because the analyses, Table 1.38, showed that web buckling was the critical failure mode. Figure 1.46 shows the test panel and the locations of the strain gages.

Table 1.39 shows the strain gage reading versus the end panel loading. Notice that strain Gage 17, from Figure 1.46, was on the titanium outer surface at the right-hand lower corner. At 25,000 pound loading, in Table 1.39, the strain Gage 17 reading was 7337 micro in./in. This resulted in 118,126 psi in the titanium if the modulus of elasticity for 6AL-4V annealed titanium is used. From

Figure 1.47 the load at this point dropped rapidly. Close inspection indicates that the titanium sheet separated from the composite substructure. Also, a crack across the composite inner face appeared above Gages 8, 10, and 12 on the composite side. Notice that these three gages dropped significantly in value when the load was raised from 24,000 pounds to 25,000 pounds. Using the 4869 micro in./in. of strain in the outer fiberglass cloth (or higher modulus of the next layer of carbon/epoxy cloth) would result in only 39,926 psi. The analysis value of critical strain of 8195 micro in./in., indicated in Table 1.13, Case 0.75-M6, was higher than the test titanium value of 7337 micro in./in. However, these panels were quite different.

In Figure 1.47, the notches in the loading curve indicate that cracking of the composites was occurring. Cracking noises were heard at the low load of only 15,000 pounds. Starting from 23,000 pounds, Table 1.39, values were circled for strain gage readings that reduce at higher loads. These reductions indicate a local failure. Notice that the even-numbered gages were on the composites side and the odd numbers on the titanium side, see strain gage locations, Figure 1.46. After 23,000 pounds loading, the even-numbered composite strains reduced. This happened to composite side strain Gages 2, 6, 8, 10, 12, 14, 16, and 18. The only odd-numbered gage that reduced at 25,000 pounds was Gage 11, on the titanium side. Therefore, some cracking was occurring on the composite side and it finally failed at 25,700 pounds. This was at a relatively low value for the composites with only 4869 micro in./in. for Gage Number 8 or 4938 micro in./in. for Gage Number 16. Gage Number 8 was at the right center location and Gage Number 16, was at the bottom, middle location, see Figure 1.46.

A cross-section of Panel J1 is shown in Figure 1.48. Notice that the composite sheet now has the facings of carbon/epoxy cloth and the three-core sheet of fiberglass. This was the most desirable configuration for weight and surface waviness according to the analyses reported in Case Number .75-M7 in Table 1.13. The critical

micro in./in. strain by analysis was 7996 micro in./in. However, this was for the web critical failure mode. The web Gage 12, Figure 1.49 showed a maximum strain of only 5166 micro in./in., Table 1.40. Actually, the critical failure mode was believed to be the titanium separating from the composites at 8645 micro in./in. at Gage 5. The gage was at the right upper corner on the titanium face. Similar to the H1 panel, which failed at the lower right corner (at Gage 17, Figure 1.46), the corner edge fixity may be so rigid it takes more of the loading and does not redistribute it to the rest of the panel. Notice that Gages 1 and 3 at the top, and 13, 15, and 17 at the bottom were more evenly distributed. Notice that only one strain gage, Number 11, decreased in value at 26,000 pounds. The head travel was linear almost up to failure, see Figure 1.47. The theoretical failure mode was 6605 lb/in., and the actual loading was 26,000 pounds divided by the 4.2-inch width, from Figure 1.49, which yields 6190 lb/in. This value was 94 percent of the theoretical value from Table 1.13 where the web was the critical buckling mode. Actually, the web strain Gage 12 showed a decrease in value at 24,000 pounds compared to the 22,000 pound strain gage value, (see circled values in Table 1.40). However, the load increased until the titanium at Gage Number 5 sustained 8645 micro in./in. Therefore, the buckling of the titanium away from the composite substructure at 139,185 psi was probably the cause of the failure, since it was close to the maximum titanium yield strength. This concept was close to optimum. However, this was at room temperature. Later tests showed that these levels would seriously deteriorate at cold and hot conditions before the bonding cure cycle was improved.

5.2.4 The cross-section of Panel G1 was shown in Figure 1.44. Notice the "pad" that was bonded to the titanium face sheet to increase the pressure drop through the remaining 0.25-inch open section. This sandwich pad helps to distribute the loading in the titanium. Notice in Figure 1.50, at Section X-X, that Gage Numbers 3, 9, and 13 were used to determine the strain gage variation across the pad. The ultimate load was 31,250 pounds and the strain gage values were shown

56

in Tables 1.41 and 1.42. At 31,000 pounds, Gage Number 3 was 5843 micro in./in., Gage Number 9 was 5927 micro in./in., and Gage Number 13 was 4865 micro in./in. These values were significantly better since they were lower than the 8645 micro in./in. at Gage Number 5 for the $J1_1$ configuration, see Figure 1.49 and Table 1.40. The G1 panel achieved a loading of 31,250 divided by 4.2 inches, which was 7440 lb/in. The G1 concept achieved a loading 20 percent higher than the $J1_1$ concept, and the maximum G1 loading is 31,250 pounds which is 24.5 percent higher than the $h1_1$ concept. The maximum loading with shims obtained 31,250 pounds compared to only 26,000 pounds without shims in Table 1.40.

For this test, the aluminum shims added, helped to redistribute the loading as seen by reviewing the strain gages in Tables 1.41 and 1.42. The top titanium face Gages 1 and 5, at 31,000 pounds, were shown to be 5916 for Gage 1, and 6234 micro in./in. for Gage 5. The average of these was 6075. The deviation is 159, which was only 2.62 percent of the mean. For Panel $J1_1$, the values at 26,000 pounds, were 5038 micro in./in. for Gage 1, Table 1.40, 5150 for Gage 3, and 8645 for Gage 5. The average was 6278 micro in./in. and the largest deviation was 2367 micro in./in. at Gage 5, which was a 37.7 percent deviation from the mean. The three aluminum foils of one-mil each added to the top and base of the Panel $G1_1$, plus the pads mentioned above, helped redistribute the load. Therefore, the pads and the shims at the ends of the panels for load redistribution have been adopted as desirable for obtaining high compression axial strength and strains.

At 30,000 pounds loading, (Table 1.42) many of the composite strain gages achieved their maximum values. Notice that Gage Number 16 shows a 6862 micro in./in. This gage was at the lower center location in Figure 1.50, on the composite side of the lower face sandwich skin.

Post failure inspection indicated a composite failure across the panel on the inner face near the top. Notice that Gages 2, 4, and 6 show large reductions in values for the composite inner face sheet from 30,000 pounds to 31,000 pounds; Gage 2 decreased from 4611 micro in./in. to 3564, Gage 4 from 5584 micro in./in. to 2854 and Gage 6 from 5029 micro in./in. to 2357. Strain Gages 1, 5, 7, 9, 15, and 17, all on the titanium face sheet, increased to the 31,000 pound level without decreasing. This would indicate that the composite failed first. However, the post failure appearance also indicates a separation of the titanium and the composite substructure at the top of the panel. Whether this was a result of the composite failure, or happened first, was difficult to determine. At Gage 5, at the top of the panel at 31,000 pounds, the highest strain in the titanium sheet was 6234 micro in./in., which was analyzed to be 100,367 psi. The highest composite strain of 6862 micro in./in., at Gage 16, was not where the panel failed, and was only 56,268 psi, using the modulus for the carbon/epoxy cloth. Since these stresses were low, it was assumed that further gains could be obtained by improving the bonding.

For the J1 and G1 configurations, the bond cure of the titanium to the composite substructure was increased to one hour at room temperature and one hour at 250°F. This was double the time used for Configuration $H1_1$. Double shear laboratory tests showed a five percent improvement using this cure cycle.

5.2.5 Referring again to the listing of the short compression 3- by 3-inch panels, shown in Tables 1.9 and 1.10, the A1-1 to A1-4, 3- by 3-inch specimens were tested. Figure 1.51 shows the improved cap width for the LA1-2 configuration, from 0.375 to 0.510 inches, and five fiberglass cloth laminates for the webs versus four. The increased cap width and the pads reduced the stresses and therefore further improved the bond shear of the titanium to the composite substructure. Using the LA1-2 geometry, and correcting the size for the test rigidity, Table 1.43, showed the expected results for the 3- by 3-inch specimen. The theoretical web buckling improved to

7202 lb/in. and the strain expected was 8060 micro in./in. Cases A1-1 and A1-2 were room temperature, dry, axial load tests. The failure loads were 31,500 pounds for A1-1 and 28,150 pounds for A1-2, see Tables 1.44 and 1.45. These values were 11 percent apart. The loadings were 10,093 lb/in. and 8605 lb/in. (dividing the loads by their appropriate widths). The A1-2 panel buckling value was 19 percent higher than the theoretical web buckling value. The strain of 10,603 micro in./in. at 31,000 pounds, Table 1.44, for the titanium side of the A1-1, indicated a very high stress in the titanium sheet of 132,000 psi (using the Mil-Handbook-5D Stress-Strain Diagram). Above 29,000 pounds, the 7175 micro in./in. strain on the composite side began to decrease. The notches in the head travel (Figure 1.52) were probably the yielding in the composite substructure and/or the bonding of the titanium. At failure the inner composite sandwich sheet had separated from the flutes, and the titanium sheet had separated from the pad, and the pad separated from the flutes.

5.2.6   The 3- by 3-inch panels, A1-3 and A1-4, were soaked in water for two weeks. The A1-3 failure was at 28,300 pounds and the A1-4 at 29,050 pounds, see Tables 1.44 and 1.45. The average of 28,675 pounds (wet) was four percent lower than the dry 29,825 pound average for the A1-1 and A1-2 panels.

5.2.7   The Al_2P, perforated titanium panel, when compared to the unperforated Panel Al_1, showed a 18,000 pound failure load compared to 20,400 pounds, see Table 1.46. This was a 12 percent reduction. However, Figure 1.53 showed that the head travel had a local "notch" change. The strain Gage 5 reading, Table 1.46, also shows a very rapid increase in strain on the composite side from 13,000 pounds to 14,000 pounds, (almost doubling in value). This indicates a premature failure. Other perforated titanium 3- by 3-inch tests at room temperature, discussed later in the program (after failure cure cycle development), namely AA1, AA2, and AA3 panels, showed 31,050 to 34,050 pounds for failure loads. These loads are significantly

higher than those panels in Table 1.46. In the next paragraph, Panels A1-9 and A1-10, which also were perforated and axially loaded at room temperature, are reported. These tests were not much different in their failure loads, compared with panel Al_2P.

5.2.8   Five 3- by 3-inch panels, A1-9 to A1-13, with perforated titanium face sheets, were tested at room temperature. The results are shown in Figure 1.54. Panels A1-9 and A1-10 were loaded axially.

The A1-9 specimen (2.896 by 2.898 inches) reached a 17,820 pound maximum axial load and the A1-10 specimen (2.895 by 2.896 inches) achieved a 19,760 pound maximum load. Dividing by their respective widths of 2.896 inches, the test loadings achieved were 6149 lb/in. and 6826 lb/in., respectively. An earlier test, Al_2P, with perforated sheet, reached an axial loading of 18,000 pounds maximum or 6002 lb/in. The analyses for simply supported non-perforated (3- by 3-inch) panels are shown in Table 1.47, and showed an estimated 7187 lb/in. with a strain of 8043 micro in./in. Panel A1-9 has an axial load strain of 5050 micro in./in. at 17,000 pounds, see Table 1.48. At the ultimate load of 17,820 pounds, the strain is estimated to be 5297 micro in./in. For Panel A1-10 the strain is 5928 micro in./in. at 19,000 pounds, and at the failure load of 19,760 pounds, the maximum strain is estimated to be 6165 micro in./in. These values were lower than the theoretical maximum strain of 8043 micro in./in. for non-perforated titanium sheet, but were well above the 4500 micro in./in. requirement. The corresponding maximum loadings of 6149 lb/in., for A1-9, and 6826 lb/in. were similarly lower than the theoretical analysis value of 7187 lb/in. for non-perforated sheet, but exceed requirements.

The lateral loads and strains of tests A1-11, A1-12, and A1-13 were well above those expected for the chordwise direction; the chordwise loads are reacted primarily by the ribs and the local airloads are transmitted by the panels to the ribs. Compression lateral loads of 6130, 4510, and 4330 pounds (see Figure 1.54) were sustained by the

60

panels. A lateral loading of only 450 pounds per inch is the maximum lateral load actually expected (3.75g maneuver). Dividing the test lateral loads by their respective lengths, one obtains 6130/2.9 = 2114 lb/in., 4510/2.896 = 1557.3 lb/in., and 4330/2.896 = 1495 lb/in. These panel lateral strengths were considerably above the maximum lateral load requirement.

5.2.9 **Two (4.5- by 10-inch) Compression Panels With Configuration LA1-1**: The details of two panels, $LA1-1-2_1$ and $LA1-1-2_2$, are shown in Figure 1.55. The dial indicators showed that for Panel $LA1-1-2_1$, for loads up to 20,000 pounds, the titanium face moved away from the observer at the top, center, and bottom locations where the dials were located. From 20,000 pounds to 40,000 pounds the titanium face sheet moved toward the observer with the lower dial indicating up to +0.0050 inches movement (see Table 1.49). From 40,000 pounds to failure at 50,000 pounds, the top dial moved very little, the middle dial moved away (by -0.0050 inches), and the bottom dial continued to move toward the observer (by +0.0071 inches), which was the largest movement versus loading. These dial gage movements are difficult to analyze. The end rigidity is almost full fixity and prevents lateral movement while the middle dial indicator can move from panel bowing. However, any column eccentricity or edge rotation caused by edge crushing, composite, titanium failures, and/or the end titanium sheet penetrating the aluminum shims at the higher loads, causes additional dial indicator movement.

The strain gages on the bottom, (see Figure 1.56), Gages 13, 15, and 17 for the titanium sheet, and Gages 14, 16, and 18 for the composites, showed high readings, see Tables 1.50 and 1.51. For example, Gage 15 showed a value of 8305 micro in./in. This corresponds to a stress of 125,000 psi for the titanium. This is close to the compression yield of the titanium 6AL-4V annealed material which, from Reference 4, the B value is $Fc_y = 139,000$ psi. At the middle of the panel, strain gage location Number 9 gave a slightly higher value of strain of 8519 micro in./in., indicating a

stress of 127,000 psi, using the Stress-Strain Diagram in MIL HDBK 5D, for titanium. The composite material, with a strain of 10,236 micro in./in. at Gage Number 16, was stressed to 83,935 psi, which was close to its short compression yield allowable of 93,100 psi. Failure occurred soon after these readings of the gages.

The actual failure looks like it occurred near strain Gages 1, 3, and 5 at the top of the specimen, by buckling of the titanium. On the composites side, cracks appear close to Gages 2, 4, and 6. Strain Gage 5 on the titanium side reached a value of 8456 micro in./in., and behind Gage 5, on the composite side, Gage 6 showed a strain of 9335 micro in./in. These values were close to the maximum strain values reached at the center of the panel at failure.

Another 4.5- by 10-inch specimen, LA1-1-2$_2$, with similar construction, was tested and failed at 47,000 pounds. Table 1.52 shows the dial gage readings. In this case, all locations bowed away from the observer, with the bottom gage moving -0.0076 difference from the recorded 5000 pound load position and the middle gage -0.0060 inches, at the 47,000 pound loading. Location Gage Numbers 9 and 11, on the titanium side, in the middle of the panel, had the highest strain readings of 8135 and 8153 micro in./in., respectively. Gage 18 on the bottom side of the panel (composites) had the highest composite reading. The failure of this panel was similar to that of Panel LA1-1-2$_1$, at the top; the titanium buckled and the composite cracked on the back face.

Another panel tested at room temperature was Panel LA1-5-2$_2$, a 5.0- by 12-inch panel, which used an adhesive process, 2175, (cured at 265°F for four hours with a pressure of 37 psi). Six shims of 0.001 inches thick were used at each end to better distribute the axial end loading into the panel. The test results are presented in Table 1.53 and Figure 1.57. The strains in the composite inner sandwich sheet at the bottom Gages 14, 16, and 18, showed high values of 7958 micro in./in., 8042 micro in./in., and 9528 micro in./in., respectively.

Both the composite side and the titanium side failed by bowing away at the bottom. It is difficult to know which side failed first. Preliminary analysis indicates the high value of 9528 micro in./in., for the carbon/epoxy cloth and/or the fiberglass cloth, would cause yielding and/or failure. Yielding or failure of the composite side would then cause the adhesive (at the titanium face) to fail, and allow the titanium sheet to buckle without any early warning.

The above results were compared with that of an earlier panel specimen $11E_2$ tested at room temperature, 4.5 by 11.0 inches long, with perforated holes that were 0.004 inches wide and 0.008 inches long and 0.05 inches on center. The average axial loading per inch of width was 7333 lb/in. versus 8000 lb/in. for Specimen $LA1-5-2_2$. The maximum strain readings were 15 to 29 percent higher for Specimen $LA1-5-2_2$ than $11E_2$. This can be accounted for by the better cure cycle, 2175 versus 2174, and the longer (1 hour versus 1/2 hour) priming cycle for the $LA1-5-2_2$ configuration.

The slot-type perforated holes may also have contributed to the lower maximum strains achieved by the $11E_2$ configuration. The 0.004 wide holes at 0.050 spacing reduced the area by eight percent. Much smaller holes, with a diameter of 0.0025, were used for the later test panels.

5.2.10 <u>Long (8- by 20-inch) Compression Panel Test of Configuration LA1-3-2,</u> <u>Tested at Room Temperature</u>: This panel, identified as Specimen LA1-3-2, was similar in construction details to Panel LA1-1, shown in Figure 1.55. The strain gage readings for preliminary and final loadings are shown in Tables 1.56, 1.59 and 1.58. The maximum load at failure was 70,000 pounds which is equivalent to 8750 pounds per inch. The analysis for simply supported elements shows a strength of 7188 lb/in., Table 1.54, and a strain of 8044 micro in./in. Another analysis, using full fixity at the ends of the elements, shows a failure of the webs at 14,854 lb/in. and a strain of 16,623 micro in./in., (Table 1.55). However, this was an elastic element analysis

63

and should be cut off at the strain that causes compression yielding. This cutoff is obtained from Reference 4, at Fc_y = 120,000 psi, for 6Al-4V annealed titanium. Dividing by the modulus for titanium of 16.1 x 10^6 psi, a maximum strain of 7453 micro in./in. results. The actual maximum strain in the titanium, from the test, was 6685 micro in./in., see Table 1.58, at Gage Number 3, which is in the middle of the top three gages, as shown in Figure 1.56. Extrapolating the strain in proportion to the failure load, of 70,000 pounds, a strain of 70,000/65,000 x 6685 = 7199 micro in./in. results. This value is 3.5 percent less than the failure yield strain from Reference 4.

The maximum strain level achieved in the test panel is 11 percent less than the theoretical simply supported "average" strain of 8044 micro in./in. based on the web buckling mode, Table 1.54. As already described, the actual panel had a maximum load level of 8750 lb/in. which was 22 percent higher than the value of 7188 lb/in. from the analysis, for buckling of the web. The actual web has more fixity than the "simply supported" web used in the analysis, and did not appear to fail first. The additional end moment due to fixity at the panel ends, may have induced the failure, and resulted in a four percent higher strain of 6685 micro in./in. at the top (Gage 3) compared to 6407 micro in./in. at the middle of the panel (Gage 7), equivalent to 6407 x 70,000/65,000 = 6900 micro in./in. at failure. The simply supported condition used for analysis was more representative than full fixity, and should be used for panel elements. An assumption of full fixity elements would yield unconservative analytical values.

If the average strain at the top of panel Gages 1 and 2, 3 and 4, and 5 and 6 were calculated; (6482 + 9321) x 1/2 = 7902, (6685 + 6871) x 1/2 = 6778, (6582 + 10,984) x 1/2 = 8783; (7902 + 6778 + 8783) x 1/3 = 7821 and multiplied by 70,000/65,000, this resulted in an "average" maximum strain of 8423 micro in./in. This test value average was five percent higher than the average analyses strain of 8044 micro in./in. using simply supported elements.

The actual test failure occurred in three places. Near the top, the titanium sheet bowed away from the substructure - opposite this, on the composite side, a crack occurred across the panel. A crack also occurred on the composite side at the bottom of the panel.

It is significant that the failures occurred near the ends. The average strain of the Gages 7, 8, 9, 10, 11, and 12, at the center of the panel was 6316 micro in./in., which was much lower than the 7.821 micro in./in. average strain of Gages 1 to 6 at the top and the 6722 micro in./in. average strain of Gages 13 to 18 at the bottom. The average top and bottom strain was 7272 micro in./in. which was 15 percent higher than the average strain at the center. The end strains caused the failure due to the end fixing moment.

Based on previous panel testing at DAC, the 20-inch panel length is equivalent to a rib spacing of 20 divided by 3.55/2.0 = 1.332, which is a rib spacing of 15.1 inches. The estimated value of the end fixity is 3.55 due to the potted ends that are machined square where the load is applied by the test machine, whereas 2.0 is the value of the fixation that would occur with rib supports. Thus, although the panel condition between ribs is represented, the end fixation outside the bay is too high. Failure then occurs outside this bay, near the panel ends, giving a conservative test result. More representative simulation of the panel and ribs is more complicated. It requires almost twice the panel length, and the addition of representative ribs and supports.

It would be necessary to duplicate two bays (one on each side of the center rib), and the axial load would need to be applied far enough away from the end ribs to avoid affecting the fixity at the ribs. This would have resulted in higher material and fabrication costs compared to the method of potting the ends of a 20-inch panel to get a 15-inch effective length. However, the increased fixity at the ends results in a 15 percent stress increase at the ends which can be treated as a margin of safety, or can be accounted for in the final design.

Figures 1.58, 1.59, and 1.60 are photographs of two small (3- by 3-inch) Panels A1-6 and A1-7, the LA1-3-2 (8- by 20-inch) panel, after test, and the two (4 1/2- by 10-inch) Panels LA1-1-2$_2$ and La1-1-2$_1$, after test. Figure 1.58 shows the titanium face, Figure 1.59 shows the composite face, and Figure 1.60 shows the side of all the panels and the titanium faces. Notice in Figure 1.58 that the titanium bows at the top right of the large panel, and that in Figure 1.59 a crack runs across the panel at both top and bottom.

5.2.11 Compression Tests on 3- by 3-inch Panels at Elevated Temperature (+160'F) and Cold (-65'F) Conditions: Table 1.59 shows the results of short compression tests of Specimens A1-5, A1-6, A1-7 and A1-8. All these specimens were of the LA1-1 configuration shown in Figure 1.55. The previous room temperature tests, A1-1, A1-2, A1-3, and A1-4, shown in Table 1.9, had an average ultimate load of 29,250 pounds. The composite side average strain was 6174 micro in./in., and the titanium side average strain was 8193 micro in./in. for the four A1-1 to A1-4 specimens.

For A1-5 and A1-6 the average hot (+160°F) test load ultimate was 17,250 pounds, which was only 59 percent of the room temperature average failing load. The average maximum strain of the composite face was -4740 micro in./in., which was 77 percent of the average room temperature failure strain. On the titanium face, the average maximum strain of 4696 micro in./in. was only 57.3 percent of the average 8193 micro in./in. strain of the titanium face at room temperature. This 42.7 percent reduction was larger than expected. The adhesive failure was at the junction of the fiberglass cap to the fiberglass pad on the titanium side.

The adhesives failed first in both the hot and cold tests. Typical overlap shear (psi) values at -67°F and 180°F for a 350°F cure (for 60 minutes at 150 psi) were shown in Table 1.17. The 180°F overlap shear of 2850 divided by the room temperature value of 3700, was 77 percent. The -67°F value was 73 percent of the room temperature

value. There was previously from Table 1.17 only 23 percent reduction for hot conditions, versus an average of 41 percent for the hot (+160°F) small panel test results. For cold conditions, using an average of 15,000 pounds divided by 29,250 pounds, which equals 51.3 percent for the actual cold (-65°F) test, was a 48.7 percent reduction. These strength reductions were significantly more than in Table 1.17 (by a factor of almost two).

The room temperature average strain of 8193 micro in./in., for Al-1 to Al-4 from Table 1.9, on the titanium side, (which is approximately at 131,907 psi) is much more than the required 4500 micro in./in. that a typical subsonic transport wing (i.e. DC-9) will undergo at ultimate loading. Therefore, this value was considered adequate to provide a margin of safety for hot and cold conditions, scale-up eccentricity, and thermal bowing of the larger panels and joints. However, the large reductions for hot and cold conditions resulted in an average of only 4740 micro in./in. for the composite side, and 4696 micro in./in. for the titanium side. The development of better adhesive characteristics, as discussed in sections 4.3 and 4.4 was therefore needed.

5.2.12 Compression Testing of 3- by 3-inch Panel Specimens, Using the Final Selected Cure Cycles, at Room Temperature, Dry, Wet, Hot, and Cold: Before the panels were cut to the 3- by 3-inch panels, they were measured for warpage. Figure 1.61 shows how the chordwise warpage was measured, and a typical result. Any waviness between the center lines of the numbered flutes can also be measured in addition to any overall panel bowing.

Fifteen 3- by 3-inch panel specimens with perforated titanium on one face were tested in compression at room temperature, dry, and wet, (after 24 hour soak), soaked and hot at +160°F, and soaked and cold at -65°F. These panels had the improved titanium bond to the

carbon/epoxy cloth and the "Ftc" cure, or the chosen "Gcf" bonding cure cycle. These selections were discussed in Sections 4.3 and 4.4. The test results verified that these selections significantly improved the strength of the larger panels.

The test results of the 3- by 3-inch panels were found to be very dependant on the edge support reinforcements. The recently developed increased shear strength of the bonding of the titanium to the pad, and the pad to the composite substructure, resulted in the 3- by 3-inch small panels holding together until the loads were high enough, prior to panel failure, for the titanium perforated sheet to cut through the aluminum foil, provided at the ends to distribute the end axial load. This relieved the load in the titanium sheet so that the load then crushed the fiberglass cloth webs and the fiberglass-carbon/epoxy cloth backing face of the sandwich. The crushed webs expanded sideways, causing a tension, peel, or bending failure of the bond to the titanium. This mode of failure was evident in the load versus head deflection.

When this problem was overcome by the addition of titanium and aluminum sheets at the ends, the titanium sustained load almost up to its compression yield strength (without any adhesive failure). This improvement was especially evident for the cold (-65°F) tests, which then sustained more load than the room temperature tests.

Sufficient test data on compression loads and strains, (from the 3- by 3-inch tests), throughout the temperature range, were obtained to provide an assurance that a scale-up to larger test panels could be made using the layup, design, and cure cycles developed.

The test conditions and test results for the fifteen 3- by 3-inch panels, with the "Ftc" cure cycle used for bonding the perforated titanium to the pad of outer sandwich face sheets of carbon/epoxy cloth, and the"Gcf" cure cycle for bonding the titanium and pad to the composite substructure are summarized in Figure 1.62. These

panels had perforated titanium sheet material on the outer surface. Previous tests of 3- by 3-inch panels with perforated titanium did not achieve anywhere near the results achieved in these tests. The better cure cycle and the increased edge supports accounted for the improvements. Note the chamfers at the corners to reduce loading of the stabilized edges.

A properly supported panel is one whose edges are supported so that no local buckling or eccentricity will cause the edge to fail first and cause premature failure of the main body of the panel. The last column of Figure 1.62 shows the methods used to avoid uneven loading due to machine interface tolerances. Four 0.001-inch aluminum foils were located between each loaded edge of the panel and the test apparatus for good load distribution.

Panels AA1, AA2, and AA3, tested at room temperature, showed good cohesive failure of the carbon cloth to the titanium. Table 1.13 and Table 1.20 showed that the highest room temperature lap shear strength was obtained with carbon/epoxy cloth bonded to the titanium sheet. Panels AA2 and AA3 showed carbon cohesive failure and titanium primer failure. The AA2 panel, Figure 1.63, showed that the top two flute caps had carbon cohesive cloth failures of the inner pad, and titanium primer cohesive failure at the bottom.

Notice that the web and composite edges have been crushed slightly. The titanium face sheet was observed to have cut through the aluminum foil because the load was sufficient to cause shear failure in the aluminum shims. Panel AA3, Figure 1.64, also showed two flute caps with carbon/epoxy cloth failure and one flute cap with a titanium primer failure. Notice that the web crushing was a little more severe than in Figure 1.63. The titanium also cut through the aluminum foil shims on the edge, crushing the web and causing the composite sandwich face sheet to be more highly loaded. The load versus head travel for AA4 and AA5 is shown in Figure 1.65. Notice that notches begin to form at about two-thirds of the peak load. A

0.02-inch 2024 aluminum plate was used instead of the aluminum foil for panel AA6, Figure 1.66. This reduced the notches slightly at the lower loads. For Panel AA7, at -65°F, a particularly large notch, occurred at about 80 percent of maximum load, see Figure 1.67. The strain gage readings, in Table 1.60, show that the titanium strain, which was usually more than the composites strain, was actually less than the composite strain starting at 16,000 pounds. The composites were, therefore, sustaining more load than the titanium face sheet, indicating that the composite substructure is peeling from the titanium sheet and the bond was failing in tension or bending, caused initially by penetration of the aluminum foil by the titanium sheet. A similar condition occurred for Panel AA8.

To correct the edge loading condition, a 0.025-inch titanium sheet was subsequently added at each edge in addition to the 0.020-inch aluminum sheet. With this arrangement, the titanium face sheet remained intact for the first time and did not cut through either the 0.025-inch titanium sheet or the 0.020-inch aluminum sheet. The failure then occurred at the much higher load of 47,700 pounds, see Figure 1.68 and Table 1.61. Notice in Figure 1.68 that up to 36,000 pounds the notches were very slight. Also, in Table 1.61, the titanium strain was higher than the composite strain up to 46,000 pounds.

Using the titanium sheet as an end shim has significantly helped to increase the loadings and failure strains for the 3- by 3-inch specimens with the stronger Ftc and Gcf cures. A photograph of the AA9 panel failure is shown in Figure 1.69. There appears to be a cohesive primer failure on the titanium and a cohesive failure of the AF31 adhesive between the pad and the flute cap. It was difficult to know which failed first.

Two smaller 2 1/2- by 3-inch panels were also tested using the aluminum and titanium end sheets. The AA14 panel had a premature failure of the titanium to the substructure at 14,000 pounds,

Table 1.61. Notice that the composites continued to support loads until 8920 micro in./in., Table 1.61, and 24,000 pounds. It also appears to be a cohesive failure of the primer on the titanium. The AA15 panel, which is similar to Panel AA14 in all respects, behaved very well, failing at 36,000 pounds, with the titanium strain at 11,816 micro in./in. and the composites strain at 9991 micro in./in. Figure 1.70 shows slight "notches" near the peak loads. For the -65°F condition, the MIL HDBK 5D showed a stress of 146,000 psi for 6AL-4V annealed titanium at this strain, (11,816 micro in./in.). This was a very high value and proves that the adhesives and cure cycles selected were strong enough to go to the full failure strengths of the materials used, and the strain far exceeded the 4500 micro in./in. required for strain compatibility with the wing. However, as discussed later, approximately 50 percent margin must be provided to sustain the beam column effect of lateral loading and thermal loading.

With the success of testing the smaller 3- by 3-inch panels, especially for the hot and cold conditions, further scale-up to larger panels was initiated.

5.2.13   <u>Testing of Four Large Panels</u>: Four large panels, described in Table 1.62 and shown together in Figure 1.71, have been tested and the results verify that the structural design concepts used will be more than adequate for a hybrid laminar flow leading edge structure that is planned to be attached to a typical aluminum wing of a commercial transport.

The four panels tested indicated that the design was more than adequate to meet all strength requirements. Additional analyses showed that the panel design achieved sufficient maximum failure loadings and strains to be able to sustain the additional lateral pressures and thermal deflections for the required design conditions at -65°F and +160°F.

The required axial static strength loading per inch for a 4500 micro in./in. strain (at the ultimate load factor of 3.75g for a transport aircraft) is 3721.6 pounds per inch for the selected design concept. The designs tested, at an equivalent rib spacing of 15 inches, achieved 6336 pounds per inch minimum (at +160°F), Table 1.62, which is 70 percent higher than required. When the panels were analytically deformed, for lateral loadings and thermal deflections, and then treated as a beam-column with the initial calculated bowing, the panel design was found to be more than adequate.

The first panel, identified in Figure 1.71 as LA1-14P, starting from the left, was 10-inch wide and 27-inch long. In the center of the panel, two aluminum angles were bonded to the panel and then wrapped with fiberglass cloth. A plate of aluminum was bolted between the angles and a universal joint was mounted in the hole in the plate. This universal joint was to allow angular rotation of the panel at the central support. The side support plate with its attachment pin can be seen in the foreground, at the bottom of the photograph, Figure 1.71. This plate was clamped at the other end, to support beams, as shown in Figure 1.72. Notice the dial gages shown in Figure 1.73. The panel on the extreme right, in Figure 1.71, Panel LA1-11-2P, was 10 inches wide and 20 inches long. The next panel, second from the left in Figure 1.71, Panel LA1-12-2P, was 7 inches wide and 15 inches long. All the above three panels have the end and edges locally reinforced with 70 percent aluminum fill in epoxy. This was to prevent the edges of the titanium and composite sheets from buckling locally at the extremities, particularly if the load is applied unequally distributed at the ends due to the panel being machined "out of square". The end aluminum and titanium shims also help to redistribute the load.

The white cap shown on the third panel from the left, in Figure 1.71, Panel LA1-12-1P, has ceramic powder in a mixture called "Sauereisen" to help distribute the end and edge loads. This ceramic filler has a low coefficient of expansion and therefore will not expand enough,

when heated to the +160°F condition, to cause additional stresses. A fifth large panel, LA1-3-2, which was 8 inches wide and 20 inches long, had already been tested. This panel was the second one shown in Table 1.62 and was listed to show its room temperature values. It was fabricated using the "old" Cure Cycle "A" of 265°F for four hours with 37 psi pressure. This panel was tested at room temperature where the original adhesive properties are good.

The +160°F LA1-11-2P and LA1-12-1P panels, and the -65°F LA1-12-2P panel were tested in an environmental chamber box. Figure 1.74 shows the Panel LA1-11-2P, 10- by 20-inch, prior to test with all the strain gages on. The box behind the test panel, and the door with two hinges in the open position, can be seen. Figure 1.75 shows a close-up of this test set-up. Three "after failure" photographs of test Panel LA1-12-2P, tested at -65°F, and test panel LA1-12-1P, tested at +160°F, are shown in Figures 1.76, 1.77, and 1.78. Figure 1.76 shows the titanium side of both panels. The LA1-12-2P titanium panel buckled at the end. Figure 1.78 shows that the titanium sheet separated from the pad, or the pad separated from the composite substructure. Figure 1.79 also shows a failure of Panel LA1-12-2P from a crack across the width of the composite side. The LA1-12-1P panel, in Figure 1.78, shows that the "Sauereisen" ceramic filler was unsatisfactory. It crumpled and caused separation of both the titanium sheet and the composite back-up sheet.

Close inspection revealed that for the LA1-12-2P panel, the composite failure was a cohesive failure of the carbon cloth. It is hard to know whether the carbon cloth failed first or the titanium separated from the composite substructure first. Table 1.62 shows that at -65°F the loading was very high at failure, 12,917 pounds per inch. The average titanium strain of 8626 micro in./in. results in over 134,000 psi for the titanium using the stress strain curves from MIL HDBK 5D. Therefore, the adhesive almost held up to the yield strength of the titanium material.

73

Starting with the strain requirement of 4500 micro in./in. for an aluminum aircraft, the corresponding loading for a composite sandwich panel with a titanium porous outer skin was 3721.6 pounds per inch, using the computer output of EA/in. = 827,018 from Table 1.8, and Young's formula P/AE = $\mathcal{E}$. The lowest load at failure was 6336 pounds per inch at +160°F, from Table 1.62, which is 1.70 times what is required to meet the 4500 micro in./in. axial requirement.

To account for the lateral loading, any thermal bowing, and the amplification of the bowing due to the beam-column effect, the computer output for mid-way between fully fixed and simply supported conditions, with a magnification factor of $\mathcal{OC}$ = 0.3, yields 0.032-inch mid-bay deflection, using the data from Table 1.14 reduced proportionately to the latest pressure information. Adding the thermal deflection for a thermal gradient from the cure temperature of 300°F to a -65°F condition (ΔT = 365°F) yields an additional 0.00051 inches for a total of 0.0325 inches of deflection.

The data in Figure 1.79, from Page 366 of Reference 5, shows that with the initial eccentricity = 0.0325 inches and K = 0.25864, the a/k value is 0.1237 and the B value is 0.9485, which results in an Fc/Fmax of 0.71. The Pc/A divided by Pmax/A is also 0.71. The allowable Pc/in. with initial eccentricity is reduced to 0.71 x 6336 lb/in. = 4498.6 lb/in. The allowable ratio of 4498.6/3721.6 = 1.21, which indicates a panel loading 21 percent more than that at 4500 micro in./in. (or 1.21g x 3.75g = 4.35g), for an equivalent 15-inch rib spacing at +160°F. Actually, the +160°F condition, which results in the lowest strength in Table 1.62, is only likely to occur during takeoff in a hot desert. When the aircraft is airborne it cools significantly, and when it reaches cruise altitude ambient conditions are closer to the -65°F condition which has a much higher allowable, for example, 12,917 pounds per inch, see Table 1.62. Therefore, for all practical purposes, the bending and thermal deflections reduce the allowable loading by 29 percent. The hot (+160°F) condition would have a margin of safety of 21 percent.

However, the -65°F condition, (which compares with a -48°F, 30,000-foot cruise altitude condition), where the laminar flow control is on most of the time, has a 12,917 pounds per inch allowable. Using the 71 percent factor results in a 9171 lb/in. allowable. Then, the margin of safety, at the ultimate condition, is (9171/3721.6 - 1) which equals 1.46, or 146 percent. Therefore, the margin of safety varies between 21 percent for an unlikely "hot" condition, to 146 percent for the more likely "cold" condition.

The optimum rib spacing was selected as 15 inches. This is consistent with the 21 percent margin of safety.

Increasing the B value, which is 0.97, to an Fc/Fmax = 0.71/1.21 = 0.587 would result in a B value of 1.13, see Figure 1.79. Then the L value, rib spacing, would be 1.13 x 15 = 17 inches, if the a/k value remained at 0.1237. However, with a 17-inch rib spacing, the deflection at the mid-bay would increase as the cube of the rib spacing. Therefore, the "a" value would increase by $(17/15)^3$ = 1.46. This would then yield an a/k value of 0.18. Using 0.18 for a/k, and going down, parallel, to the 0.2 value of a/k in Figure 1.79, until Fc/Fmax of 0.587 is obtained, the B value of 1.10 was obtained. This gives a revised rib spacing of 1.10 x 15 = 16.5 inches. Therefore, for the hot (+160°F) condition, the margin of safety of 21 percent could be reduced to zero by increasing the rib spacing to 16.5 inches.

However, since only a small number of panels were tested, and there is a relatively wide variations in shear values obtained for the materials and adhesive strengths, a 21 percent margin of safety was retained. Therefore, a 15-inch rib spacing would be recommended until further testing. A flight panel would have some curvature which should allow a rib spacing greater than 16.5 inches, provided that a fully representative nose section were tested.

The work done in this task verifies that a feasible structural concept is available for a flight demonstration model.

Before a production model is initiated, chordwise and spanwise joints to meet the structural and aerodynamic requirements and provide for interchangeability must be developed. Fatigue and damage tolerance testing for at least a 60,000-hour aircraft operating life are also necessary. See Section 3.2 for further details of recommendations.

6.0 CONCLUSIONS AND RECOMMENDATIONS

6.1 CONCLUSIONS

6.1.1 A low-cost suction panel for laminar flow control can be fabricated using a perforated titanium sheet as the outer face sheet of an efficient sandwich structure, with fiberglass cloth and carbon/epoxy cloth used to form the active (suction) and inactive core flutes and inner face of the sandwich.

6.1.2 It is possible to design the panel so that the perforated titanium outer sheet is sufficiently supported by the composite substructure for failure in compression to occur at higher than 4500 micro in./in., and for the panel waviness at 1.5g to be within the designated limits to avoid causing transition to turbulence.

6.1.3 The test results with the small 3- by 3- inch panels proved the success of the adhesive bonding and short column strength and strain capacity of the panel, at room temperature, +160°F, and -65°F conditions.

6.1.4 The 4- by 10-inch test panels gave additional data on the ability of a longer column to sustain compression strain. The data correlated well with the analytical program results using simply supported elements.

6.1.5 The next step, a one-bay, 8- by 20-inch panel, when tested with almost rigid ends, was equivalent to a 15-inch supporting rib pitch with a C=2 end fixity factor (continuous structure across the rib). This end fixity is usually sufficient to cause the strains to be 15 percent higher at the ends than at mid-bay. This is a good indication of the expected level of strain because slight eccentricity can easily cause increased strain at the panel ends.

6.1.6   This type of structure can be fabricated cheaply for test and demonstration programs and could be used on a production airplane. The basic fiberglass cloth that is formed into flutes is easily fabricated with rubber mandrels. The carbon/epoxy layers are used to balance thermal expansion and for added strength, rigidity, and for increased adhesive bond strength (especially the perforated titanium to the carbon/epoxy cloth). By using a few laminates of carbon/epoxy cloth at strategic locations, (i.e. - sandwich facings of the inner skin and sandwich pad), it is possible to build up a laminated substructure of composites that is low in cost, is thermally balanced, and has high resistance to compression. The carbon/epoxy cloth is of relatively high cost ($150 per pound versus $16 per pound for fiberglass cloth). Therefore, only the necessary amount of carbon/epoxy cloth is used.

6.1.7   The long two-bay 27-inch panel provided the closest representation of actual strains. The results indicated a sufficient margin of safety to allow for the additional eccentricity of a beam-column caused by the lateral pressure loading and any warpage from the thermal gradients. Therefore, the final panel design can be recommended for the next phase of flight testing and is structurally adequate for flight with induced compressive strain levels of 4500 micro in./in.

6.2   RECOMMENDATIONS

6.2.1   The lap shear tests of the AF31 adhesive were used to determine the best cure cycle. However, from the high magnification photographs, it was obvious that the degree of ductility at the interface influences the strength. The effects of fatigue, environmental factors, foreign object damage, and tension and bending in the adhesive over the operating temperature range could also influence the selection of the optimum cure cycle. Therefore, it is recommended that smooth fatigue lap shear tests, tension and bending tests, with and without notches and flaws, at room temperature, -65°F, and +160°F are desirable before using the design on a

commercial transport with a 60,000 hour life. These tests should be performed for the equivalent of 2 x 60,000 hours life before final selection of the materials and concepts are made for a production design.

6.2.2   Since the beam-column magnification of the lateral deflection from the end compression and lateral loading was found to be a strong factor, and was accounted for by analyses only, it would be prudent to test this effect. The lateral loads could be applied as tension pulloffs with the panel in the test rig used for the two-bay compression test. These lateral loads should be imposed separately on a hot (+160°F), a cold (-65°F), and a room temperature panel. This would require three two-bay test panels. The initial testing should be with flat panels to minimize cost. This could be followed by representative full scale leading edge curved panels tied to representative ribs and wing front spar, with the tension pulloffs perpendicular to the curved panel surface. Typical chordwise and spanwise joints should be included.

6.2.3   The analyses indicated that when each element is considered simply supported (pin-ended), it yields slightly conservative answers when compared to test panels that have almost complete rigid (C=4) panel ends due to their being potted and end-loaded with wide compression blocks. When the analyses were done using full fixity, they yielded unconservative results (the loads and strains obtained analytically were much higher than the test results). Therefore, revision of the analytical program, to provide various fixity values at the ends of each element would enable the analyst to input a design value of C=2 for the condition over a rib and C=4 for the ends in order to be more representative of test conditions. This is needed to analytically predict with more accuracy the critical design loads, stresses, and strains, based on test results.

6.2.4   The layup of the composite panels that were tested is very labor intensive. Possible design changes to reduce the labor and speed up the fabrication of the panels should be studied. These should include using SPF/DB titanium sandwich, or SPF aluminum substructure. The relative cost, weight, maintenance, and replacement in the field, should be considered.

6.2.5   The adhesive development accomplished in this program should be studied still further. Cure temperatures higher than 300°F with variations in time and pressure might result in significant additional improvements. The "G" cure cycle pressure was limited to 75 psi to prevent bowing of the flute webs. These webs could be redesigned if a cure cycle temperature higher than 300°F showed significant advantages. For example, carbon/epoxy cloth strips could be layed up in the webs to withstand the pressure loads at higher than 300°F without buckling the webs.

7.0   REFERENCES:

1. Timoshenko, S. - "Theory of Plates and Shells", McGraw-Hill Book Company, Inc., New York, 1940.

Other DAC reports that provided the base for this study;

1. NASA-CR-159252 - Evaluation of Laminar Flow Control Systems Concepts for Subsonic Commercial Transport Aircraft - Executive Summary, W. E. Pearce, DAC-ACEE-01-FR-2995, N83-17551, December 1982.

2. NASA-CR-159251 - Evaluation of Laminar Flow Control Systems for Subsonic Transport Aircraft, W. E. Pearce et. al., 86N28077, June 1983.

3. NASA-CR-172424 - Development of Laminar Flow Control Wing Surface Porous Structure, W. E. Pearce et. al., 84x10438, July 1984.

4. MIL-HDBK-5D - Military Standardization Handbook, Metallic Materials and Elements for Aeorspace Vehicle Structures, Department of Defense, Washington, D.C., 20025, June 1, 1983, Project No. 1560-0126.

5. Peery, D. J. - Aircraft Structures, McGraw-Hill Book Company, Inc., New York, Toronto, London, 1950.

6. NASA-CR-178006 - Final Report - Evaluation of Superplastic Forming and Co-Diffusion Bonding of Ti-6A1-4V Titanium Alloy for Supersonic Cruise Aircraft Research, Contract NASI-15527, J. E. Fischler et. al., December 1985.

LIST OF FIGURES

82

LIST OF FIGURES

LIST OF FIGURES

LIST OF TABLES

8.0 APPENDIX

Governing differential equation for the buckling of laminated composite panel is:

$$D_{11} \frac{\partial^4 w}{\partial x^4} + 2(D_{12} + 2D_{66}) \frac{\partial^4 w}{\partial x^2 \partial y^2} + D_{22} \frac{\partial^4 w}{\partial y^4} = N_x \frac{\partial^2 w}{\partial x^2} + N_{xy} \frac{\partial^2 w}{\partial x \partial y} \quad (1)$$

The above equation assumes that the composite laminates are symmetric and balance, i.e., Bij = D16 = D26 = 0.0.

Taking the deflection surface of the buckled panel or panel elements in the form of a double trigonometric series:

$$w = \sum_{m=1}^{\infty} \sum_{n=1}^{\infty} a_{mn} \sin \frac{m \pi x}{a} \sin \frac{n \pi y}{b} \quad (2)$$

Equation (2) satisfies the requirements of simple support boundary condition at all four edges. Solving for the Nx (assuming Nxy=0) of the general buckling Equation (1) gives:

$$N_{x_{CR}} = \frac{\pi^2}{a^2} \left[D_{11} m^2 + 2(D_{12} + 2D_{66})\left(\frac{a}{b}\right)^2 + D_{22} \frac{n^4}{m^2}\left(\frac{a}{b}\right)^4 \right]_{MIN} \quad (3)$$

Now it is a matter of defining flexural rigidities (D11, D12, D22, and D66) for the panel as a whole and for each element in the panel to obtain critical buckling load for the respective element.

Many instances in actual structure, boundary conditions may not necessarily be a perfectly simple support nor clamped, rather somewhere in between. The normal method to account for this discrepancy is to use fixity factor. J. H. Argyris recommended a fixity factor of 1.12 in his paper, "Flexure-Torsion Failure of Panels", and it seems to agree fairly well with test results. Thus, the fixity factor of 1.12 is used in calculating the critical buckling load of skin, base, cap, and web.

Each element has its own stiffness and critical buckling load, and they are related to the overall stiffness and to overall column load, Nx, of the panel. A method employed to relate these is a uniform strain method. Under uniform strain, the load carried by each element is related to overall load by ratio of element stiffness to the overall column stiffness. Similarly, the critical buckling load of each element can be normalized to column load by considering the ratio of stiffness between element and overall column.

In the case of critical shear buckling, due to the difficulty in getting close form solution, a numerical solution is used. The critical shear buckling of composite panel can be expressed as follows:

$$N_{xy_{CR}} = K_s \frac{\pi^2}{b^2} \sqrt[4]{D_{11} D_{22}^3} \quad FOR \quad D_{11} > D_{22} \tag{4}$$

$$N_{xy_{CR}} = K_s \frac{\pi^2}{b^2} \sqrt[4]{D_{11}^3 D_{22}} \quad FOR \quad D_{22} > D_{11} \tag{5}$$

The values of Ks can be obtained from curves in Figure 1.80. This plot is the result of finite difference analysis conducted by NASA on the orthotropic panels. For a computer application, this plot has been numerically input into a data file, and the values are read off from the data file by using double quadratic interpolation technique.

STIFFENER GEOMETRY
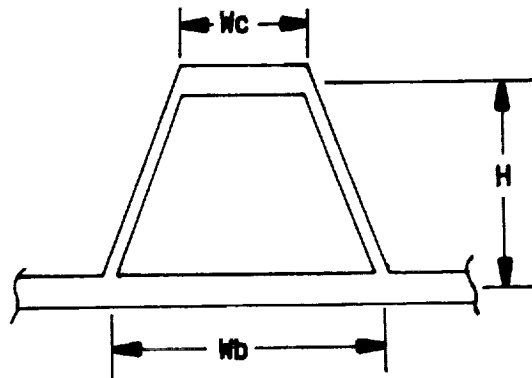
Wc = WIDTH OF CAP (IN.)
Wb = WIDTH OF BASE (IN.)
H = HEIGHT (DISTANCE FROM MIDDLE OF
     HAT CAP TO MIDDLE OF SKIN) (IN.)

PANEL GEOMETRY
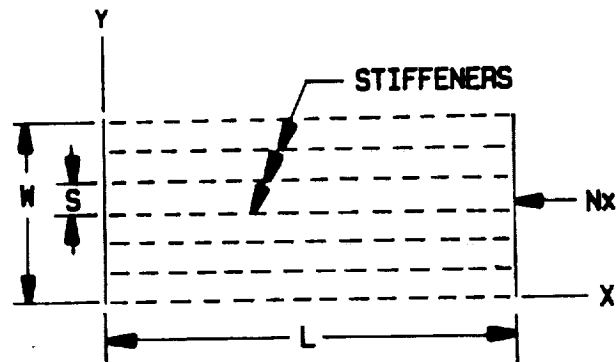
LENGTH (L) = 30 IN.
WIDTH (W) = 20 IN.
STIFFENER SPACING = S
PANEL LOADING = Nx LB/IN.

FIGURE 1.1 STIFFENER AND PANEL GEOMETRY FOR THE
ANALYTICAL MODEL
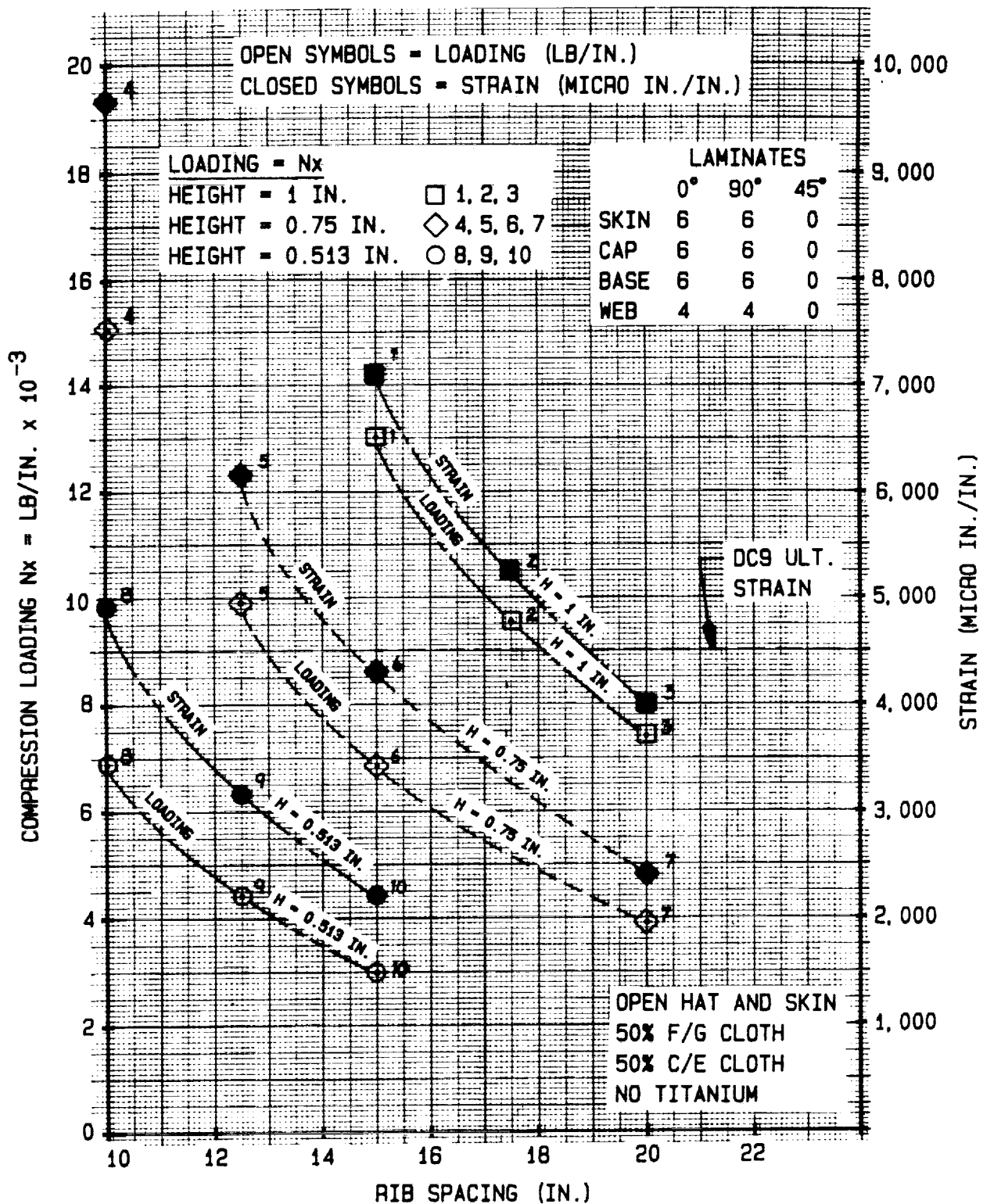
FIGURE 1.2 COMPRESSION LOADING AND STRAIN VERSUS RIB SPACING FOR VARIOUS PANEL HEIGHTS FOR OPEN HAT AND SKIN – COMPOSITES ONLY

C-2
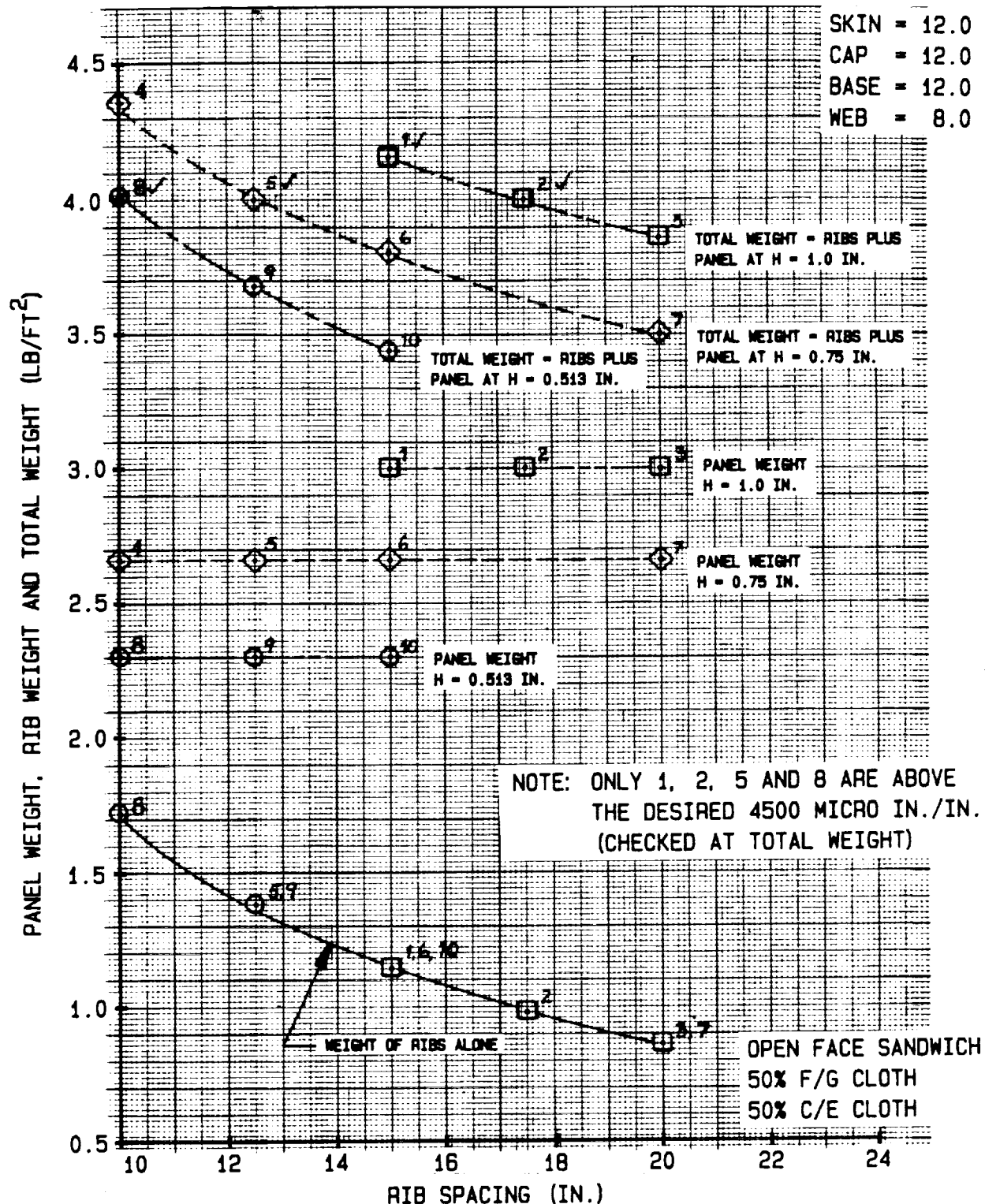
FIGURE 1.3 PANEL WEIGHT, RIB WEIGHT, AND TOTAL WEIGHT VERSUS
RIB SPACING FOR OPEN HAT AND SKIN — COMPOSITES ONLY

SEE TABLE 1.7 FOR DEFINITION OF CASE PARAMETERS
AND WEIGHTS FOR SELECTED CASES
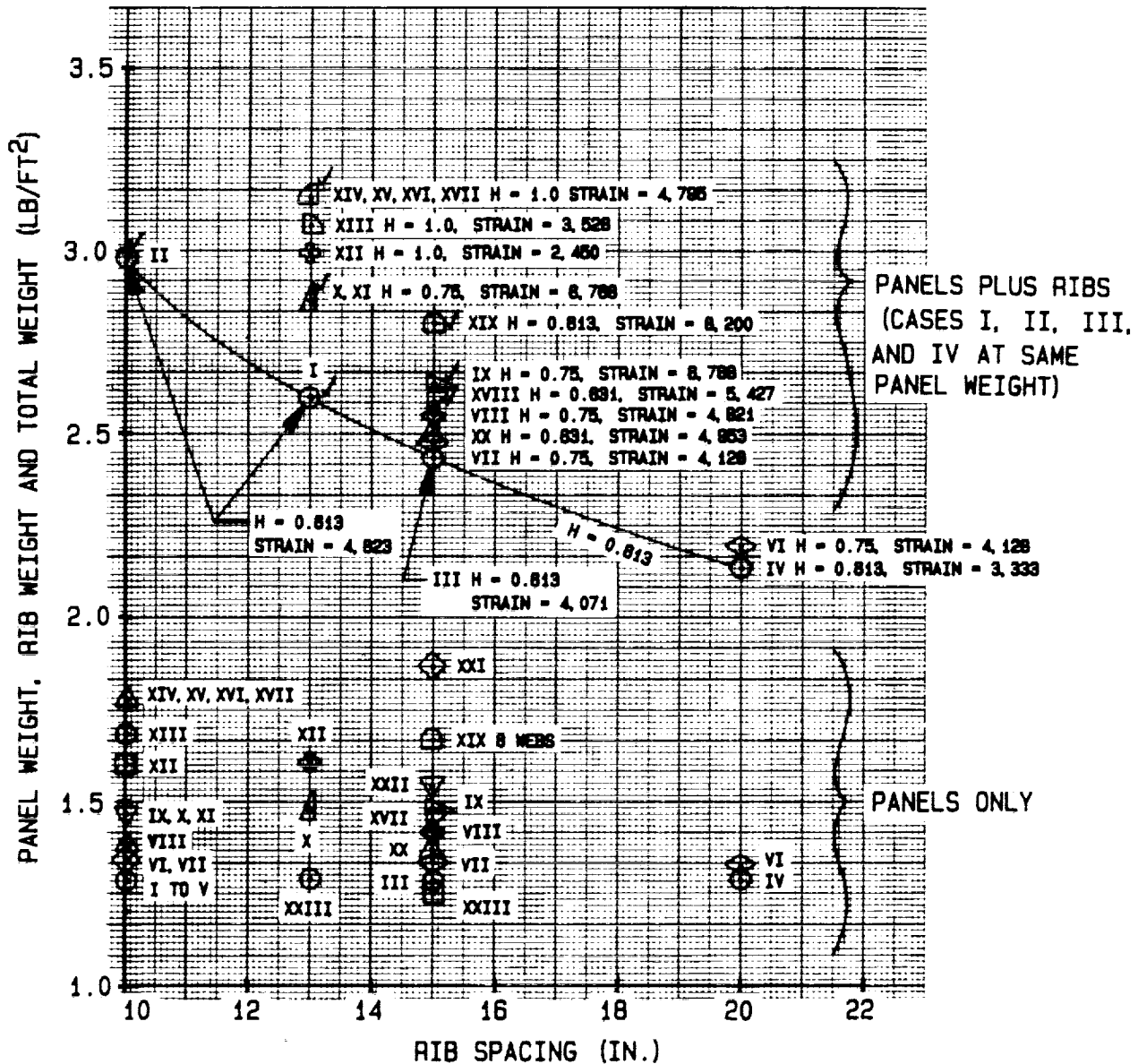
FIGURE 1.4 CLOSED SANDWICH PANEL WEIGHTS, RIB WEIGHTS, TOTAL
WEIGHTS, WITH STRAINS AND PANEL HEIGHTS NOTED FOR VARIOUS RIB
SPACINGS

94

C-2

CORRUGATED SANDWICH GEOMETRY
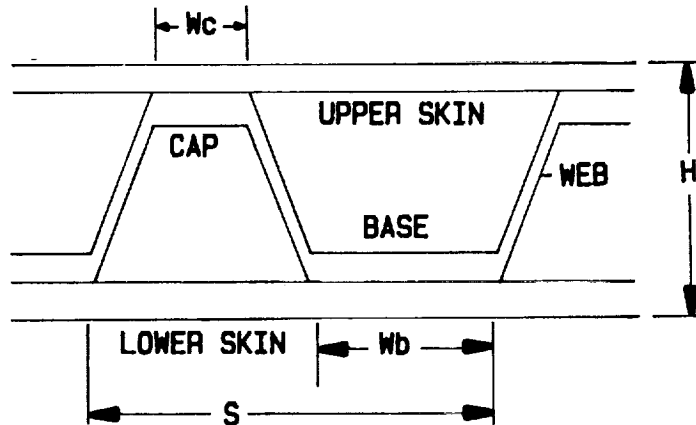
Wc = WIDTH OF CAP (IN.)
Wb = WIDTH OF BASE (IN.)
H = HEIGHT (IN.)
S = PITCH (IN.)

FIGURE 1.5 CORRUGATED SANDWICH GEOMETRY FOR
MIXED MATERIALS
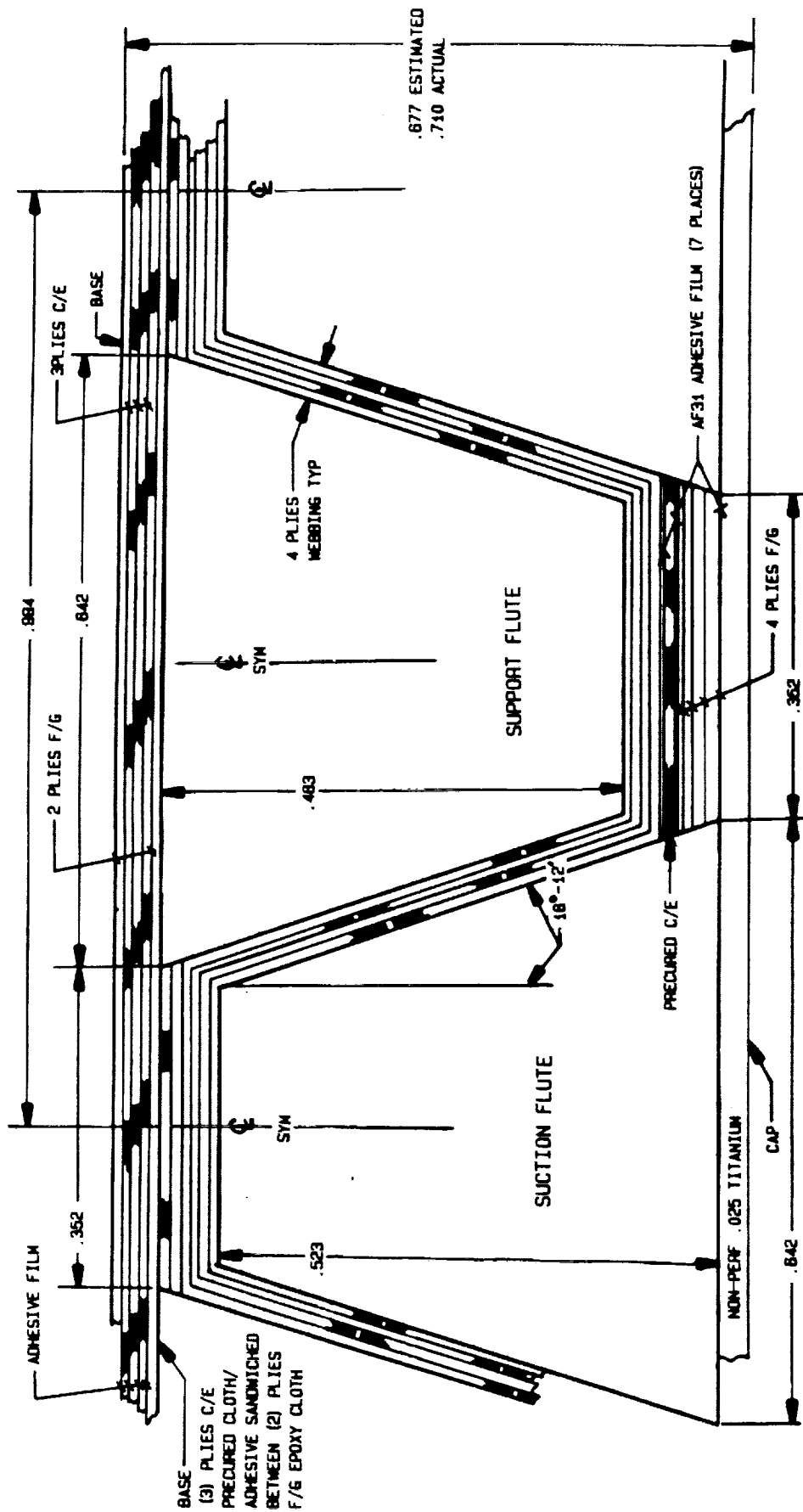
FIGURE 1.6 DETAILS OF PANELS WITH CONFIGURATION 13F

$13F_1$ = 30,000 LB ULT COMP STRENGTH
$13F_2$ = 27,000 LB ULT COMP STRENGTH

CLOSED SANDWICH

OPEN SYMBOLS = Nx (LOADING)
CLOSED SYMBOLS = STRAIN (MICRO IN./IN.)

SEE TABLE 1.7 FOR
DEFINITION OF CASE PARAMETERS
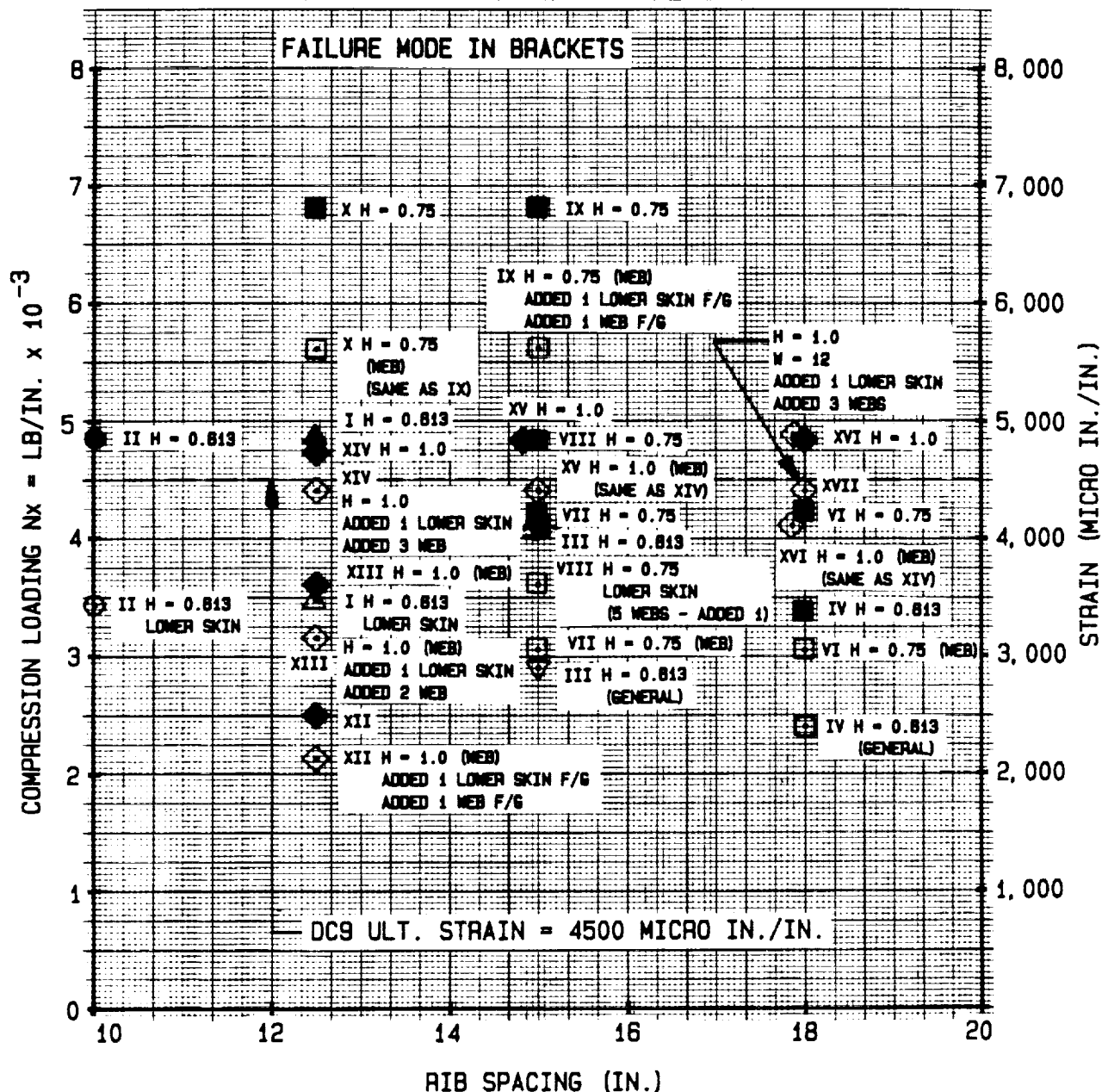
FIGURE 1.7 CLOSED SANDWICH LOADINGS, STRAINS, PANEL HEIGHTS,
AND RIB SPACING — CASES I TO XVII

CLOSED SANDWICH

OPEN SYMBOLS = Nx (LOADING)
CLOSED SYMBOLS = STRAIN (MICRO IN./IN.)
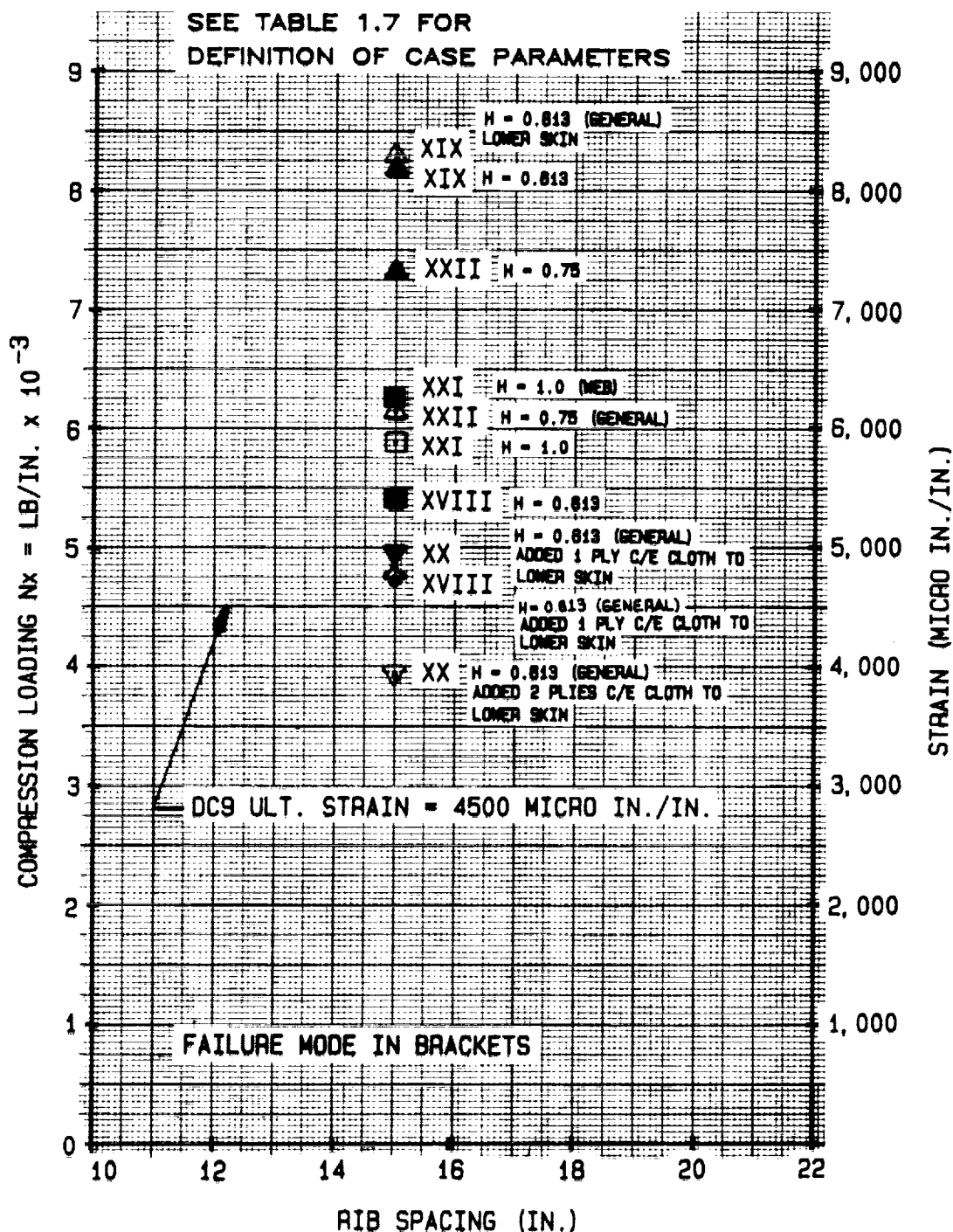
FIGURE 1.8 CLOSED SANDWICH LOADINGS, STRAINS, PANEL HEIGHTS,
AND RIB SPACING — CASES XVIII TO XXII

FIGURE 1.9 DETAILS OF PANELS WITH CONFIGURATION LA1-2

FIGURE 1.10 PANEL LA1-7, CROSS-SECTION DETAILS
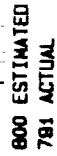
100
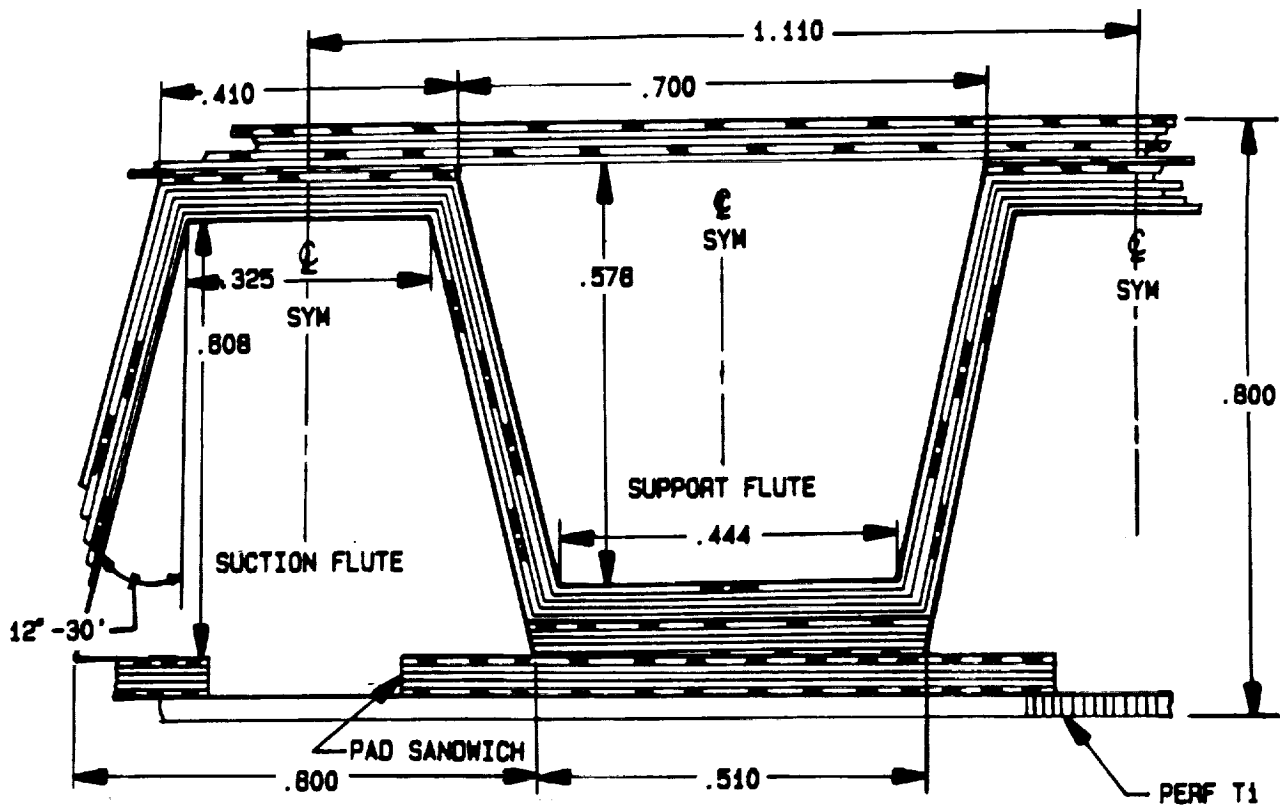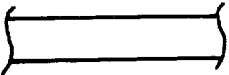
- T1 PHOSPHORIC ACID ANODIZED AND PRIMED PER LFC LAB OUTLINE (REV. C)

- F/G PLIES SHOWN THUS:

- C/E PLIES SHOWN THUS:

- ADHESIVE PLIES SHOWN THUS:

FIGURE 1.11 LAYUP OF PANEL LA1-11-1

101

LFC SURFACE WAVINESS TOLERANCE
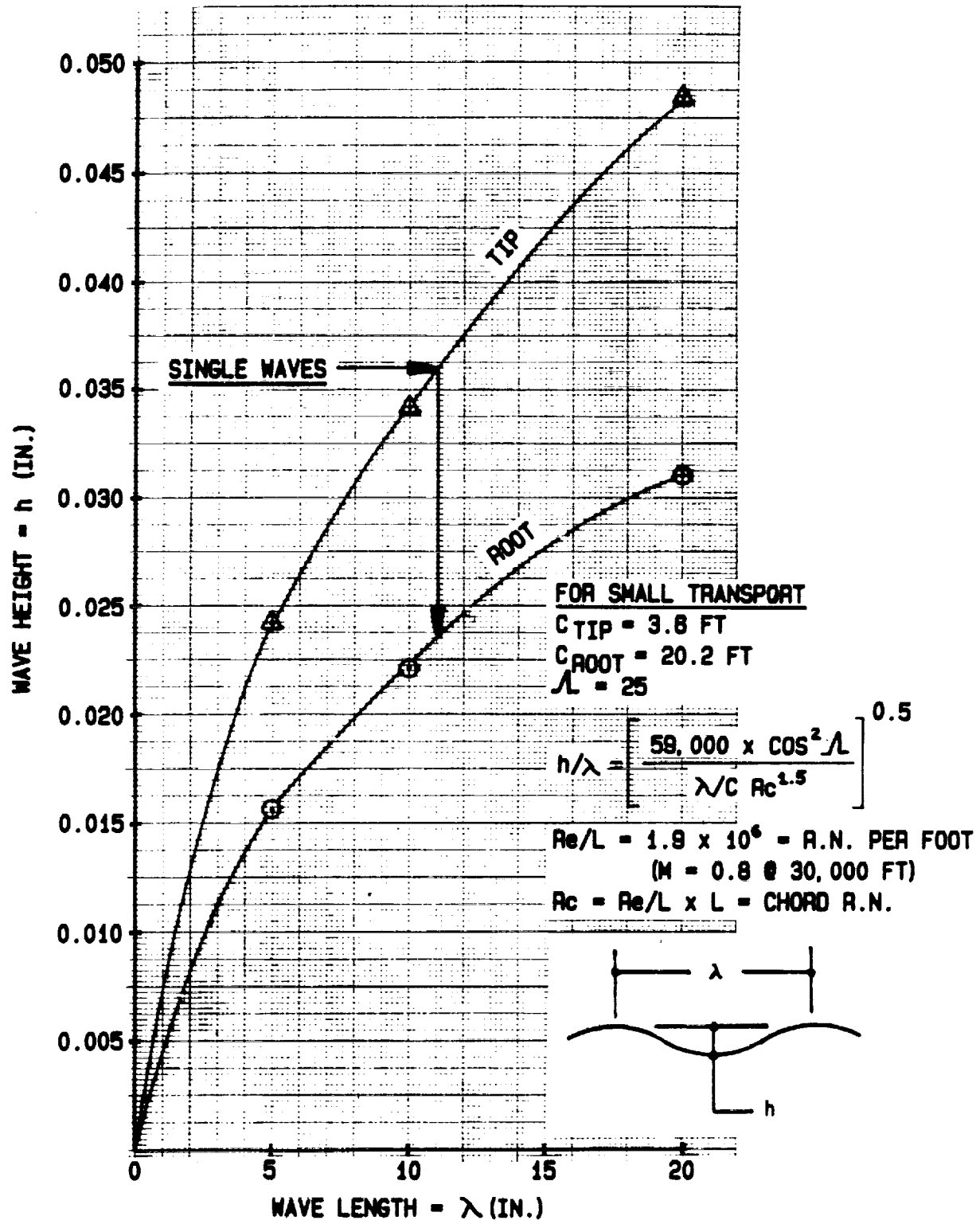
FIGURE 1.12 WAVE HEIGHT VERSUS WAVE LENGTH AT WING
TIP AND ROOT TO AVOID TURBULENCE

102

CHORDWISE SLOPE FOR LAMINAR FLOW VS PANEL WEIGHT AND
ALLOWABLE COMPRESSION LOADING AND PANEL HEIGHT
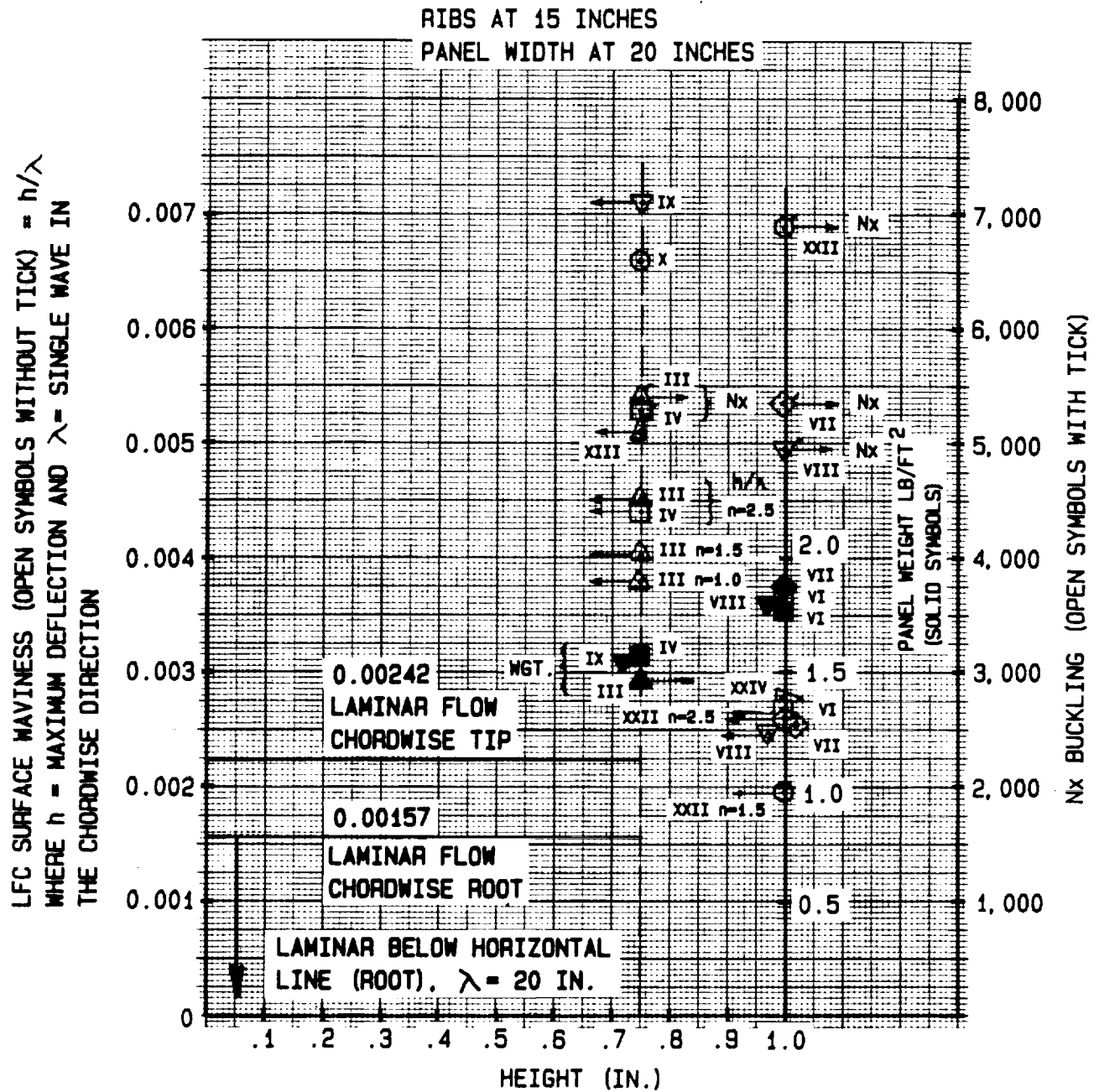
FIGURE 1.13 SURFACE WAVINESS FOR PANEL HEIGHTS OF 0.75
AND 1.0 INCHES
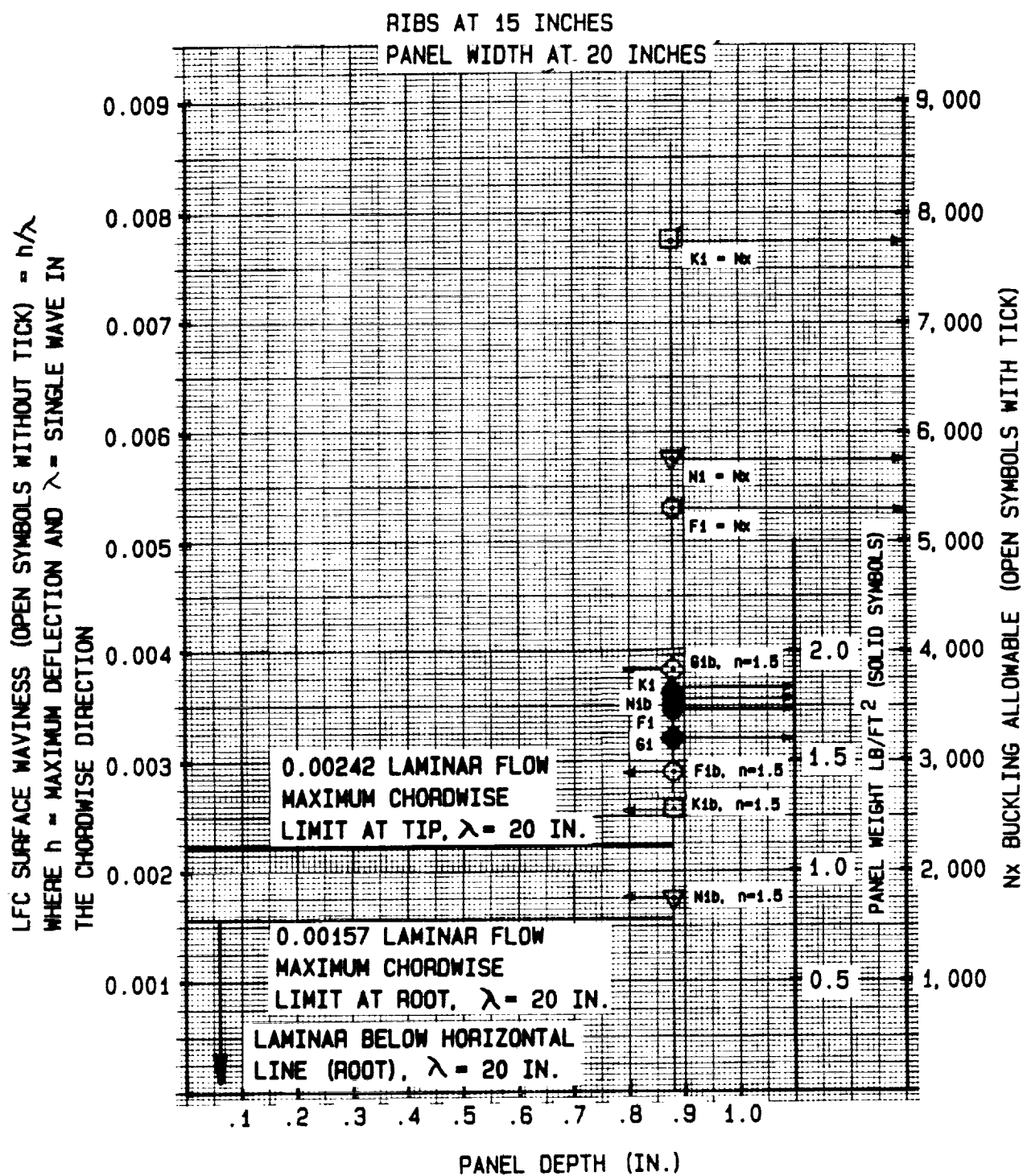
FIGURE 1.14 SURFACE WAVINESS FOR PANEL HEIGHT OF
0.875 INCHES
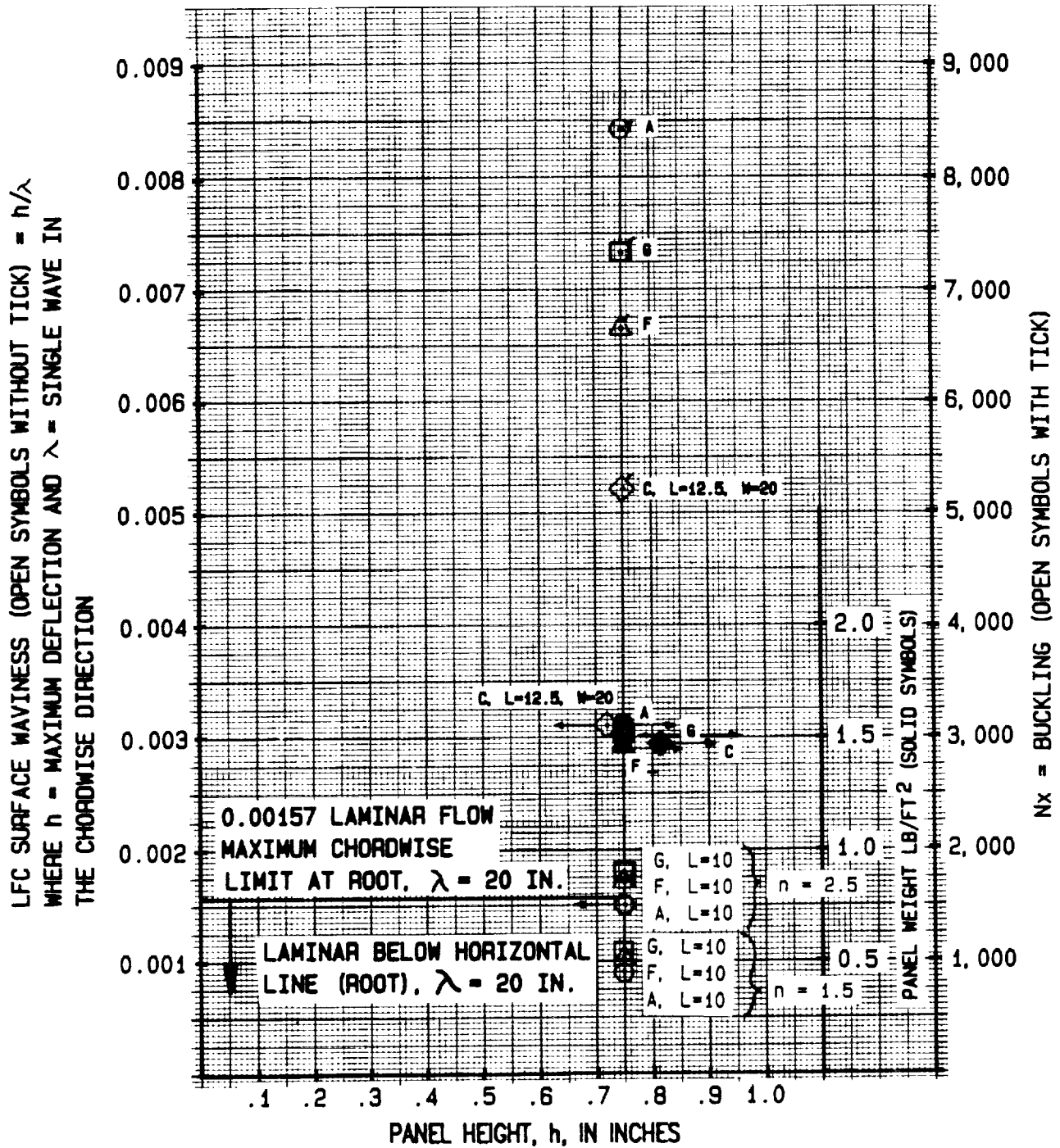
FIGURE 1.15 SURFACE WAVINESS FOR PANEL HEIGHT OF 0.75
INCHES AND COLUMN LENGTH OF 10 INCHES

LAYER #1   PERFORATED TITANIUM TAB
LAYER #2   PRIMER (EC2174)
LAYER #3   AF31 ADHESIVE
LAYER #4   PRIMER (EC2174)
LAYER #5   FIBERGLASS TAB (DMS 2127-8)

FIGURE 1.16 LAYER DESCRIPTION FOR TABLE 1.11 OF LAP
            SHEAR SPECIMEN FOR PERFORATED TITANIUM BONDED
            TO FIBERGLASS CLOTH
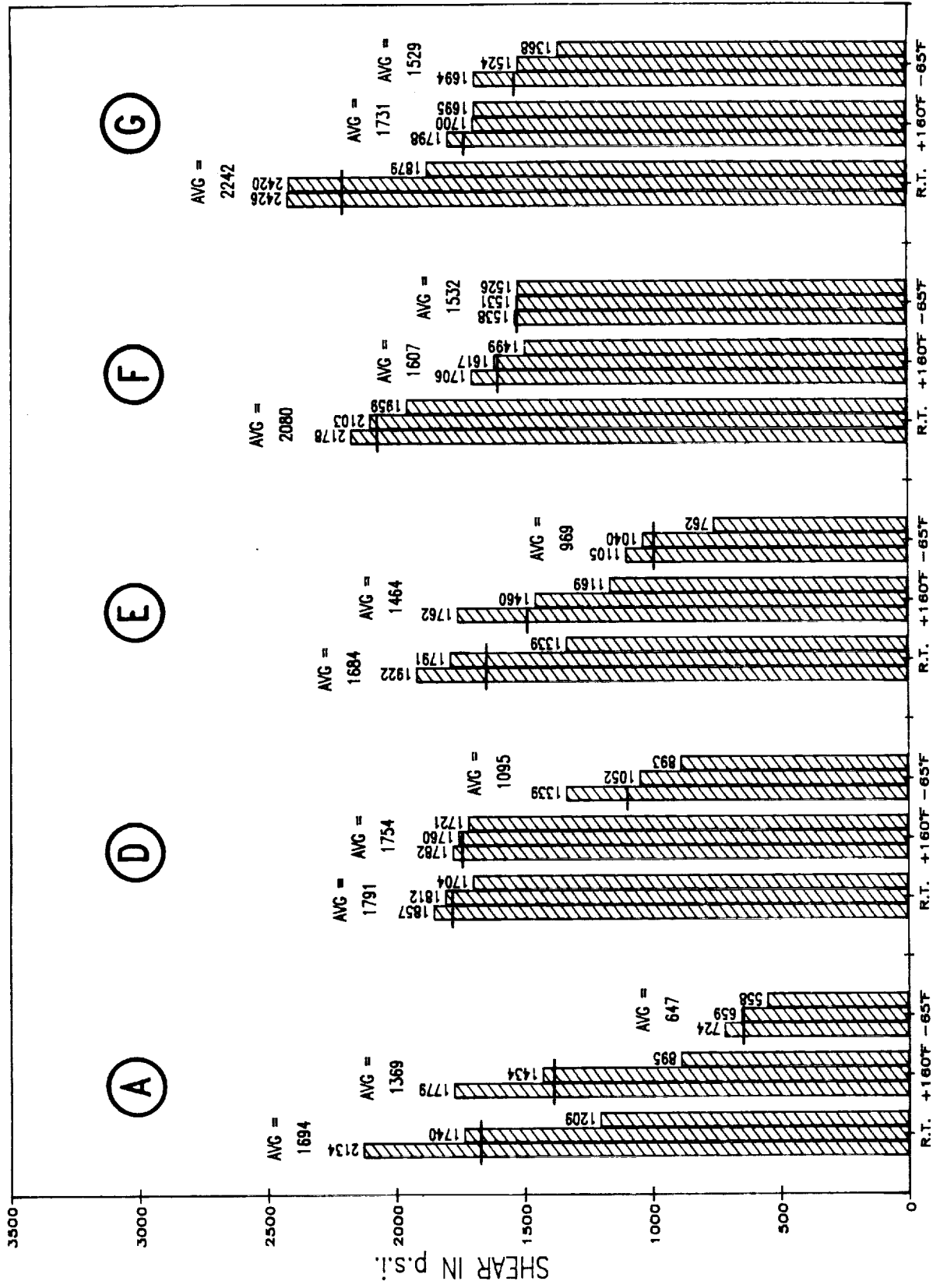
FIGURE 1.17 FIBERGLASS ADHESIVELY BONDED TO TITANIUM
WITH A, D, E, F, AND G CURES
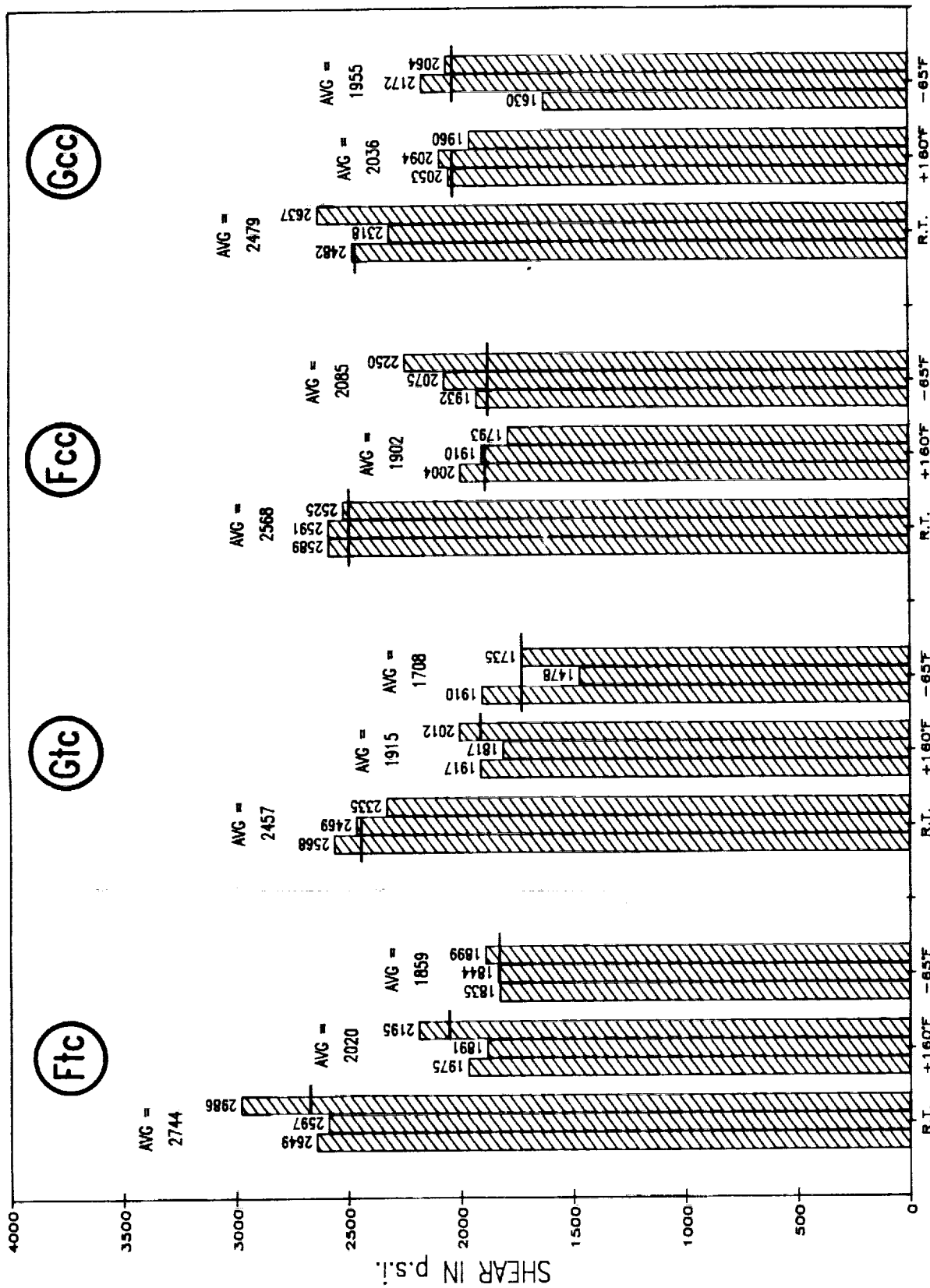
FIGURE 1.18 PERFORATED TITANIUM BONDED TO CARBON/EPOXY CLOTH
AND CARBON/EPOXY CLOTH BONDED TO CARBON/EPOXY CLOTH
WITH F AND G CURES
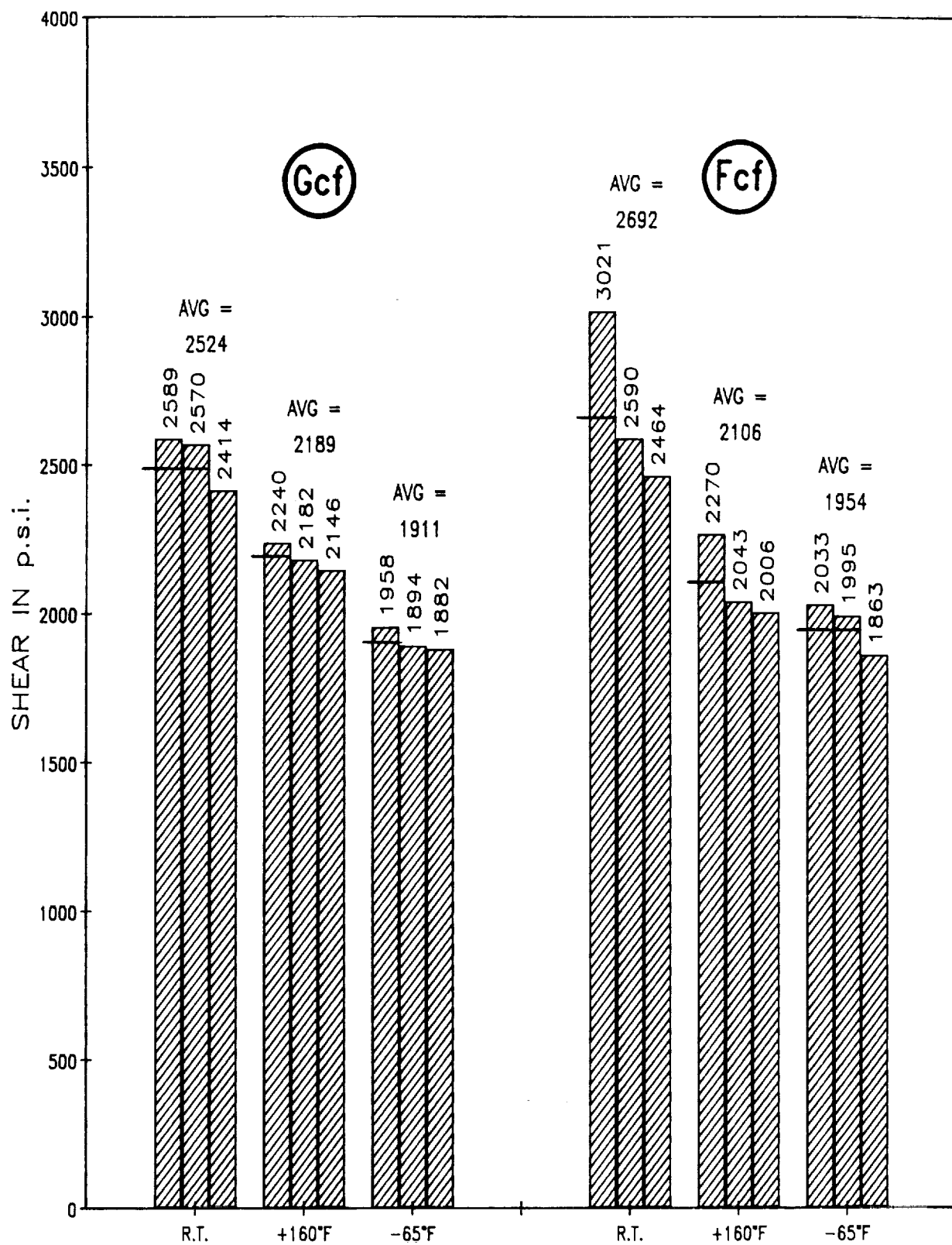
FIGURE 1.19 CARBON/EPOXY CLOTH ADHESIVELY BONDED TO
FIBERGLASS CLOTH WITH F AND G CURES
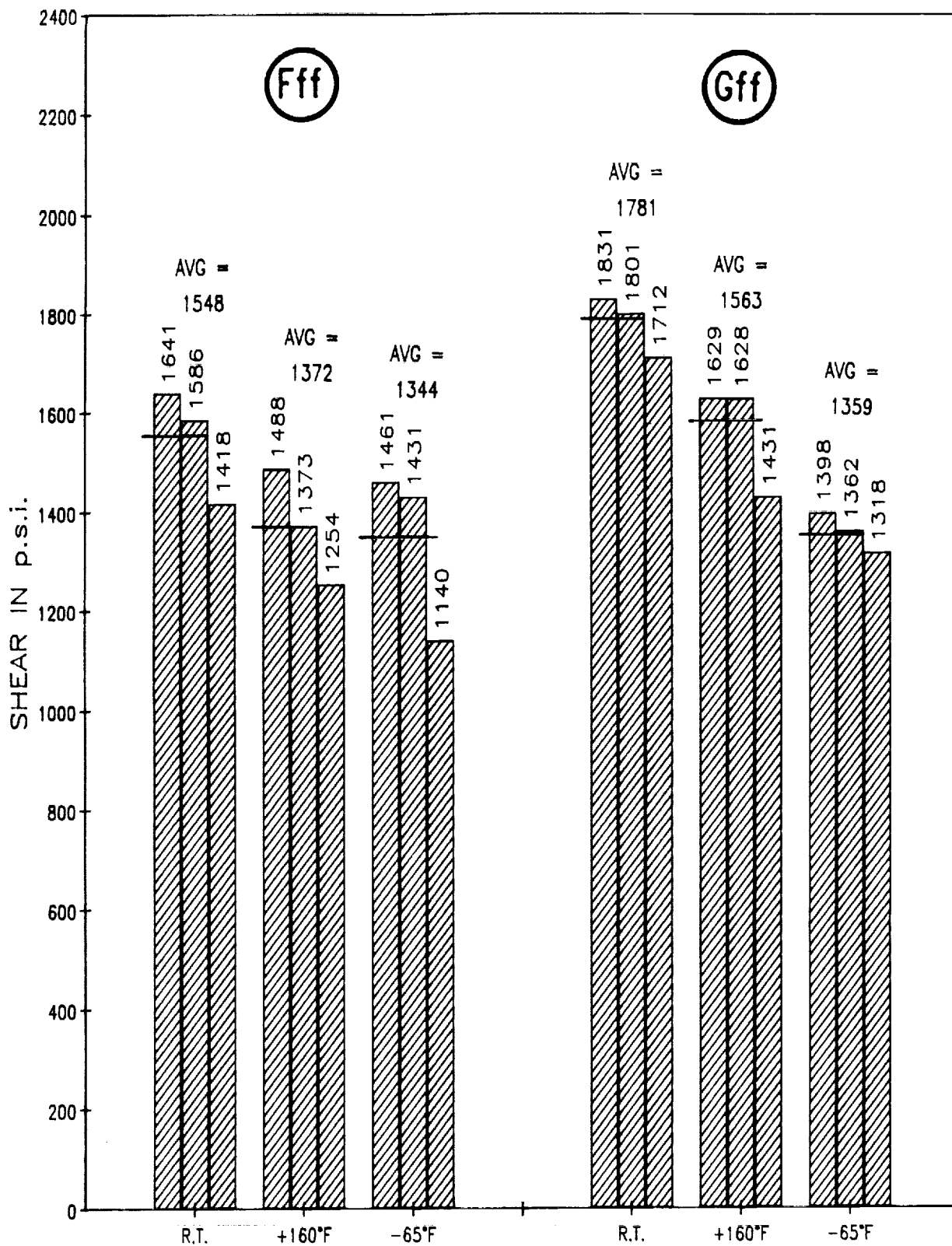
FIGURE 1.20 FIBERGLASS CLOTH ADHESIVELY BONDED TO
FIBERGLASS CLOTH WITH F AND G CURES

110
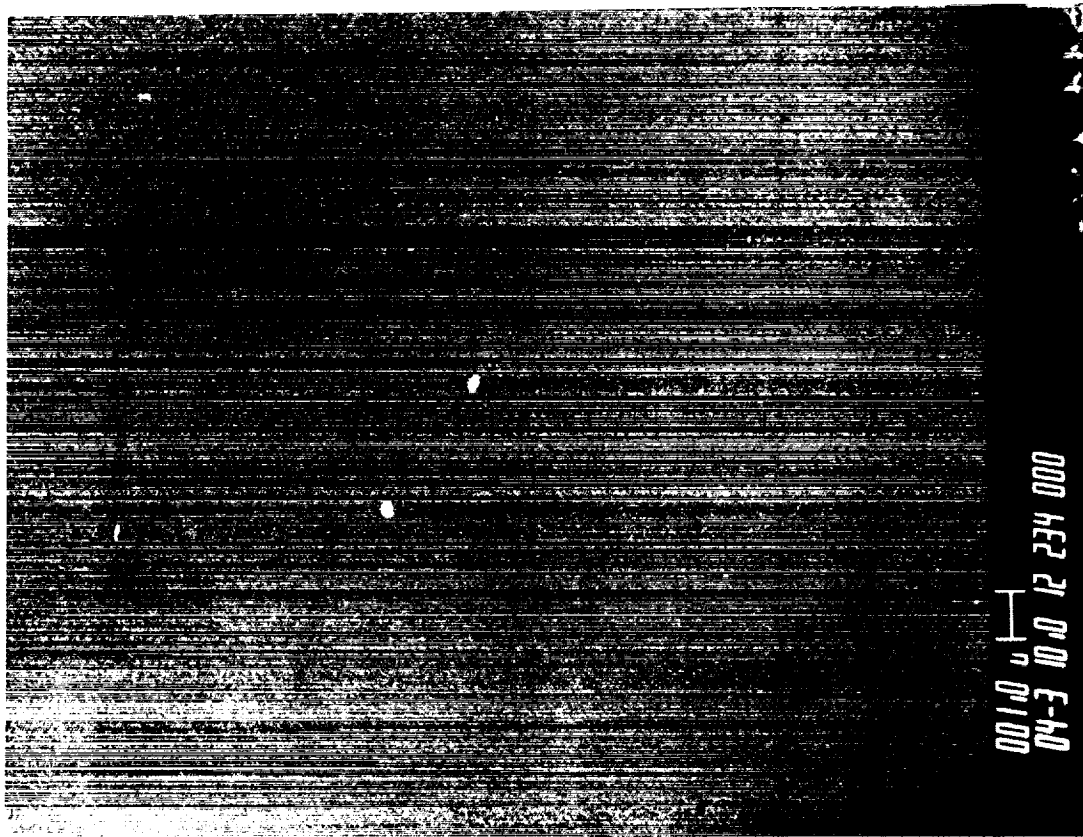
PRIMER SURFACE, Ti – CLEANED AND PRIMED
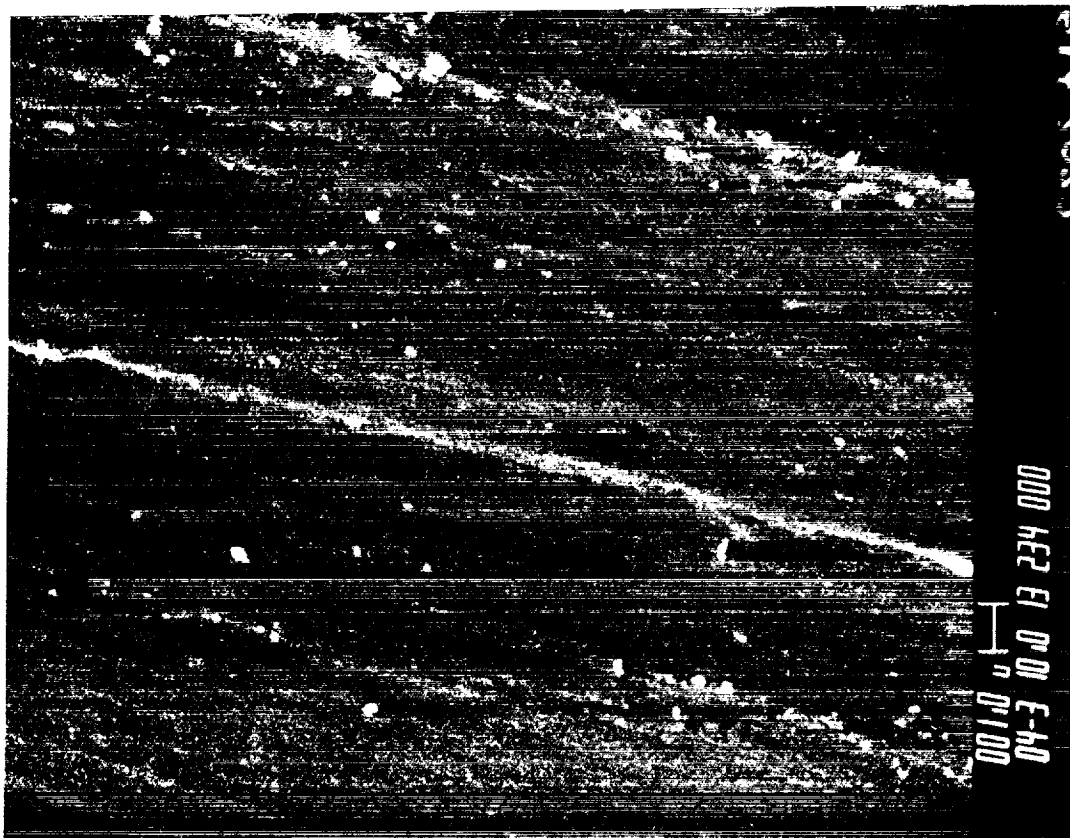
Ti SURFACE, Ti – CLEANED AND SCRAPED

FIGURE 1.21 TITANIUM AND TITANIUM WITH PRIMER SURFACES BEFORE
CURE CYCLING AND BONDING, 4000X MAGNIFICATION

111

1.22 (c) 23.77% Si – Ti, SANDED, CLEANED, AND PRIMED, XES

1.22 (b) 4.5% Si – Ti SANDED AND CLEANED, XES

1.22 (a) 3.16% Si – Ti CLEANED AND SCRAPED, XES

FIGURE 1.22 PHOTOGRAPHS OF TITANIUM SURFACE BEFORE BONDING

112
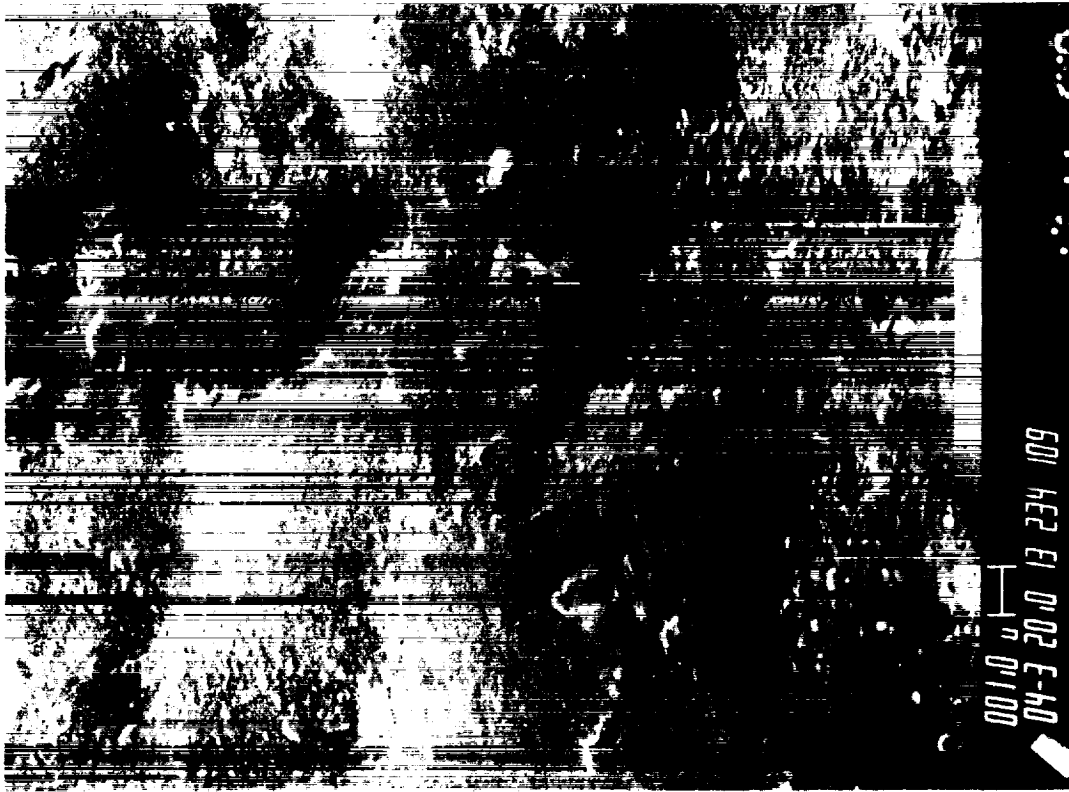
A9 – AF31 SURFACE –
55% PRIMER FAILURE, 45% AF31 FAILURE –

A1 – PRIMER SURFACE –
91% PRIMER FAILURE

FIGURE 1.23 A1 AND A9 FAILURE SURFACES, 4000X MAGNIFICATION
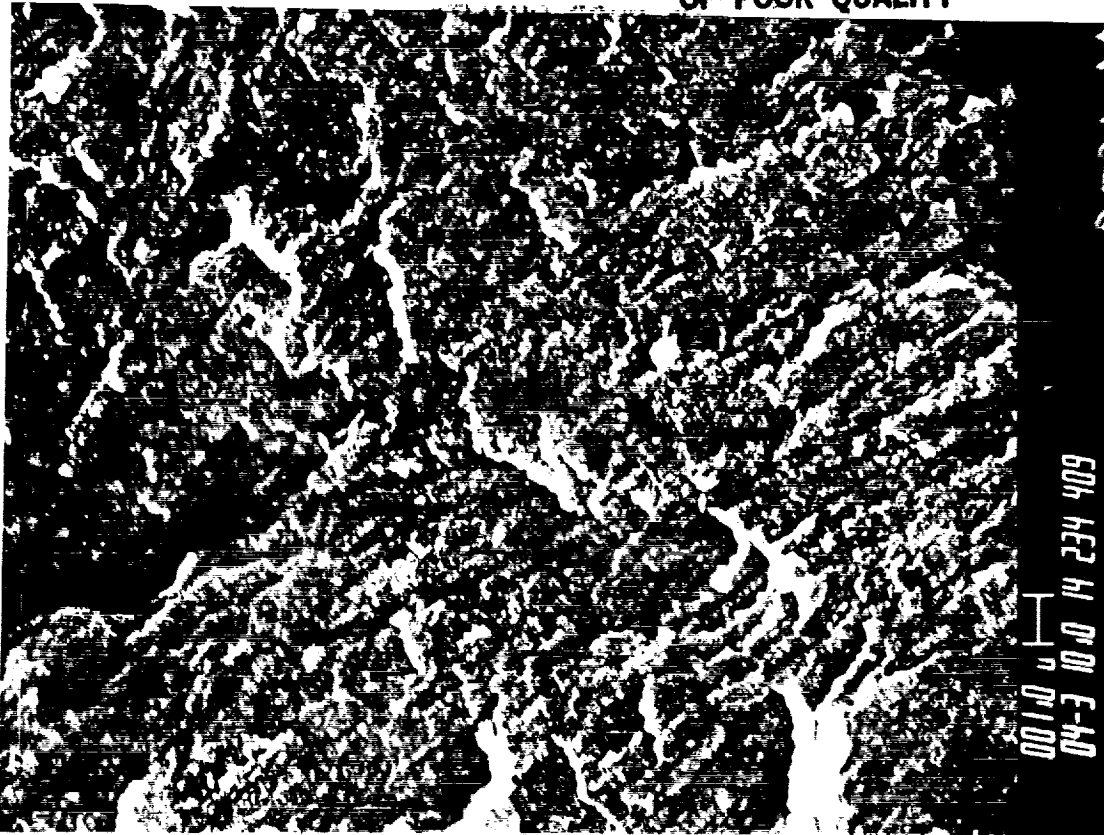
F9 - AF31 SURFACE -
48% AF31 FAILURE
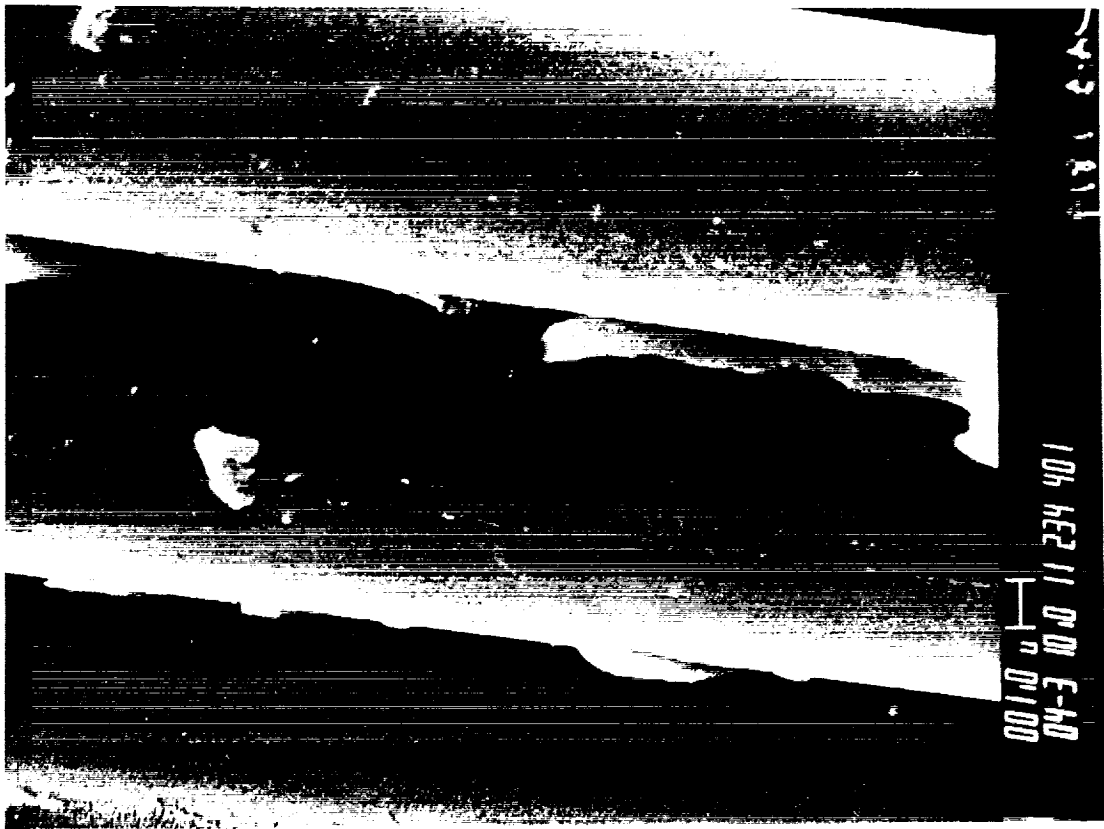
F1 - FIBERGLASS PRIMER SURFACE -
98% FIBERGLASS PRIMER FAILURE

FIGURE 1.24 F1 AND F9 FAILURE SURFACES, 4000X MAGNIFICATION

114
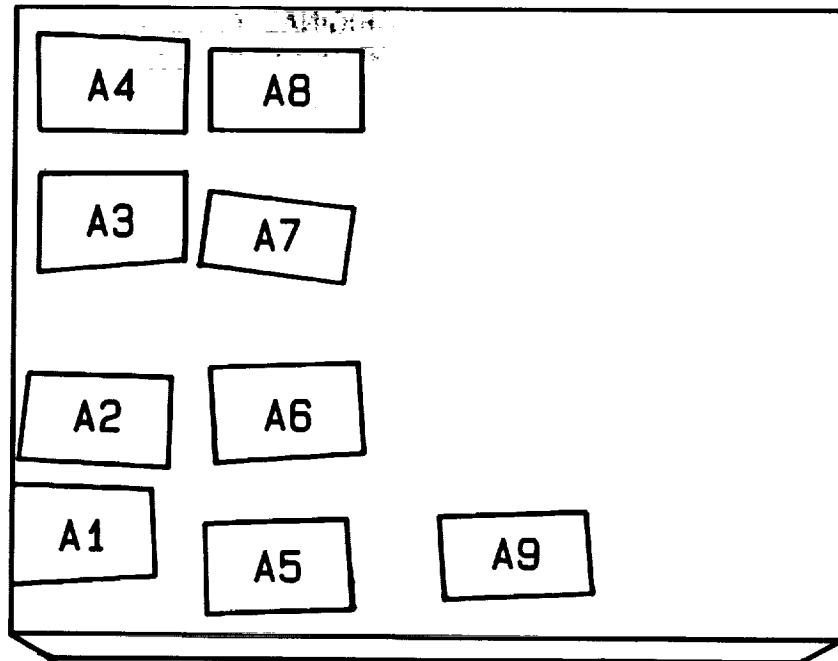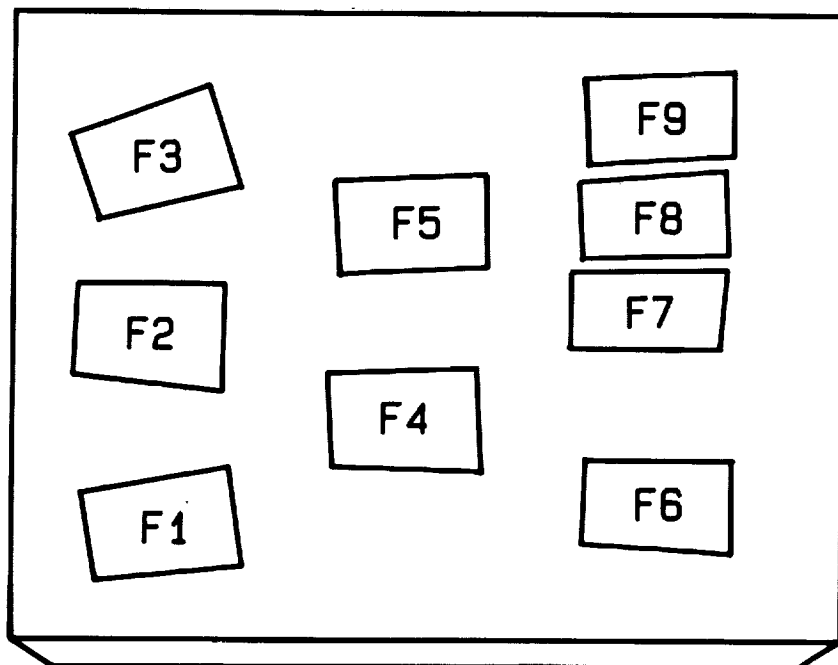
"A" SPECIMENS

"F" SPECIMENS

FIGURE 1.25 SHEAR SPECIMEN KEY FOR THE CURE "A" AND
"F" CYCLES (FIGURES 1.26 AND 1.28, AND FIGURES
1.27 AND 1.29, RESPECTIVELY)

115
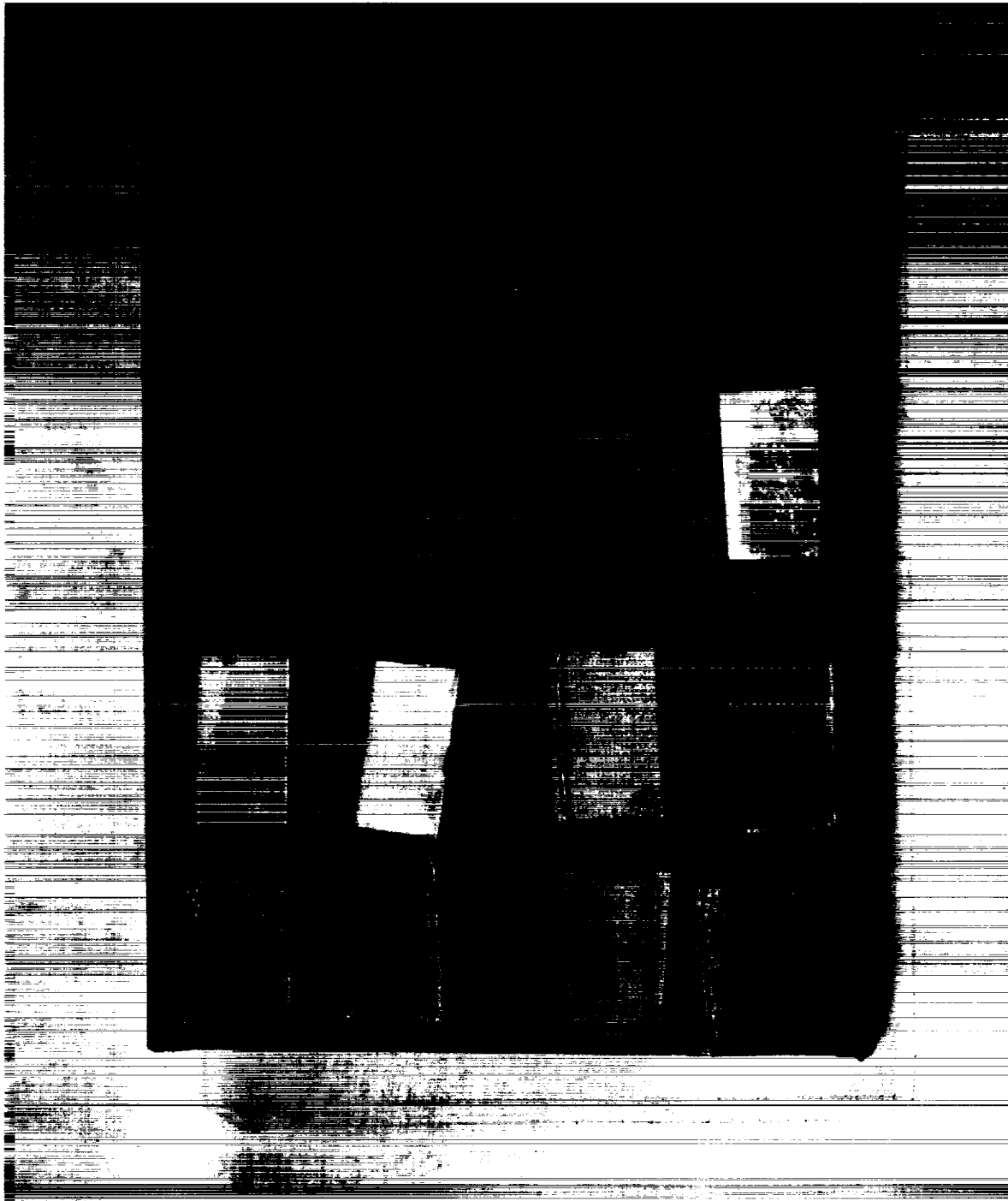
FIGURE 1.26 PHOTOGRAPH OF "A" CURE CYCLE SHEAR SPECIMENS

116
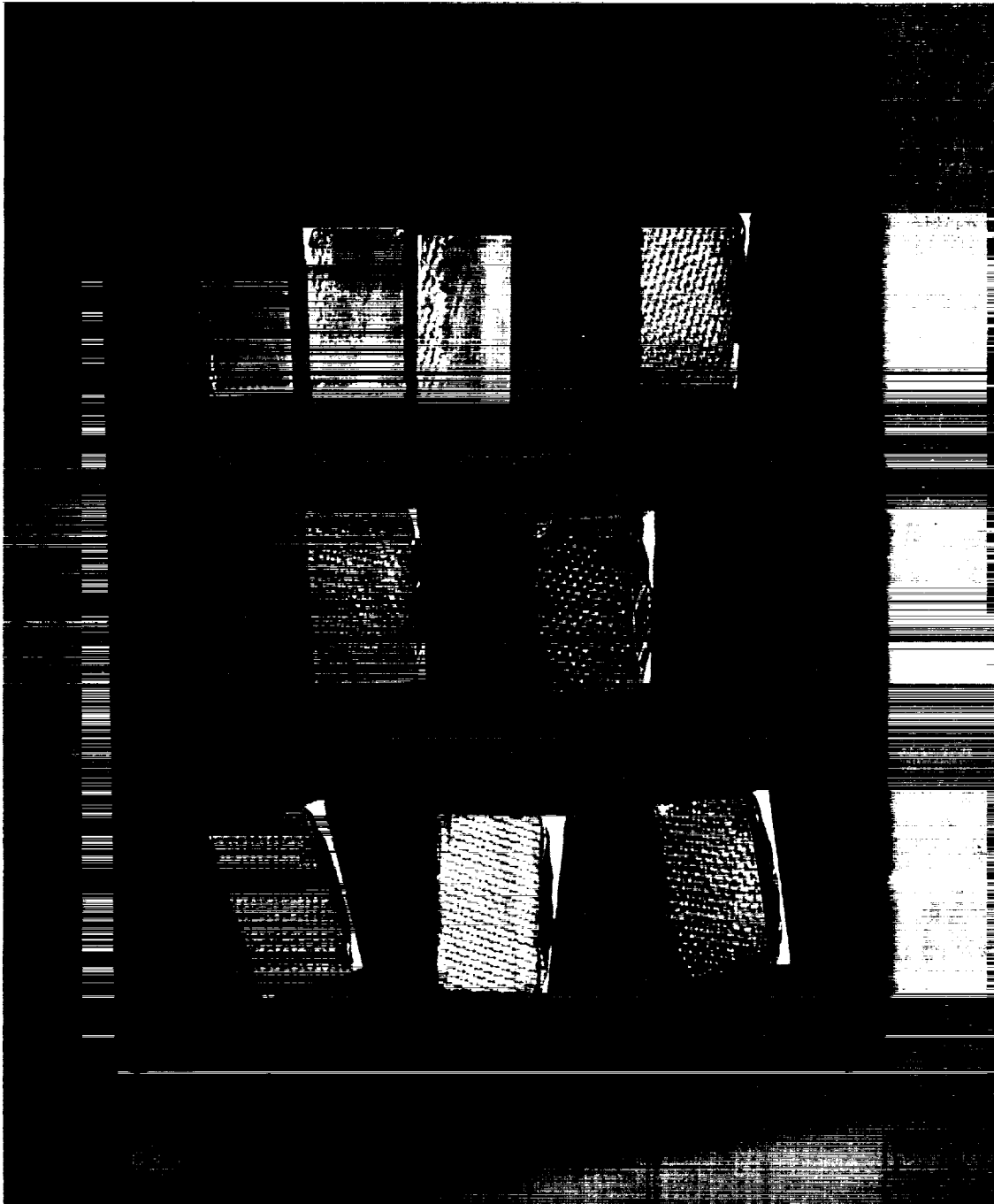
FIGURE 1.27 PHOTOGRAPH OF "F" CURE CYCLE SHEAR SPECIMENS

117
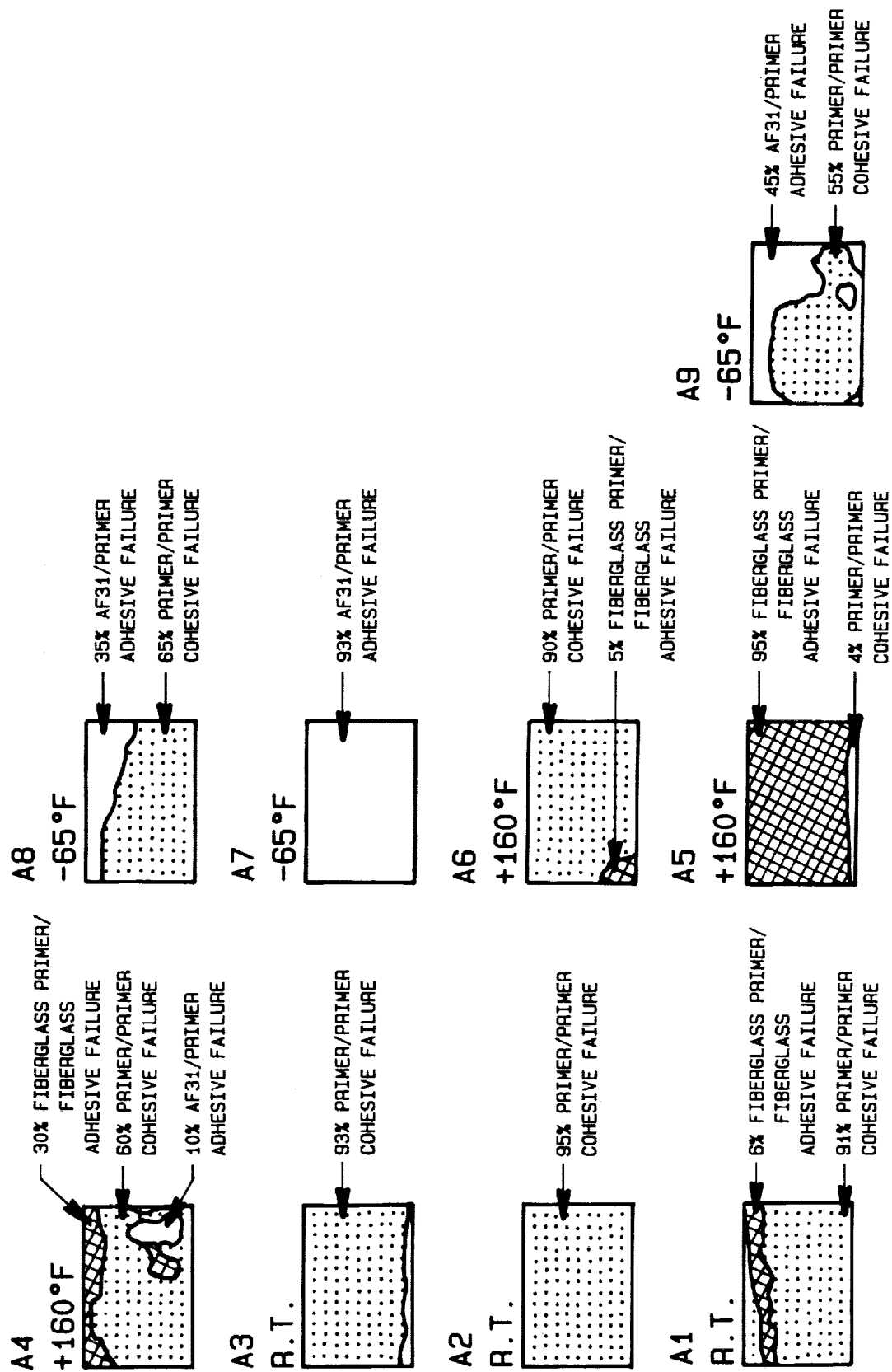
FIGURE 1.28 FAILURE FACES FOR "A" CURE CYCLE SHEAR SPECIMENS
(SEE FIGURE 1.26 PHOTOGRAPH)

F9 −65°F

48% PRIMER/PRIMER COHESIVE FAILURE

48% AF31/PRIMER ADHESIVE FAILURE

F8 −65°F

14% FIBERGLASS PRIMER/ FIBERGLASS ADHESIVE FAILURE

48% AF31/PRIMER ADHESIVE FAILURE

38% PRIMER/PRIMER COHESIVE FAILURE

F7 −65°F

15% FIBERGLASS PRIMER/ FIBERGLASS ADHESIVE FAILURE

45% AF31/PRIMER ADHESIVE FAILURE

40% PRIMER/PRIMER COHESIVE FAILURE

F6 +160°F

96% FIBERGLASS PRIMER/ FIBERGLASS ADHESIVE FAILURE

F5 +160°F

97% FIBERGLASS PRIMER/ FIBERGLASS ADHESIVE FAILURE

F4 +160°F

97% FIBERGLASS PRIMER/ FIBERGLASS ADHESIVE FAILURE

F3 R.T.

97% FIBERGLASS PRIMER/ FIBERGLASS ADHESIVE FAILURE

F2 R.T.

98% FIBERGLASS PRIMER/ FIBERGLASS ADHESIVE FAILURE

F1 R.T.

98% FIBERGLASS PRIMER/ FIBERGLASS ADHESIVE FAILURE

FIGURE 1.29 FAILURE FACES FOR "F" CURE CYCLE SHEAR SPECIMENS
(SEE FIGURE 1.27 PHOTOGRAPH)
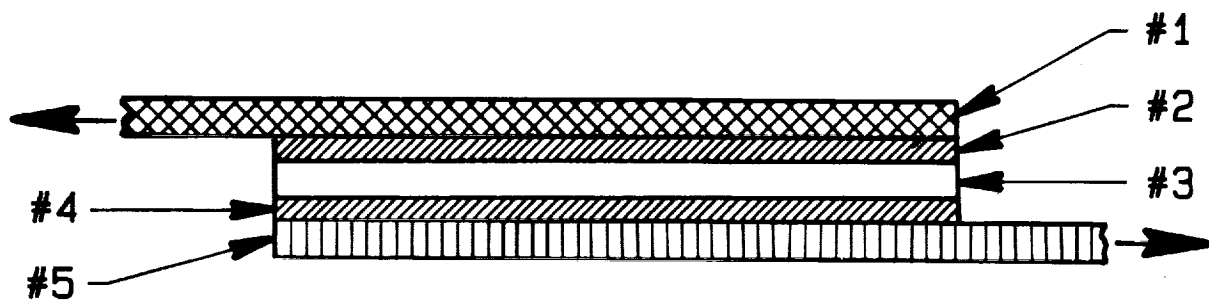
119

```
LAYER #1   CARBON
LAYER #2   PRIMER (EC2174)
LAYER #3   AF31 ADHESIVE
LAYER #4   PRIMER (EC2174)
LAYER #5   FIBERGLASS
```

FIGURE 1.30 CARBON/FIBERGLASS LAYER DESCRIPTION FOR
TABLES 1.30 AND 1.31 LAP SHEAR TESTS
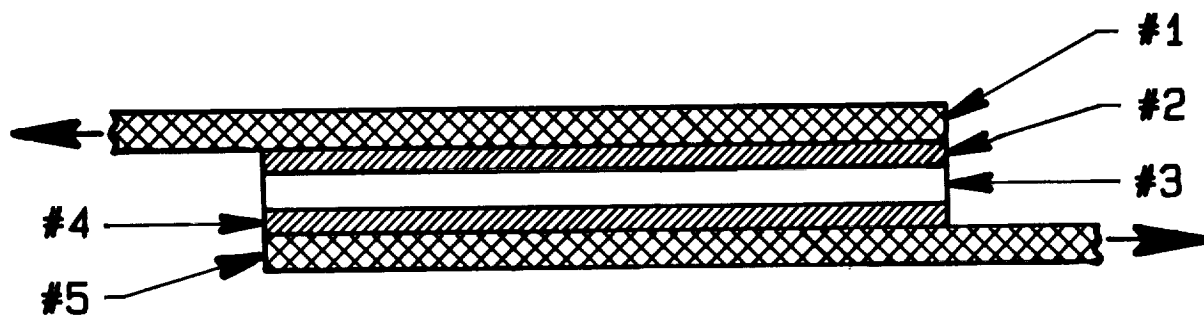
```
LAYER #1   CARBON
LAYER #2   PRIMER (EC2174)
LAYER #3   AF31 ADHESIVE
LAYER #4   PRIMER (EC2174)
LAYER #5   CARBON
```

FIGURE 1.31 CARBON/CARBON LAYER DESCRIPTION FOR
TABLES 1.32 AND 1.33 LAP SHEAR TESTS
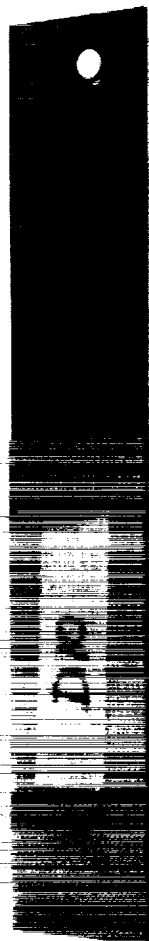
FIGURE 1.32 LAP SHEAR SPECIMEN D10 — FIBERGLASS CLOTH
BONDED TO PERFORATED TITANIUM

FIGURE 1.33 COMPRESSION SPECIMEN PANEL 10E
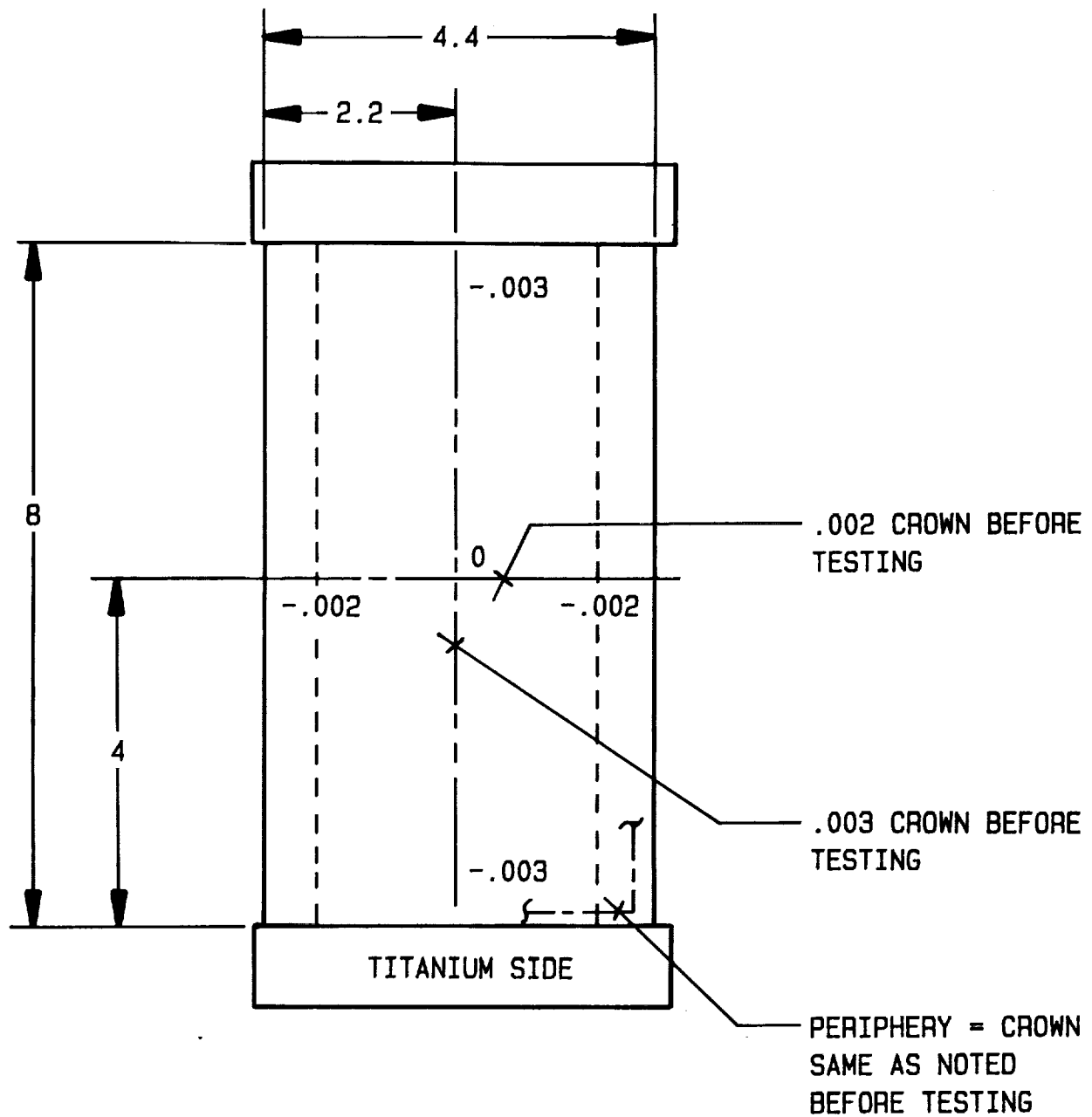
NOTE: ALL DIMENSIONS IN INCHES

FIGURE 1.34 FAILURE OF TEST SPECIMEN 10E

124

FIGURE 1.35 SEPARATION OF TITANIUM FROM COMPOSITE
SUBSTRUCTURE, SPECIMEN 10E

125

FIGURE 1.36 VIEW OF TITANIUM SHEET TO COMPOSITE
SUBSTRUCTURE AFTER FAILURE, PANEL 10E

FIUGRE 1.37 ADDITIONAL VIEW OF TITANIUM SHEET TO COMPOSITE
SUBSTRUCTURE AFTER FAILURE, PANEL 10E

127
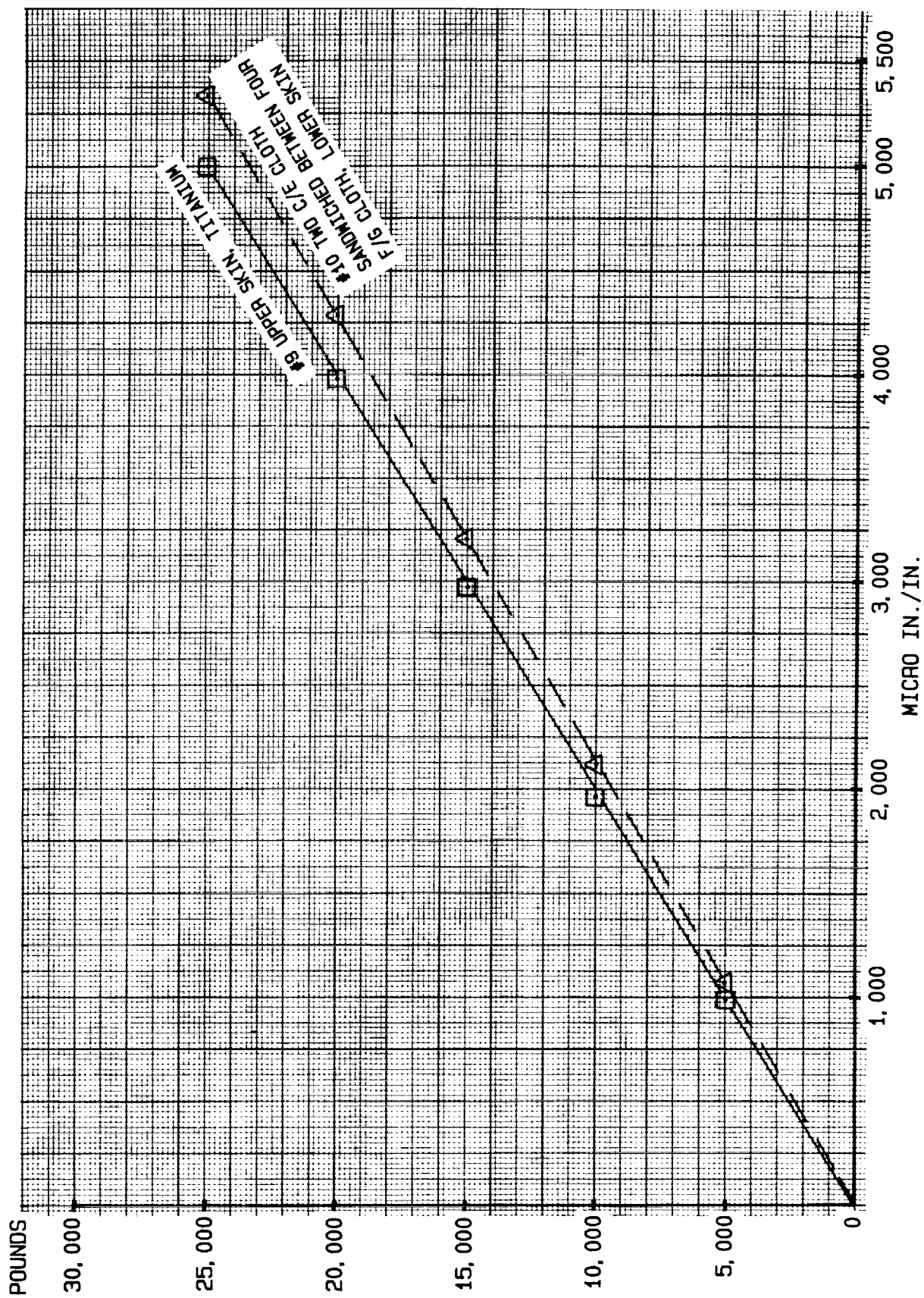
FIGURE 1.38 COMPRESSION TEST, 4.4— BY 8–INCH TEST PANEL, SPECIMEN 10E

128

FIGURE 1.39 COMPRESSION TEST, SPECIMEN 10E
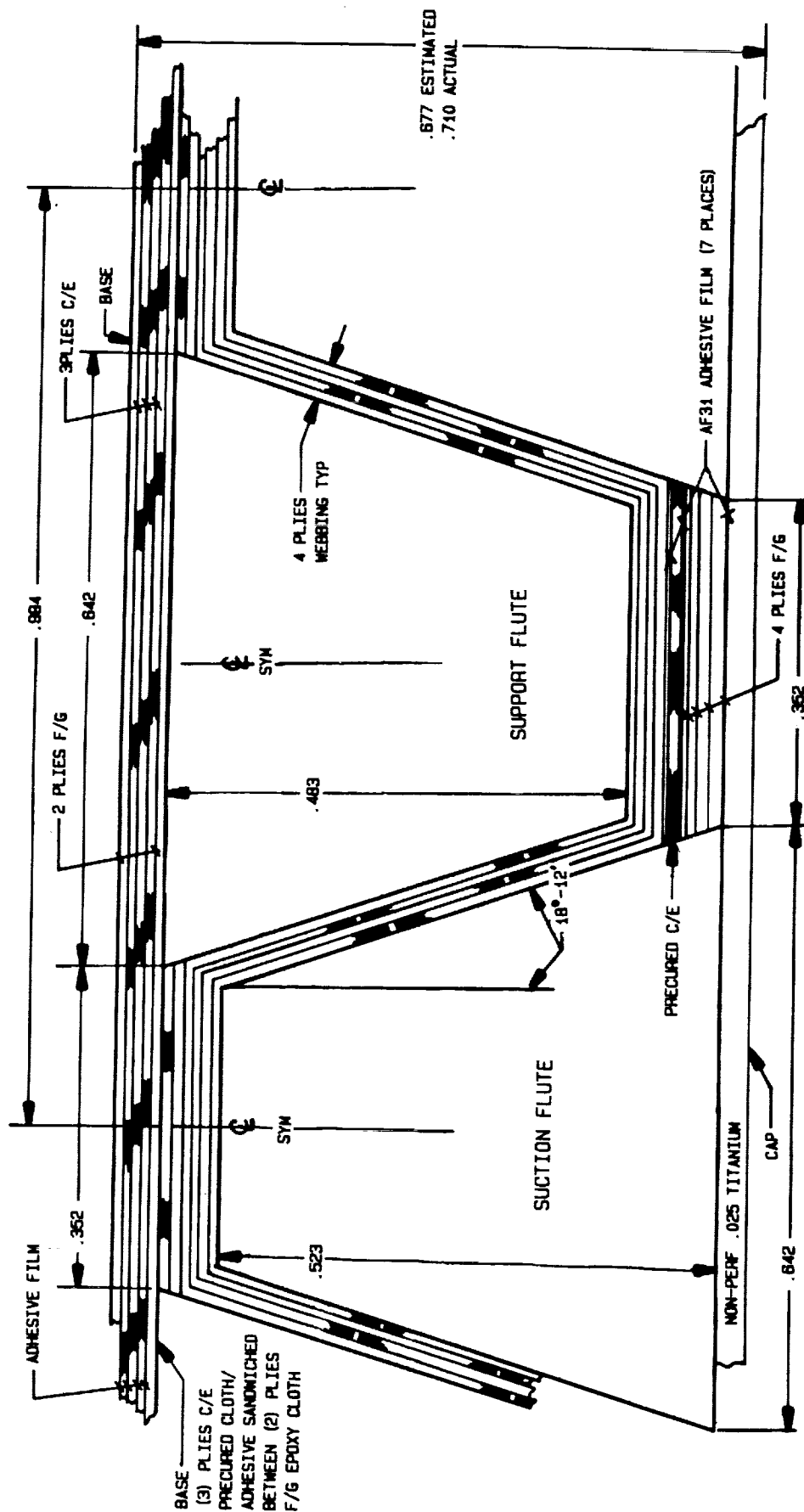
FIGURE 1.40 DETAILS OF PANELS WITH CONFIGURATION 13F

130
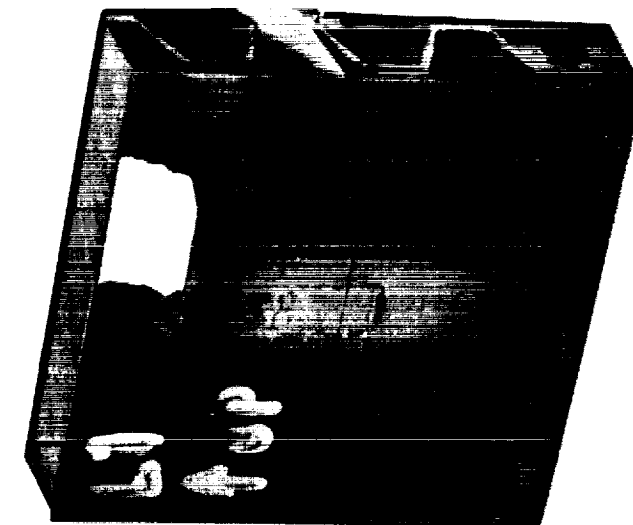
FIGURE 1.41 SHORT COMPRESSION PANEL A1 (LEFT FIGURE) – AXIALLY LOADED TITANIUM SHEET L1 (RIGHT FIGURE) – TRANSVERSE LOADED
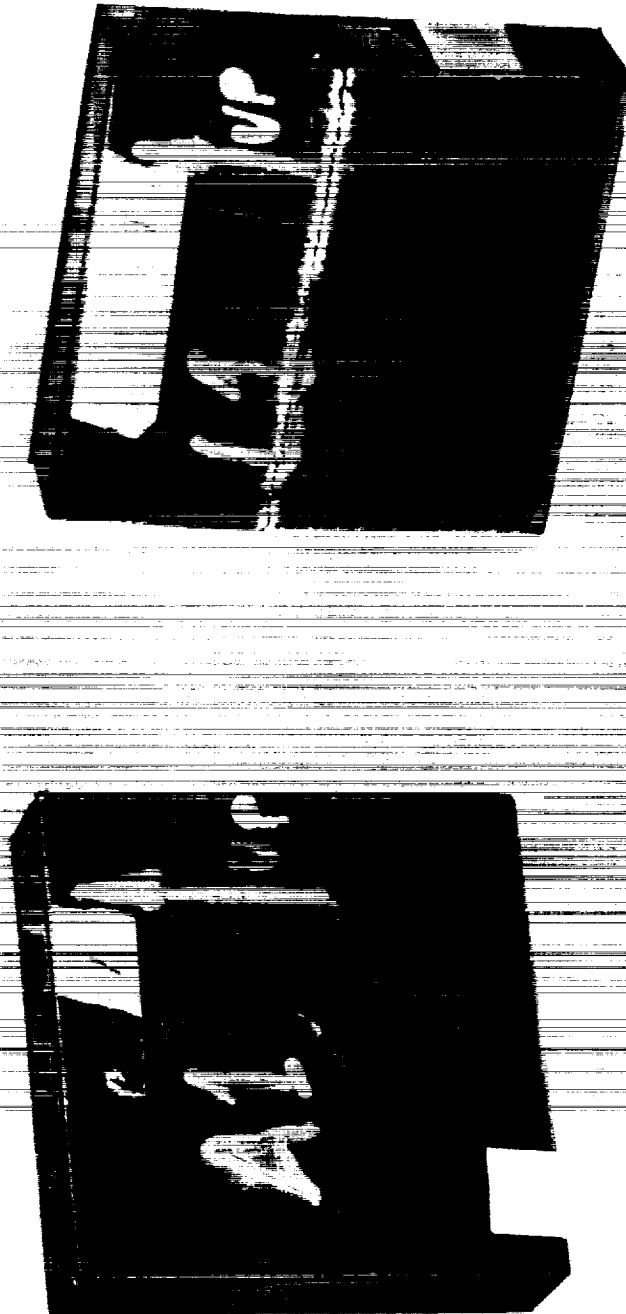
FIGURE 1.42 SHORT COMPRESSION PANEL A1 (LEFT FIGURE) – AXIALLY LOADED COMPOSITE SIDE, L1 (RIGHT FIGURE) – TRANSVERSE LOADED

132
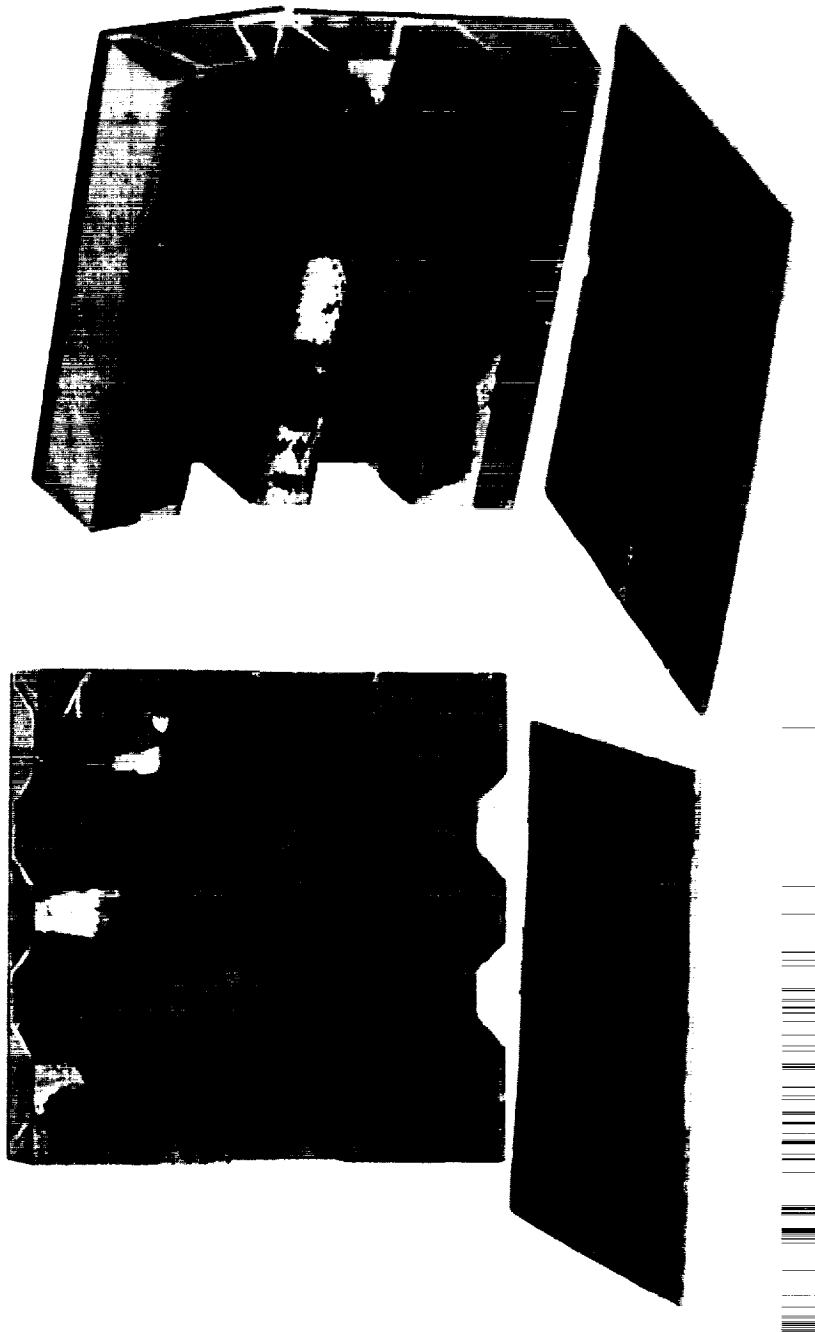
FIGURE 1.43 TITANIUM SHEET ROTATED 90 DEGREES SHOWING EXPOSED
BOND LAYER ON A1 AND L1 SPECIMENS
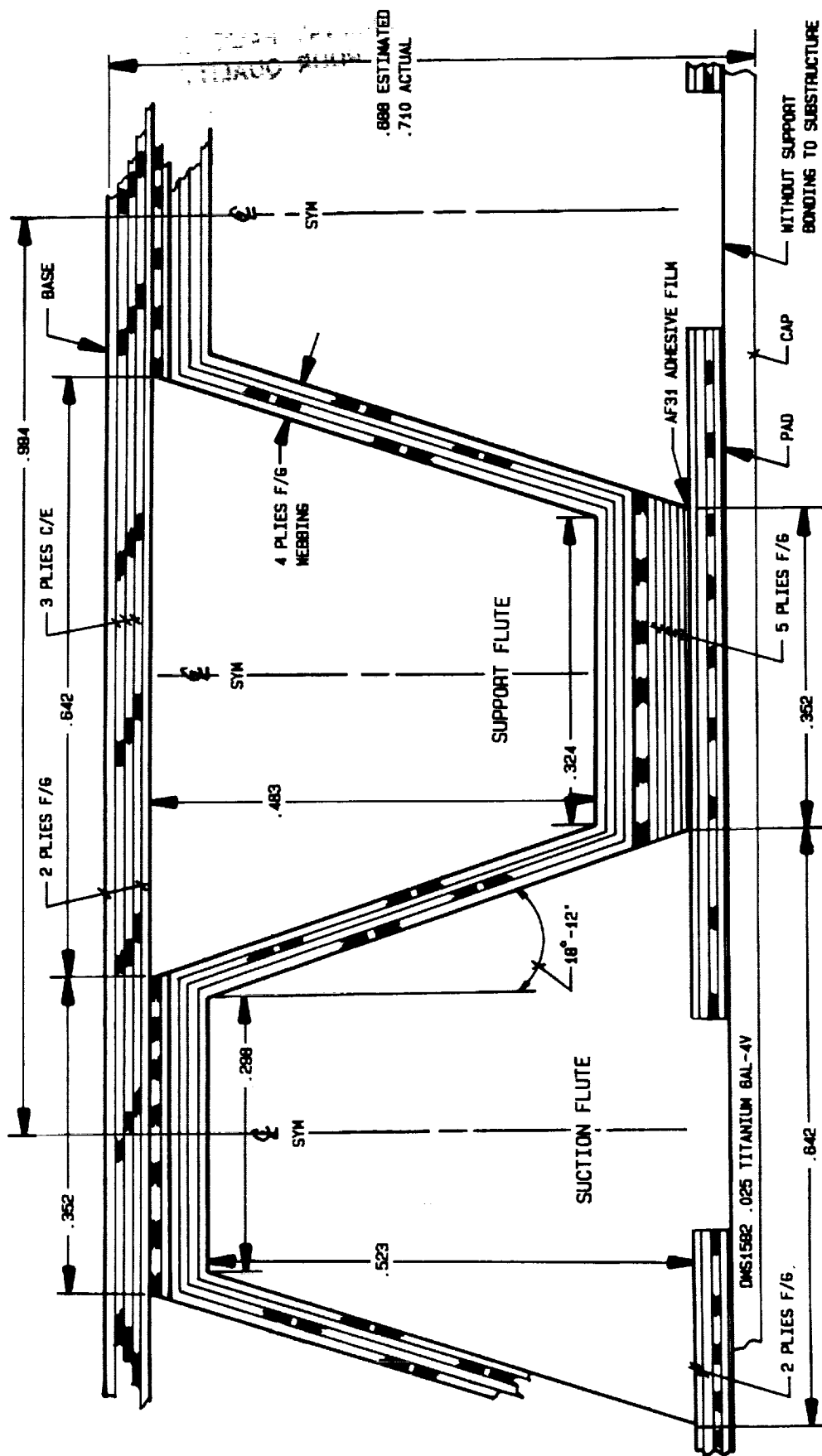
AVERAGE DEPTH $\varnothing$ SUCTION FLUTE AFTER REMOVING MANDRELS = -0.0009

$G1_1$ = 31,250 LB ULT COMP STRENGTH

FIGURE 1.44 CONFIGURATION $G1_1$, WITH PADS, TESTED AT ROOM TEMPERATURE, SPECIAL PRIMER AND CURE, EXISTING MANDRELS

134

ORIGINAL PAGE IS OF POOR QUALITY
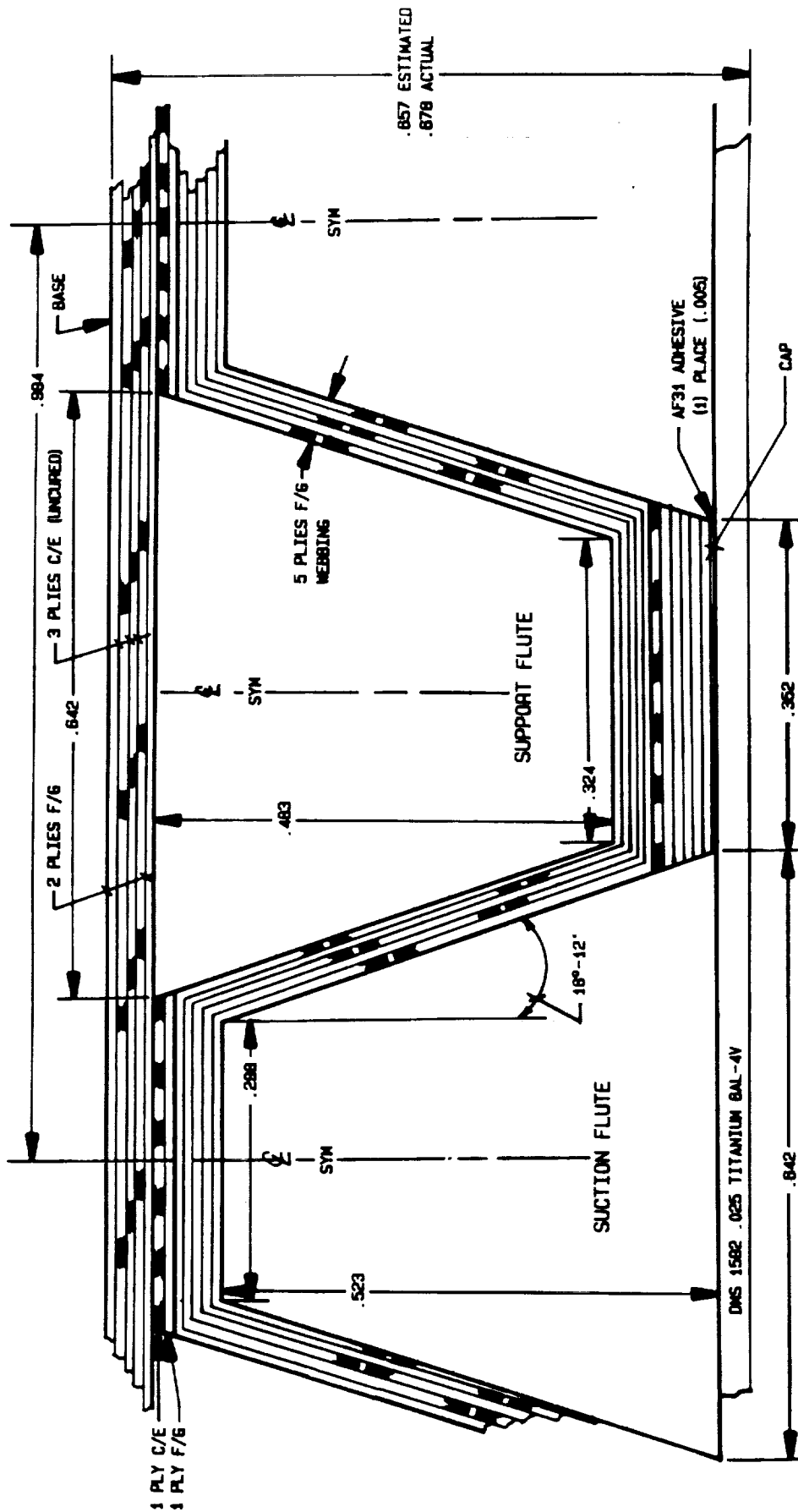
FIGURE 1.45 CONFIGURATION H1₁

.857 ESTIMATED
.678 ACTUAL

BASE

.994

3 PLIES C/E (UNCURED)

5 PLIES F/G WEBBING

SUPPORT FLUTE

2 PLIES F/G

.642

.483

.324

18°-12'

.288

SUCTION FLUTE

.523

1 PLY C/E
1 PLY F/G

SYM

AF31 ADHESIVE (1) PLACE (.006)

CAP

.352

.842

DMS 1582 .025 TITANIUM 6AL-4V

AVERAGE ₵ WAVINESS = -0.0007 FOR #H1 NON-PERF TITANIUM

AVERAGE ₵ WAVINESS = -0.00036 FOR #H2 PERF TITANIUM

AVERAGE ₵ WAVINESS = -0.0006 FOR #H3 NON-PERF TITANIUM

135
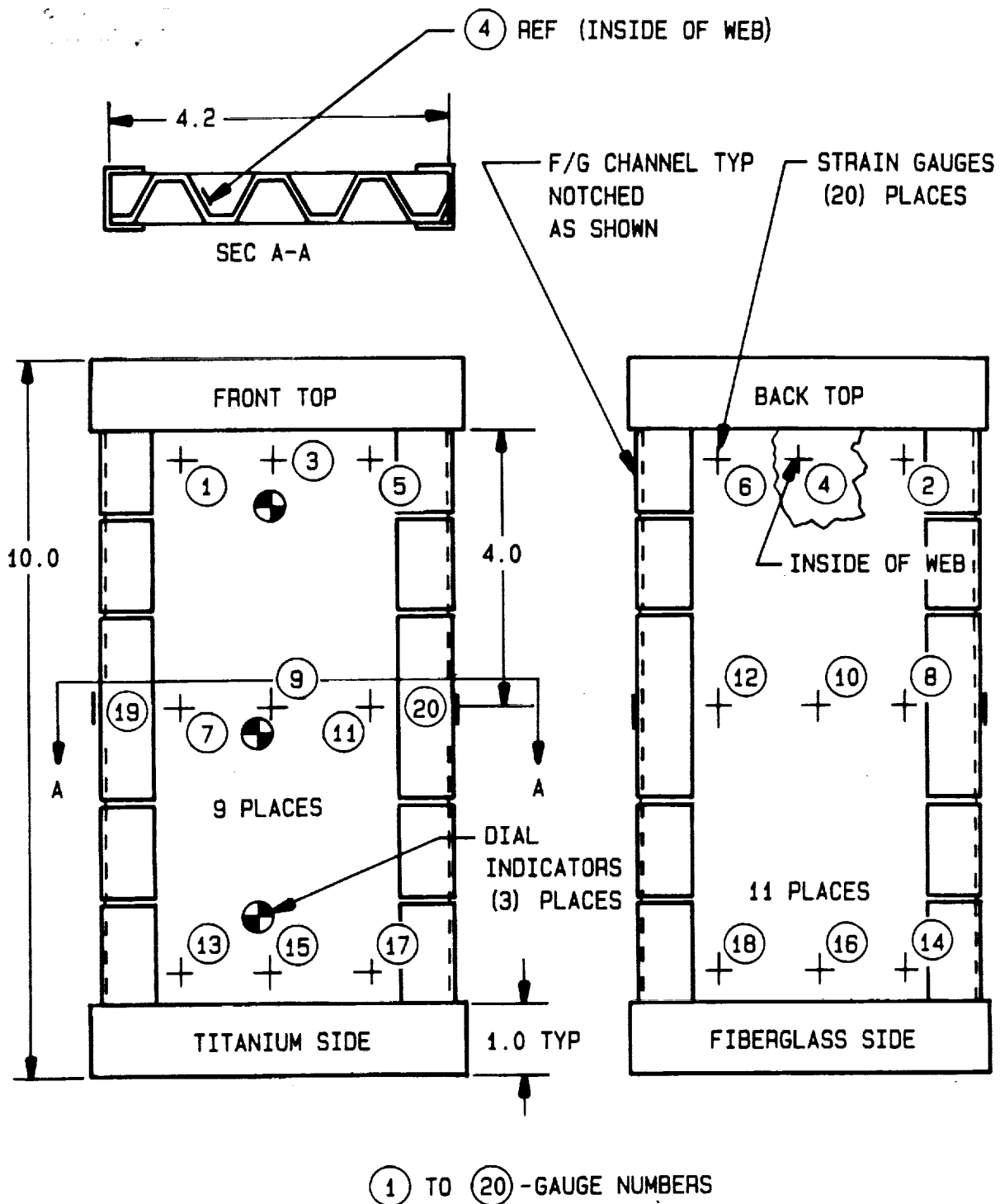
FIGURE 1.46 STRAIN GAGE AND DIAL GAGE LOCATIONS FOR
CONFIGURATION H1₁
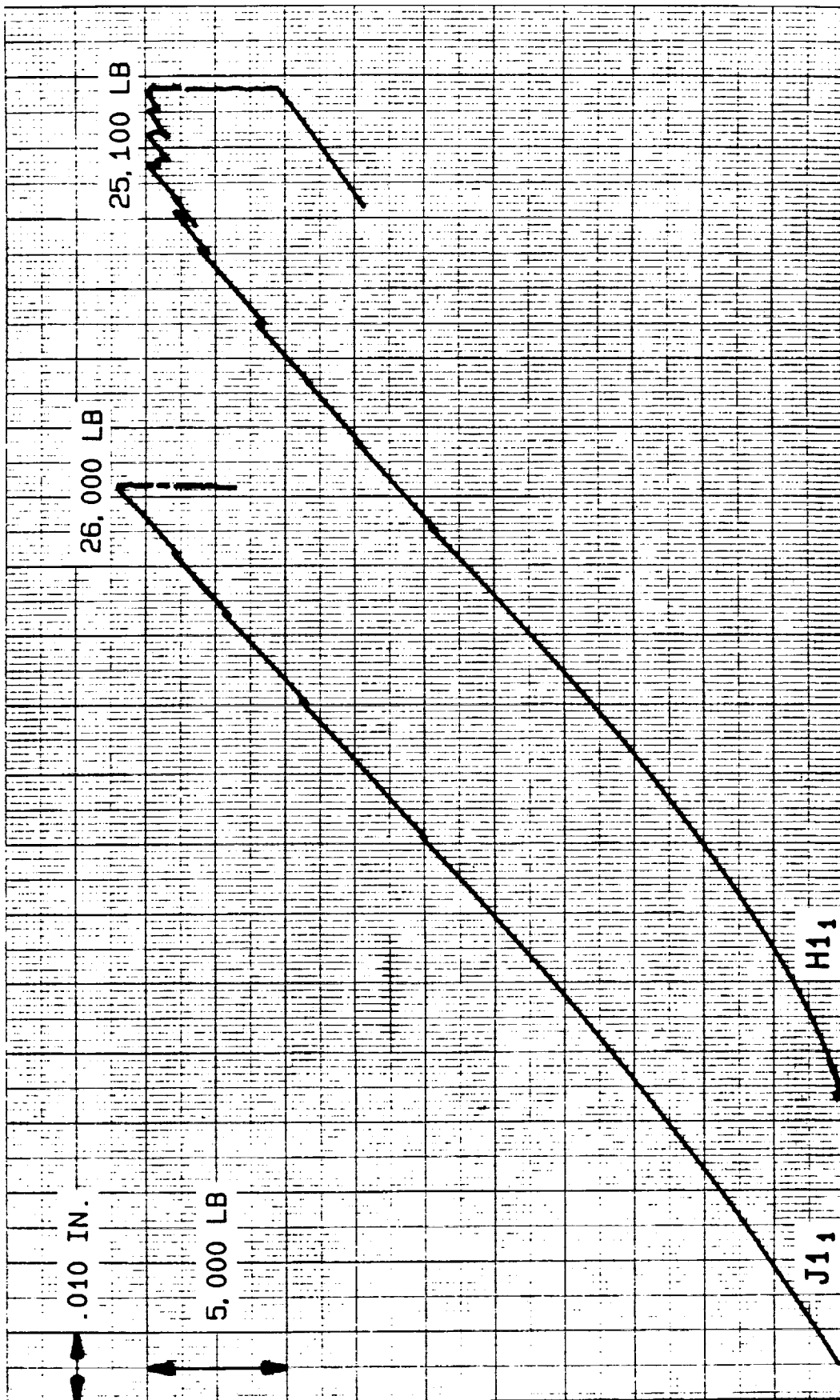
FIGURE 1.47 LOAD VERSUS HEAD TRAVEL AT ROOM TEMPERATURE FOR
PANELS H1₁ AND J1₁

137

FIGURE 1.48 CONFIGURATION $J1_1$

$J1_1 = 26,000$ LB ULT COMP STRENGTH

.875 ESTIMATED
.882 ACTUAL

$\overline{C}$ SYM

CAP

18°-12'

2 PLIES F/G

AF31 ADHESIVE
(1) PLACE (.005)

5 PLIES F/G
WEBBING

5 PLIES F/G

.984

.352

SUPPORT FLUTE

2 C/E + 3 F/G (5 PLIES TOTAL)

$\overline{C}$ SYM

.483

.324

.642

C/E REF

.288

$\overline{C}$ SYM

SUCTION FLUTE

.025 TITANIUM 6AL-4V

.842

.523

1 C/E + 3 F/G
(4 PLACES TOTAL)

138

SEC A-A
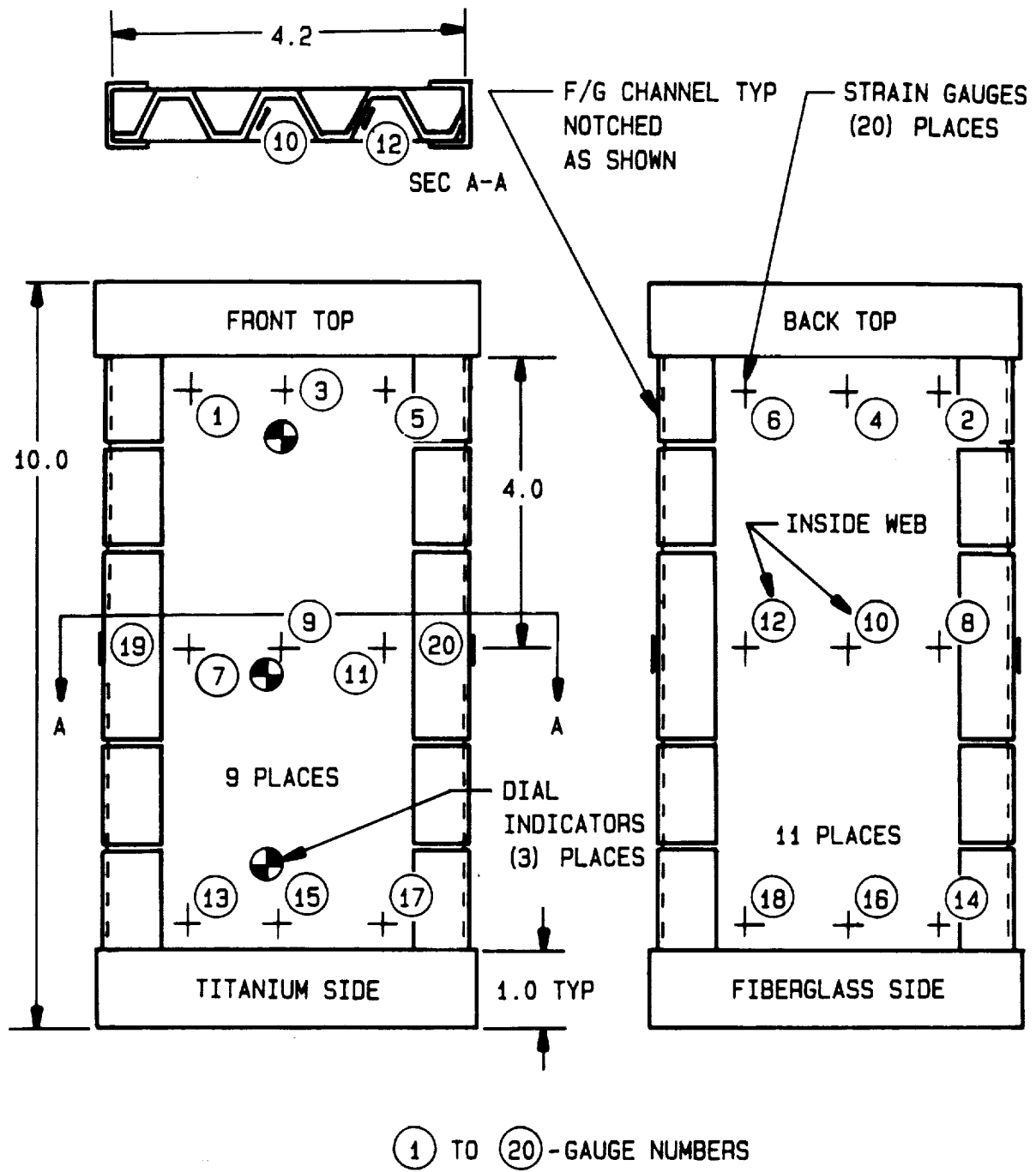
FIGURE 1.49 STRAIN GAGE AND DIAL GAGE LOCATIONS,
CONFIGURATION J1$_1$

139
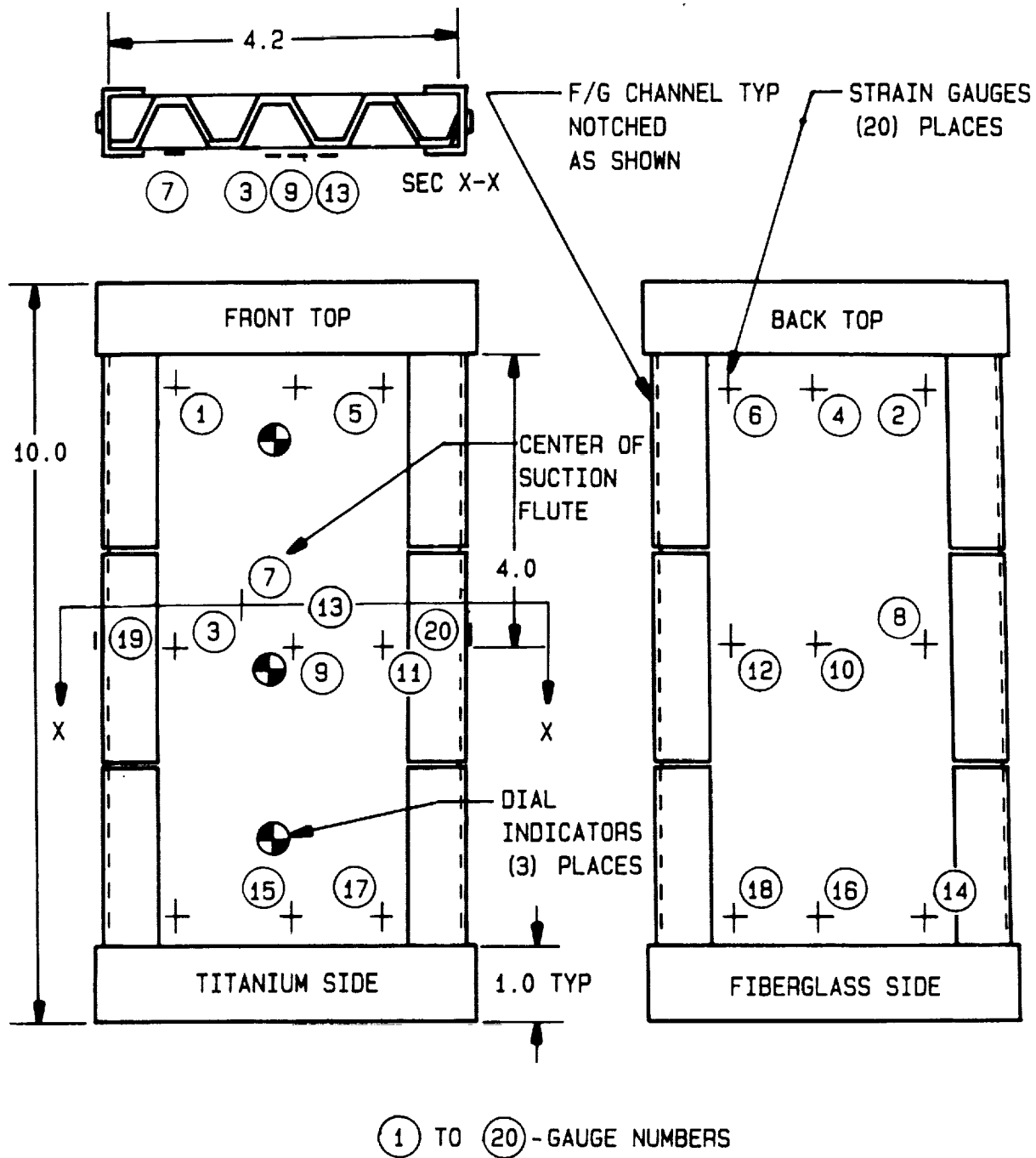
FIGURE 1.50 STRAIN GAGE AND DIAL GAGE LOCATIONS
FOR CONFIGURATION $G1_1$
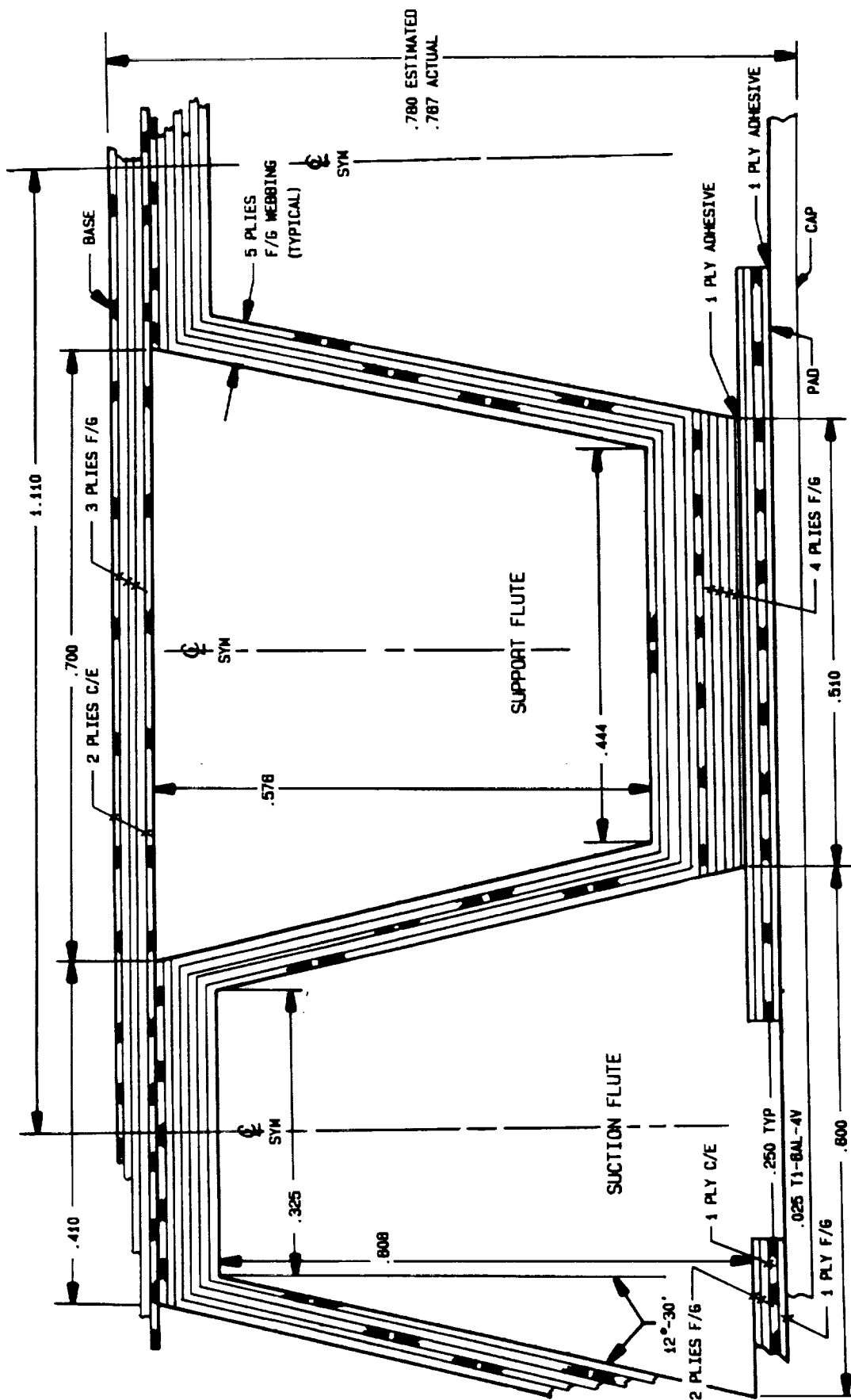
FIGURE 1.51 DETAILS OF PANELS WITH CONFIGURATION LA1-2

141

.010 IN.

5,000 LB

31,500 LB

A1-1
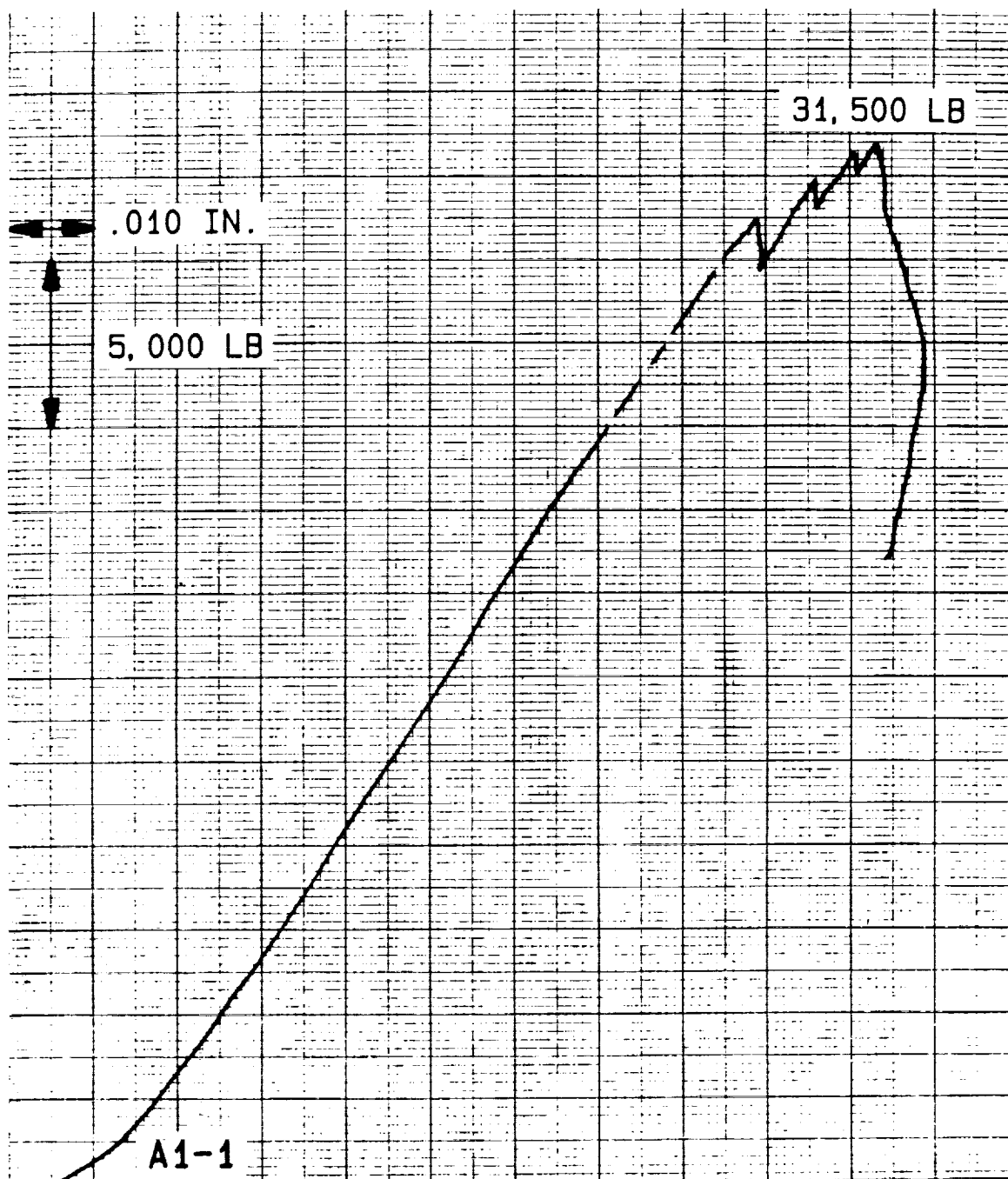
FIGURE 1.52 LOAD VERSUS HEAD TRAVEL FOR PANEL A1-1

142
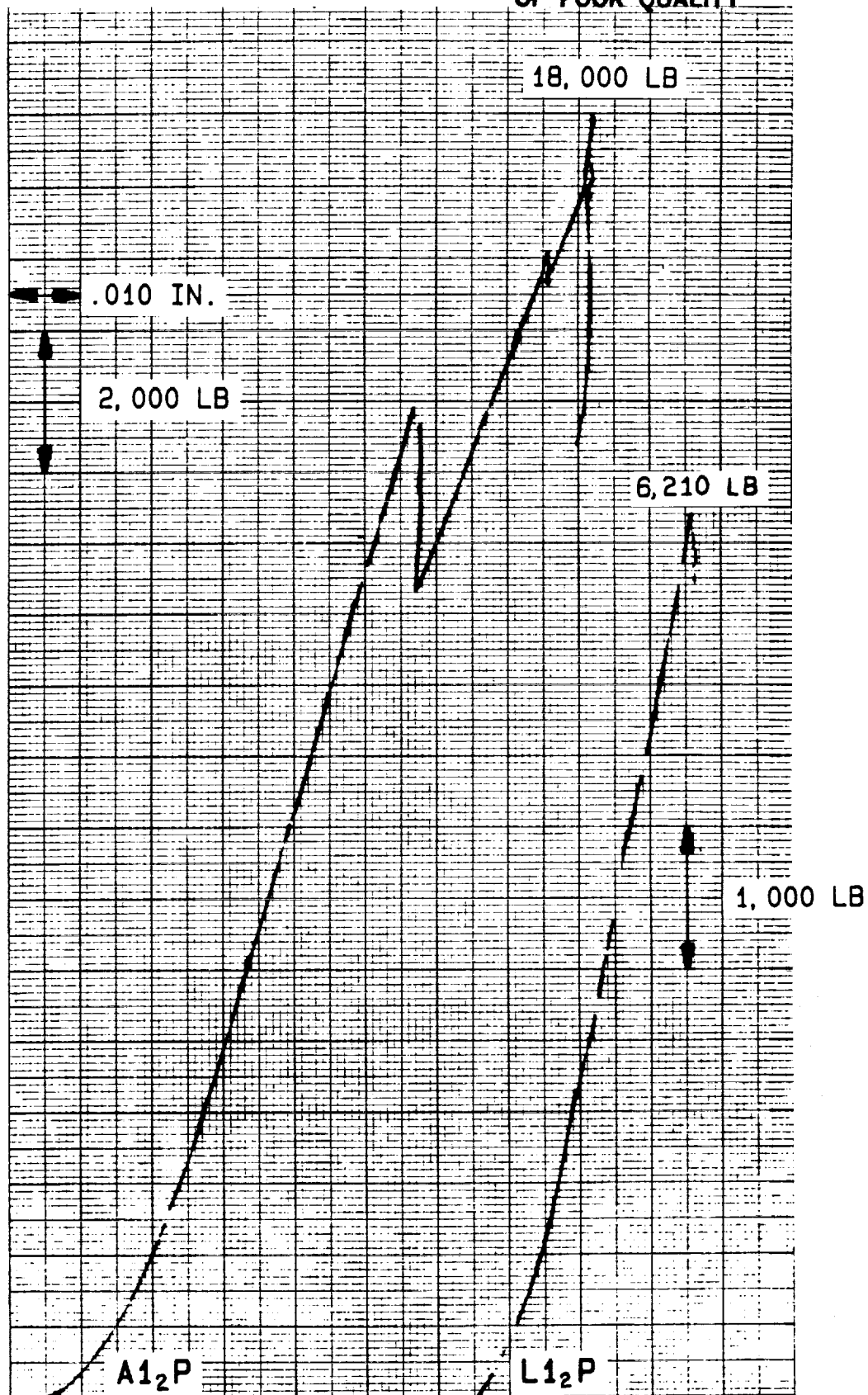
FIGURE 1.53 LOAD VERSUS HEAD TRAVEL FOR PANELS A1$_2$P AND L1$_2$P

143
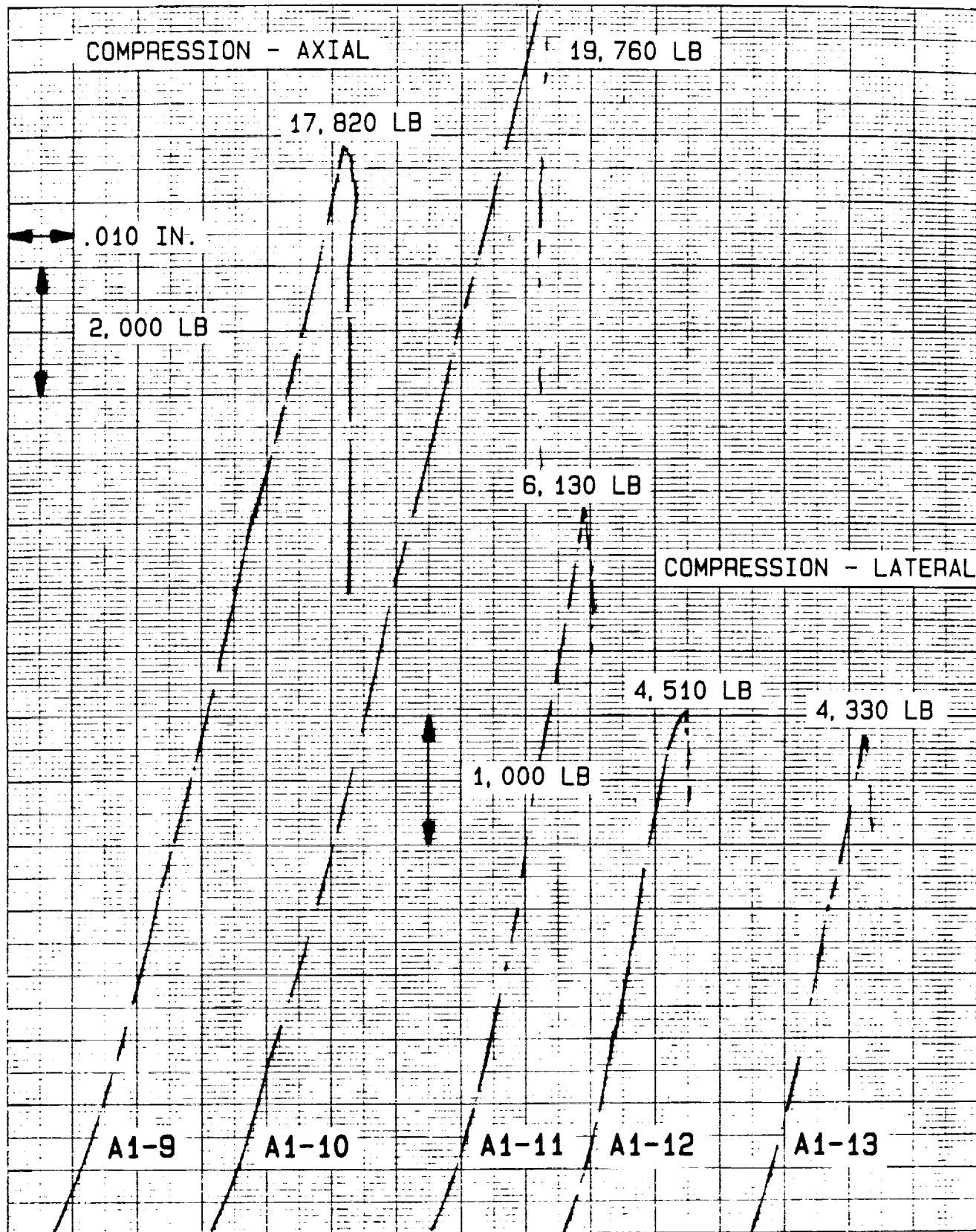
FIGURE 1.54 LOAD VERSUS HEAD TRAVEL FOR 3- BY 3-INCH
COMPRESSION TESTS FOR PANELS A1-9 TO A1-13

144

ORIGINAL PAGE IS OF POOR QUALITY
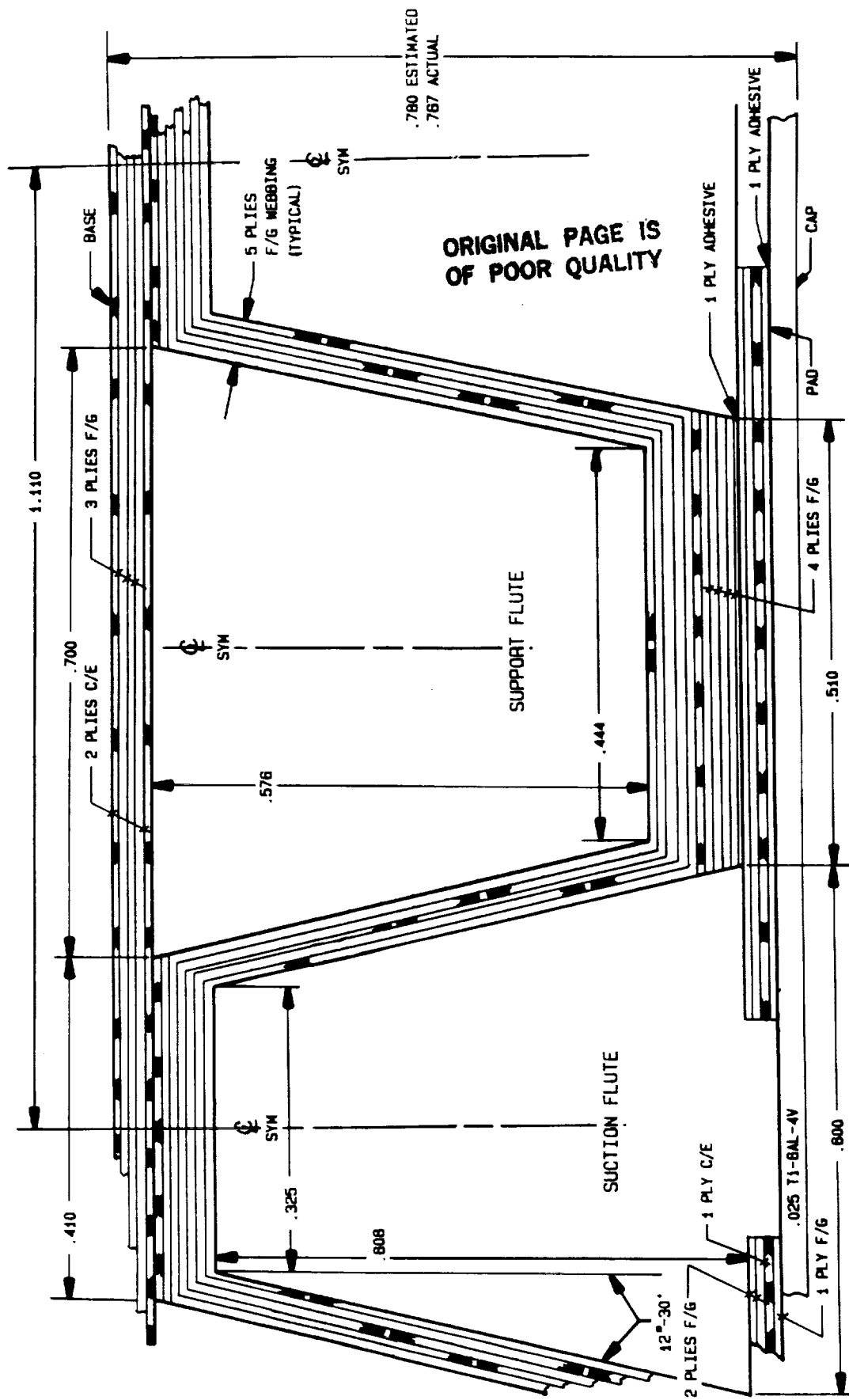
FIGURE 1.55 DETAILS OF PANELS WITH CONFIGURATION LA1-1

145
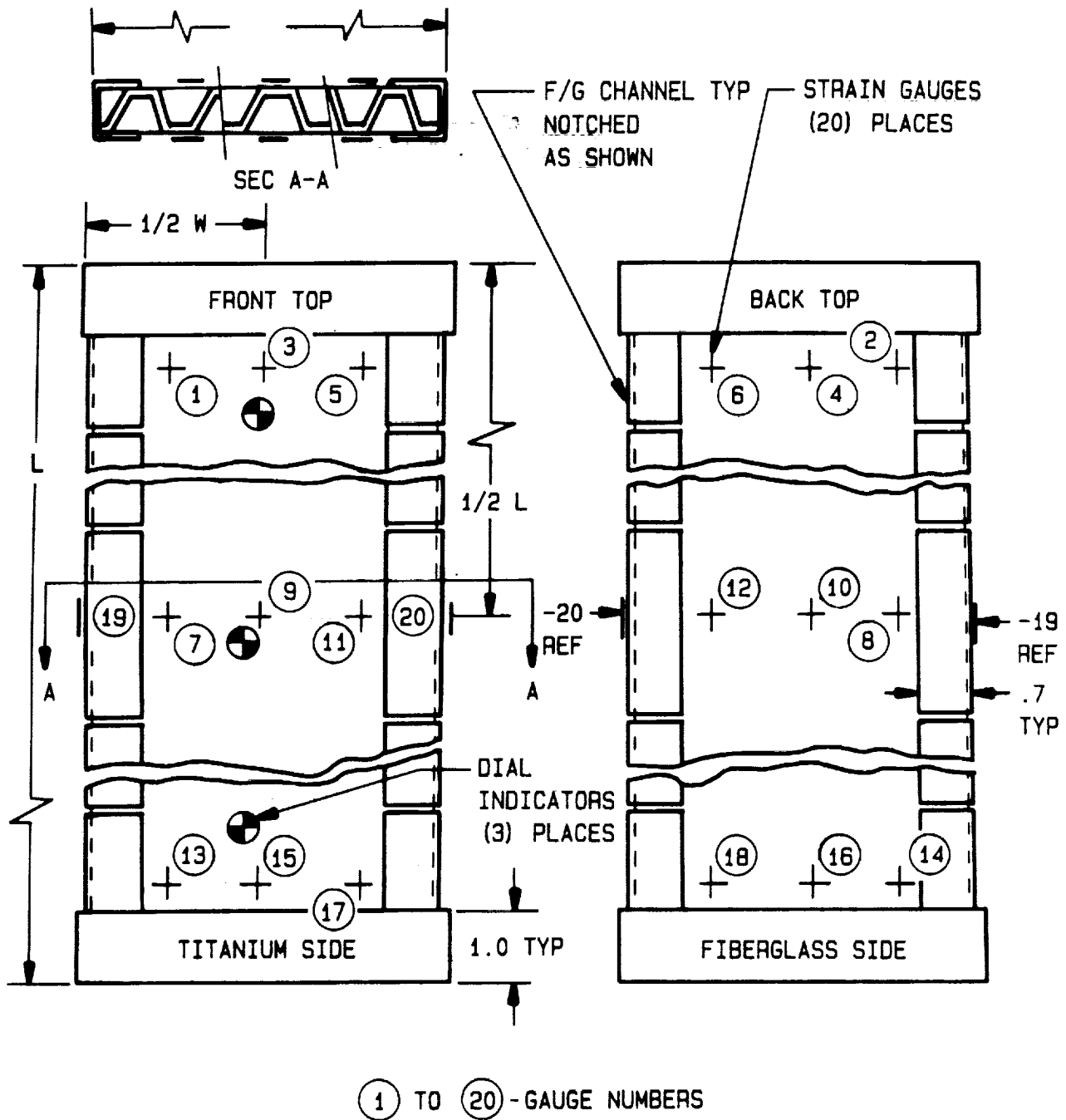
FIGURE 1.56 STRAIN GAGE AND DIAL GAGE LOCATIONS FOR
LONG COLUMN COMPRESSION SPECIMENS

146
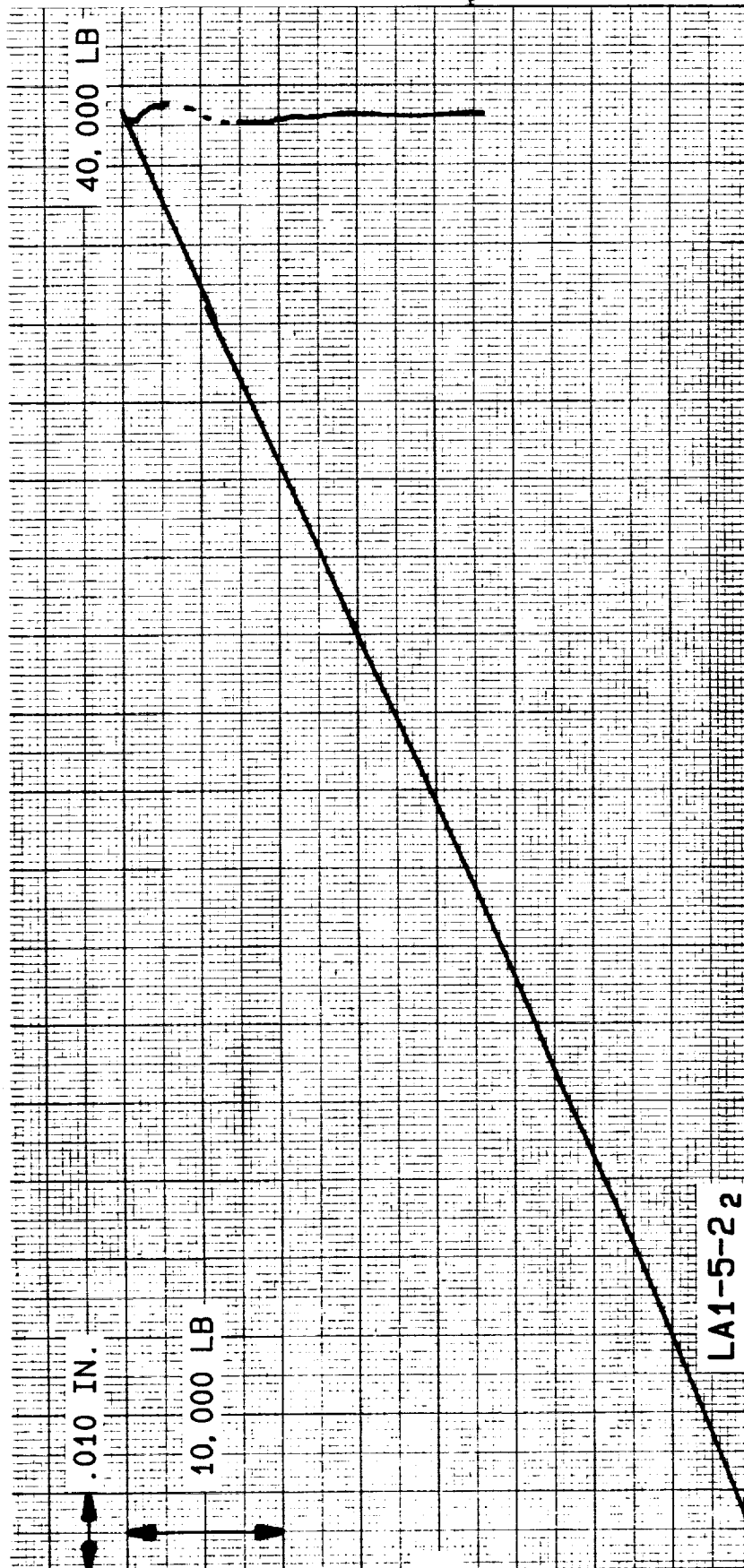
FIGURE 1.57 LOAD VERSUS HEAD TRAVEL AT ROOM TEMPERATURE
FOR PANEL LA1-5-2$_2$
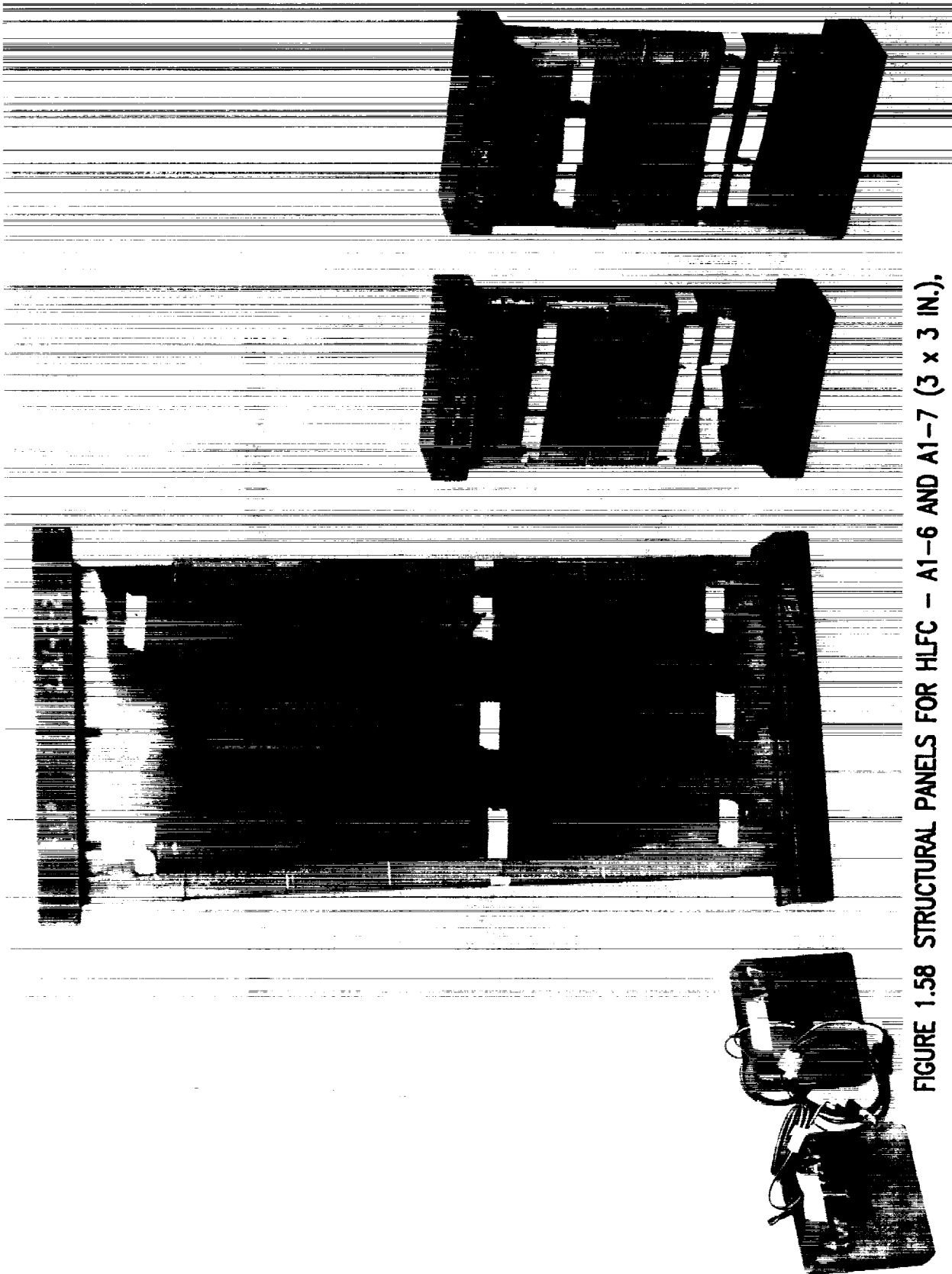
FIGURE 1.58 STRUCTURAL PANELS FOR HLFC — A1–6 AND A1–7 (3 x 3 IN.), LA1–3–2 (8 x 20 IN.), AND LA1–1–2₂ AND LA1–1–2₁ (4.5 x 10 IN.) — TITANIUM SIDE
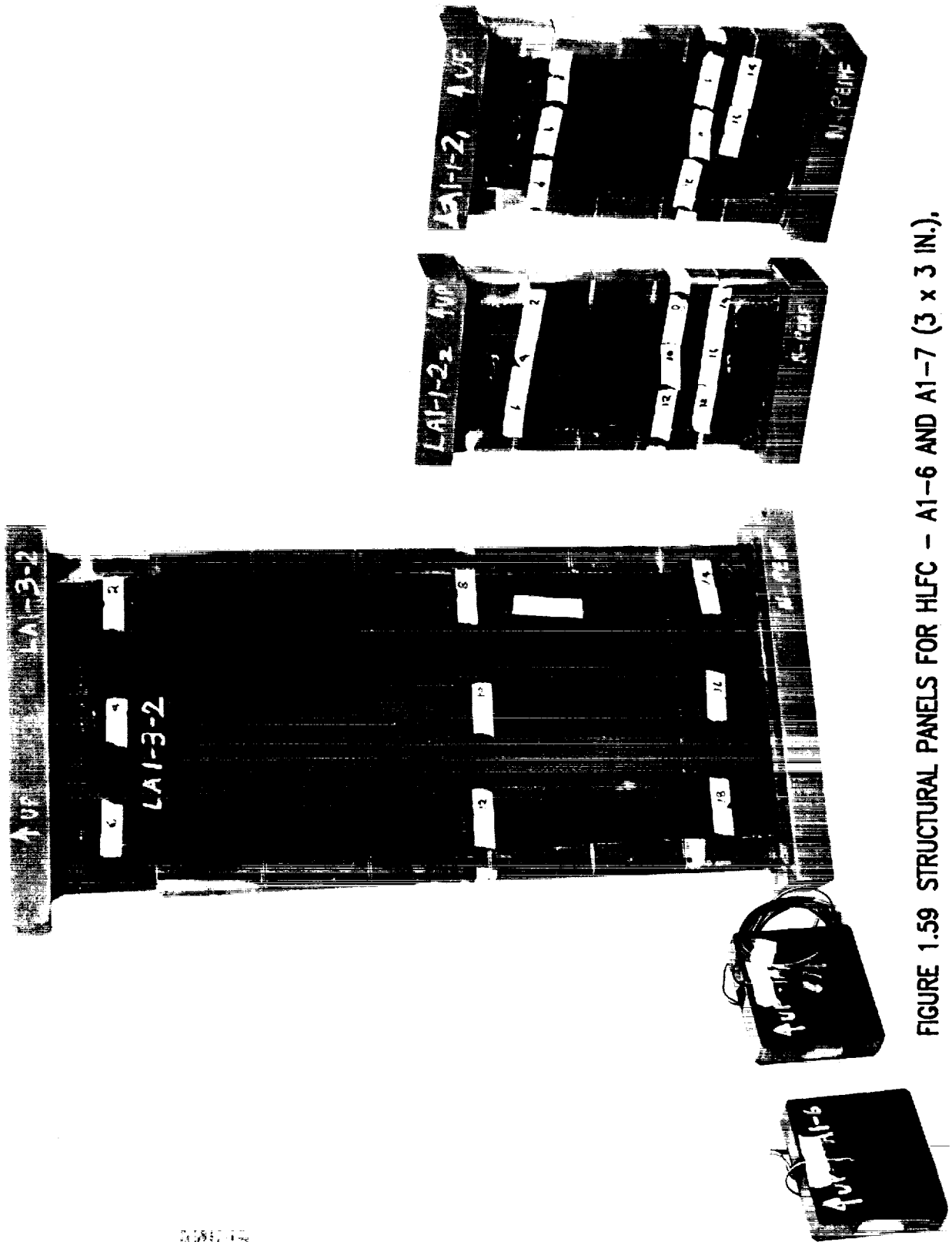
FIGURE 1.59 STRUCTURAL PANELS FOR HLFC — A1–6 AND A1–7 (3 x 3 IN.), LA1–3–2 (8 x 20 IN.), AND LA1–1–2₂ AND LA1–1–2₁ (4.5 x 10 IN.) — COMPOSITE SIDE
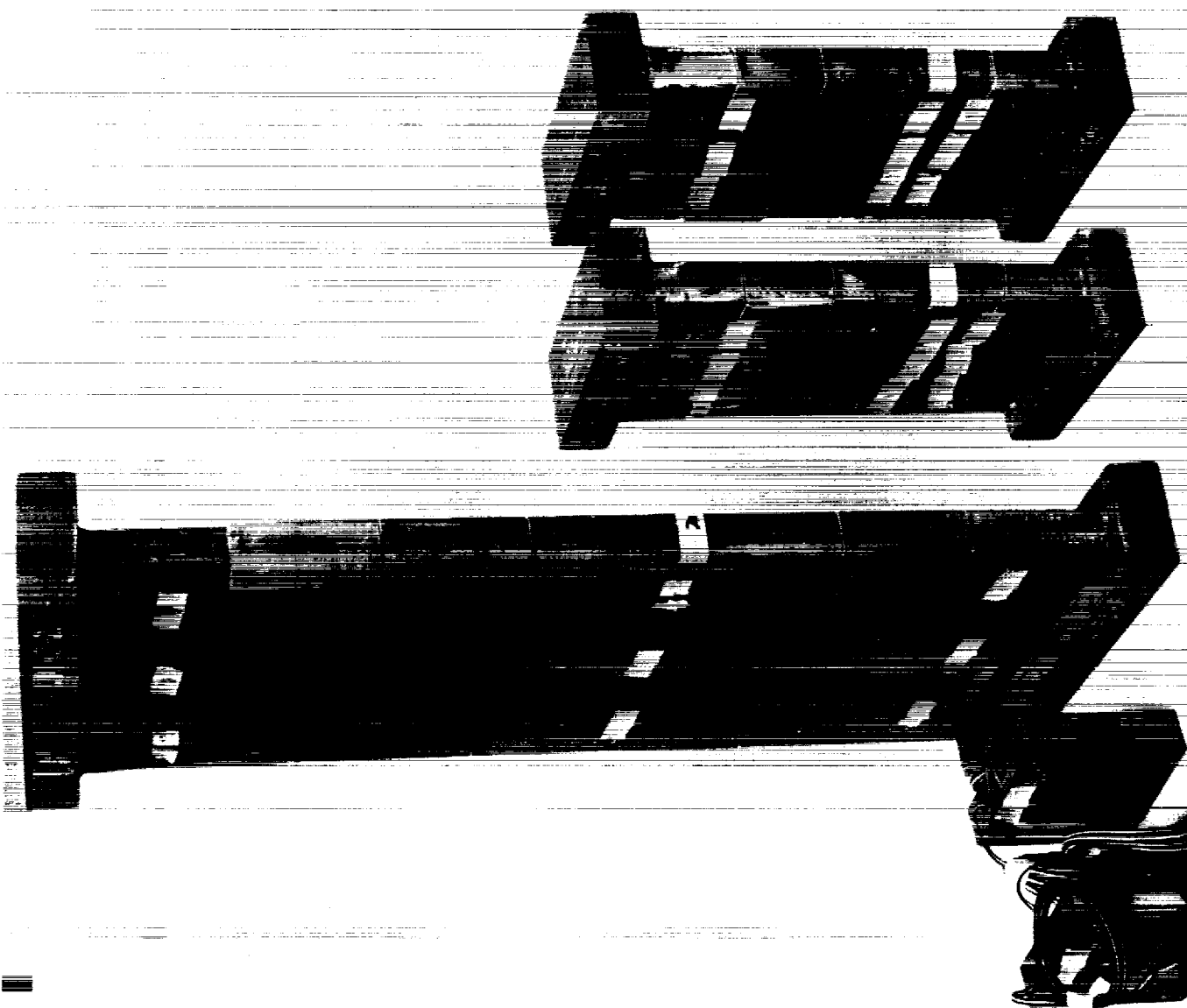
FIGURE 1.60 STRUCTURAL PANELS FOR HLFC — A1–6 AND A1–7 (3 x 3 IN.), LA1–3–2 (8 x 20 IN.), AND LA1–1–2$_2$ AND LA1–1–2$_1$ (4.5 x 10 IN.) — SIDE VIEW
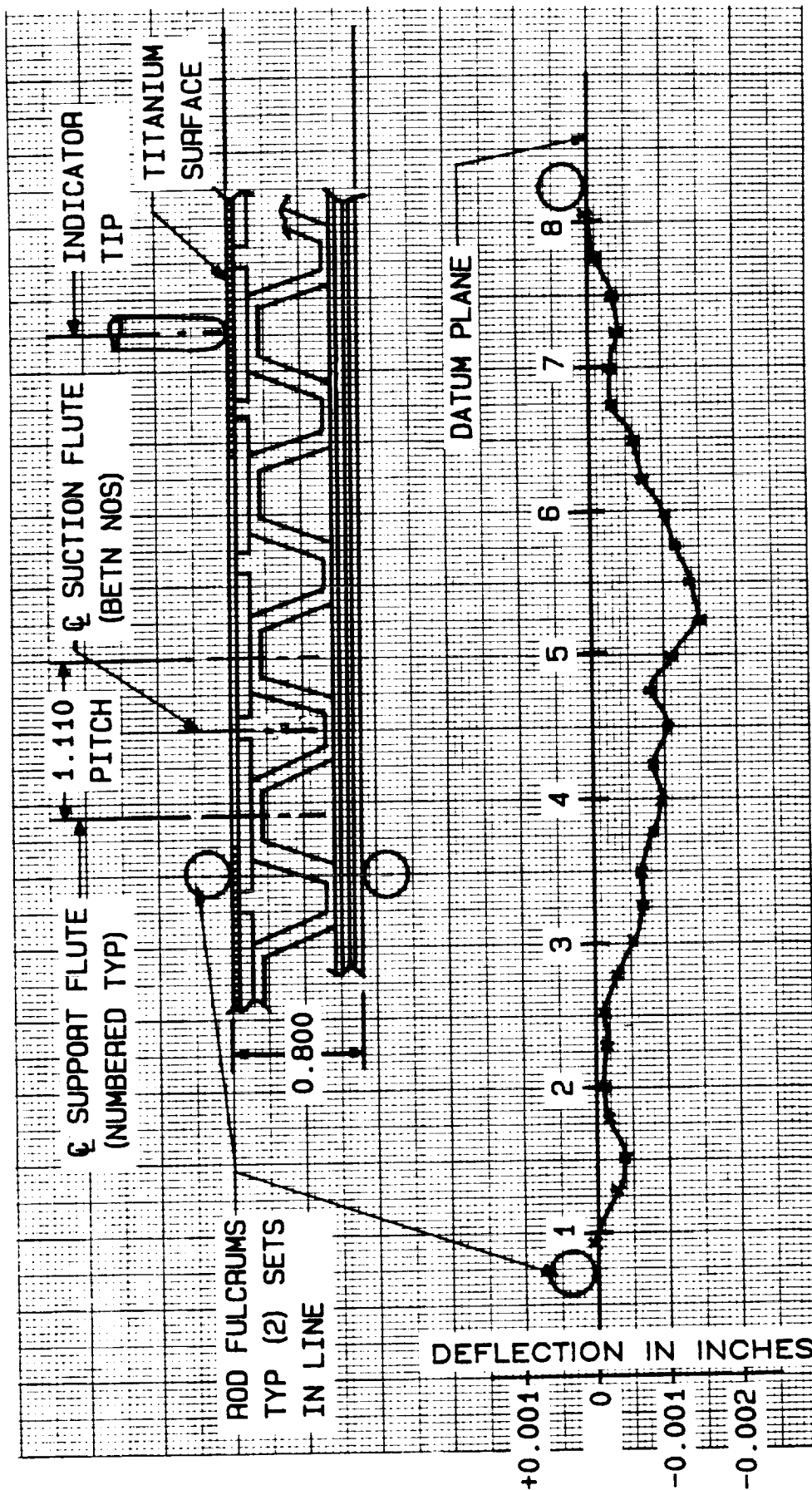
FIGURE 1.61 WAVINESS AND WARPAGE DEFLECTIONS FOR PANEL LA1-11-1
(PERFORATED 12- BY 20-INCH PANEL)
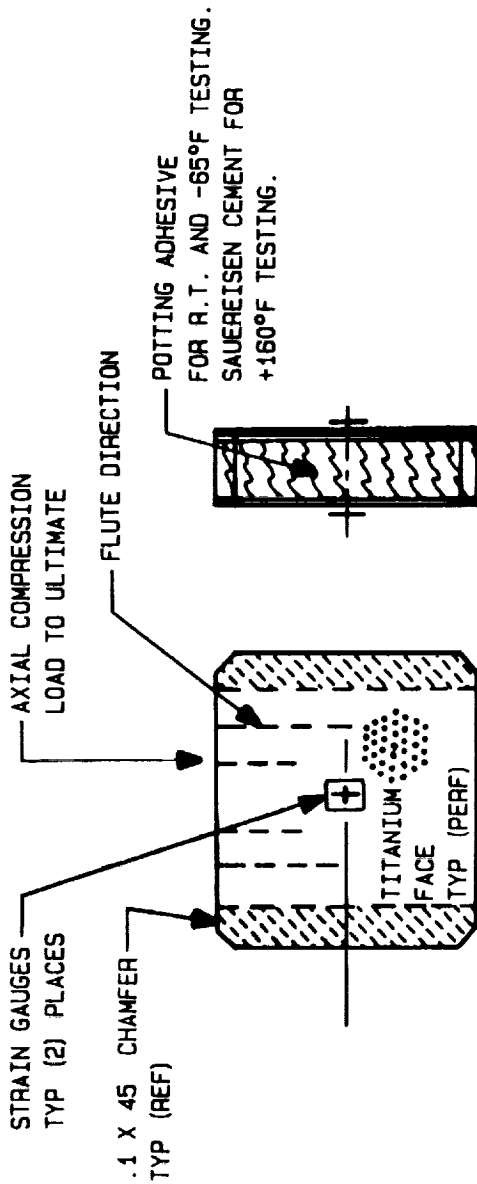
SIZE (IN.)	BATCH NO.	IDENT. NO.	TEST CONDITIONS	ULTIMATE LOAD (LBS)	MAXIMUM STRAIN TI (MICRO IN./IN.)	MAXIMUM STRAIN C/E (MICRO IN./IN.)	DATE TEST	LOADING SURFACES
3W x 3H	LA1-11-1P	AA1	DRY R.T.	31,050	-8,220	-6,330	10-28-85	(4) Al FOIL
		AA2	DRY R.T.	33,900	-8,454	-6,483	10-28-85	(4) Al FOIL
		AA3	WET R.T. ▲	34,050	-8,279	-7,890	10-28-85	(4) Al FOIL
		AA4	DRY +160°F	25,250	-7,034	-6,254	10-28-85	(4) Al FOIL
		AA5	DRY +160°F	22,000	-5,770	-5,230	10-28-85	(4) Al FOIL
		AA6	WET +160°F ▲	21,650	-5,991	-5,664	10-28-85	Al SHEET *
		AA7	DRY -65°F	29,850	-4,815	-7,343	10-30-85	Al SHEET *
		AA8	DRY -65°F	25,700	-4,842	-7,310	10-30-85	Al SHEET *
		AA9	WET -65°F ▲	47,700	-12,195	-9,912	10-30-85	Al & Ti SHEETS **
2 1/2W x 3H	LA1-12-1P	AA10	DRY R.T.	23,850	-7,580	-5,390	10-28-85	(4) Al FOIL
		AA11	DRY +160°F	16,060	-5,410	-3,755	10-28-85	Al SHEET *
		AA12	DRY +160°F	15,980	-4,702	-4,365	10-28-85	Al SHEET *
		AA13	DRY R.T.	23,850	-7,670	-5,285	10-28-85	(4) Al FOIL
		AA14	DRY -65°F	25,000	-4,617	-8,920	10-30-85	Al & Ti SHEETS **
		AA15	DRY -65°F	36,000	-11,816	-9,991	10-30-85	Al & Ti SHEETS **

▲ 24 HOUR WATER SOAK PRIOR TO TESTING

* Al SHEET = .020 THICK 2024-0

** Al & Ti SHEETS — Al SHEET = .020 THICK 2024-0
   — Ti SHEET = .025 THICK Ti-6Al-4V

STRAIN GAUGES TYP (2) PLACES

.1 X 45 CHAMFER TYP (REF)

AXIAL COMPRESSION LOAD TO ULTIMATE

FLUTE DIRECTION

POTTING ADHESIVE FOR R.T. AND -65°F TESTING. SAUEREISEN CEMENT FOR +160°F TESTING.

TITANIUM FACE TYP (PERF)

FIGURE 1.62 SUMMARY OF 3- BY 3-INCH PANELS WITH "F" AND "G" CURE CYCLES - LOAD AND STRAIN

FIGURE 1.63 3– BY 3–INCH PANEL AA2, FROM BATCH NO. LA1–11–1P, DRY AT ROOM TEMPERATURE

153

FIGURE 1.64 3- BY 3-INCH PANEL AA3, FROM BATCH NO. LA1-11-1P, WET AT ROOM TEMPERATURE
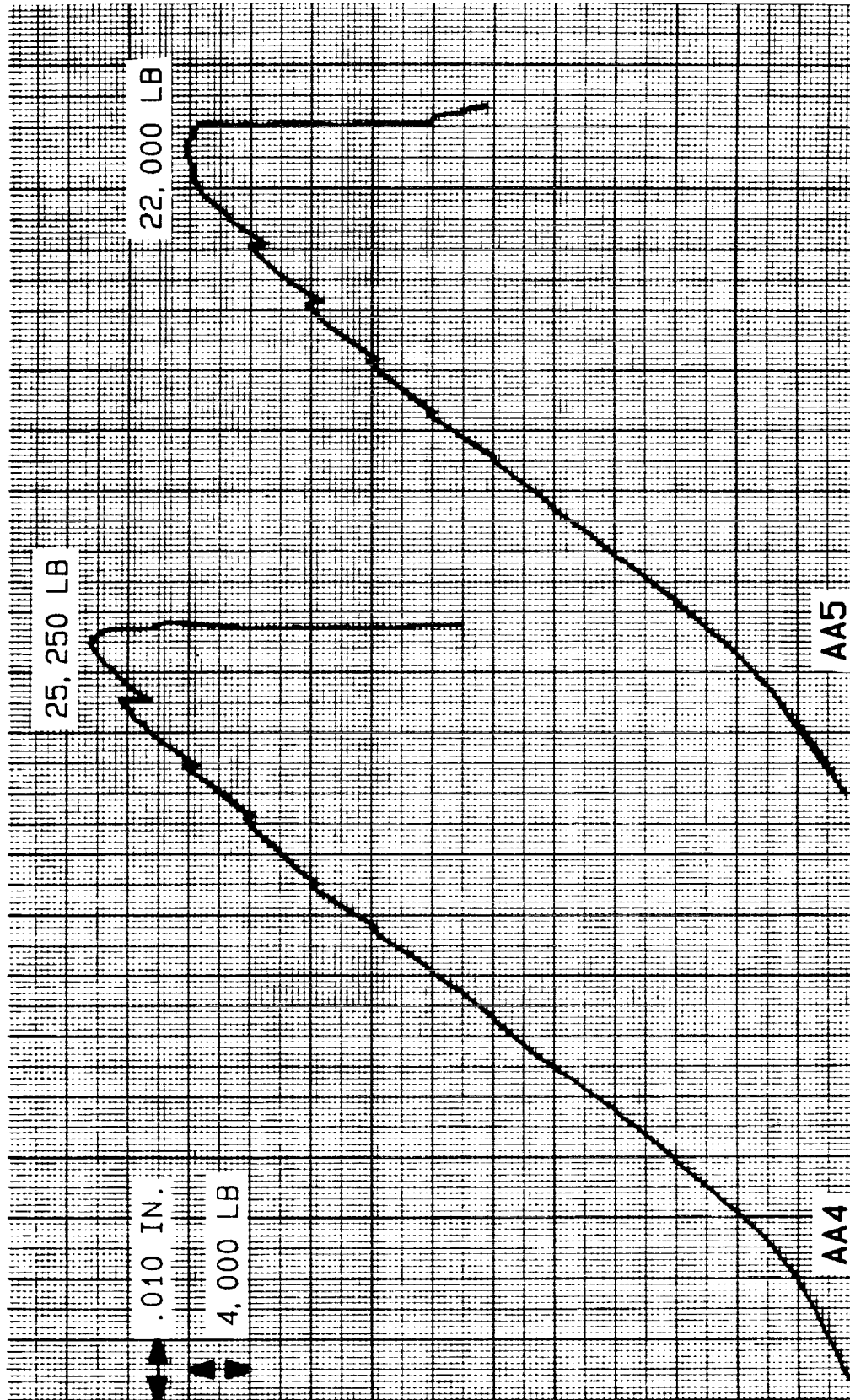
FIGURE 1.65 LOAD VERSUS HEAD TRAVEL FOR PANELS
AA4 AND AA5 AT +160°F

155
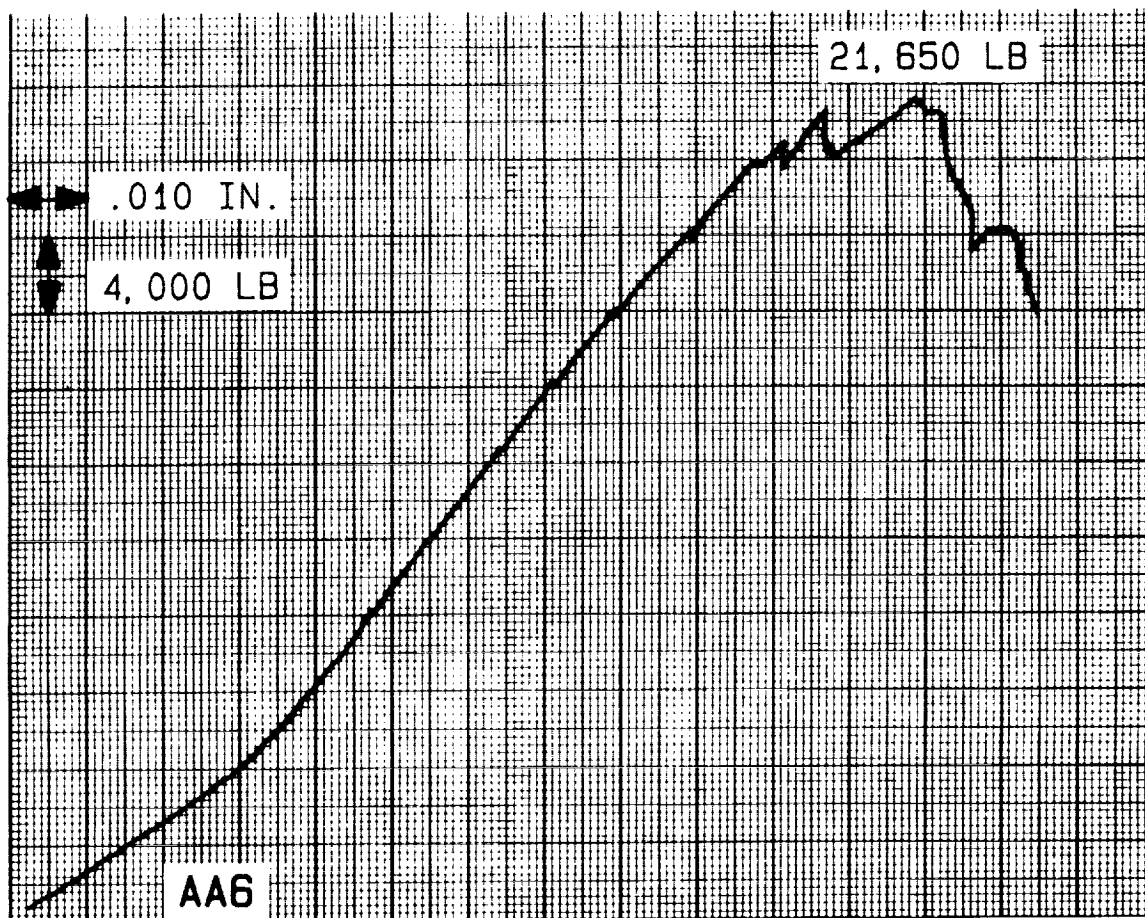
FIGURE 1.66 LOAD VERSUS HEAD TRAVEL FOR PANEL AA6 AT +160°F, WET
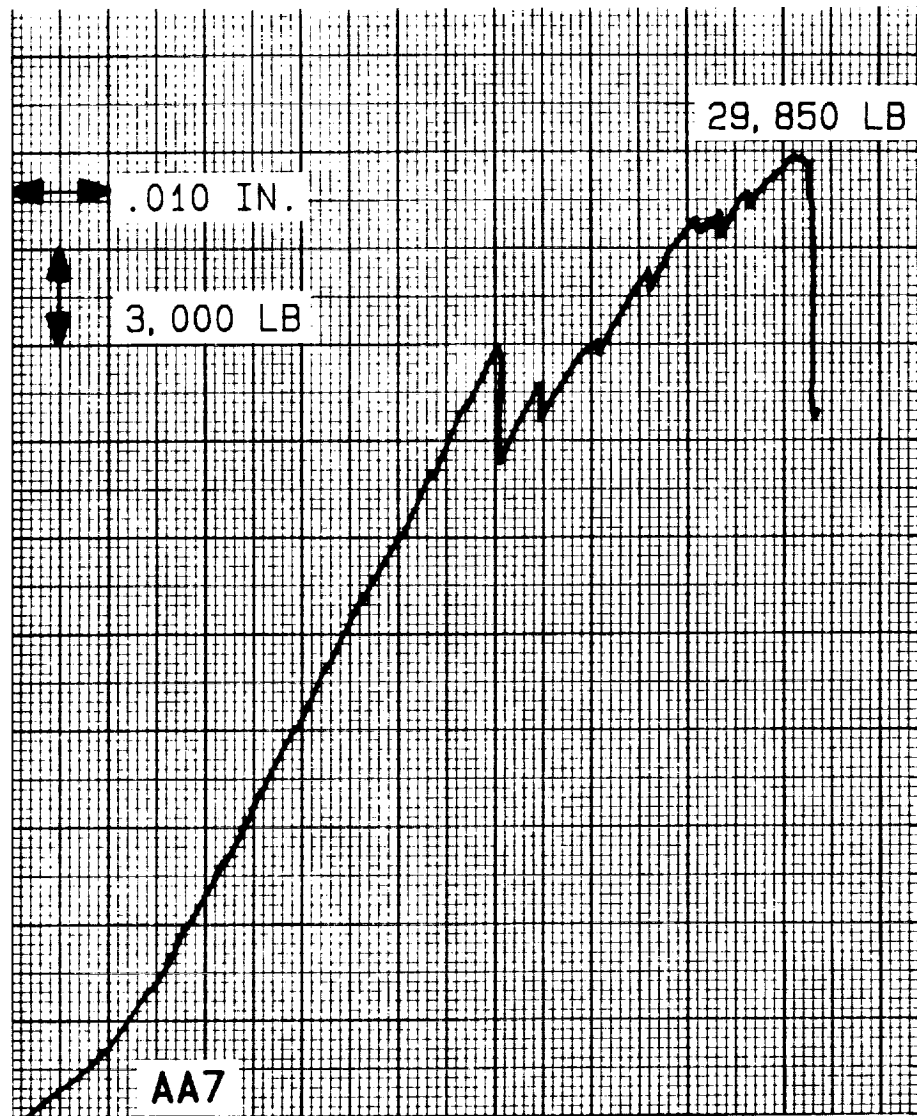
FIGURE 1.67 LOAD VERSUS HEAD TRAVEL FOR PANEL AA7 AT −65°F
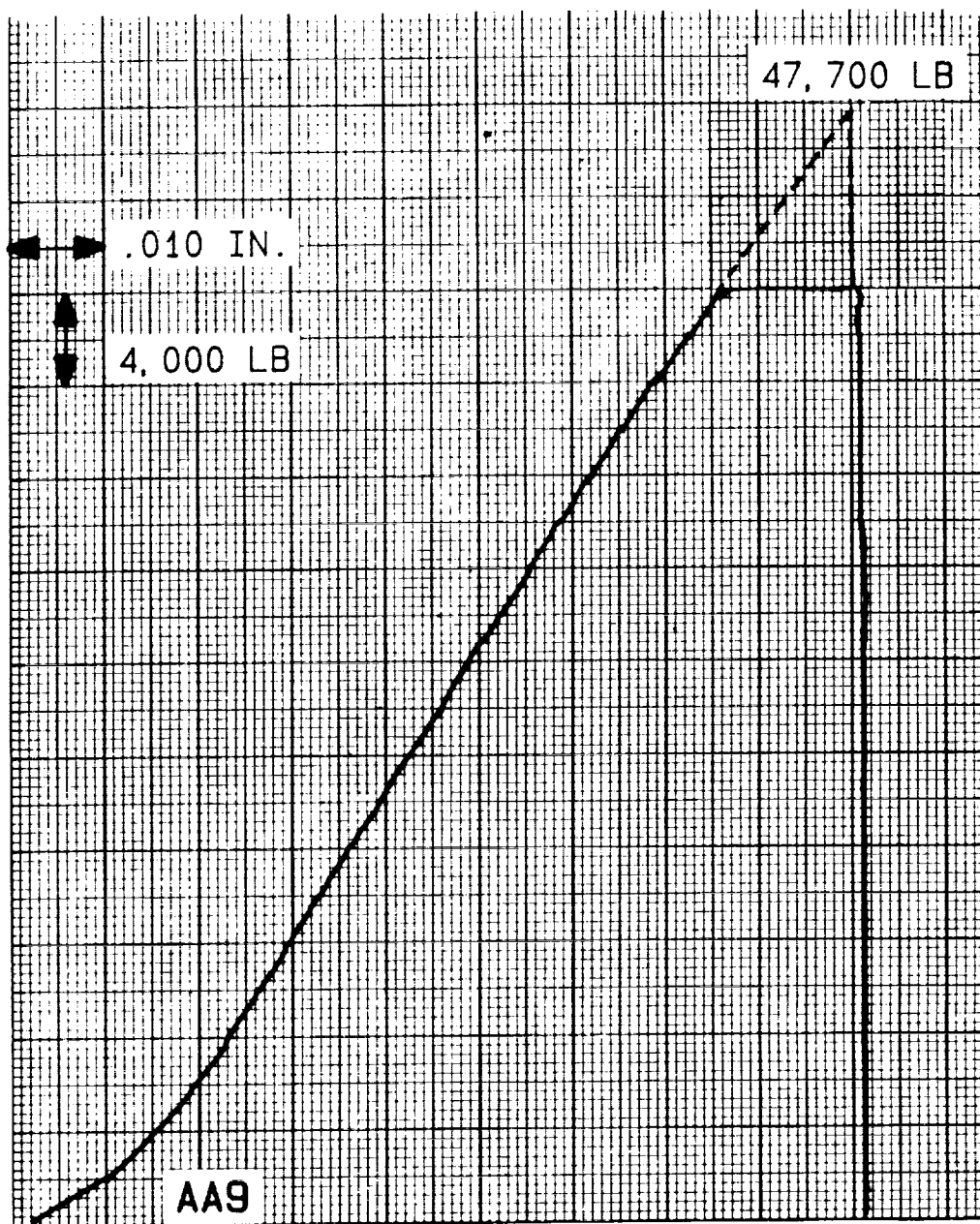
FIGURE 1.68 LOAD VERSUS HEAD TRAVEL FOR PANEL AA9 AT −65°F, WET

FIGURE 1.69 3— BY 3—INCH PANEL AA9, FROM BATCH NO. LA1—11—1P, WET AT —65F

159
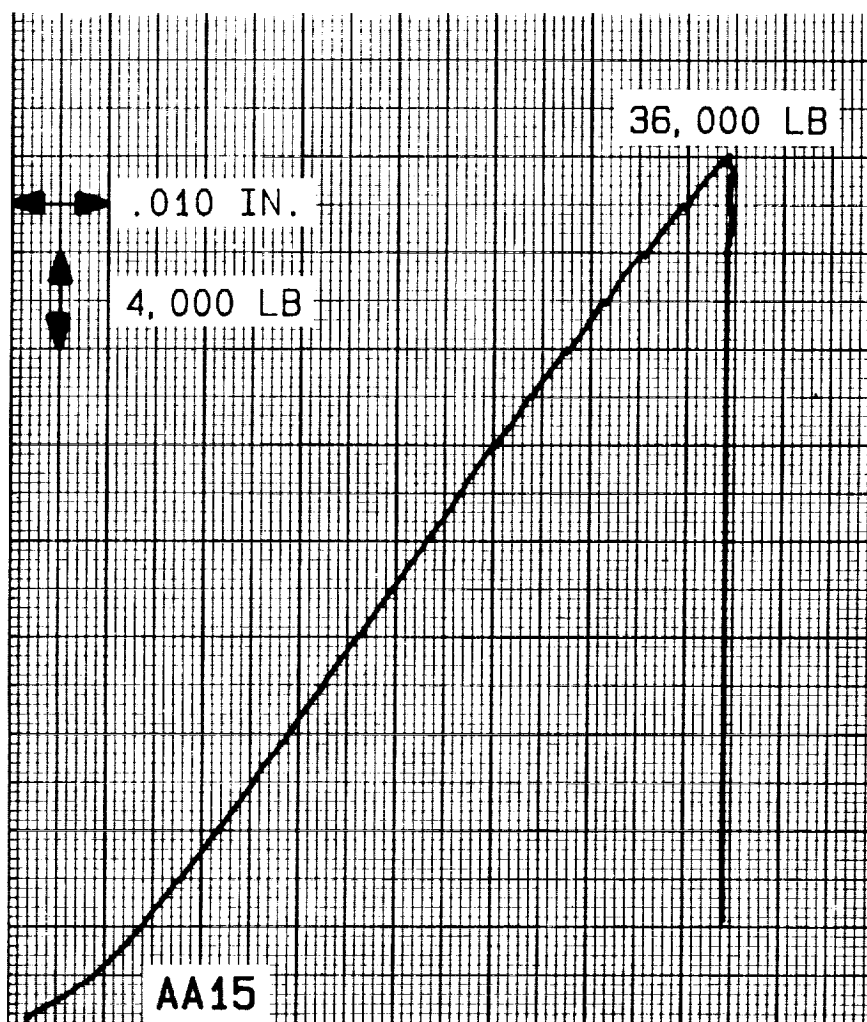
FIGURE 1.70 LOAD VERSUS HEAD TRAVEL FOR PANEL AA15 AT −65°F

↑TOP

FIGURE 1.71 FINAL TEST PANELS – BEFORE TESTING
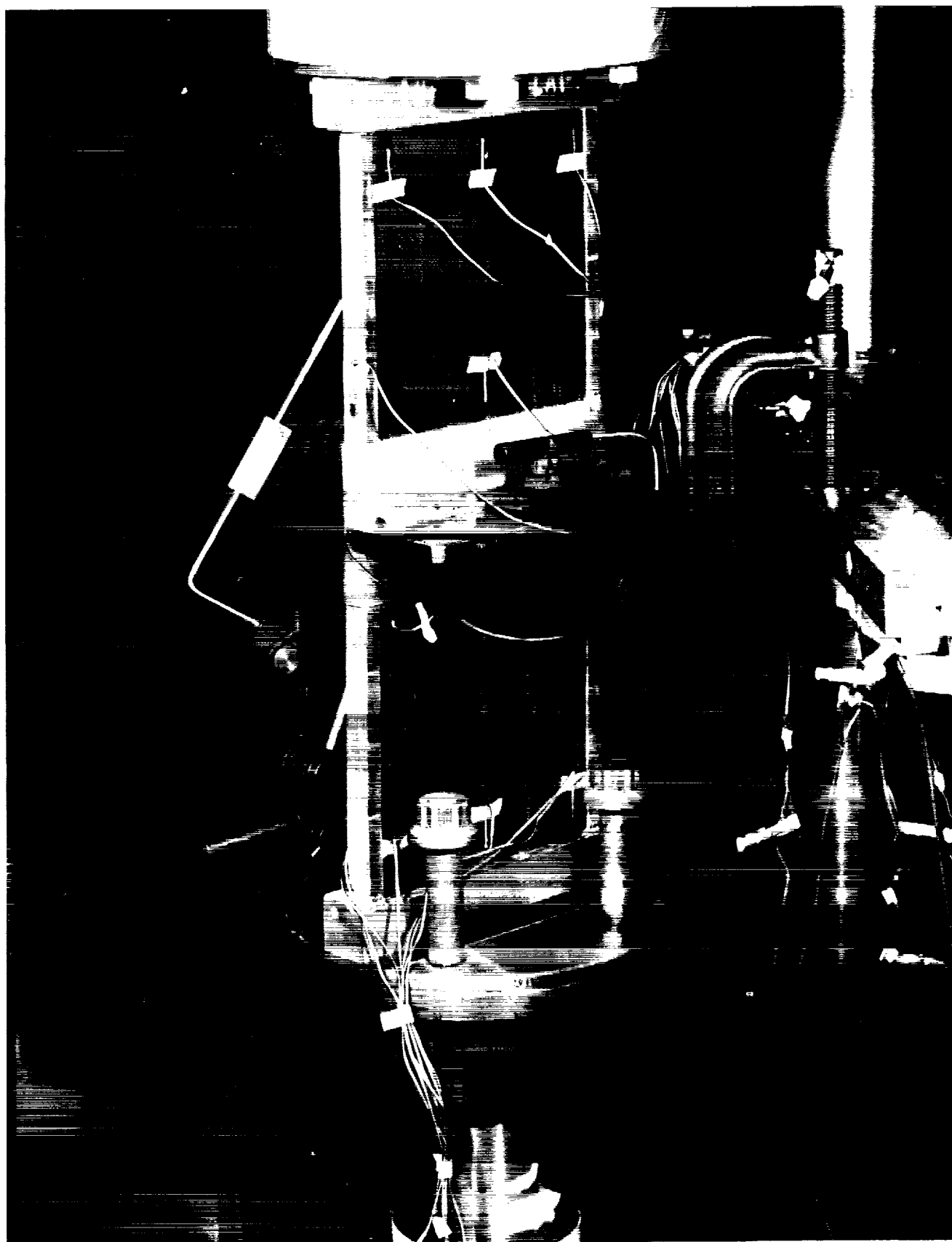
FIGURE 1.72 PANEL LA1-14P COMPRESSION TEST SET-UP -
COMPOSITE SIDE - BEFORE TEST

162
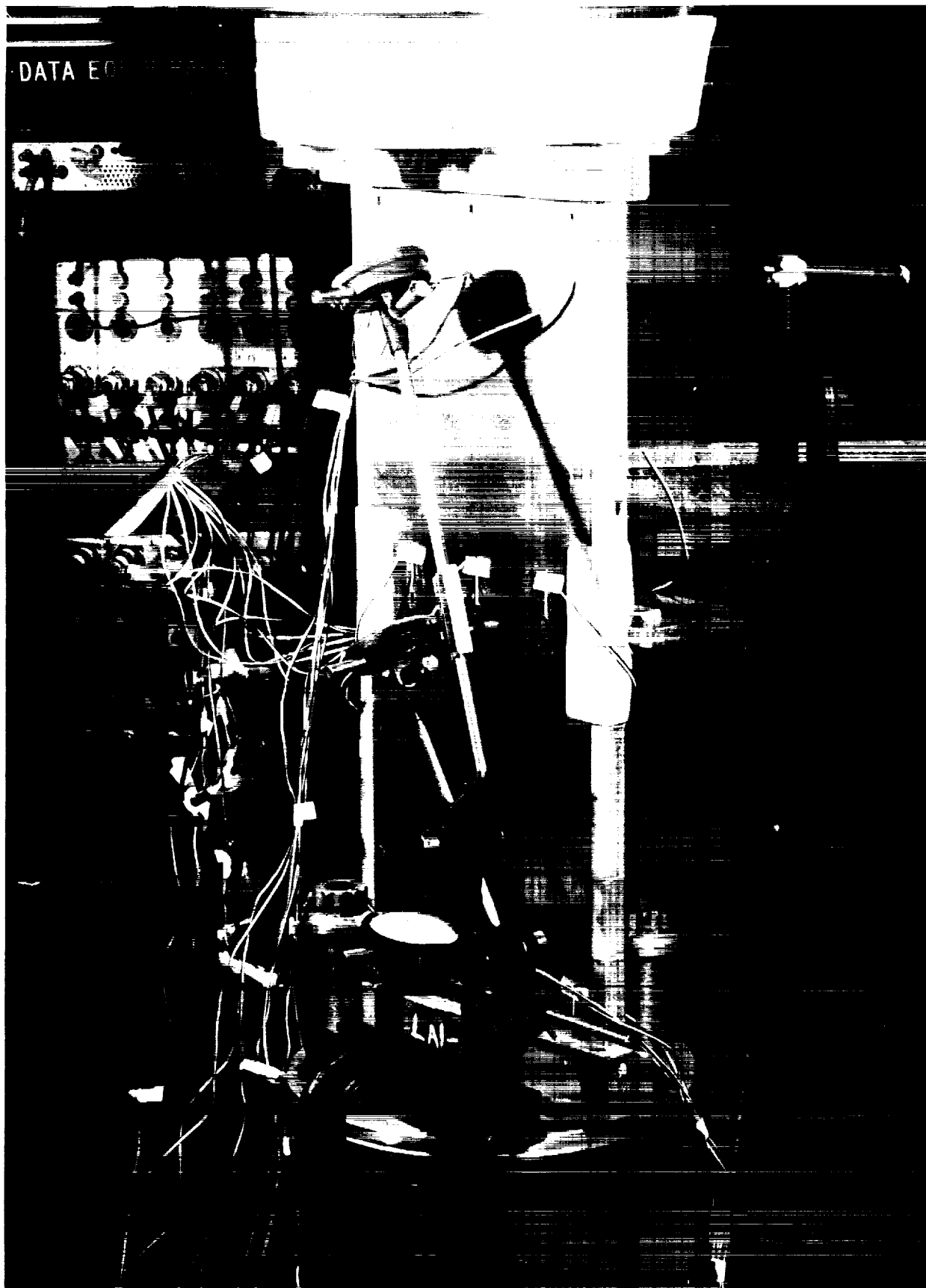
FIGURE 1.73 PANEL LA1-14P COMPRESSION TEST SET-UP -
TITANIUM SIDE - BEFORE TEST

163
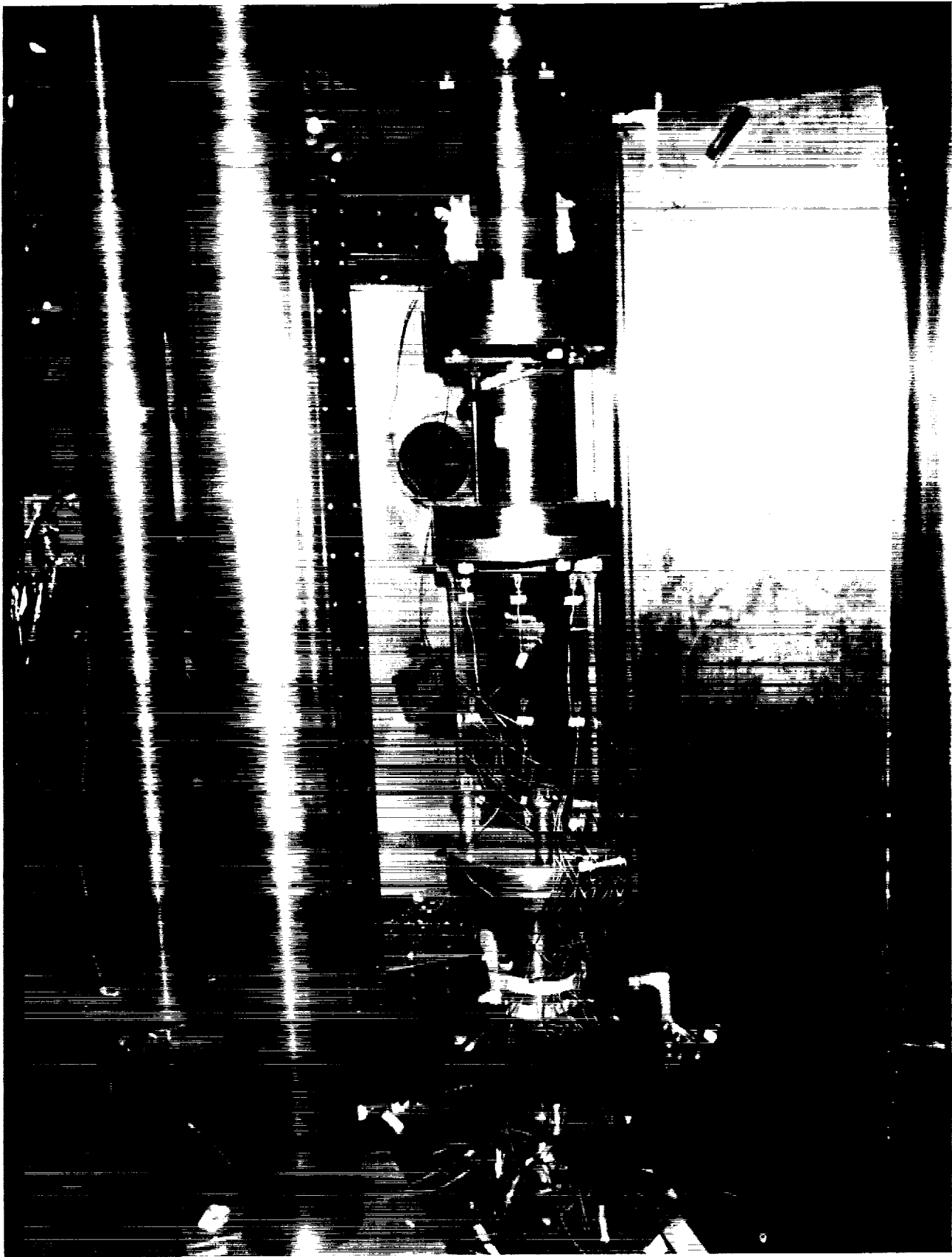
FIGURE 1.74 TEST PANEL LA1-11-2P IN THE ENVIRONMENTAL
CHAMBER READY FOR TEST
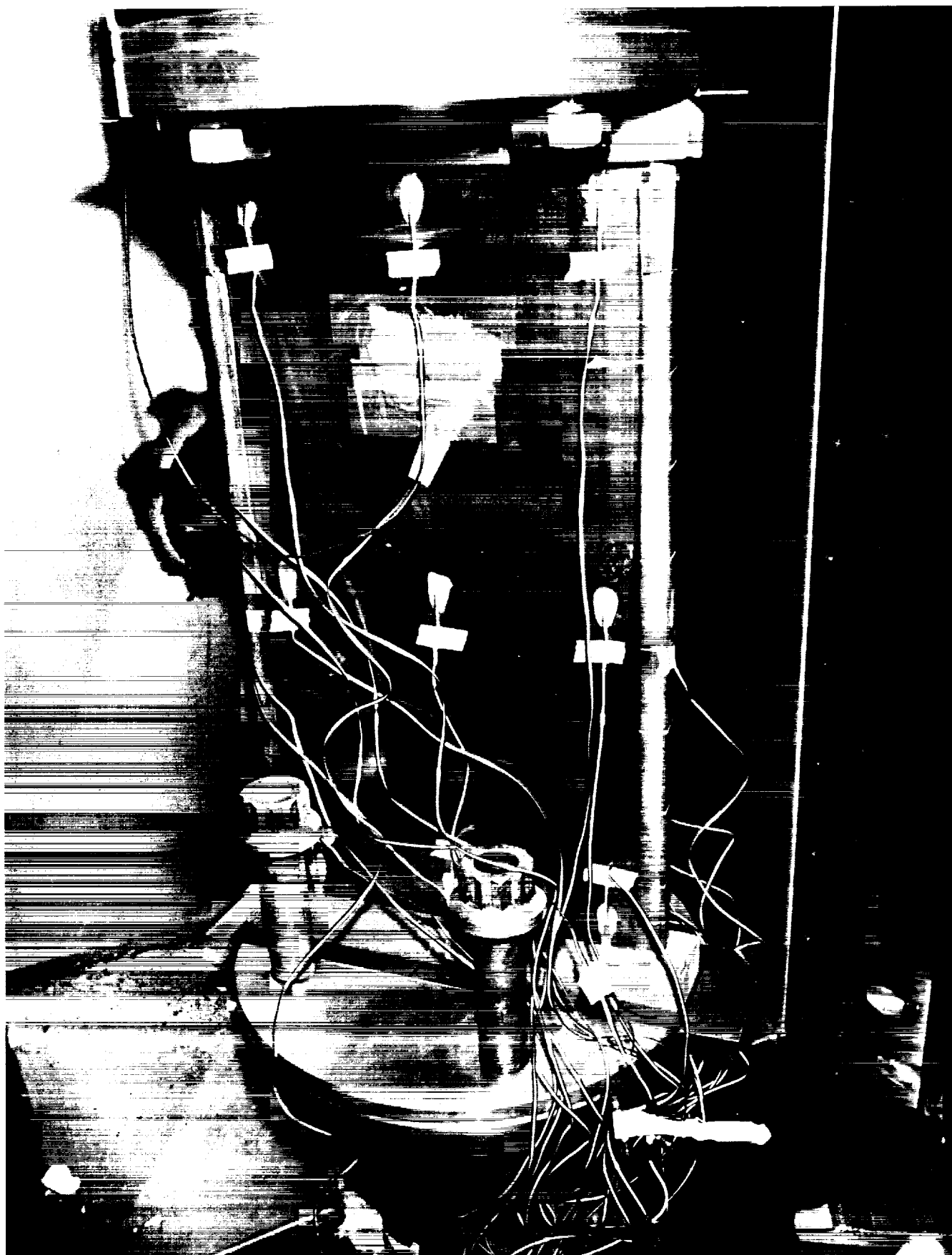
FIGURE 1.75 CLOSE-UP OF TEST SET-UP IN ENVIRONMENTAL CHAMBER BOX — PANEL LA1–11–2P

LA1-12-2P

LA1-12-1P

FIGURE 1.76 TITANIUM SIDE, AFTER FAILURE, LA1-12-1P PANEL ON
RIGHT SIDE AND LA1-12-2P PANEL ON LEFT SIDE

166

FIGURE 1.77 COMPOSITE SIDE, AFTER TESTING, PANEL LA1–12–1P TESTED AT −65°F AND PANEL LA1–12–2P TESTED AT +160°F

FIGURE 1.78 END VIEW, AFTER TEST, PANELS LA1-12-2P AND LA1-12-1P
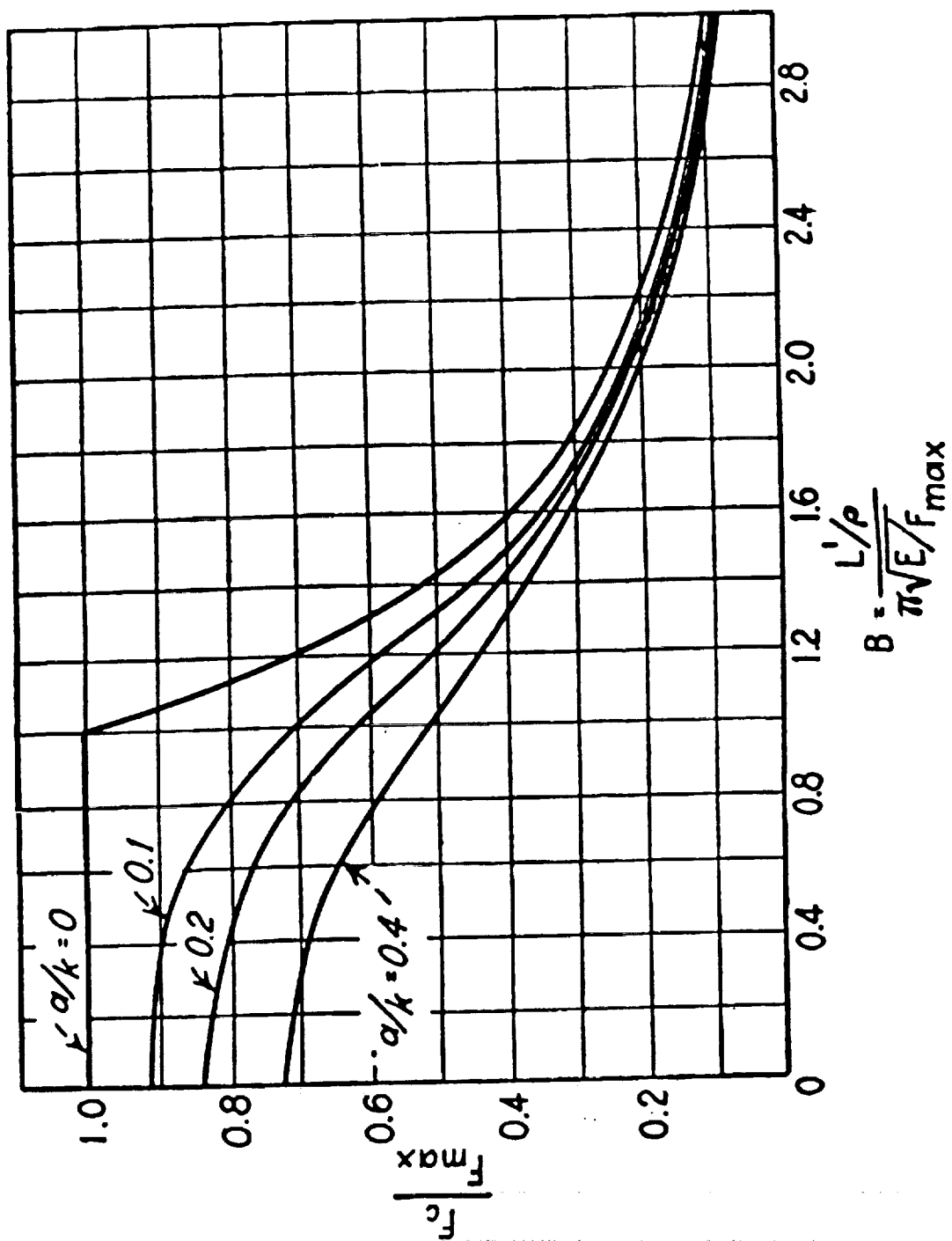
FIGURE 1.79 ECCENTRICITY REDUCTION IN ALLOWABLES
(REF. – AIRCRAFT STRUCTURES, PEERY)
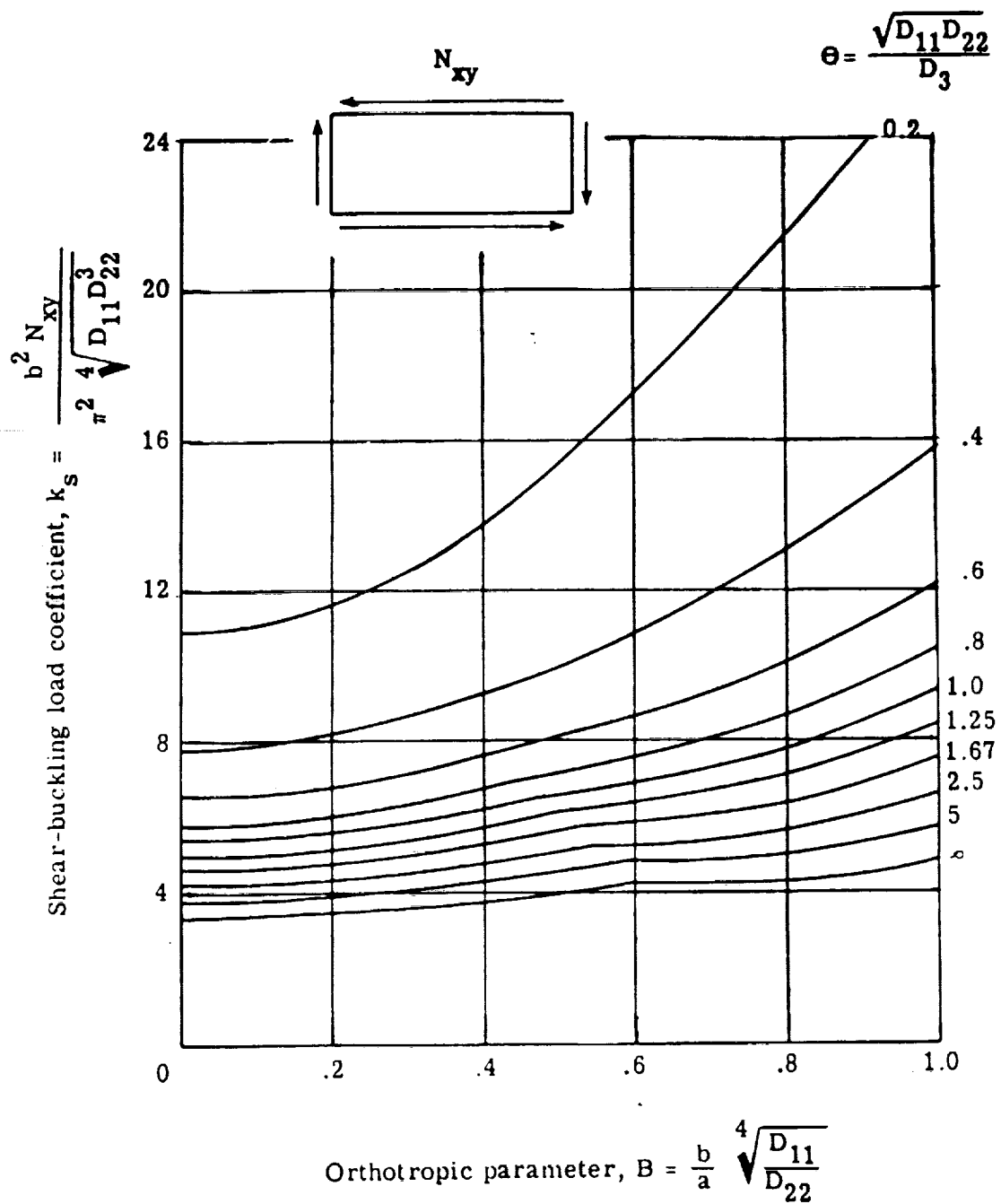
FIGURE 1.80 SHEAR-BUCKLING LOAD COEFFICIENTS FOR RECTANGULAR
ORTHOTROPIC PLATES WITH ALL EDGES SIMPLY SUPPORTED

TABLE 1.1

BUCKLING ANALYSIS OF HAT-STIFFENED MODEL — CASE "A"

PANEL GEOMETRY			MONOLAYER PROPERTIES		
LENGTH	30 IN.		ELASTIC MODULUS ALONG FIBER	12,020,000 psi	
WIDTH	20 IN.		ELASTIC MODULUS ACROSS FIBER	11,300,000 psi	
SPACING	1.300 IN.		SHEAR MODULUS	570,000 psi	
CAP (Wc)	0.800 IN.		POISSONS RATIO	0.0880	
BASE (Wb)	1.200 IN.		THICKNESS	0.0130 IN.	
HEIGHT	0.600 IN.		WEIGHT PER UNIT VOLUME	0.0560 pci	

PLY ORIENTATION

	0°	90°	45°	
SKIN	2	0	2	
CAP	2	0	0	NO. OF LAYERS
BASE	2	0	2	
WEB	0	0	2	

LOCAL AND GENERAL BUCKLING
NORMALIZED TO COLUMN LOAD

SKIN	Nx = 2,179,452 LB/IN.
BASE	Nx = 5,518 LB/IN.
CAP	Nx = 1,517 LB/IN.
WEB	Nx = 23,588 LB/IN.
GENERAL	Nx = 680 LB/IN.

SHEAR BUCKLING

SKIN	Nxy = 1,047,258 LB/IN.
GENERAL	Nxy = 728 LB/IN.

STRAIN = 1,007 MICRO IN./IN. AT Nx = 680 LB/IN.

PROPERTIES OF PANEL

D_{11} = 50,500.3   AREA PER INCH =   0.0933 SQ IN./IN.
D_{22} =   136.9   EA PER INCH   = 674,907 LB/IN.
D_{12} =   50.8   WEIGHT   =   0.7524 psf
D_{66} = 1,173.3

SEE GENERAL DISCUSSION IN THE APPENDIX FOR THE DESCRIPTION OF D_{11}, D_{22}, D_{12}, AND D_{66} WHICH ARE COEFFICIENTS IN THE GOVERNING DIFFERENTIAL EQUATION FOR GENERAL BUCKLING OF THE PANEL

TABLE 1.2

BUCKLING ANALYSIS OF HAT-STIFFENED MODEL – CASE "B"

PANEL GEOMETRY

LENGTH	30 IN.
WIDTH	20 IN.
SPACING	0.638 IN.
CAP (Wc)	0.500 IN.
BASE (Wb)	0.700 IN.
HEIGHT	0.638 IN.

MONOLAYER PROPERTIES

ELASTIC MODULUS ALONG FIBER	8,400,000 psi
ELASTIC MODULUS ACROSS FIBER	2,500,000 psi
SHEAR MODULUS	800,000 psi
POISSONS RATIO	0.2200
THICKNESS	0.0051 IN.
WEIGHT PER UNIT VOLUME	0.0920 pci

PLY ORIENTATION

	0°	90°	45°
SKIN	6	6	0
CAP	6	6	0
BASE	6	6	0
WEB	4	4	0

$\left.\right\}$ NO. OF LAYERS

LOCAL AND GENERAL BUCKLING
NORMALIZED TO COLUMN LOAD

SKIN	N_x = 1,169,863 LB/IN.
BASE	N_x = 23,413 LB/IN.
CAP	N_x = 40,689 LB/IN.
WEB	N_x = 10,842 LB/IN.
GENERAL	N_x = 958 LB/IN.

SHEAR BUCKLING

| SKIN | N_{xy} = 410,910 LB/IN. |
| GENERAL | N_{xy} = 922 LB/IN. |

STRAIN = 912 MICRO IN./IN. AT N_x = 958 LB/IN.

PROPERTIES OF PANEL

D_{11} = 76,664.7
D_{22} = 178.4
D_{12} = 18.0
D_{66} = 1,075.3

AREA PER INCH = 0.1918 SQ IN./IN.
EA PER INCH = 1,049,560 LB/IN.
WEIGHT = 2.5404 psf

SEE GENERAL DISCUSSION IN THE APPENDIX FOR THE DESCRIPTION OF D_{11}, D_{22}, D_{12}, AND D_{66} WHICH ARE COEFFICIENTS IN THE GOVERNING DIFFERENTIAL EQUATION FOR GENERAL BUCKLING OF THE PANEL

TABLE 1.3

BUCKLING ANALYSIS OF HAT-STIFFENED MODEL – CASE "C"

PANEL GEOMETRY			MONOLAYER PROPERTIES		
LENGTH	20 IN.		ELASTIC MODULUS ALONG FIBER	8,400,000 psi	
WIDTH	20 IN.		ELASTIC MODULUS ACROSS FIBER	2,500,000 psi	
SPACING	0.638 IN.		SHEAR MODULUS	800,000 psi	
CAP (Wc)	0.500 IN.		POISSONS RATIO	0.2200	
BASE (Wb)	0.700 IN.		THICKNESS	0.0051 IN.	
HEIGHT	0.638 IN.		WEIGHT PER UNIT VOLUME	0.0920 pci	

PLY ORIENTATION

	0°	90°	45°	
SKIN	6	6	0	
CAP	6	6	0	NO. OF LAYERS
BASE	6	6	0	
WEB	4	4	0	

LOCAL AND GENERAL BUCKLING
NORMALIZED TO COLUMN LOAD

SKIN	Nx = 962,581 LB/IN.
BASE	Nx = 23,413 LB/IN.
CAP	Nx = 40,689 LB/IN.
WEB	Nx = 10,841 LB/IN.
GENERAL	Nx = 2,003 LB/IN.

SHEAR BUCKLING

SKIN	Nxy = 410,939 LB/IN.
GENERAL	Nxy = 1,965 LB/IN.

STRAIN = 1,908 MICRO IN./IN. AT Nx = 2,003 LB/IN.

PROPERTIES OF PANEL

D_{11} = 76,664.7   AREA PER INCH =   0.1918 SQ IN./IN.
D_{22} =   178.4   EA PER INCH   = 1,049,560 LB/IN.
D_{12} =   18.0   WEIGHT   =   2.5404 psf
D_{66} =   1,075.3

SEE GENERAL DISCUSSION IN THE APPENDIX FOR THE DESCRIPTION OF D_{11}, D_{22}, D_{12}, AND D_{66} WHICH ARE COEFFICIENTS IN THE GOVERNING DIFFERENTIAL EQUATION FOR GENERAL BUCKLING OF THE PANEL

173

TABLE 1.4

BUCKLING ANALYSIS OF HAT-STIFFENED MODEL - CASE "D"

PANEL GEOMETRY

		MONOLAYER PROPERTIES	
LENGTH	15 IN.	ELASTIC MODULUS ALONG FIBER	8,400,000 psi
WIDTH	20 IN.	ELASTIC MODULUS ACROSS FIBER	2,500,000 psi
SPACING	0.638 IN.	SHEAR MODULUS	800,000 psi
CAP (Wc)	0.500 IN.	POISSONS RATIO	0.2200
BASE (Wb)	0.700 IN.	THICKNESS	0.0051 IN.
HEIGHT	0.638 IN.	WEIGHT PER UNIT VOLUME	0.0920 pci

PLY ORIENTATION

	0°	90°	45°	
SKIN	6	6	0	
CAP	6	6	0	NO. OF LAYERS
BASE	6	6	0	
WEB	4	4	0	

LOCAL AND GENERAL BUCKLING
NORMALIZED TO COLUMN LOAD

SKIN	Nx = 962,574 LB/IN.
BASE	Nx = 23,413 LB/IN.
CAP	Nx = 40,689 LB/IN.
WEB	Nx = 10,842 LB/IN.
GENERAL	Nx = 3,472 LB/IN.

SHEAR BUCKLING

SKIN	Nxy = 410,971 LB/IN.
GENERAL	Nxy = 3,428 LB/IN.

STRAIN = 3,308 MICRO IN./IN. AT Nx = 3,472 LB/IN.

PROPERTIES OF PANEL

D_{11} = 76,664.7   AREA PER INCH =   0.1918 SQ IN./IN.
D_{22} =   178.4   EA PER INCH   = 1,049,560 LB/IN.
D_{12} =   18.0   WEIGHT   =   2.5404 psf
D_{66} =   1,075.3

SEE GENERAL DISCUSSION IN THE APPENDIX FOR THE DESCRIPTION OF D_{11}, D_{22}, D_{12}, AND D_{66} WHICH ARE COEFFICIENTS IN THE GOVERNING DIFFERENTIAL EQUATION FOR GENERAL BUCKLING OF THE PANEL

174

TABLE 1.5

BUCKLING ANALYSIS OF HAT-STIFFENED MODEL – CASE "1"

PANEL GEOMETRY			MONOLAYER PROPERTIES
LENGTH	15 IN.		ELASTIC MODULUS ALONG FIBER	5,550,000 psi
WIDTH	30 IN.		ELASTIC MODULUS ACROSS FIBER	5,550,000 psi
SPACING	0.980 IN.		SHEAR MODULUS	435,000 psi
CAP (Wc)	0.360 IN.		POISSONS RATIO	0.1145
BASE (Wb)	0.660 IN.		THICKNESS	0.0100 IN.
HEIGHT	1.000 IN.		WEIGHT PER UNIT VOLUME	0.0636 pci

PLY ORIENTATION

	0°	90°	45°	
SKIN	6	6	0
CAP	6	6	0	NO. OF LAYERS
BASE	6	6	0
WEB	4	4	0

LOCAL AND GENERAL BUCKLING
NORMALIZED TO COLUMN LOAD

			SHEAR BUCKLING
SKIN	N_x = 1,082,255 LB/IN.		SKIN	N_{xy} = 542,334 LB/IN.
BASE	N_x = 185,298 LB/IN.		GENERAL	N_{xy} = 11,396 LB/IN.
CAP	N_x = 481,002 LB/IN.
WEB	N_x = 27,099 LB/IN.
GENERAL	N_x = 12,997 LB/IN.

STRAIN = 7,114 MICRO IN./IN. AT N_x = 12,997 LB/IN.

PROPERTIES OF PANEL

D_{11} = 295,154.8   AREA PER INCH =   0.3292 SQ IN./IN.
D_{22} =   989.8   EA PER INCH = 1,826,913 LB/IN.
D_{12} =   113.3   WEIGHT   =   3.0147 psf
D_{66} = 1,025.3

SEE GENERAL DISCUSSION IN THE APPENDIX FOR THE DESCRIPTION OF D_{11}, D_{22}, D_{12}, AND D_{66} WHICH ARE COEFFICIENTS IN THE GOVERNING DIFFERENTIAL EQUATION FOR GENERAL BUCKLING OF THE PANEL

175

TABLE 1.6

BUCKLING ANALYSIS OF CORRUGATED SANDWICH MODEL – CASE XVIII

MATERIAL CODES FOR LAMINA (INCHES)
```
1 - CARBON/EPOXY TAPE          (T=0.005)    5 - E-GLASS CLOTH          (T=0.010)
2 - CARBON/EPOXY CLOTH         (T=0.010)    6 - F584/IM6 CARBON/EPOXY  (T=0.0055)
3 - KEVLAR/EPOXY CLOTH         (T=0.010)    7 - TITANIUM MATERIAL      (T=0.0050)
4 - K/E THIN COCURED FACINGS   (T=0.010)    8 - ADDITIONAL MATERIAL IF ANY
```

MONOLAYER PROPERTIES FOR LAMINA

CODE	E_L (psi)	E_T (psi)	G_{LT} (psi)	ν_{LT}	Rho (pci)
2	0.8200E+07	0.8200E+07	0.5700E+06	0.0990	0.0571
5	0.2900E+07	0.2900E+07	0.3000E+06	0.1300	0.0700
7	0.1640E+08	0.1640E+08	0.6200E+07	0.3100	0.1600

PANEL GEOMETRY AND STIFFENER SPACING (INCHES)
```
LENGTH = 15.000     WIDTH = 20.000      SPACING = 1.020
BASE   =  0.400     CAP   =  0.510      HEIGHT  = 0.613
```

ANGLE (A) AND MATERIAL CODE (C) OF EACH PLY (P)
```
ONLY FOR UPPER SKIN
P   1    2    3    4    5
A   0    0    0    0    0
C   7    7    7    7    7
ONLY FOR LOWER SKIN
P   1    2    3    4    5
A   0    0    0    0    0
C   5    2    2    2    5
ONLY FOR BASE
P   1    2    3    4    5
A   0    0    0    0    0
C   5    5    5    5    2
ONLY FOR CAP
P   1    2    3    4    5    6    7    8    9
A   0    0    0    0    0    0    0    0    0
C   5    5    5    5    2    5    5    5    5
ONLY FOR WEB
P   1    2    3    4
A   0    0    0    0
C   5    5    5    5
```

LOCAL AND GENERAL BUCKLING
NORMALIZED TO COLUMN LOAD

			SHEAR BUCKLING NORMALIZED TO PANEL LOAD		
UPPER SKIN	Nx =	9,508 LB/IN.	UPPER SKIN	Nxy =	3,650 LB/IN.
LOWER SKIN	Nx =	19,024 LB/IN.	LOWER SKIN	Nxy =	35,982 LB/IN.
WEB	Nx =	8,524 LB/IN.	WEB	Nxy =	88,792 LB/IN.
GENERAL	Nx =	4,747 LB/IN.	GENERAL	Nxy =	14,767 LB/IN.

STRAIN = 5,427 MICRO IN./IN. AT Nx = 4,747 LB/IN.

PROPERTIES OF PANEL
```
D11 = 65,725.0     AREA PER INCH = 0.1181 SQ IN./IN.
D22 = 55,530.2     EA PER INCH   = 874,834 LB/IN.
D12 = 10,170.9     WEIGHT        = 1.4420 psf
D66 =  5,995.8
```
17€

TABLE 1.7
CLOSED SANDWICH PANEL DETAILS — CASES I TO XXIII

KEY DESCRIPTION PARAMETERS: L = LENGTH OF PANEL, W = WIDTH OF PANEL, S = SPACING OF PANEL, b = BASE, c = CAP

CASE NUMBER	KEY DESCRIPTION PARAMETERS	UPPER SKIN BUCKLING (LB/IN.)	LOWER SKIN BUCKLING (LB/IN.)	WEB BUCKLING (LB/IN.)	GENERAL BUCKLING (LB/IN.)	CRITICAL STRAIN (MICRO IN./IN.)	CRITICAL LOADING (LB/IN.)	HEIGHT OF PANEL (IN.)	PLIES OF TITANIUM AT 0.005 IN./PLY	PLIES OF C/E CLOTH UPPER SKIN IN./PLY	PLIES OF C/E CLOTH FOR LOWER SKIN	PLIES OF F/G CLOTH FOR LOWER SKIN	PLIES OF C/E CLOTH FOR BASE	PLIES OF F/G CLOTH FOR BASE	PLIES OF C/E CLOTH FOR CAP	PLIES OF F/G CLOTH FOR CAP	PLIES OF C/E CLOTH FOR WEB	PLIES OF F/G CLOTH FOR WEB	WEIGHT IN LB/FT2 PANEL	>4500 MICRO IN./IN. ?	ASTERISK ?
I	L=12.5, W=20.0, S=1.02, b=0.51, c=0.4	7750	3439	6141	3634	4823✓	3439	0.613	5	1	2	1	4	1	8	0	4	1	1.285	✓	*
II	L=10.0, W=20.0, S=1.02, b=0.51, c=0.4	7750	3439	6141	5112	4823✓	3439	0.613	5	1	2	1	4	1	8	0	4	1	1.285	✓	*
III	L=15.0, W=20.0, S=1.02, b=0.51, c=0.4	7750	3438	6140	2903	4071	2903	0.613	5	1	2	1	4	1	8	0	4	1	1.285	✗	-
IV	L=20.0, W=20.0, S=1.02, b=0.51, c=0.4	7750	3437	6139	2376	3333	2376	0.613	5	1	2	1	4	1	8	0	4	1	1.285	✗	-
V	COMPLETE REPLICATION OF CASE IV																				
VI	L=20.0, W=20.0, S=1.02, b=0.51, c=0.4	7919	3512	3008	3648	4128	3008	0.75	1	1	2	1	4	1	8	0	4	1	1.3393	✗	-
VII	L=15.0, W=20.0, S=1.02, b=0.51, c=0.4	7919	3513	3008	4481	4128	3008	0.75	1	1	2	1	4	1	8	0	4	1	1.3393	✗	-
VIII	L=15.0, W=20.0, S=1.02, b=0.51, c=0.4	8113	3599	4814	4542	4821✓	3599	0.75	1	1	2	1	4	1	8	0	5	1	1.4013	✓	*
IX	L=15.0, W=20.0, S=1.02, b=0.51, c=0.4	8989	9512	5598	6097	6768✓	5598	0.75	2	1	2	1	4	1	8	0	5	1	1.4786	✓	*
X	L=12.5, W=20.0, S=1.02, b=0.51, c=0.4	8989	9512	5598	7519	6768✓	5598	0.75	2	1	2	1	4	1	8	0	5	1	1.4786	✓	*
XI	COMPLETE REPLACATION OF CASE X																				
XII	L=12.5, W=20.0, S=1.02, b=0.51, c=0.4	9374	9922	2113	13998	2450	2113	1.00	2	1	2	1	4	1	8	0	5	1	1.6018	✗	-
XIII	L=12.5, W=20.0, S=1.02, b=0.51, c=0.4	9642	10206	3129	14201	3528	3129	1.00	2	1	2	1	4	1	8	0	6	1	1.6875	✗	-
XIV	L=12.5, W=20.0, S=1.02, b=0.51, c=0.4	9910	10489	4378	14414	4801✓	4378	1.00	2	1	2	1	4	1	8	0	7	1	1.7731	✓	-
XV	L=15.0, W=20.0, S=1.02, b=0.51, c=0.4	9910	10486	4374	11585	4797✓	4374	1.00	2	1	2	1	4	1	8	0	7	1	1.7731	✓	-
XVI	L=20.0, W=20.0, S=1.02, b=0.51, c=0.4	9910	10486	4372	9590	4795✓	4372	1.00	2	1	2	1	4	1	8	0	7	1	1.7731	✓	-
XVII	L=12.0, W=20.0, S=1.02, b=0.51, c=0.4	9910	10486	4372	29280	4795✓	4372	1.00	2	1	2	1	4	1	8	0	7	1	1.7731	✓	-
XVIII	L=15.0, W=20.0, S=1.02, b=0.51, c=0.4	9508	19024	8524	4747	5427✓	4747	0.613	3	1	2	1	4	1	8	0	4	1	1.4420	✓	✱
XIX	L=15.0, W=20.0, S=1.02, b=0.51, c=0.4	10994	19755	8977	8294	8200✓	8294	0.613	PLIES OF Ti-5: 1	1	2	1	4	1	8	0	7	1	1.6764	✗	-
XX	L=15.0, W=20.0, S=1.02, b=0.51, c=0.4	8629	9131	7267	3932	4953✓	3932	0.613	2	1	2	1	4	1	8	0	4	1	1.3637	✗	*
XXI	L=15.0, W=20.0, S=1.02, b=0.51, c=0.4	10177	10770	5867	11738	6266✓	5867	1.00	2	1	2	1	4	1	8	0	8	1	1.859	✓	-
XXII	L=15.0, W=20.0, S=1.02, b=0.51, c=0.4	9179	9714	8232	6143	7274✓	6143	0.75	2	1	2	1	4	1	8	0	6	1	1.5396	✓	*
XXIII	L=15.0, W=20.0, S=1.02, b=0.51, c=0.4	7750	3438	6140	2903	4071	2903	0.613	1	1	2	1	4	1	8	0	4	1	1.2854	✗	-

TABLE 1.8

BUCKLING ANALYSIS OF CORRUGATED SANDWICH MODEL – CASE IX

MATERIAL CODES FOR LAMINA (INCHES)
```
1 - CARBON/EPOXY TAPE        (T=0.005)    5 - E-GLASS CLOTH         (T=0.010)
2 - CARBON/EPOXY CLOTH       (T=0.010)    6 - F584/IM6 CARBON/EPOXY (T=0.0055)
3 - KEVLAR/EPOXY CLOTH       (T=0.010)    7 - TITANIUM MATERIAL     (T=0.0050)
4 - K/E THIN COCURED FACINGS (T=0.010)    8 - ADDITIONAL MATERIAL IF ANY
```

MONOLAYER PROPERTIES FOR LAMINA

CODE	E_L (psi)	E_T (psi)	G_{LT} (psi)	ν_{LT}	Rho (pci)
2	0.8200E+07	0.8200E+07	0.5700E+06	0.0990	0.0571
5	0.2900E+07	0.2900E+07	0.3000E+06	0.1300	0.0700
7	0.1640E+08	0.1640E+08	0.6200E+07	0.3100	0.1600

PANEL GEOMETRY AND STIFFENER SPACING (INCHES)
```
LENGTH = 15.000     WIDTH = 20.000     SPACING = 1.020
BASE   =  0.400     CAP   =  0.510     HEIGHT  = 0.750
```

ANGLE (A) AND MATERIAL CODE (C) OF EACH PLY (P)
```
ONLY FOR UPPER SKIN
P    1    2    3    4    5
A    0    0    0    0    0
C    7    7    7    7    7
ONLY FOR LOWER SKIN
P    1    2    3    4
A    0    0    0    0
C    5    2    2    5
ONLY FOR BASE
P    1    2    3    4    5
A    0    0    0    0    0
C    5    5    5    5    2
ONLY FOR CAP
P    1    2    3    4    5    6    7    8    9
A    0    0    0    0    0    0    0    0    0
C    5    5    5    5    2    5    5    5    5
ONLY FOR WEB
P    1    2    3    4    5
A    0    0    0    0    0
C    5    5    5    5    5
```

```
LOCAL AND GENERAL BUCKLING           SHEAR BUCKLING
NORMALIZED TO COLUMN LOAD            NORMALIZED TO PANEL LOAD
UPPER SKIN  Nx = 8,989 LB/IN.       UPPER SKIN  Nxy =   3,531 LB/IN.
LOWER SKIN  Nx = 9,512 LB/IN.       LOWER SKIN  Nxy =  17,980 LB/IN.
WEB         Nx = 5,598 LB/IN.       WEB         Nxy = 102,477 LB/IN.
GENERAL     Nx = 6,097 LB/IN.       GENERAL     Nxy =  18,920 LB/IN.
```

STRAIN = 6,768 MICRO IN./IN. AT Nx = 5,598 LB/IN.

PROPERTIES OF PANEL
```
D11 = 88,737.5      AREA PER INCH = 0.1199 SQ IN./IN.
D22 = 68,545.5      EA PER INCH   = 827,018 LB/IN.
D12 = 11,638.6      WEIGHT        = 1.4786 psf
D66 =  6,877.9
```
178

TABLE 1.9
EARLY 3— BY 3-INCH COMPRESSION PANELS

SPECIMEN I.D.	BATCH CONFIG.	AXIAL	LATERAL	SIZE (IN.) W	SIZE (IN.) L	SIZE (IN.) t	ULT. LOAD (LB)	AVERAGE (LB)	TEMP.	PERCENT OF R.T.	AVERAGE MICRO IN./IN.	MAX. STRAIN C/E SIDE (#1) GAGE (MICRO IN./IN.)	MAX. STRAIN T1 SIDE (#2) GAGE (MICRO IN./IN.)	AVERAGE MICRO IN./IN.	TEST R.T.	TEST -65°	TEST +160°	TEST D	TEST W
L1	13F		X	2.923	2.881	.706	5,625					-2,440	- 2,948		X			X	
A1	13F	X		2.882	2.922	.717	13,250	17,217				-4,296	- 3,669		X			X	
A1₁	13F	X		2.921	2.880	.717	20,400					-6,175	- 7,743		X			X	
A1₂P	H2	X		2.999	2.995	.675	18,000					-9,371	- 5,694		X			X	
L1₁P	H2		X	2.997	2.995	.670	6,990					-3,379	- 1,195		X			X	
L1₂P	H2		X	2.982	2.999	.668	6,210					-3,610	- 3,496		X			X	
A1-1	LA1-2-3	X		3.121	3.010	.775	31,500	29,250 AT R.T.			6,174	-7,175	-10,603	8,193	X			X	
A1-2	LA1-2-3	X		3.271	2.969	.766	28,150					-6,099	- 6,776		X			X	
A1-3	LA1-2-3	X		3.152	2.938	.770	28,300					-6,851	- 6,913		X				X
A1-4	LA1-2-3	X		3.138	2.981	.773	29,050					-4,571	- 8,480		X				X
A1-5	LA1-2-3	X		3.236	2.937	.767	17,200		HOT	.588		-3,605	- 5,210				X	X	
A1-6	LA1-2-3	X		3.138	2.953	.778	17,300		HOT	.591		-5,874	- 4,182				X	X	
A1-7	LA1-2-3	X		3.238	3.026	.772	12,000		COLD	.410		-1,271	- 3,021			X		X	
A1-8	LA1-2-3	X		3.107	2.942	.781	18,000		COLD	.615		-3,138	- 5,099			X		X	
A1-9	LA1-2-1	X		2.896	2.898	.768	17,820					-4,698	- 5,050		X			X	
A1-10	LA1-2-1	X		2.895	2.896	.773	19,760					-4,874	- 5,928		X			X	
A1-11	LA1-2-1		X	2.895	2.900	.766	6,130					-1,770	+ 209		X			X	
A1-12	LA1-2-2		X	2.897	2.896	.764	4,510					-1,465	- 130		X			X	
A1-13	LA1-2-2		X	2.896	2.896	.764	4,330					-1,815	+ 98		X			X	

* D - DRY
W - WET

TABLE 1.10
EARLY 3- BY 3-INCH COMPRESSION PANELS (CONT.)

SPECIMEN I.D.	BATCH CONFIG.	PADS AF31 PROGRESS	.003 LOADING SHIMS	PAA AND PRIME	PERF. Ti
Li	13F			N/C	
Al	13F			N/C	
Al_1	13F		X	N/C	
Al_2P	H2		X	N/C	X
Ll_1P	H2		X	N/C	X
Ll_2P	H2		X	N/C	X
Al-1	LA1-2-3	X	X	REV B	
Al-2	LA1-2-3	X	X	B	
Al-3	LA1-2-3	X	X	B	
Al-4	LA1-2-3	X	X	B	
Al-5	LA1-2-3	X	.006	B	
Al-6	LA1-2-3	X	.006	B	
Al-7	LA1-2-3	X	.006	B	
Al-8	LA1-2-3	X	.006	B	
Al-9	LA1-2-1	X	X	B	
Al-10	LA1-2-1	X	X	B	
Al-11	LA1-2-1	X	X	B	
Al-12	LAI-2-2	X	X	B	
Al-13	LA1-2-2	X	X	B	

TABLE 1.11
CLOSED SANDWICH PANEL DETAILS
CASES A1 TO O1 FOR RIB SPACING = 15 INCHES

KEY DESCRIPTION: L = LENGTH, W = WIDTH, S = SPACING, c = CAP, b = BASE.

CASE NUMBER	KEY DESCRIPTION	WEIGHT LB/FT2	PLIES OF F/G CLOTH FOR WEB	PLIES OF C/E CLOTH FOR CAP	PLIES OF F/G CLOTH FOR CAP	PLIES OF C/E CLOTH FOR BASE	PLIES OF F/G CLOTH FOR BASE	PLIES OF C/E CLOTH LOWER SKIN	PLIES OF F/G CLOTH LOWER SKIN	PLIES OF C/E CLOTH UPPER SKIN	PLIES OF T1 AT .025 IN	HEIGHT IN INCHES	CRITICAL LOADING - MICRO IN./IN.	CRITICAL STRAIN - LB/IN.	GENERAL BUCKLING - LB/IN.	WEB BUCKLING - LB/IN.	LOWER SKIN BUCKLING - LB/IN.	UNDERSKIN BUCKLING - LB/IN.
A1	L=15.0, W=20.0, S=1.3, c=0.51	1.6287	5	0	9	1	5	1	3	4	1	.75	6581	6696	8441	9395	21622	6581
B1	L=15.0, W=20.0, S=1.2, c=0.51	1.6724	5	0	9	1	5	1	3	4	1	.75	8495	8508	8495	9259	30438	9263
C1	L=15.0, W=20.0, S=1.2, c=0.51	1.6426	5	0	9	1	5	1	3	4	1	.75	7676	8240	7676	8422	23020	8643
D1	L=15.0, W=20.0, S=1.2, c=0.51	1.5162	5	0	9	1	5	1	2	3	1	.75	6286	7511	6286	7024	11341	7764
E1	L=15.0, W=20.0, S=1.2, c=0.51	1.5646	5	0	9	1	5	1	2	4	1	.75	6510	7652	6510	7317	15603	7893
XXIIa	L=15.0, W=20.0, S=1.2, c=0.51	1.8715	8	0	7	2	4	1	6	1	1	1.0	6861	7676	10629	6861	9901	7945
F1	L=15.0, W=20.0, S=1.2, c=0.51	1.7244	5	0	9	1	5	1	3	4	1	0.875	5291	5220	11821	5291	30894	9042
G1	L=15.0, W=20.0, S=1.2, c=0.51	1.6054	5	0	9	1	5	1	7	0	1	0.875	3587	4810	5990	3587	8341	6919
H1	L=15.0, W=20.0, S=1.2, c=0.51	1.821	5	0	9	1	5	1	4	4	1	0.875	5673	5448	12204	5673	47409	9660
I1	L=15.0, W=20.0, S=1.2, c=0.51	1.665	5	0	9	1	5	1	5	2	1	0.875	4406	5008	9360	4406	20893	8161
J1	L=15.0, W=20.0, S=1.2, c=0.51	1.7254	6	0	9	1	5	1	5	2	1	0.875	6470	7212	9415	6470	21307	8323
K1	L=15.0, W=20.0, S=1.2, c=0.51	1.7841	6	0	9	1	5	1	3	4	1	0.875	7748	7517	11862	7748	31417	9562
L1	L=15.0, W=20.0, S=1.3, c=0.51	1.7318	6	0	9	1	5	1	3	4	1	0.875	6780	6696	11776	4972	22275	6780
M1	L=15.0, W=20.0, S=1.4, c=0.51	1.689	6	0	9	1	5	1	3	4	1	0.875	5031	5043	11703	8074	16529	5031
N1	L=15.0, W=20.0, S=1.4, c=0.51	1.7549	4	2	9	1	5	1	3	4	1	0.875	5741	5043	12111	10273	18863	5741
O1	L=15.0, W=20.0, S=1.2, c=0.51	1.8595	4	2	9	1	5	1	3	4	1	0.875	9979	8381	12357	9979	36294	11046

TABLE 1.12

SURFACE WAVINESS (h/λ) FOR H = 0.75 INCHES

CASE NUMBER	τ	① RIB WEIGHT LB/FT²	② PANEL WEIGHT (2) LB/FT²	③ ②+③ TOTAL WEIGHT LB/FT²	④ SINGLE RIB WEIGHT (DOUBLE RIB)	⑤ ③+⑤ TOTAL RIB WEIGHT 2/2 (LB/FT²) (SINGLE RIB)	⑥ BELOW h/λ = .0027 YES OR NO	⑦ VALUE OF h/λ (IN./IN.)	⑧ HEIGHT IN INCHES	⑨ LOWER SKIN PLIES OF C/E CLOTH	⑩ LOWER SKIN PLIES OF F/G CLOTH	⑪ PLIES OF F/G WEB	⑫
.75-Aa	10	1.72	1.56	3.28	0.86	2.42	YES	.0015	.75	3	2	6	
.75-Ba	10	1.72	1.53	3.25	0.86	2.39	YES	.0016	.75	2	3	6	
.75-Ea	10	1.72	1.47	3.19	0.86	2.33	NO	.0033	.75	2	3	5	
.75-Fa	10	1.72	1.51	3.23	0.86	2.37	YES	.0017	.75	3	2	5	
.75-La	10	1.72	1.475	3.20	0.86	2.34	YES	.0021	.75	2	4	4	
.75-Ma-1	10	1.72	1.526	3.25	0.86	2.39	YES	.0018	.75	2	4	5	
.75-Ma-2	10	1.4292								2	2	5	
.75-Ma-3	10									2	2	5	
.75-Ma-4	10									2	4	5	
.75-Ma-5	10									4	2	5	

Notes on column ⑪ (PLIES OF F/G WEB):

CRITICAL STRAIN IS MARGINAL WEB BUCKLING IS LOW 4328 LB/IN. (→ 4)

GOOD WEB BUCKLING UP TO 6883 LB/IN. (CHOOSE THIS ONE) (→ 5)

TABLE 1.13

CLOSED SANDWICH CHARACTERISTICS FOR HEIGHT OF 0.75 INCHES

KEY DESCRIPTION: L - LENGTH, W - WIDTH; S - SPACING, b - BASE; c - CAP

CASE NUMBER	KEY DESCRIPTION	UPPER SKIN BUCKLING - LB/IN.	LOWER SKIN BUCKLING - LB/IN.	WEB BUCKLING - LB/IN.	GENERAL BUCKLING - LB/IN.	CRITICAL LOADING - LB/IN.	CRITICAL STRAIN - MICRO IN./IN.	HEIGHT IN INCHES	PLIES OF T1 AT 0.005/PLY UPPER SKIN	PLIES OF C/E CLOTH LOWER SKIN	PLIES OF F/C CLOTH LOWER SKIN	PLIES OF C/E FOR BASE	PLIES OF F/C FOR BASE	PLIES OF C/E FOR CAP	PLIES OF F/C FOR CAP	PLIES OF C/E FOR WEB	PLIES OF F/C FOR WEB	WEIGHT IN psf
.75-Pa	L=12.5, W=20.0, S=1.2, b=0.51, c=0.51	7791	7693	6883	7907	8195	6883	0.75	5	2	4	1	4	1	8	0	5	1.526
.75-Q	L=12.5, W=20.0, S=1.2, b=0.51, c=0.51	7981	7829	10086	7957	9160	7829	0.75	5	2	4	1	4	1	8	0	6	1.577
.75-R	L=15.0, W=20.0, S=1.2, b=0.51, c=0.51	7655	7559	4327	6431	5244	4327	0.75	5	2	4	1	4	1	8	0	4	1.475
.75-S	L=15.0, W=20.0, S=1.2, b=0.51, c=0.51							0.75	5	2	4	1	4	1	8	0	5	1.526
.75-T	L=15.0, W=20.0, S=1.2, b=0.51, c=0.51	7929	7830	10085	6497	7602	6497	0.75	5	2	4	1	4	1	8	0	6	1.577
.75-M2	L=10.0, W=20.0, S=1.2, b=0.51, c=0.51	7542	7665	6338	10217	7805	6338	0.75	*	2	2	1	4	1	8	0	5	*1.4292
.75-M3	L=10.0, W=20.0, S=1.2, b=0.51, c=0.51	7542	4444	6338	10217	5472	4444	0.75	*	2	2	1	4	1	8	0	5	1.4292
.75-M4	L=10.0, W=20.0, S=1.2, b=0.51, c=0.51	7800	7707	6883	10887	8195	6883	0.75	*	4	4	1	4	1	8	0	5	1.5259
.75-M5	L=10.0, W=20.0, S=1.2, b=0.51, c=0.51	9043	23424	8380	13756	8607	8300	0.75	*	3	2	1	4	1	8	0	5	1.5854
.75-M6	L=10.0, W=20.0, S=1.2, b=0.51, c=0.51	8292	9238	7317	12173	8195	7317	0.75	*	2	2	1	4	1	8	0	5	1.5073
.75-M7	L=10.0, W=20.0, S=1.2, b=0.51, c=0.51	7671	11212	6605	10561	7996	6605	0.75	*	2	3	1	4	1	8	0	5	*1.4776

*MOST DESIREABLE CASES FOR WEIGHT AND SURFACE WAVINESS

TABLE 1.14

PANEL DEFLECTION FOR TYPICAL 0.75-INCH HEIGHT – CASE I

MATERIAL CODES FOR LAMINA (INCHES)
```
1 - CARBON/EPOXY TAPE      (T=0.005)   5 - E-GLASS CLOTH          (T=0.010)
2 - CARBON/EPOXY CLOTH     (T=0.010)   6 - F584/IM6 CARBON/EPOXY (T=0.0055)
3 - KEVLAR/EPOXY CLOTH     (T=0.010)   7 - TITANIUM MATERIAL      (T=0.0050)
4 - K/E THIN COCURED FACINGS (T=0.010) 8 - ADDITIONAL MATERIAL IF ANY
```

MONOLAYER PROPERTIES FOR LAMINA

CODE	E_L (psi)	E_T (psi)	G_{LT} (psi)	v_{LT}	Rho (pci)
2	0.8200E+07	0.8200E+07	0.5700E+06	0.0990	0.0571
5	0.2900E+07	0.2900E+07	0.3000E+06	0.1300	0.0700
7	0.1640E+08	0.1640E+08	0.6200E+07	0.3100	0.1600

PANEL GEOMETRY AND STIFFENER SPACING (INCHES)
```
LENGTH = 15.000    WIDTH = 20.000    SPACING = 1.020    PRESSURE = 8.000
BASE   =  0.400    CAP   =  0.510    HEIGHT  = 0.750    ALPHA    = 0.300
```

ANGLE (A) AND MATERIAL CODE (C) OF EACH PLY (P)
```
ONLY FOR UPPER SKIN
P    1    2    3    4    5
A    0    0    0    0    0
C    7    7    7    7    7
ONLY FOR LOWER SKIN
P    1    2    3    4
A    0    0    0    0
C    5    2    2    5
ONLY FOR BASE
P    1    2    3    4    5
A    0    0    0    0    0
C    5    5    5    5    2
ONLY FOR CAP
P    1    2    3    4    5    6    7    8    9
A    0    0    0    0    0    0    0    0    0
C    5    5    5    5    2    5    5    5    5
ONLY FOR WEB
P    1    2    3    4    5
A    0    0    0    0    0
C    5    5    5    5    5
```

PANEL DEFLECTION AT CENTER
WITHOUT AXIAL LOAD
SIMPLY SUPPORTED
DEFLECTION W = 0.0919 IN.
CLAMPED
DEFLECTION W = 0.0459 IN.

PANEL DEFLECTION AT CENTER
WITH AXIAL LOAD
SIMPLY SUPPORTED
DEFLECTION Wa = 0.1313 IN.
CLAMPED
DEFLECTION Wa = 0.0656 IN.

PROPERTIES OF PANEL
```
D_QX = 7,157.9     D_QY        = 155.3
D_11 = 88,737.5    AREA PER INCH = 0.1199 SQ IN./IN.
D_22 = 68,545.5    EA PER INCH   = 827,018 LB/IN.
D_12 = 11,638.6    WEIGHT        = 1.4786 psf
D_66 =  6,877.9
```

TABLE 1.15

PANEL DEFLECTION FOR TYPICAL 1.0-INCH HEIGHT – CASE XXIIb

MATERIAL CODES FOR LAMINA (INCHES)
```
1 - CARBON/EPOXY TAPE        (T=0.005)   5 - E-GLASS CLOTH         (T=0.010)
2 - CARBON/EPOXY CLOTH       (T=0.010)   6 - F584/IM6 CARBON/EPOXY (T=0.0055)
3 - KEVLAR/EPOXY CLOTH       (T=0.010)   7 - TITANIUM MATERIAL     (T=0.0050)
4 - K/E THIN COCURED FACINGS (T=0.010)   8 - ADDITIONAL MATERIAL IF ANY
```

MONOLAYER PROPERTIES FOR LAMINA

CODE	E_L (psi)	E_T (psi)	G_{LT} (psi)	ν_{LT}	Rho (pci)
2	0.8200E+07	0.8200E+07	0.5700E+06	0.0990	0.0571
5	0.2900E+07	0.2900E+07	0.3000E+06	0.1300	0.0700
7	0.1640E+08	0.1640E+08	0.6200E+07	0.3100	0.1600

PANEL GEOMETRY AND STIFFENER SPACING (INCHES)
```
LENGTH = 15.000    WIDTH = 20.000    SPACING = 1.200    PRESSURE = 8.000
BASE   =  0.600    CAP   =  0.500    HEIGHT  = 1.000    ALPHA    = 0.300
```

ANGLE (A) AND MATERIAL CODE (C) OF EACH PLY (P)
```
ONLY FOR UPPER SKIN
P    1    2    3    4    5
A    0    0    0    0    0
C    7    7    7    7    7
ONLY FOR LOWER SKIN
P    1    2    3    4    5    6    7
A    0    0    0    0    0    0    0
C    5    5    2    5    5    5    5
ONLY FOR BASE
P    1    2    3    4    5
A    0    0    0    0    0
C    5    5    5    5    2
ONLY FOR CAP
P    1    2    3    4    5    6    7    8    9
A    0    0    0    0    0    0    0    0    0
C    5    5    5    5    2    5    5    5    5
ONLY FOR WEB
P    1    2    3    4    5    6    7    8    9
A    0    0    0    0    0    0    0    0    0
C    5    5    5    5    5    5    5    5    5
```

PANEL DEFLECTION AT CENTER WITHOUT AXIAL LOAD	PANEL DEFLECTION AT CENTER WITH AXIAL LOAD
SIMPLY SUPPORTED	SIMPLY SUPPORTED
DEFLECTION W = 0.0486 IN.	DEFLECTION Wa = 0.0694 IN.
CLAMPED	CLAMPED
DEFLECTION W = 0.0226 IN.	DEFLECTION Wa = 0.0323 IN.

PROPERTIES OF PANEL
```
DQX = 14,974.7     DQY          = 512.4
D11 = 163,405.8    AREA PER INCH = 0.1651 SQ IN./IN.
D22 = 110,154.4    EA PER INCH   = 902,309 LB/IN.
D12 =  18,538.1    WEIGHT        = 1.9523 psf
D66 =  12,483.8
```

TABLE 1.16

SUMMARY OF WAVINESS AND WARPAGE FOR LA1 PANELS

CONFIGURATION	NON-PERFORATED	PERFORATED	ACTUAL HEIGHT (INCHES)	PADS	CHORDWISE DISH FOR 10 IN. (INCHES)	CHORDWISE DISH FOR 8 IN. (INCHES)	MAXIMUM FLUTE WAVE (INCHES)	INNER SANDWICH FACE, CLOTH LAMINATES	DATE OF TEST	$\frac{y}{4}$ = SINGLE WAVE LENGTH DEFLECTION $\times 10^{-4}$
										$\times 10^{-4}$
LA1-1	X	–	.767	–		.0028	.0002	3F/G 2C/E	3/12/85	2.8
LA1-2	X	X	.78	–		-.001	.0003		3/19/85 &3/27/85	1.0
LA1-3	X	X	.761	–		-.0014	.0005			1.4
LA1-4	X	X	.768	X		-.0026	.0007		4/10/85	2.6
LA1-5	X	X	.771	X		-.0025	.0006		4/23/85	2.5
LA1-6	X	–	.770	X	-.0025		.0004		5/15/85	3.125
LA1-7	X	–	.791	X	-.0018		.0003	3F/G 3C/E	6/17/85	2.25
LA1-8	X	–	.793	X	-.0016		.0005	3F/G 3C/E	7/2/85	2.0

TABLE 1.17

OVERLAP SHEAR (psi) FOR DIFFERENT CURE CYCLES
(FROM 3M CORPORATION DATA)

TEST	TEST TEMPERATURE	TYPICAL PROPERTIES
SHEAR STRENGTH	-67°F + 2°F	2750 psi
	73.5°F + 2°F	4430 psi
	280°F + 2°F	2700 psi
	300°F + 2°F	2550 psi
	350°F + 2°F	2350 psi
CREEP RUPTURE (192 HOURS)	73.5°F + 2°F	.003"
	300°F + 2°F	.008"

AF-31 T-PEEL ON ALUMINUM

T-PEEL BONDS CONSIST OF BONDED AREAS OF 1" x 6" 2024 T3 CLAD 1" x 8" x .032" PANELS WITH ONE LAYER OF AF-31 FILM ADHESIVE. EACH METAL SKIN OF THE T-PEEL PANELS WERE PULLED AT A 90° ANGLE TO THE BOND LINE OR 180°F IN RELATION TO THEMSELVES WITH A JAW SEPARATION RATE OF 20 INCHES PER MINUTE.

A. ORIGINAL PROPERTIES

CURE CYCLE	T-PEEL (LB/IN. WIDTH)					
	-40°F	75°F	180°F	250°F	350°F	450°F
NORMAL CURE CYCLE - 350°F 60 MIN., 150 psi, 200°F PER MIN. RISE RATE TO CURE TEMPERATURE.	4	25	12	8	7	4
FAST CURE CYCLE - 450°F PRESS TEMPERATURE, 350 psi, 15 SECONDS IN THE PRESS, MAXIMUM BOND LINE TEMPERATURE ATTAINED 412°F.	4	27	11	8	7	4

AF-31 OVERLAP SHEAR ON ALUMINUM USING VARIED CURE TIMES, TEMPS., AND PRESSURES

THE FOLLOWING DATA SHOWS TYPICAL VALUES OBTAINED WITH AF-31 IN ALUMINUM OVERLAP BONDS. ALL PROPERTIES WERE MEASURED ON 1" WIDE, 1/2" OVERLAP SPECIMENS CUT FROM .063" THICK 4" x 7" BONDED PANELS OF 2024 T3 CLAD ALUMINUM. TESTS WERE CONDUCTED ACCORDING TO MMM-A-132 METHODS. ALL BONDS WERE FORMED IN A PLATEN PRESS.

CURE CYCLE				OVERLAP SHEAR (psi)									
TEMP. (°F)	TIME (MIN.)	PRESSURE (psi)	RISE RATE (°F/MIN.)	-67°F	75°F	180°F	250°F	300°F	350°F	TEST TEMP. 400°F	450°F	500°F	600°F
350	60	150	200	2700	3700	2850	2500	2390	1700	1150	1100	800	250
350	10	150	200	2850	4200		2430	1975					
350	5	150	200	2260	4200		2260	1610					
350	60	45	200	2675	3740			2050					
350	60	45	9	2800	3700			2100			1300		
350	120	100	10					2647		2185		1790	
250	120	75	10		4285			1225					
250	24 HRS	75	10		4375			2090					
260	120	75	10		4150			1510					
260	8 HRS	75	10		4360			2000					
325	60	20	200	2720	3360	1830	1370	840					
350	60	20	200	2820	3280	2020	1720	1530					

TABLE 1.18

OVERLAP SHEAR TESTS

AUTOCLAVE CURE CYCLES
SINGLE OVERLAP SHEARS (1/2 x 1 SQ IN.)

TABS: Ti-PERF, FIBERGLASS; AF31-.010 ADHESIVE

CURE I.D.	TEMPERATURE	TIME	PRESSURE	COMMENT
"A"	265°F	4 HRS	37 PSI	OLD STD (FAST HEAT RISE)
"B"	350°F	1 HR	150 PSI	PREHEATED AUTOCLAVE (PER 3M STD)
"C"	265°F	4 HRS	150 PSI	
"D"	300°F	1 HR	75 PSI	
"E"	300°F	2 HRS	100 PSI	
"F"	300°F	1 HR	100 PSI	
"G"	300°F	2 HRS	75 PSI	

TABS: FIBERGLASS BONDED TO FIBERGLASS; AF31-.010 ADHESIVE CALLED F_{FF} AND G_{FF} CURE CYCLES

"F" AND "G" - SAME AS ABOVE CURE CYCLES

TABS: FIBERGLASS BONDED TO CARBON EPOXY CLOTH; AF31-.010 ADHESIVE CALLED F_{CF} AND G_{CF} CURE CYCLES

"F" AND "G" - SAME AS ABOVE CURE CYCLES

TABS: CARBON EPOXY CLOTH BONDED TO TITANIUM CALLED F_{TC} AND G_{TC} CURE CYCLES

"F" AND "G" - SAME AS ABOVE CURE CYCLES

TABS: CARBON EPOXY CLOTH BONDED TO CARBON EPOXY CLOTH CALLED F_{CC} AND G_{CC} CURE CYCLES

"F" - SAME AS ABOVE CURE CYCLE

TABLE 1.19
SINGLE LAP SHEAR DATA
AVERAGE SHEAR VALUES FOR MATERIALS OF INTEREST

STRESS (PSI) AVERAGE OF (3) COUPONS EACH

TITANIUM TO PADS

NO.	TABS	CURE IDENT.	ROOM TEMP.	+160°F	−65°F
I	Ti/C	Ftc	(2744)	(2020)	(1859)
II	Ti/C	Gtc	2457	1915	1708
III	Ti/F	Ftf	2080	1607	(1532)
IV	Ti/F	Gtf	(2242)	(1731)	1529

TITANIUM PADS TO SUBSTRUCTURE

NO.	TABS	CURE IDENT.	ROOM TEMP.	+160°F	−65°F
V	F/F	Fff	1548	1372	1344
VI	F/F	Gff	(1781)	(1563)	(1359)
VII	C/F	Fcf	2524	(2189)	1911
VIII	C/F	Gcf	(2692)	2106	(1954)
IX	C/C	Fcc	(2568)	1902	(2085)
X	C/C	Gcc	2479	(2036)	1955

189

TABLE 1.20
FAILURE MODE FROM MAGNIFICATION PHOTOGRAPHS
(A1 TO A9)

IDENT. OF SPECIMEN AND TEMP.	MATERIAL IDENT. ON TITANIUM SURFACE	LAYERS OF SEPARATION	FAILURE MODE IDENT.	FAILURE CONCLUSION
A1 R.T.	#2 91% PRIMER	PRIMER/PRIMER	COHESIVE	91% PRIMER COHESIVE FAILURE
	#3 3% AF31	AF31/PRIMER	ADHESIVE	
	#4 6% FIBERGLASS PRIMER	FIBERGLASS PRIMER/FIBERGLASS	ADHESIVE	
A2 R.T.	#2 95% PRIMER	PRIMER/PRIMER	COHESIVE	95% PRIMER COHESIVE FAILURE
	#3 3% AF31	AF31/PRIMER	ADHESIVE	
	#4 2% FIBERGLASS PRIMER	FIBERGLASS PRIMER/FIBERGLASS	ADHESIVE	
A3 R.T.	#2 93% PRIMER	PRIMER/PRIMER	COHESIVE	93% PRIMER COHESIVE FAILURE
	#3 3% AF31	AF31/PRIMER	ADHESIVE	
	#4 4% FIBERGLASS PRIMER	FIBERGLASS PRIMER/FIBERGLASS	ADHESIVE	
A4 +160°F	#2 60% PRIMER	PRIMER/PRIMER	COHESIVE	60% PRIMER COHESIVE FAILURE
	#3 10% AF31	AF31/PRIMER	ADHESIVE	
	#4 30% FIBERGLASS PRIMER	FIBERGLASS PRIMER/FIBERGLASS	ADHESIVE	30% FIBERGLASS PRIMER ADHESIVE FAILURE
A5 +160°F	#2 4% PRIMER	PRIMER/PRIMER	COHESIVE	
	#3 1% AF31	AF31/PRIMER	ADHESIVE	
	#4 95% FIBERGLASS PRIMER	FIBERGLASS PRIMER/FIBERGLASS	ADHESIVE	95% FIBERGLASS PRIMER ADHESIVE FAILURE
A6 +160°F	#2 90% PRIMER	PRIMER/PRIMER	COHESIVE	90% PRIMER COHESIVE FAILURE
	#3 5% AF31	AF31/PRIMER	ADHESIVE	
	#4 5% FIBERGLASS PRIMER	FIBERGLASS PRIMER/FIBERGLASS	ADHESIVE	
A7 -65°F	#2 5% PRIMER	PRIMER/PRIMER	COHESIVE	
	#3 93% AF31	AF31/PRIMER	ADHESIVE	93% AF31 ADHESIVE FAILURE
	#4 2% FIBERGLASS PRIMER	FIBERGLASS PRIMER/FIBERGLASS	ADHESIVE	
A8 -65°F	#2 65% PRIMER	PRIMER/PRIMER	COHESIVE	65% PRIMER COHESIVE FAILURE
	#3 35% AF31	AF31/PRIMER	ADHESIVE	35% AF31 ADHESIVE FAILURE
	#4 0% FIBERGLASS PRIMER	FIBERGLASS PRIMER/FIBERGLASS	ADHESIVE	
A9 -65°F	#2 55% PRIMER	PRIMER/PRIMER	COHESIVE	55% PRIMER COHESIVE FAILURE
	#3 45% AF31	AF31/PRIMER	ADHESIVE	45% AF31 ADHESIVE FAILURE
	#4 0% FIBERGLASS PRIMER	FIBERGLASS PRIMER/FIBERGLASS	ADHESIVE	

190

TABLE 1.21
FAILURE MODE FROM MAGNIFICATION PHOTOGRAPHS
(D1 TO D9)

IDENT. OF SPECIMEN AND TEMP.	MATERIAL IDENT. ON TITANIUM SURFACE	LAYERS OF SEPARATION	FAILURE MODE IDENT.	FAILURE CONCLUSION
D1 R.T.	#2 90% PRIMER	PRIMER/PRIMER	COHESIVE	90% PRIMER COHESIVE FAILURE
	#3 5% AF31	AF31/PRIMER	ADHESIVE	
	#4 5% FIBERGLASS PRIMER	FIBERGLASS PRIMER/FIBERGLASS	ADHESIVE	
D2 R.T.	#2 80% PRIMER	PRIMER/PRIMER	COHESIVE	80% PRIMER COHESIVE FAILURE
	#3 10% AF31	AF31/PRIMER	ADHESIVE	
	#4 10% FIBERGLASS PRIMER	FIBERGLASS PRIMER/FIBERGLASS	ADHESIVE	
D3 R.T.	#2 70% PRIMER	PRIMER/PRIMER	COHESIVE	70% PRIMER COHESIVE FAILURE
	#3 10% AF31	AF31/PRIMER	ADHESIVE	20% FIBERGLASS PRIMER ADHESIVE FAILURE
	#4 20% FIBERGLASS PRIMER	FIBERGLASS PRIMER/FIBERGLASS	ADHESIVE	
D4 +160°F	#2 9% PRIMER	PRIMER/PRIMER	COHESIVE	
	#3 1% AF31	AF31/PRIMER	ADHESIVE	
	#4 90% FIBERGLASS PRIMER	FIBERGLASS PRIMER/FIBERGLASS	ADHESIVE	90% FIBERGLASS PRIMER ADHESIVE FAILURE
D5 +160°F	#2 20% PRIMER	PRIMER/PRIMER	COHESIVE	20% PRIMER COHESIVE FAILURE
	#3 5% AF31	AF31/PRIMER	ADHESIVE	
	#4 75% FIBERGLASS PRIMER	FIBERGLASS PRIMER/FIBERGLASS	ADHESIVE	75% FIBERGLASS PRIMER ADHESIVE FAILURE
D6 +160°F	#2 12% PRIMER	PRIMER/PRIMER	COHESIVE	12% PRIMER COHESIVE FAILURE
	#3 8% AF31	AF31/PRIMER	ADHESIVE	
	#4 80% FIBERGLASS PRIMER	FIBERGLASS PRIMER/FIBERGLASS	ADHESIVE	80% FIBERGLASS PRIMER ADHESIVE FAILURE
D7 -65°F	#2 70% PRIMER	PRIMER/PRIMER	COHESIVE	70% PRIMER COHESIVE FAILURE
	#3 25% AF31	AF31/PRIMER	ADHESIVE	25% AF31 ADHESIVE FAILURE
	#4 5% FIBERGLASS PRIMER	FIBERGLASS PRIMER/FIBERGLASS	ADHESIVE	
D8 -65°F	#2 75% PRIMER	PRIMER/PRIMER	COHESIVE	75% PRIMER COHESIVE FAILURE
	#3 20% AF31	AF31/PRIMER	ADHESIVE	20% AF31 ADHESIVE FAILURE
	#4 5% FIBERGLASS PRIMER	FIBERGLASS PRIMER/FIBERGLASS	ADHESIVE	
D9 -65°F	#2 80% PRIMER	PRIMER/PRIMER	COHESIVE	80% PRIMER COHESIVE FAILURE
	#3 17% AF31	AF31/PRIMER	ADHESIVE	17% AF31 ADHESIVE FAILURE
	#4 3% FIBERGLASS PRIMER	FIBERGLASS PRIMER/FIBERGLASS	ADHESIVE	

C-2

TABLE 1.22

FAILURE MODE FROM MAGNIFICATION PHOTOGRAPHS

(E1 TO E9)

IDENT. OF SPECIMEN AND TEMP.	MATERIAL IDENT. ON TITANIUM SURFACE	LAYERS OF SEPARATION	FAILURE MODE IDENT.	FAILURE CONCLUSION
E1 R.T.	#2 9% PRIMER #3 1% AF31 #4 90% FIBERGLASS PRIMER	PRIMER/PRIMER AF31/PRIMER FIBERGLASS PRIMER/FIBERGLASS	COHESIVE ADHESIVE ADHESIVE	90% FIBERGLASS PRIMER ADHESIVE FAILURE
E2 R.T.	#2 95% PRIMER #3 3% AF31 #4 2% FIBERGLASS PRIMER	PRIMER/PRIMER AF31/PRIMER FIBERGLASS PRIMER/FIBERGLASS	COHESIVE ADHESIVE ADHESIVE	95% PRIMER COHESIVE FAILURE
E3 R.T.	#2 7% PRIMER #3 1% AF31 #4 92% FIBERGLASS PRIMER	PRIMER/PRIMER AF31/PRIMER FIBERGLASS PRIMER/FIBERGLASS	COHESIVE ADHESIVE ADHESIVE	92% FIBERGLASS PRIMER ADHESIVE FAILURE
E4 +160°F	#2 75% PRIMER #3 5% AF31 #4 20% FIBERGLASS PRIMER	PRIMER/PRIMER AF31/PRIMER FIBERGLASS PRIMER/FIBERGLASS	COHESIVE ADHESIVE ADHESIVE	75% PRIMER COHESIVE FAILURE
E5 +160°F	#2 2% PRIMER #3 2% AF31 #4 96% FIBERGLASS PRIMER	PRIMER/PRIMER AF31/PRIMER FIBERGLASS PRIMER/FIBERGLASS	COHESIVE ADHESIVE ADHESIVE	96% FIBERGLASS PRIMER ADHESIVE FAILURE
E6 +160°F	#2 73% PRIMER #3 5% AF31 #4 22% FIBERGLASS PRIMER	PRIMER/PRIMER AF31/PRIMER FIBERGLASS PRIMER/FIBERGLASS	COHESIVE ADHESIVE ADHESIVE	73% PRIMER COHESIVE FAILURE 22% FIBERGLASS PRIMER ADHESIVE FAILURE
E7 -65°F	#2 80% PRIMER #3 15% AF31 #4 5% FIBERGLASS PRIMER	PRIMER/PRIMER AF31/PRIMER FIBERGLASS PRIMER/FIBERGLASS	COHESIVE ADHESIVE ADHESIVE	80% PRIMER COHESIVE FAILURE 15% AF31 ADHESIVE FAILURE
E8 -65°F	#2 83% PRIMER #3 12% AF31 #4 5% FIBERGLASS PRIMER	PRIMER/PRIMER AF31/PRIMER FIBERGLASS PRIMER/FIBERGLASS	COHESIVE ADHESIVE ADHESIVE	83% PRIMER COHESIVE FAILURE 12% AF31 ADHESIVE FAILURE
E9 -65°F	#2 83% PRIMER #3 12% AF31 #4 5% FIBERGLASS PRIMER	PRIMER/PRIMER AF31/PRIMER FIBERGLASS PRIMER/FIBERGLASS	COHESIVE ADHESIVE ADHESIVE	83% PRIMER COHESIVE FAILURE 12% AF31 ADHESIVE FAILURE

TABLE 1.23

FAILURE MODE FROM MAGNIFICATION PHOTOGRAPHS

(F1 TO F9)

IDENT. OF SPECIMEN AND TEMP.	MATERIAL IDENT. ON TITANIUM SURFACE	LAYERS OF SEPARATION	FAILURE MODE IDENT.	FAILURE CONCLUSION
F1 R.T.	#2 1% PRIMER #3 1% AF31 #4 98% FIBERGLASS PRIMER	PRIMER/PRIMER AF31/PRIMER FIBERGLASS PRIMER/FIBERGLASS	COHESIVE ADHESIVE ADHESIVE	98% FIBERGLASS PRIMER ADHESIVE FAILURE
F2 R.T.	#2 1% PRIMER #3 1% AF31 #4 98% FIBERGLASS PRIMER	PRIMER/PRIMER AF31/PRIMER FIBERGLASS PRIMER/FIBERGLASS	COHESIVE ADHESIVE ADHESIVE	98% FIBERGLASS PRIMER ADHESIVE FAILURE
F3 R.T.	#2 1% PRIMER #3 2% AF31 #4 97% FIBERGLASS PRIMER	PRIMER/PRIMER AF31/PRIMER FIBERGLASS PRIMER/FIBERGLASS	COHESIVE ADHESIVE ADHESIVE	97% FIBERGLASS PRIMER ADHESIVE FAILURE
F4 +160°F	#2 1% PRIMER #3 2% AF31 #4 97% FIBERGLASS PRIMER	PRIMER/PRIMER AF31/PRIMER FIBERGLASS PRIMER/FIBERGLASS	COHESIVE ADHESIVE ADHESIVE	97% FIBERGLASS PRIMER ADHESIVE FAILURE
F5 +160°F	#2 1% PRIMER #3 2% AF31 #4 97% FIBERGLASS PRIMER	PRIMER/PRIMER AF31/PRIMER FIBERGLASS PRIMER/FIBERGLASS	COHESIVE ADHESIVE ADHESIVE	97% FIBERGLASS PRIMER ADHESIVE FAILURE
F6 +160°F	#2 1% PRIMER #3 3% AF31 #4 98% FIBERGLASS PRIMER	PRIMER/PRIMER AF31/PRIMER FIBERGLASS PRIMER/FIBERGLASS	COHESIVE ADHESIVE ADHESIVE	98% FIBERGLASS PRIMER ADHESIVE FAILURE
F7 -65°F	#2 40% PRIMER #3 45% AF31 #4 15% FIBERGLASS PRIMER	PRIMER/PRIMER AF31/PRIMER FIBERGLASS PRIMER/FIBERGLASS	COHESIVE ADHESIVE ADHESIVE	40% PRIMER COHESIVE FAILURE 45% AF31 ADHESIVE FAILURE
F8 -65°F	#2 38% PRIMER #3 48% AF31 #4 14% FIBERGLASS PRIMER	PRIMER/PRIMER AF31/PRIMER FIBERGLASS PRIMER/FIBERGLASS	COHESIVE ADHESIVE ADHESIVE	38% PRIMER COHESIVE FAILURE 48% AF31 ADHESIVE FAILURE
F9 -65°F	#2 48% PRIMER #3 48% AF31 #4 4% FIBERGLASS PRIMER	PRIMER/PRIMER AF31/PRIMER FIBERGLASS PRIMER/FIBERGLASS	COHESIVE ADHESIVE ADHESIVE	48% PRIMER COHESIVE FAILURE 48% AF31 ADHESIVE FAILURE

TABLE 1.24

FAILURE MODE FROM MAGNIFICATION PHOTOGRAPHS

(G1 TO G9)

IDENT. OF SPECIMEN AND TEMP.	MATERIAL IDENT. ON TITANIUM SURFACE	LAYERS OF SEPARATION	FAILURE MODE IDENT.	FAILURE CONCLUSION
G1 R.T.	#2 4% PRIMER #3 1% AF31 #4 95% FIBERGLASS PRIMER	PRIMER/PRIMER AF31/PRIMER FIBERGLASS PRIMER/FIBERGLASS	COHESIVE ADHESIVE ADHESIVE	95% FIBERGLASS PRIMER ADHESIVE FAILURE
G2 R.T.	#2 2% PRIMER #3 1% AF31 #4 97% FIBERGLASS PRIMER	PRIMER/PRIMER AF31/PRIMER FIBERGLASS PRIMER/FIBERGLASS	COHESIVE ADHESIVE ADHESIVE	97% FIBERGLASS PRIMER ADHESIVE FAILURE
G3 R.T.	#2 1% PRIMER #3 1% AF31 #4 98% FIBERGLASS PRIMER	PRIMER/PRIMER AF31/PRIMER FIBERGLASS PRIMER/FIBERGLASS	COHESIVE ADHESIVE ADHESIVE	98% FIBERGLASS PRIMER ADHESIVE FAILURE
G4 +160°F	#2 1% PRIMER #3 1% AF31 #4 98% FIBERGLASS PRIMER	PRIMER/PRIMER AF31/PRIMER FIBERGLASS PRIMER/FIBERGLASS	COHESIVE ADHESIVE ADHESIVE	98% FIBERGLASS PRIMER ADHESIVE FAILURE
G5 +160°F	#2 2% PRIMER #3 1% AF31 #4 97% FIBERGLASS PRIMER	PRIMER/PRIMER AF31/PRIMER FIBERGLASS PRIMER/FIBERGLASS	COHESIVE ADHESIVE ADHESIVE	97% FIBERGLASS PRIMER ADHESIVE FAILURE
G6 +160°F	#2 1% PRIMER #3 1% AF31 #4 98% FIBERGLASS PRIMER	PRIMER/PRIMER AF31/PRIMER FIBERGLASS PRIMER/FIBERGLASS	COHESIVE ADHESIVE ADHESIVE	98% FIBERGLASS PRIMER ADHESIVE FAILURE
G7 -65°F	#2 10% PRIMER #3 80% AF31 #4 10% FIBERGLASS PRIMER	PRIMER/PRIMER AF31/PRIMER FIBERGLASS PRIMER/FIBERGLASS	COHESIVE ADHESIVE ADHESIVE	10% PRIMER COHESIVE FAILURE 80% AF31 ADHESIVE FAILURE
G8 -65°F	#2 30% PRIMER #3 55% AF31 #4 15% FIBERGLASS PRIMER	PRIMER/PRIMER AF31/PRIMER FIBERGLASS PRIMER/FIBERGLASS	COHESIVE ADHESIVE ADHESIVE	30% PRIMER COHESIVE FAILURE 55% AF31 ADHESIVE FAILURE
G9 -65°F	#2 15% PRIMER #3 75% AF31 #4 10% FIBERGLASS PRIMER	PRIMER/PRIMER AF31/PRIMER FIBERGLASS PRIMER/FIBERGLASS	COHESIVE ADHESIVE ADHESIVE	15% PRIMER COHESIVE FAILURE 75% AF31 ADHESIVE FAILURE

TABLE 1.25

LAP SHEAR TESTS OF ADHESIVE WITH DIFFERENT CURE CYCLES
(CURES A1 TO A10 AND B1 TO B3)

SPECIMEN ID	W (IN.)	OVERLAP (IN.)	AREA (SQ IN.)	ULT LOAD (LB)	STRESS (PSI)	AVERAGE FAILURE STRESS (PSI)	PERCENT OF ROOM TEMP FAILURE STRESS
ROOM TEMPERATURE							
A1	.983	.526	.5171	900	1740	1694	
A2	.994	.524	.5209	630	1209		
A3	.992	.548	.5436	1160	2134		
+160°F							
A4	.992	.540	.5357	768	1434	1369	81%
A5	.990	.546	.5788	923	1779		
A6	.985	.540	.5319	476	895		
-65°F							
A7	.995	.500	.4975	328	659	647	38%
A8	.993	.570	.5660	316	558		
A9	.992	.520	.5218	378	724		
EXTRA +160°F							
A10	.954	.560		833	1543		91%
ROOM TEMPERATURE							
B1	.987	.472	.4659	495	1062	1052	
B2	.986	.439	.4329	420	970		
B3	.985	.488	.4807	540	1123		

TABLE 1.26

LAP SHEAR TESTS OF ADHESIVE WITH DIFFERENT CURE CYCLES
(CURES B4 TO B9 AND C1 TO C6)

SPECIMEN ID	W (IN.)	OVERLAP (IN.)	AREA (SQ IN.)	ULT LOAD (LB)	STRESS (PSI)	AVERAGE FAILURE STRESS (PSI)	PERCENT OF ROOM TEMP FAILURE STRESS
+180°F							
B4	.990	.514	.5089	487	957	964	92%
B5	.969	.490	.4749	479	1009		
B6	.982	.480	.4714	437	927		
-67°F							
B7	.990	.480	.4752	258	543	700	67%
B8	.992	.503	.4990	335	671		
B9	.995	.478	.4756	422	887		
ROOM TEMPERATURE							
C1	.984	.490	.4822	755	1566	1216	
C2	.983	.490	.4817	550	1142		
C3	.986	.496	.4891	460	940		
+160°F							
C4	.996	.515	.5729	742	1446	1453	119.5%
C5	.990	.503	.4980	689	1384		
C6	.988	.493	.4871	745	1529		

TABLE 1.27

LAP SHEAR TESTS OF ADHESIVE WITH DIFFERENT CURE CYCLES
(CURES C7 TO C10 AND D1 TO D9)

SPECIMEN ID	W (IN.)	OVERLAP (IN.)	AREA (SQ IN.)	ULT LOAD (LB)	STRESS (PSI)	AVERAGE FAILURE STRESS (PSI)	PERCENT OF ROOM TEMP FAILURE STRESS
-65°F							
C7	.987	.498	.4915	525	865	753	62%
C8	.996	.486	.4841	294	607		
C9	.959	.497	.4766	375	787		
EXTRA							
C10	.998						
ROOM TEMPERATURE							
D1	.978	.492	.4812	820	1704	1791	
D2	.959	.480	.4603	855	1857		
D3	.976	.492	.4802	870	1812		
+160°F							
D4	.989	.476	.4708	810	1721	1754	98%
D5	.943	.497	.4687	835	1782		
D6	.984	.455	.4477	788	1760		
-65°F							
D7	.976	.479	.4675	492	1052	1095	61%
D8	.968	.495	.4792	428	893		
D9	.975	.501	.4885	654	1339		

TABLE 1.28

LAP SHEAR TESTS – FIBERGLASS TO PERFORATED TITANIUM

(CURES E AND F)

SPECIMEN ID	W (IN.)	OVERLAP (IN.)	AREA (SQ IN.)	ULT LOAD (LB)	STRESS (PSI)	AVERAGE FAILURE STRESS (PSI)	PERCENT OF ROOM TEMP FAILURE STRESS
ROOM TEMPERATURE							
E-1	.982	.506	.4969	955	1922	1684	100%
E-2	.978	.498	.4870	652	1339		
E-3	.977	.452	.4416	791	1791		
+160°F							
E-4	.975	.494	.4817	703	1460	1464	87%
E-5	.975	.418	.4076	718	1762		
E-6	.978	.523	.5115	598	1169		
-65°F							
E-7	.986	.434	.4279	455	1040	969	58%
E-8	.972	.470	.4568	505	1105		
E-9	.983	.478	.4699	358	762		
ROOM TEMPERATURE							
F-1	.965	.521	.5028	1095	2178	2080	100%
F-2	.974	.535	.5211	1021	1595		
F-3	.977	.530	.5178	1089	2103		
+160°F							
F-4	.970	.542	.5257	850	1617	1607	77%
F-5	.962	.568	.5464	819	1499		
F-6	.968	.497	.4811	821	1706		
-65°F							
F-7	.977	.510	.4983	763	1531	1532	74%
F-8	.972	.442	.4296	661	1538		
F-9	.969	.510	.4942	754	1526		

198

TABLE 1.29
LAP SHEAR TESTS – FIBERGLASS TO PERFORATED TITANIUM
(CURE G)

SPECIMEN ID	W (IN.)	OVERLAP (IN.)	AREA (SQ IN.)	ULT LOAD (LB)	STRESS (PSI)	AVERAGE FAILURE STRESS (PSI)	PERCENT OF ROOM TEMP FAILURE STRESS
ROOM TEMPERATURE							
G-1	.989	.495	.4896	1188	2426	2242	100%
G-2	.980	.522	.5115	1238	2420		
G-3	.990	.492	.4871	915	1879		
+160°F							
G-4	.987	.599	.5517	938	1700	1731	77%
G-5	.983	.506	.4974	843	1695		
G-6	.976	.497	.4851	872	1798		
-65°F							
G-7	.986	.504	.4969	680	1368	1529	68%
G-8	.992	.494	.4900	830	1694		
G-9	.989	.501	.4955	755	1524		

TABLE 1.30

FAILURE MODE DESCRIPTION OF CARBON/FIBERGLASS FROM
MAGNIFIED EXAMINATION (Fcf1 TO Fcf9)

IDENT. OF SPECIMEN AND TEMP.	MATERIAL IDENT. ON CARBON SURFACE	LAYERS OF SEPARATION	FAILURE MODE IDENT.	FAILURE CONCLUSION
FcF1 R.T.	#1 100% CARBON #2 0% PRIMER #3 0% AF31 #4 0% PRIMER #5 0% FIBERGLASS	CARBON/CARBON PRIMER/PRIMER AF31/PRIMER PRIMER/PRIMER FIBERGLASS/FIBERGLASS	COHESIVE COHESIVE ADHESIVE COHESIVE COHESIVE	100% CARBON COHESIVE FAILURE
FcF2 R.T.	#1 70% CARBON #2 1% PRIMER #3 7% AF31 #4 2% PRIMER #5 20% FIBERGLASS	CARBON/CARBON PRIMER/PRIMER AF31/PRIMER PRIMER/PRIMER FIBERGLASS/FIBERGLASS	COHESIVE COHESIVE ADHESIVE COHESIVE COHESIVE	70% CARBON COHESIVE FAILURE
FcF3 R.T.	#1 60% CARBON #2 0% PRIMER #3 4% AF31 #4 1% PRIMER #5 35% FIBERGLASS	CARBON/CARBON PRIMER/PRIMER AF31/PRIMER PRIMER/PRIMER FIBERGLASS/FIBERGLASS	COHESIVE COHESIVE ADHESIVE COHESIVE COHESIVE	60% CARBON COHESIVE FAILURE
FcF4 +160°F	#1 50% CARBON #2 10% PRIMER #3 4% AF31 #4 6% PRIMER #5 30% FIBERGLASS	CARBON/CARBON PRIMER/PRIMER AF31/PRIMER PRIMER/PRIMER FIBERGLASS/FIBERGLASS	COHESIVE COHESIVE ADHESIVE COHESIVE COHESIVE	50% CARBON COHESIVE FAILURE 30% FIBERGLASS COHESIVE FAILURE
FcF5 +160°F	#1 30% CARBON #2 12% PRIMER #3 10% AF31 #4 3% PRIMER #5 45% FIBERGLASS	CARBON/CARBON PRIMER/PRIMER AF31/PRIMER PRIMER/PRIMER FIBERGLASS/FIBERGLASS	COHESIVE COHESIVE ADHESIVE COHESIVE COHESIVE	30% CARBON COHESIVE FAILURE 45% FIBERGLASS COHESIVE FAILURE
FcF6 +160°F	#1 40% CARBON #2 10% PRIMER #3 10% AF31 #4 10% PRIMER #5 30% FIBERGLASS	CARBON/CARBON PRIMER/PRIMER AF31/PRIMER PRIMER/PRIMER FIBERGLASS/FIBERGLASS	COHESIVE COHESIVE ADHESIVE COHESIVE COHESIVE	40% CARBON COHESIVE FAILURE
FcF7 -65°F	#1 60% CARBON #2 2% PRIMER #3 5% AF31 #4 8% PRIMER #5 25% FIBERGLASS	CARBON/CARBON PRIMER/PRIMER AF31/PRIMER PRIMER/PRIMER FIBERGLASS/FIBERGLASS	COHESIVE COHESIVE ADHESIVE COHESIVE COHESIVE	70% CARBON COHESIVE FAILURE
FcF8 -65°F	#1 70% CARBON #2 4% PRIMER #3 5% AF31 #4 1% PRIMER #5 20% FIBERGLASS	CARBON/CARBON PRIMER/PRIMER AF31/PRIMER PRIMER/PRIMER FIBERGLASS/FIBERGLASS	COHESIVE COHESIVE ADHESIVE COHESIVE COHESIVE	80% CARBON COHESIVE FAILURE
FcF9 -65°F	#1 80% CARBON #2 2% PRIMER #3 6% AF31 #4 2% PRIMER #5 10% FIBERGLASS	CARBON/CARBON PRIMER/PRIMER AF31/PRIMER PRIMER/PRIMER FIBERGLASS/FIBERGLASS	COHESIVE COHESIVE ADHESIVE COHESIVE COHESIVE	80% CARBON COHESIVE FAILURE

TABLE 1.31

FAILURE MODE DESCRIPTION OF CARBON/FIBERGLASS FROM MAGNIFIED EXAMINATION (Gcf1 TO Gcf9)

IDENT. OF SPECIMEN AND TEMP.	MATERIAL IDENT. ON CARBON SURFACE	LAYERS OF SEPARATION	FAILURE MODE IDENT.	FAILURE CONCLUSION
Gcf1 R.T.	#1 65% CARBON #2 5% PRIMER #3 5% AF31 #4 5% PRIMER #5 20% FIBERGLASS	CARBON/CARBON PRIMER/PRIMER AF31/PRIMER PRIMER/PRIMER FIBERGLASS/FIBERGLASS	COHESIVE COHESIVE ADHESIVE COHESIVE COHESIVE	65% CARBON COHESIVE FAILURE
Gcf2 R.T.	#1 70% CARBON #2 5% PRIMER #3 3% AF31 #4 2% PRIMER #5 20% FIBERGLASS	CARBON/CARBON PRIMER/PRIMER AF31/PRIMER PRIMER/PRIMER FIBERGLASS/FIBERGLASS	COHESIVE COHESIVE ADHESIVE COHESIVE COHESIVE	70% CARBON COHESIVE FAILURE
Gcf3 R.T.	#1 90% CARBON #2 1% PRIMER #3 5% AF31 #4 1% PRIMER #5 3% FIBERGLASS	CARBON/CARBON PRIMER/PRIMER AF31/PRIMER PRIMER/PRIMER FIBERGLASS/FIBERGLASS	COHESIVE COHESIVE ADHESIVE COHESIVE COHESIVE	90% CARBON COHESIVE FAILURE
Gcf4 +160°F	#1 45% CARBON #2 7% PRIMER #3 20% AF31 #4 3% PRIMER #5 15% FIBERGLASS	CARBON/CARBON PRIMER/PRIMER AF31/PRIMER PRIMER/PRIMER FIBERGLASS/FIBERGLASS	COHESIVE COHESIVE ADHESIVE COHESIVE COHESIVE	45% CARBON COHESIVE FAILURE
Gcf5 +160°F	#1 40% CARBON #2 5% PRIMER #3 15% AF31 #4 15% PRIMER #5 25% FIBERGLASS	CARBON/CARBON PRIMER/PRIMER AF31/PRIMER PRIMER/PRIMER FIBERGLASS/FIBERGLASS	COHESIVE COHESIVE ADHESIVE COHESIVE COHESIVE	40% CARBON COHESIVE FAILURE
Gcf6 +160°F	#1 25% CARBON #2 10% PRIMER #3 25% AF31 #4 20% PRIMER #5 20% FIBERGLASS	CARBON/CARBON PRIMER/PRIMER AF31/PRIMER PRIMER/PRIMER FIBERGLASS/FIBERGLASS	COHESIVE COHESIVE ADHESIVE COHESIVE COHESIVE	25% CARBON COHESIVE FAILURE 20% PRIMER COHESIVE FAILURE
Gcf7 -65°F	#1 90% CARBON #2 0% PRIMER #3 4% AF31 #4 1% PRIMER #5 5% FIBERGLASS	CARBON/CARBON PRIMER/PRIMER AF31/PRIMER PRIMER/PRIMER FIBERGLASS/FIBERGLASS	COHESIVE COHESIVE ADHESIVE COHESIVE COHESIVE	90% CARBON COHESIVE FAILURE
Gcf8 -65°F	#1 80% CARBON #2 0% PRIMER #3 5% AF31 #4 0% PRIMER #5 15% FIBERGLASS	CARBON/CARBON PRIMER/PRIMER AF31/PRIMER PRIMER/PRIMER FIBERGLASS/FIBERGLASS	COHESIVE COHESIVE ADHESIVE COHESIVE COHESIVE	80% CARBON COHESIVE FAILURE
Gcf9 -65°F	#1 70% CARBON #2 2% PRIMER #3 8% AF31 #4 0% PRIMER #5 20% FIBERGLASS	CARBON/CARBON PRIMER/PRIMER AF31/PRIMER PRIMER/PRIMER FIBERGLASS/FIBERGLASS	COHESIVE COHESIVE ADHESIVE COHESIVE COHESIVE	70% CARBON COHESIVE FAILURE

TABLE 1.32

FAILURE MODE DESCRIPTION OF CARBON/CARBON FROM
MAGNIFIED EXAMINATION (Fcc1 TO Fcc9)

IDENT. OF SPECIMEN AND TEMP.	MATERIAL IDENT. ON CARBON SURFACE	LAYERS OF SEPARATION	FAILURE MODE IDENT.	FAILURE CONCLUSION
Fcc1 R.T.	#1 75% CARBON #2 0% PRIMER #3 20% AF31 #4 0% PRIMER #5 5% CARBON	CARBON/CARBON PRIMER/PRIMER AF31/PRIMER PRIMER/PRIMER CARBON/CARBON	COHESIVE COHESIVE ADHESIVE COHESIVE COHESIVE	75% CARBON COHESIVE FAILURE
Fcc2 R.T.	#1 60% CARBON #2 5% PRIMER #3 15% AF31 #4 0% PRIMER #5 20% CARBON	CARBON/CARBON PRIMER/PRIMER AF31/PRIMER PRIMER/PRIMER CARBON/CARBON	COHESIVE COHESIVE ADHESIVE COHESIVE COHESIVE	60% CARBON COHESIVE FAILURE
Fcc3 R.T.	#1 80% CARBON #2 4% PRIMER #3 15% AF31 #4 0% PRIMER #5 1% CARBON	CARBON/CARBON PRIMER/PRIMER AF31/PRIMER PRIMER/PRIMER CARBON/CARBON	COHESIVE COHESIVE ADHESIVE COHESIVE COHESIVE	80% CARBON COHESIVE FAILURE
Fcc4 +160°F	#1 5% CARBON #2 3% PRIMER #2 60% AF31 #4 7% PRIMER #5 25% CARBON	CARBON/CARBON PRIMER/PRIMER AF31/PRIMER PRIMER/PRIMER CARBON/CARBON	COHESIVE COHESIVE ADHESIVE COHESIVE COHESIVE	80% AF31 ADHESIVE FAILURE 25% CARBON COHESIVE FAILURE
Fcc5 +160°F	#1 30% CARBON #2 7% PRIMER #3 55% AF31 #4 5% PRIMER #5 3% CARBON	CARBON/CARBON PRIMER/PRIMER AF31/PRIMER PRIMER/PRIMER CARBON/CARBON	COHESIVE COHESIVE ADHESIVE COHESIVE COHESIVE	30% CARBON COHESIVE FAILURE 55% AF31 ADHESIVE FAILURE
Fcc6 +160°F	#1 3% CARBON #2 5% PRIMER #3 25% AF31 #4 2% PRIMER #5 65% CARBON	CARBON/CARBON PRIMER/PRIMER AF31/PRIMER PRIMER/PRIMER CARBON/CARBON	COHESIVE COHESIVE ADHESIVE COHESIVE COHESIVE	 85% CARBON COHESIVE FAILURE
Fcc7 -65°F	#1 2% CARBON #2 4% PRIMER #3 8% AF31 #4 1% PRIMER #5 85% CARBON	CARBON/CARBON PRIMER/PRIMER AF31/PRIMER PRIMER/PRIMER CARBON/CARBON	COHESIVE COHESIVE ADHESIVE COHESIVE COHESIVE	 85% CARBON COHESIVE FAILURE
Fcc8 -65°F	#1 90% CARBON #2 2% PRIMER #3 5% AF31 #4 2% PRIMER #5 1% CARBON	CARBON/CARBON PRIMER/PRIMER AF31/PRIMER PRIMER/PRIMER CARBON/CARBON	COHESIVE COHESIVE ADHESIVE COHESIVE COHESIVE	90% CARBON COHESIVE FAILURE
Fcc9 -65°F	#1 7% CARBON #2 10% PRIMER #3 75% AF31 #4 3% PRIMER #5 5% CARBON	CARBON/CARBON PRIMER/PRIMER AF31/PRIMER PRIMER/PRIMER CARBON/CARBON	COHESIVE COHESIVE ADHESIVE COHESIVE COHESIVE	75% AF31 ADHESIVE FAILURE

TABLE 1.33

ORIGINAL PAGE IS
OF POOR QUALITY

FAILURE MODE DESCRIPTION OF CARBON/CARBON FROM
MAGNIFIED EXAMINATION (Gcc1 TO Gcc9)

IDENT. OF SPECIMEN AND TEMP.	MATERIAL IDENT. ON CARBON SURFACE	LAYERS OF SEPARATION	FAILURE MODE IDENT.	FAILURE CONCLUSION
Gcc1 R.T.	#1 60% CARBON #2 9% PRIMER #3 30% AF31 #4 1% PRIMER #5 0% CARBON	CARBON/CARBON PRIMER/PRIMER AF31/PRIMER PRIMER/PRIMER CARBON/CARBON	COHESIVE COHESIVE ADHESIVE COHESIVE COHESIVE	60% CARBON COHESIVE FAILURE
Gcc2 R.T.	#1 1% CARBON #2 1% PRIMER #3 50% AF31 #4 3% PRIMER #5 45% CARBON	CARBON/CARBON PRIMER/PRIMER AF31/PRIMER PRIMER/PRIMER CARBON/CARBON	COHESIVE COHESIVE ADHESIVE COHESIVE COHESIVE	50% AF31 ADHESIVE FAILURE 45% CARBON COHESIVE FAILURE
Gcc3 R.T.	#1 1% CARBON #2 1% PRIMER #3 55% AF31 #4 3% PRIMER #5 40% CARBON	CARBON/CARBON PRIMER/PRIMER AF31/PRIMER PRIMER/PRIMER CARBON/CARBON	COHESIVE COHESIVE ADHESIVE COHESIVE COHESIVE	55% AF31 ADHESIVE FAILURE 40% CARBON COHESIVE FAILURE
Gcc4 +160°F	#1 3% CARBON #2 1% PRIMER #2 90% AF31 #4 5% PRIMER #5 1% CARBON	CARBON/CARBON PRIMER/PRIMER AF31/PRIMER PRIMER/PRIMER CARBON/CARBON	COHESIVE COHESIVE ADHESIVE COHESIVE COHESIVE	90% AF31 ADHESIVE FAILURE
Gcc5 +160°F	#1 55% CARBON #2 5% PRIMER #3 35% AF31 #4 2% PRIMER #5 3% CARBON	CARBON/CARBON PRIMER/PRIMER AF31/PRIMER PRIMER/PRIMER CARBON/CARBON	COHESIVE COHESIVE ADHESIVE COHESIVE COHESIVE	55% CARBON COHESIVE FAILURE
Gcc6 +160°F	#1 1% CARBON #2 2% PRIMER #3 90% AF31 #4 3% PRIMER #5 5% CARBON	CARBON/CARBON PRIMER/PRIMER AF31/PRIMER PRIMER/PRIMER CARBON/CARBON	COHESIVE COHESIVE ADHESIVE COHESIVE COHESIVE	90% AF31 ADHESIVE FAILURE
Gcc7 -65°F	#1 5% CARBON #2 3% PRIMER #3 8% AF31 #4 2% PRIMER #5 82% CARBON	CARBON/CARBON PRIMER/PRIMER AF31/PRIMER PRIMER/PRIMER CARBON/CARBON	COHESIVE COHESIVE ADHESIVE COHESIVE COHESIVE	82% CARBON COHESIVE FAILURE
Gcc8 -65°F	#1 60% CARBON #2 5% PRIMER #3 30% AF31 #4 2% PRIMER #5 3% CARBON	CARBON/CARBON PRIMER/PRIMER AF31/PRIMER PRIMER/PRIMER CARBON/CARBON	COHESIVE COHESIVE ADHESIVE COHESIVE COHESIVE	60% CARBON COHESIVE FAILURE
Gcc9 -65°F	#1 45% CARBON #2 5% PRIMER #3 40% AF31 #4 5% PRIMER #5 5% CARBON	CARBON/CARBON PRIMER/PRIMER AF31/PRIMER PRIMER/PRIMER CARBON/CARBON	COHESIVE COHESIVE ADHESIVE COHESIVE COHESIVE	45% CARBON COHESIVE FAILURE

TABLE 1.34

LAP SHEAR STRENGTH OF PERFORATED TITANIUM TO
CARBON/EPOXY CLOTH

SPECIMEN ID	W (IN.)	OVERLAP (IN.)	AREA (SQ IN.)	ULT LOAD (LB)	STRESS (PSI)	AVERAGE FAILURE STRESS (PSI)	PERCENT OF ROOM TEMP FAILURE STRESS
ROOM TEMPERATURE							
F_{TC}-1	1.004	.502	.5040	1335	2649	2744	100%
F_{TC}-2	.996	.491	.4890	1270	2597		
F_{TC}-3	1.006	.516	.5191	1550	2986		
+160°F							
F_{TC}-4	1.004	.484	.4859	960	1975	2020	74%
F_{TC}-5	.999	.487	.4865	920	1891		
F_{TC}-6	1.000	.492	.4920	1080	2195		
-65°F							
F_{TC}-7	.993	.494	.4905	900	1835	1859	68%
F_{TC}-8	1.003	.500	.5015	925	1844		
F_{TC}-9	1.006	.492	.4950	940	1899		
ROOM TEMPERATURE							
G_{TC}-1	1.001	.498	.4985	1280	2568	2457	100%
G_{TC}-2	.996	.522	.5043	1245	2469		
G_{TC}-3	.998	.502	.5010	1170	2335		
+160°F							
G_{TC}-4	1.000	.506	.5060	970	1917	1915	78%
G_{TC}-5	.999	.504	.5035	915	1817		
G_{TC}-6	1.002	.486	.4870	980	2012		
-65°F							
G_{TC}-7	.996	.502	.5000	955	1910	1708	70%
G_{TC}-8	.994	.514	.5109	755	1478		
G_{TC}-9	.988	.522	.5157	895	1735		

TABLE 1.35

LAP SHEAR TESTS

CARBON/EPOXY CLOTH TO FIBERGLASS CLOTH

SPECIMEN ID	W (IN.)	OVERLAP (IN.)	AREA (SQ IN.)	ULT LOAD (LB)	STRESS (PSI)	AVERAGE FAILURE STRESS (PSI)	PERCENT OF ROOM TEMP FAILURE STRESS
ROOM TEMPERATURE							
F_G-1	.969	.498	.4826	1165	2414	2524	
F_G-10					2570		
F_G-3	.984	.524	.5156	1335	2589		
+160°F							
F_G-4	.990	.523	.5178	1130	2182	2189	87%
F_G-5	.980	.501	.5910	1100	2240		
F_G-6	.990	.480	.4752	1020	2146		
-65°F							
F_G-7	.991	.501	.4965	972	1958	1911	76%
F_G-8	.988	.512	.5059	952	1882		
F_G-9	.982	.500	.4910	930	1894		
ROOM TEMPERATURE							
G_G-1	.993	.500	.4965	1500	3021	2692	100%
G_G-2	1.002	.495	.4960	1285	2590		
G_G-3	.991	.475	.4707	1160	2464		
+160°F							
G_G-4	.990	.514	.5089	1155	2270	2106	78%
G_G-5	.981	.498	.4885	980	2006		
G_G-6	1.000	.509	.5090	1040	2043		
-65°F							
G_G-7	1.002	.540	.5411	1100	2033	1964	73%
G_G-8	.999	.505	.5045	940	1863		
G_G-9	.960	.509	.4886	975	1995		

TABLE 1.36

LAP SHEAR STRENGTH OF CARBON/EPOXY CLOTH TO
CARBON/EPOXY CLOTH

SPECIMEN ID	W (IN.)	OVERLAP (IN.)	AREA (SQ IN.)	ULT LOAD (LB)	STRESS (PSI)	AVERAGE FAILURE STRESS (PSI)	PERCENT OF ROOM TEMP FAILURE STRESS
ROOM TEMPERATURE							
F_{CC}-1	.988	.514	.5078	1315	2589	2568	100%
F_{CC}-2	.981	.480	.4709	1220	2591		
F_{CC}-3	.990	.474	.4693	1185	2525		
+160°F							
F_{CC}-4	.992	.493	.4891	980	2004	1902	74%
F_{CC}-5	.991	.486	.4816	920	1910		
F_{CC}-6	.994	.488	.4851	870	1793		
-65°F							
F_{CC}-7	1.001	.530	.5305	1025	1932	2085	81%
F_{CC}-8	.989	.502	.4965	1030	2075		
F_{CC}-9	.992	.448	.4444	1000	2250		
ROOM TEMPERATURE							
G_{CC}-1	.995	.500	.4975	1235	2482	2479	100%
G_{CC}-2	.984	.502	.4940	1145	2318		
G_{CC}-3	.990	.498	.4930	1300	2637		
+160°F							
G_{CC}-4	.989	.517	.5113	1050	2053	2036	82%
G_{CC}-5	.993	.464	.4608	965	2094		
G_{CC}-6	.987	.504	.4974	975	1960		
-65°F							
G_{CC}-7	.994	.506	.5030	820	1630	1955	79%
G_{CC}-8	.993	.510	.5064	1100	2172		
G_{CC}-9	.994	.502	.4990	1030	2064		

TABLE 1.37

LAP SHEAR TESTS

FIBERGLASS CLOTH TO FIBERGLASS CLOTH

SPECIMEN ID	W (IN.)	OVERLAP (IN.)	AREA (SQ IN.)	ULT LOAD (LB)	STRESS (PSI)	AVERAGE FAILURE STRESS (PSI)	PERCENT OF ROOM TEMP FAILURE STRESS
ROOM TEMPERATURE							
F_F-1	.968	.510	.4937	700	1418	1548	100%
F_F-2	.952	.510	.4855	770	1586		
F_F-3	.957	.515	.4929	809	1641		
+160°F							
F_F-4	.979	.513	.5022	630	1254	1372	89%
F_F-5	.967	.518	.5009	688	1373		
F_F-6	.985	.485	.4777	711	1488		
-65°F							
F_F-7	.983	.536	.5269	770	1461	1344	87%
F_F-8	.974	.508	.4948	708	1431		
F_F-9	.977	.509	.4973	567	1140		
ROOM TEMPERATURE							
G_F-1	.965	.515	.4970	851	1712	1781	100%
G_F-2	.973	.505	.4914	885	1801		
G_F-3	.971	.501	.4865	891	1831		
+160°F							
G_F-4	.975	.515	.5021	818	1629	1563	88%
G_F-5	.962	.515	.4954	709	1431		
G_F-6	.982	.516	.5067	825	1628		
-65°F							
G_F-7	.974	.520	.5065	690	1362	1359	100%
G_F-8	.975	.516	.5031	663	1318		
G_F-9	.979	.510	.4993	698	1398		

TABLE 1.38

TEST NO. 1, SPECIMEN 10E

CLOSED CORRUGATED SANDWICH PANEL

MATERIAL CODES FOR LAMINA (INCHES)

1 - CARBON/EPOXY TAPE (T=0.005)	5 - E-GLASS CLOTH (T=0.010)
2 - CARBON/EPOXY CLOTH (T=0.010)	6 - F584/IM6 CARBON/EPOXY (T=0.0055)
3 - KEVLAR/EPOXY CLOTH (T=0.010)	7 - TITANIUM MATERIAL (T=0.0050)
4 - K/E THIN COCURED FACINGS (T=0.010)	8 - ADDITIONAL MATERIAL IF ANY

MONOLAYER PROPERTIES FOR LAMINA

CODE	E_L (psi)	E_T (psi)	G_{LT} (psi)	ν_{LT}	Rho (pci)
2	0.8200E+07	0.8200E+07	0.5700E+06	0.0990	0.0571
5	0.2900E+07	0.2900E+07	0.3000E+06	0.1300	0.0700
7	0.1640E+08	0.1640E+08	0.6200E+07	0.3100	0.1600

PANEL GEOMETRY AND STIFFENER SPACING (INCHES)

LENGTH = 8.500	WIDTH = 4.330	SPACING = 1.000
BASE = 0.400	CAP = 0.404	HEIGHT = 0.683

ANGLE (A) AND MATERIAL CODE (C) OF EACH PLY (P)

ONLY FOR UPPER SKIN

P	1	2	3	4	5
A	0	0	0	0	0
C	7	7	7	7	7

ONLY FOR LOWER SKIN

P	1	2	3	4	5	6
A	0	0	0	0	0	0
C	5	5	5	5	2	2

ONLY FOR BASE

P	1	2	3	4	5	6
A	0	0	0	0	0	0
C	5	5	5	5	5	5

ONLY FOR CAP

P	1	2	3	4	5	6	7	8	9	10
A	0	0	0	0	0	0	0	0	0	0
C	5	5	5	5	2	2	5	5	5	5

ONLY FOR WEB

P	1	2	3	4
A	0	0	0	0
C	5	5	5	5

LOCAL AND GENERAL BUCKLING
NORMALIZED TO COLUMN LOAD

UPPER SKIN	Nx =	9,613 LB/IN.
LOWER SKIN	Nx =	11,684 LB/IN.
WEB	Nx =	5,053 LB/IN.
GENERAL	Nx =	85,703 LB/IN.

SHEAR BUCKLING
NORMALIZED TO PANEL LOAD

UPPER SKIN	Nxy =	3,877 LB/IN.
LOWER SKIN	Nxy =	25,287 LB/IN.
WEB	Nxy =	35,130 LB/IN.
GENERAL	Nxy =	153,439 LB/IN.

STRAIN = 6,307 MICRO IN./IN. AT Nx = 5,053 LB/IN.

PROPERTIES OF PANEL

D_{11} = 65,121.9	AREA PER INCH = 0.1216 SQ IN./IN.
D_{22} = 53,802.0	EA PER INCH = 801,137 LB/IN.
D_{12} = 9,316.0	WEIGHT = 1.4979 psf
D_{66} = 6,186.6	

TABLE 1.39

STRAIN GAGE READINGS FOR CONFIGURATION H1$_1$

LABORATORY TEST DATA
COMPRESSION TEST NO. 19439

STRAIN GAGE NO.	LOAD (LBS) 5,000	10,000	15,000	17,000	19,000	21,000	23,000	24,000	25,000
				STRAIN IN MICRO IN./IN.					
1	375	1252	2154	2512	2894	3311	3711	4065	4247
2	1277	1901	2400	2522	2572	2560	2248	1623	1200
3	532	1414	2318	2674	3013	3441	3790	4160	4355
4	941	1693	2725	3075	3538	3931	4374	4580	4711
5	576	1460	2343	2682	3032	3482	3821	4204	4850
6	1460	2380	3339	3708	4149	4240	4593	4090	3352
7	702	1629	2590	2969	3379	3768	4195	4441	4670
8	1122	2047	2962	3325	3692	4114	4504	4869	1450
9	799	1753	2730	3115	3530	3917	4342	4604	4631
10	1246	2227	3157	3536	3865	4344	4254	5301	1454
11	893	1892	2915	3314	3748	4146	4538	4860	4426
12	1207	2155	3103	3479	3868	4459	4834	4568	3612
13	972	1907	2836	3208	3594	4038	4465	4826	5647
14	910	1893	2883	3278	3701	4115	4568	4728	4499
15	1049	1949	2838	3196	3554	3981	4358	4696	5593
16	1005	2053	3100	3517	3962	4366	4826	4938	4362
17	1150	2108	3087	3484	3906	4345	4860	5221	7337
18	819	1759	2722	3099	3505	3740	4137	4065	3632
19	520	1098	1666	1866	2087	2293	2514	2589	2923
20	713	1346	1971	2206	2458	2857	3127	3393	3593

SPECIMEN ID H1$_1$ ULT. 25,100 LBS

TABLE 1.40

STRAIN GAGE READINGS FOR CONFIGURATION J1₁

LABORATORY TEST DATA
COMPRESSION TEST FIBERGLASS C/E/Ti NO. 19437

STRAIN GAGE NO.	LOAD (LBS) 5,000	10,000	15,000	20,000	22,000	24,000	26,000
			STRAIN IN MICRO IN./IN.				
1	1006	1958	2884	3840	4228	4617	5038
2	900	1784	2669	3592	3978	4348	4734
3	1071	2004	2938	3905	4317	4716	5150
4	1006	1912	2823	3754	4149	4529	4957
5	1115	2154	3240	4604	5825	7537	8645
6	877	1799	2700	3638	4032	4400	4775
7	891	1810	2724	3653	4037	4415	4800
8	1000	2013	3049	4150	4627	5080	5560
9	921	1845	2767	3704	4103	4483	4874
10	940	1855	2768	3719	4121	4509	4910
11	961	1933	2903	3400	4306	4642	3836
12	986	1953	2921	3924	4345	4255	5166
13	858	1727	2612	3536	3917	4292	4678
14	1141	2215	3277	4363	4810	5241	5694
15	858	1718	2596	3496	3877	4245	4622
16	1299	2412	3523	4665	5189	5663	6168
17	846	1795	2774	3832	4300	4780	5282
18	1127	2110	3072	4036	4431	4807	5195
19	600	1218	1820	2415	2645	2865	3099
20	584	1145	1680	2196	2377	2557	2742

SPECIMEN ID J1₁

TABLE 1.41

STRAIN GAGE READINGS FOR CONFIGURATION G1$_1$

TO 26,000 POUNDS

LABORATORY TEST DATA
COMPRESSION TEST

STRAIN GAGE NO.	LOAD (LBS) 5,000	10,000	15,000	17,000	19,000	21,000	23,000	24,000	25,000	26,000
				STRAIN IN MICRO IN./IN.						
1	931	1830	2704	3071	3414	3765	4067	4257	4430	4593
2	827	1659	2496	2854	3192	3534	3842	4028	4191	4360
3	857	1723	2591	2972	3310	3666	3980	4176	4347	4525
4	1002	1899	2795	3177	3523	3883	4196	4381	4556	4714
5	881	1759	2633	3002	3354	3706	4025	4220	4395	4587
6	867	1715	2555	2911	3233	3563	3845	4017	4170	4320
7	871	1742	2618	2971	3319	3672	4032	4230	4406	4582
8	891	1769	2661	3024	3378	3741	4111	4313	4498	4674
9	863	1731	2602	2959	3304	3660	4019	4219	4395	4564
10	992	1908	2843	3244	3599	3984	4396	4613	4807	4999
11	820	1675	2531	2883	3222	3568	3924	4114	4288	4458
12	935	1831	2744	3132	3500	3898	4311	4540	4752	4964
13	848	1716	2585	2938	3280	3635	3993	4192	4369	4514
14	928	1795	2658	3009	3354	3704	4065	4259	4442	4608
15	886	1718	2561	2899	3232	3573	3923	4110	4283	4451
16	1280	2270	3258	3657	4063	4489	4937	5195	5430	5667
17	772	1643	2516	2870	3212	3570	3930	4120	4300	4472
18	1049	1936	2787	3124	3448	3787	4121	4298	4455	4613
19	454	1108	1679	1904	2124	2355	2580	2696	2802	2905
20	665	1340	2000	2270	2524	2787	3055	3191	3315	3432

TABLE 1.42

STRAIN GAGE READINGS FOR CONFIGURATION G1₁

TO 31,250 POUNDS

LABORATORY TEST DATA
COMPRESSION TEST

STRAIN GAGE NO.	LOAD (LBS) 27,000	28,000	29,000	30,000	31,000
		STRAIN IN MICRO IN./IN			
1	4766	5169	5439	5662	5916
2	4539	4505	4600	4611	3564
3	4711	4944	5177	5390	5843
4	4883	5154	5387	5584	2854
5	4751	4951	5173	5379	6234
6	4755	4672	4898	5029	2357
7	4765	4987	5198	5394	5778
8	4861	4804	4961	5050	4222
9	4753	5000	5214	5416	5927
10	5196	5465	5679	5881	4339
11	4641	4872	5070	5289	5254
12	5196	5499	5982	6060	4400
13	4725	4968	5181	5379	4865
14	4794	4893	5075	5242	4922
15	4626	4844	5042	5248	5285
16	5939	6202	6536	6862	6115
17	4655	4910	5118	5327	5354
18	4781	4930	5155	5340	4881
19	3013	2895	2971	3043	3000
20	3575	3744	3884	4016	2882

31,250 LBS MAXIMUM

212

TABLE 1.43

CONFIGURATION A1-1 ANALYSES

(LENGTH AND WIDTH CORRECTED FOR EDGE STIFFNESS)

MATERIAL CODES FOR LAMINA (INCHES)
```
1 - CARBON/EPOXY TAPE          (T=0.005)   5 - E-GLASS CLOTH          (T=0.010)
2 - CARBON/EPOXY CLOTH         (T=0.010)   6 - F584/IM6 CARBON/EPOXY (T=0.0055)
3 - KEVLAR/EPOXY CLOTH         (T=0.010)   7 - TITANIUM MATERIAL      (T=0.0050)
4 - K/E THIN COCURED FACINGS (T=0.010)     8 - ADDITIONAL MATERIAL IF ANY
```

MONOLAYER PROPERTIES FOR LAMINA

CODE	E_L (psi)	E_T (psi)	G_{LT} (psi)	ν_{LT}	Rho (pci)
2	0.8200E+07	0.8200E+07	0.5700E+06	0.0990	0.0571
5	0.2900E+07	0.2900E+07	0.3000E+06	0.1300	0.0700
7	0.1640E+08	0.1640E+08	0.6200E+07	0.3100	0.1600

PANEL GEOMETRY AND STIFFENER SPACING (INCHES)
```
LENGTH = 2.310     WIDTH = 2.310      SPACING = 1.110
BASE   = 0.410     CAP   = 0.510      HEIGHT  = 0.767
```

ANGLE (A) AND MATERIAL CODE (C) OF EACH PLY (P)

ONLY FOR UPPER SKIN

P	1	2	3	4	5
A	0	0	0	0	0
C	7	7	7	7	7

ONLY FOR LOWER SKIN

P	1	2	3	4	5
A	0	0	0	0	0
C	2	5	5	5	2

ONLY FOR BASE

P	1	2	3	4	5	6	7
A	0	0	0	0	0	0	0
C	5	5	5	5	5	5	2

ONLY FOR CAP

P	1	2	3	4	5	6	7	8	9	10	11	12	13
A	0	0	0	0	0	0	0	0	0	0	0	0	0
C	2	5	5	5	5	5	5	2	5	5	5	5	5

ONLY FOR WEB

P	1	2	3	4	5
A	0	0	0	0	0
C	5	5	5	5	5

```
LOCAL AND GENERAL BUCKLING          SHEAR BUCKLING
NORMALIZED TO COLUMN LOAD           NORMALIZED TO PANEL LOAD
UPPER SKIN   Nx =  11,678 LB/IN.    UPPER SKIN   Nxy =     4,048 LB/IN.
LOWER SKIN   Nx =  10,883 LB/IN.    LOWER SKIN   Nxy =    25,442 LB/IN.
WEB          Nx =   7,202 LB/IN.    WEB          Nxy =    65,318 LB/IN.
GENERAL      Nx = 421,412 LB/IN.    GENERAL      Nxy = 1,002,998 LB/IN.
```

STRAIN = 8,060 MICRO IN./IN. AT Nx = 7,202 LB/IN.

PROPERTIES OF PANEL
```
D11 = 96,165.8    AREA PER INCH = 0.1362 SQ IN./IN.
D22 = 74,877.3    EA PER INCH   = 893,574 LB/IN.
D12 = 12,728.0    WEIGHT        = 1.6362 psf
D66 =  7,832.9
```

TABLE 1.44

A1-1, A1-3, AND L1$_1$P STRAIN GAGE DATA

SPECIMEN GEOMETRY

ID	W (IN.)	L (IN.)	T (IN.)	ULTIMATE LOAD (LBS)
A1-1	3.121	3.010	.7755	31500
A1-3	3.152	2.938	.7705	28300
L1$_1$P	2.997	2.995	.6696	6990

ID=IDENTIFICATION, W=WIDTH, L=LENGTH, T=THICKNESS

SPECIMEN A1-1

LOAD (LBS)	STRAIN (MICRO IN./IN.) GAGE 1	GAGE 2
1000	+ 55	- 491
2000	- 31	- 857
3000	- 222	- 126
4000	- 482	- 1608
5000	- 716	- 1896
6000	- 960	- 2193
7000	-1205	- 2499
8000	-1476	- 2838
9000	-1783	- 3227
10000	-1933	- 3349
11000	-2212	- 3665
12000	-2487	- 3931
13000	-2744	- 4235
14000	-3037	- 4498
15000	-3287	- 4779
16000	-3564	- 5069
17000	-3848	- 5322
18000	-4137	- 5596
19000	-4432	- 5972
20000	-4760	- 6262
21000	-5047	- 6637
22000	-5376	- 7010
23000	-5674	- 7299
24000	-6095	- 8006
25000	-6090	- 7686
26000	-6308	- 7960
27000	-6694	- 8416
28000	-6981	- 8799
29000	-7175	- 9458
30000	-5706	-10505
31000	-4946	-10603

ULTIMATE LOAD 31500 LBS

SPECIMEN A1-3

LOAD (LBS)	STRAIN (MICRO IN./IN.) GAGE 1	GAGE 2
2000	- 635	- 404
4000	-1227	-1002
6000	-1745	-1534
8000	-2249	-2024
10000	-2796	-2578
12000	-3335	-3083
14000	-3852	-3594
16000	-4388	-4097
18000	-4939	-4647
20000	-5445	-5133
22000	-6001	-5676
24000	-6482	-6306
26000	-6851	-6913
28000	-	-

ULTIMATE LOAD 28300 LBS

SPECIMEN L1$_1$P

LOAD (LBS)	STRAIN (MICRO IN./IN.) GAGE 1	GAGE 2
1000	- 588	- 478
2000	-1208	- 896
3000	-1715	- 1195
4000	-2257	- 1373
5000	-2892	- 1253
6000	-3379	- 639

ULTIMATE LOAD 6990 LBS

214

TABLE 1.45

A1-2 AND A1-4 STRAIN GAGE DATA

SPECIMEN GEOMETRY

ID	W (IN.)	L (IN.)	T (IN.)	ULTIMATE LOAD (LBS)
A1-2	3.271	2.969	.766	28150
A1-4	3.138	2.981	.773	29050

ID=IDENTIFICATION, W=WIDTH, L=LENGTH, T=THICKNESS

SPECIMEN A1-2

LOAD (LBS)	STRAIN (MICRO IN./IN.)	
	GAGE 1	GAGE 2
2000	+ 4	- 932
4000	- 317	-1584
6000	- 792	-2104
8000	-1353	-2660
10000	-1803	-3088
12000	-2319	-3569
14000	-2815	-4020
16000	-3352	-4481
18000	-3904	-4936
20000	-4496	-5463
22000	-5022	-5915
24000	-5566	-6389
26000	-6099	-6776
28000	-	-

ULTIMATE LOAD 28150 LBS

SPECIMEN A1-4

LOAD (LBS)	STRAIN (MICRO IN./IN.)	
	GAGE 1	GAGE 2
2000	- 69	- 909
4000	- 330	-1552
6000	- 580	-2171
8000	- 833	-2734
10000	-1109	-3350
12000	-1360	-3917
14000	-1643	-4578
16000	-1939	-5099
18000	-2300	-5655
20000	-2723	-6221
22000	-3138	-6788
24000	-3561	-7331
26000	-4090	-7913
27000	-4343	-8234
28000	-4571	-8480

ULTIMATE LOAD 29050 LBS

TABLE 1.46

$A1_1$, $A1_2P$, AND $L1_2P$ STRAIN GAGE DATA

SPECIMEN GEOMETRY

ID	W (IN.)	L (IN.)	T (IN.)	ULTIMATE LOAD (LBS)
$A1_1$	2.921	2.880	.7175	20400
$A1_2P$	2.999	2.995	.6751	18000
$L1_2P$	2.982	2.999	.6682	6210

ID=IDENTIFICATION, W=WIDTH, L=LENGTH, T=THICKNESS

SPECIMEN $A1_1$

LOAD (LBS)	STRAIN (MICRO IN./IN.) GAGE 1	GAGE 2
2000	- 28	-1163
4000	- 571	-1941
6000	-1204	-2566
8000	-1904	-3176
9000	-2231	-3473
10000	-2570	-3723
11000	-2936	-4109
12000	-3160	-4328
13000	-3613	-4747
14000	-3920	-5008
15000	-4257	-5333
16000	-4620	-5717
17000	-5003	-6208
18000	-5363	-6643
19000	-5769	-7213
20000	-6175	-7743
21000	-	-

ULTIMATE LOAD 20400 LBS

SPECIMEN $A1_2P$

LOAD (LBS)	STRAIN (MICRO IN./IN.) GAGE 1	GAGE 2
2000	-1009	- 403
4000	-1672	-1003
6000	-2374	-1717
8000	-2986	-2337
9000	-3304	-2641
10000	-3582	-2966
11000	-3949	-3295
12000	-4247	-3626
13000	-4526	-3911
14000	-9302	-5398
15000	-9371	-5694
16000	-9106	-5430
17000	+4940	-2184

ULTIMATE LOAD 18000 LBS

SPECIMEN $L1_2P$

LOAD (LBS)	STRAIN (MICRO IN./IN.) GAGE 1	GAGE 2
1000	- 638	- 451
2000	-1092	- 895
3000	-1519	-1366
4000	-1889	-1901
5000	-2330	-2427
6000	-3610	-3496

ULTIMATE LOAD 6210 LBS

TABLE 1.47

SIMPLY SUPPORTED 3– BY 3–INCH PANEL

MATERIAL CODES FOR LAMINA (INCHES)
1 - CARBON/EPOXY TAPE   (T=0.005)   5 - E-GLASS CLOTH   (T=0.010)
2 - CARBON/EPOXY CLOTH   (T=0.010)   6 - F584/IM6 CARBON/EPOXY (T=0.0055)
3 - KEVLAR/EPOXY CLOTH   (T=0.010)   7 - TITANIUM MATERIAL   (T=0.0050)
4 - K/E THIN COCURED FACINGS (T=0.010)   8 - ADDITIONAL MATERIAL IF ANY

MONOLAYER PROPERTIES FOR LAMINA

CODE	E_L (psi)	E_T (psi)	G_{LT} (psi)	ν_{LT}	Rho (pci)
2	0.8200E+07	0.8200E+07	0.5700E+06	0.0990	0.0571
5	0.2900E+07	0.2900E+07	0.3000E+06	0.1300	0.0700
7	0.1640E+08	0.1640E+08	0.6200E+07	0.3100	0.1600

PANEL GEOMETRY AND STIFFENER SPACING (INCHES)

LENGTH = 3.000   WIDTH = 3.000   SPACING = 1.110
BASE   = 0.410   CAP   = 0.510   HEIGHT = 0.767

ANGLE (A) AND MATERIAL CODE (C) OF EACH PLY (P)

ONLY FOR UPPER SKIN

P	1	2	3	4	5
A	0	0	0	0	0
C	7	7	7	7	7

ONLY FOR LOWER SKIN

P	1	2	3	4	5
A	0	0	0	0	0
C	2	5	5	5	2

ONLY FOR BASE

P	1	2	3	4	5	6	7
A	0	0	0	0	0	0	0
C	5	5	5	5	5	5	2

ONLY FOR CAP

P	1	2	3	4	5	6	7	8	9	10	11	12	13
A	0	0	0	0	0	0	0	0	0	0	0	0	0
C	2	5	5	5	5	5	5	2	5	5	5	5	5

ONLY FOR WEB

P	1	2	3	4	5
A	0	0	0	0	0
C	5	5	5	5	5

LOCAL AND GENERAL BUCKLING   SHEAR BUCKLING
NORMALIZED TO COLUMN LOAD   NORMALIZED TO PANEL LOAD

UPPER SKIN   Nx = 11,661 LB/IN.   UPPER SKIN   Nxy =   3,934 LB/IN.
LOWER SKIN   Nx = 10,808 LB/IN.   LOWER SKIN   Nxy = 24,684 LB/IN.
WEB   Nx =   7,187 LB/IN.   WEB   Nxy = 63,828 LB/IN.
GENERAL   Nx = 249,855 LB/IN.   GENERAL   Nxy = 594,678 LB/IN.

STRAIN = 8,043 MICRO IN./IN. AT Nx = 7,187 LB/IN.

PROPERTIES OF PANEL

D_{11} = 96,165.8   AREA PER INCH = 0.1362 SQ IN./IN.
D_{22} = 74,887.3   EA PER INCH   = 893,574 LB/IN.
D_{12} = 12,728.0   WEIGHT   = 1.6362 psf
D_{66} = 7,832.9

TABLE 1.48

(3- BY 3-INCH) STRAIN VALUES FOR A1-9 TO A1-11

SPECIMEN GEOMETRY

ID	W (IN.)	T (IN.)	H (IN.)
A1-9	2.896	.768	2.898
A1-10	2.895	.773	2.895
A1-11	2.895	.766	2.900
A1-12	2.897	.764	2.896
A1-13	2.896	.764	2.896

ID=IDENTIFICATION, W=WIDTH, T=DEPTH, H=LENGTH

SPECIMEN A1-9

LOAD (LBS)	Ti STRAIN (MICRO IN./IN.) GAGE 1	COMP. GAGE 2
3000	- 945	- 745
6000	-1846	-1597
9000	-2717	-2433
10000	-2992	-2702
11000	-3287	-2990
12000	-3573	-3273
13000	-3859	-3553
14000	-4165	-3852
15000	-4456	-4131
16000	-4756	-4422
17000	-5050	-4698

ULTIMATE LOAD 17820 LBS

SPECIMEN A1-10

LOAD (LBS)	Ti STRAIN (MICRO IN./IN.) GAGE 1	COMP. GAGE 2
3000	-	-
6000	-2070	-1382
9000	-	-
10000	-3250	-2446
11000	-	-
12000	-3823	-2976
13000	-	-
14000	-4420	-3531
15000	-4710	-3796
16000	-5036	-4098
17000	-5330	-4349
18000	-5642	-4625
19000	-5928	-4874

ULTIMATE LOAD 19760 LBS

SPECIMEN A1-11

LOAD (LBS)	Ti STRAIN (MICRO IN./IN.) GAGE 1	COMP. GAGE 2
1000	-192	- 247
2000	-254	- 614
3000	-231	- 993
4000	- 96	-1390
5000	+209	-1770

ULTIMATE LOAD 6130 LBS

TABLE 1.49

PANEL LA1-1-2₁ DIAL INDICATORS (4.5- BY 10-INCH)

LOAD (LBS)	TOP	CENTER	LOWER
		DEFLECTION IN INCHES	
5,000	-.0010	-.0012	-.0018
7,000	-.0010	-.0014	-.0020
9,000	-.0008	-.0014	-.0020
11,000	-.0008	-.0010	-.0018
15,000	-.0002	-.0006	-.0014
20,000	-.0001	-.0000	-.0002
25,000	+.0001	+.0010	+.0010
29,000	+.0006	+.0018	+.0020
32,000	+.0006	+.0014	+.0032
34,000	+.0009	+.0009	+.0036
36,000	+.0006	+.0006	+.0039
38,000	+.0007	+.0000	+.0045
40,000	+.0010	-.0008	+.0050
42,000	+.0009	+.0012	+.0052
44,000	+.0010	-.0020	+.0056
46,000	+.0010	-.0028	+.0051
48,000	+.0010	-.0041	+.0070
50,000	+.0008	-.0050	+.0071

TABLE 1.50

PANEL LA1-1-2₁ STRAIN READINGS (4.5- BY 10-INCH)

STRAIN GAGE NO.	LOAD (LBS) 5,000	7,000	9,000	11,000	15,000	20,000	25,000	29,000
			STRAIN IN MICRO IN./IN.					
1	- 891	-1179	-1508	-1804	-2436	-3232	4011	4646
2	- 616	931	1256	1566	2219	3026	3828	4450
3	- 937	1241	1548	1836	2427	3188	3928	4534
4	- 786	1134	1488	1814	2499	3381	4200	4877
5	- 963	1284	1608	1923	2555	3355	4154	4800
6	- 723	1086	1452	1817	2543	3457	4344	5059
7	- 780	1096	1420	1732	2377	3187	3992	4676
8	- 789	1114	1465	1799	2477	3340	4209	4926
9	- 845	1171	1510	1826	2424	3309	4126	4780
10	- 833	1150	1488	1800	2451	3281	4097	4756
11	- 873	1217	1556	1885	2550	3399	4230	4899
12	- 810	1126	1460	1770	2399	3215	4010	4661
13	- 619	936	1256	1564	2192	3015	3897	4439
14	-1000	1350	1700	2040	2716	3608	4479	5188
15	- 866	1194	1536	1840	2488	3294	4082	4715
16	-1166	1536	1912	2768	2492	3932	4882	5644
17	- 766	1095	1420	1738	2368	3159	3923	4548
18	-1169	1515	1883	2226	2919	3827	4736	5464
19	- 590	860	1130	1387	1919	2593	3254	3780
20	- 731	1014	1293	1562	2105	2798	3466	4011

TABLE 1.51

PANEL LA1-1-2, STRAIN READINGS (4.5- BY 10-INCH) CONT.

STRAIN GAGE NO.	LOAD (LBS) 32,000	34,000	36,000	38,000	40,000	42,000	44,000	46,000	48,000	50,000
				STRAIN IN MICRO IN./IN.						
1	5134	5444	5782	6132	6450	6790	7099	7400	7709	8128
2	4956	5269	5624	5994	6328	6688	7013	7350	7711	8155
3	5008	5309	5628	5955	6362	6582	6891	7210	7558	8024
4	5418	5761	6122	6481	6845	7200	7540	7875	8244	8653
5	5271	5587	5997	6237	6548	6875	7200	7534	7903	8456
6	5631	6000	6400	6783	7164	7557	7928	8311	8739	9335
7	5145	5469	5816	6155	6491	6840	7184	7509	7877	8245
8	5489	5851	6234	6636	7027	7452	7879	8317	8850	9418
9	5302	5636	5995	6345	6689	7061	7394	7748	8123	8519
10	5260	5598	5938	6281	6619	6958	7288	7611	7989	8330
11	5416	5756	6100	6476	6864	7327	7700	8094	8523	9128
12	5164	5484	5817	6145	6457	6775	7089	7377	7716	8000
13	4945	5281	5629	5974	6305	6656	6998	7320	7682	8013
14	5740	6094	6474	6844	7224	7614	8000	8382	8830	9311
15	5210	5543	5871	6218	6551	6996	7241	7578	7958	8305
16	6263	6631	7055	7474	7889	8334	8764	9198	9700	10236
17	5078	5331	5639	5965	6272	6592	6911	7214	7513	7795
18	6043	6422	6833	7243	7640	8071	8500	8900	9396	9712
19	4189	4449	4222	5000	5265	5542	5807	6077	6383	6659
20	4420	4680	7466	5288	5576	5817	6084	6316	6551	6812

TABLE 1.52

DIAL INDICATOR DEFLECTIONS, LA1-1-2$_2$ PANEL

LOAD (LBS)	TOP	MIDDLE	LOWER
		DEFLECTION IN INCHES	
5,000	.0000	-.0015	-.0024
10,000	-.0002	-.0028	-.0040
15,000	-.0009	-.0040	-.0045
20,000	-.0014	-.0050	-.0065
25,000	-.0020	-.0055	-.0070
30,000	-.0027	-.0063	-.0072
35,000	-.0030	-.0060	-.0080
40,000	-.0034	-.0068	-.0090
43,000	-.0040	-.0070	-.0097
45,000	-.0040	-.0070	-.0097
47,000	-.0047	-.0075	-.0100
49,000	FAILURE		

TABLE 1.53

STRAIN GAGE READINGS FOR LA1-5-2₂

SPECIMEN ID	W (IN.)	T (IN.)	H (IN.)
LA1-5-2₂	5.204	.7815	12.016

STRAIN GAGE NO.	LOAD (LBS)							
	5,000	10,000	15,000	20,000	25,000	30,000	35,000	40,000
			STRAIN IN MICRO IN./IN.					
1	- 868	-1711	-2578	-3435	-4320	-5221	-6127	-7052
2	- 536	-1238	-1963	-2684	-3419	-4156	-4882	-5704
3	-1050	-1842	-2658	-3467	-4303	-5153	-6082	-6947
4	- 638	-1335	-2059	-2769	-3492	-4220	-4925	-5704
5	- 985	-1784	-2595	-3396	-4208	-5027	-5830	-6653
6	- 680	-1434	-2191	-2932	-3682	-4422	-4137	-5891
7	- 699	-1480	-2274	-3056	-3855	-4642	-5408	-6220
8	- 861	-1680	-2515	-3339	-4187	-5052	-5905	-6619
9	- 748	-1536	-2344	-3142	-3949	-4764	-5562	-6430
10	- 924	-1748	-2595	-3436	-4293	-5160	-6029	-6777
11	- 799	-1580	-2382	-3176	-3977	-4777	-5564	-6416
12	- 955	-1772	-2602	-3418	-4253	-5099	-5930	-6749
13	- 558	-1275	-2015	-2743	-3470	-4190	-4882	-5924
14	-1078	-1899	-2728	-3536	-4360	-5195	-6019	-7958
15	- 623	-1345	-2095	-2832	-3582	-4339	-5078	-5798
16	-1243	-1285	-2937	-3761	-4587	-5414	- 699	-8042
17	- 529	-1231	-1959	-2671	-3404	-4143	-4864	-5608
18	-1454	-2463	-3570	-4562	-5667	-6815	-8004	-9528

TABLE 1.54

BUCKLING ANALYSIS USING SIMPLY SUPPORTED EDGES

(8- BY 20-INCH PANEL)

MATERIAL CODES FOR LAMINA (INCHES)

1 - CARBON/EPOXY TAPE	(T=0.005)	5 - E-GLASS CLOTH (T=0.010)
2 - CARBON/EPOXY CLOTH	(T=0.010)	6 - F584/IM6 CARBON/EPOXY (T=0.0055)
3 - KEVLAR/EPOXY CLOTH	(T=0.010)	7 - TITANIUM MATERIAL (T=0.0050)
4 - K/E THIN COCURED FACINGS	(T=0.010)	8 - ADDITIONAL MATERIAL IF ANY

MONOLAYER PROPERTIES FOR LAMINA

CODE	E_L (psi)	E_T (psi)	G_{LT} (psi)	ν_{LT}	Rho (pci)
2	0.8200E+07	0.8200E+07	0.5700E+06	0.0990	0.0571
5	0.2900E+07	0.2900E+07	0.3000E+06	0.1300	0.0700
7	0.1640E+08	0.1640E+08	0.6200E+07	0.3100	0.1600

PANEL GEOMETRY AND STIFFENER SPACING (INCHES)

LENGTH = 20.000	WIDTH = 8.000	SPACING = 1.110
BASE = 0.410	CAP = 0.510	HEIGHT = 0.767

ANGLE (A) AND MATERIAL CODE (C) OF EACH PLY (P)

ONLY FOR UPPER SKIN

P	1	2	3	4	5
A	0	0	0	0	0
C	7	7	7	7	7

ONLY FOR LOWER SKIN

P	1	2	3	4	5
A	0	0	0	0	0
C	2	5	5	5	2

ONLY FOR BASE

P	1	2	3	4	5	6	7
A	0	0	0	0	0	0	0
C	5	5	5	5	5	5	2

ONLY FOR CAP

P	1	2	3	4	5	6	7	8	9	10	11	12	13
A	0	0	0	0	0	0	0	0	0	0	0	0	0
C	2	5	5	5	5	5	5	2	5	5	5	5	5

ONLY FOR WEB

P	1	2	3	4	5
A	0	0	0	0	0
C	5	5	5	5	5

LOCAL AND GENERAL BUCKLING NORMALIZED TO COLUMN LOAD		SHEAR BUCKLING NORMALIZED TO PANEL LOAD	
UPPER SKIN	Nx = 11,662 LB/IN.	UPPER SKIN Nxy = 3,817 LB/IN.	
LOWER SKIN	Nx = 10,729 LB/IN.	LOWER SKIN Nxy = 23,568 LB/IN.	
WEB	Nx = 7,188 LB/IN.	WEB Nxy = 61,790 LB/IN.	
GENERAL	Nx = 36,293 LB/IN.	GENERAL Nxy = 57,674 LB/IN.	

STRAIN = 8,044 MICRO IN./IN. AT Nx = 7,188 LB/IN.

PROPERTIES OF PANEL

D_{11} = 96,165.8	AREA PER INCH = 0.1362 SQ IN./IN.
D_{22} = 74,887.3	EA PER INCH = 893,574 LB/IN.
D_{12} = 12,728.0	WEIGHT = 1.6362 psf
D_{66} = 7,832.9	

TABLE 1.55

BUCKLING ANALYSIS USING FIXED EDGES

(8- BY 20-INCH PANEL)

MATERIAL CODES FOR LAMINA (INCHES)

1 - CARBON/EPOXY TAPE	(T=0.005)	5 - E-GLASS CLOTH	(T=0.010)
2 - CARBON/EPOXY CLOTH	(T=0.010)	6 - F584/IM6 CARBON/EPOXY	(T=0.0055)
3 - KEVLAR/EPOXY CLOTH	(T=0.010)	7 - TITANIUM MATERIAL	(T=0.0050)
4 - K/E THIN COCURED FACINGS	(T=0.010)	8 - ADDITIONAL MATERIAL IF ANY	

MONOLAYER PROPERTIES FOR LAMINA

CODE	E_L (psi)	E_T (psi)	G_{LT} (psi)	ν_{LT}	Rho (pci)
2	0.8200E+07	0.8200E+07	0.5700E+06	0.0990	0.0571
5	0.2900E+07	0.2900E+07	0.3000E+06	0.1300	0.0700
7	0.1640E+08	0.1640E+08	0.6200E+07	0.3100	0.1600

PANEL GEOMETRY AND STIFFENER SPACING (INCHES)

LENGTH = 20.000	WIDTH = 8.000	SPACING = 1.110
BASE = 0.410	CAP = 0.510	HEIGHT = 0.767

ANGLE (A) AND MATERIAL CODE (C) OF EACH PLY (P)

ONLY FOR UPPER SKIN

P	1	2	3	4	5
A	0	0	0	0	0
C	7	7	7	7	7

ONLY FOR LOWER SKIN

P	1	2	3	4	5
A	0	0	0	0	0
C	2	5	5	5	2

ONLY FOR BASE

P	1	2	3	4	5	6	7
A	0	0	0	0	0	0	0
C	5	5	5	5	5	5	2

ONLY FOR CAP

P	1	2	3	4	5	6	7	8	9	10	11	12	13
A	0	0	0	0	0	0	0	0	0	0	0	0	0
C	2	5	5	5	5	5	5	2	5	5	5	5	5

ONLY FOR WEB

P	1	2	3	4	5
A	0	0	0	0	0
C	5	5	5	5	5

LOCAL AND GENERAL BUCKLING NORMALIZED TO COLUMN LOAD	SHEAR BUCKLING NORMALIZED TO PANEL LOAD
UPPER SKIN Nx = 21,269 LB/IN.	UPPER SKIN Nxy = 6,474 LB/IN.
LOWER SKIN Nx = 22,770 LB/IN.	LOWER SKIN Nxy = 42,788 LB/IN.
WEB Nx = 14,854 LB/IN.	WEB Nxy = 110,520 LB/IN.
GENERAL Nx = 82,442 LB/IN.	GENERAL Nxy = 100,412 LB/IN.

STRAIN = 16,623 MICRO IN./IN. AT Nx = 14,854 LB/IN.

PROPERTIES OF PANEL

D_{11} = 96,165.8	AREA PER INCH = 0.1362 SQ IN./IN.
D_{22} = 74,887.3	EA PER INCH = 893,574 LB/IN.
D_{12} = 12,728.0	WEIGHT = 1.6362 psf
D_{66} = 7,832.9	

TABLE 1.56

(8- BY 20-INCH) PANEL LA1-3-2 GAGE READINGS

STRAIN GAGE NO.	LOAD (LBS) 2,000	4,000	6,000	8,000	10,000	14,000	18,000	22,000
			STRAIN IN MICRO IN./IN.					
1	-108	281	454	633	811	1165	1531	1895
2	432	656	872	1091	1305	1736	2176	2606
3	180	333	493	666	830	1172	1527	1883
4	294	454	613	779	943	1271	1611	1945
5	215	385	560	737	911	1259	1617	1977
6	115	341	587	836	1077	1573	2080	2586
7	160	335	531	717	905	1284	1672	2066
8	320	501	691	880	1070	1442	1834	2217
9	154	332	518	705	892	1263	1644	2080
10	300	480	660	855	1042	1420	1802	2191
11	130	303	482	661	840	1202	1569	1932
12	277	452	636	825	1006	1375	1750	2124
13	146	329	523	706	891	1267	1648	2027
14	445	689	927	1171	1414	1900	2403	2914
15	117	293	481	660	840	1201	1566	1926
16	491	674	860	1036	1213	1578	1919	2279
17	107	288	466	641	816	1160	1515	1864
18	408	620	849	1065	1288	1730	2178	2642
19	92	155	228	283	344	464	574	667
20	169	327	490	648	808	1128	1451	1779

TABLE 1.57

(8- BY 20-INCH) PANEL LA1-3-2 GAGE READINGS (CONT.)

STRAIN GAGE NO.	LOAD (LBS) 27,000	32,000	37,000	42,000	47,000	50,000	0
		STRAIN IN MICRO IN./IN.					
1	2334	2788	3223	3666	4084	4330	18
2	3139	3690	4255	4832	5455	5837	21
3	2313	2757	3200	3654	4107	4394	18
4	2356	2775	3178	3625	4086	4350	39
5	2405	2845	3283	3729	4174	4428	27
6	3213	3861	4531	5213	5971	6450	88
7	2531	3007	3520	4011	4533	4809	26
8	2689	3166	3644	4126	4622	4933	54
9	2485	2960	3434	3918	4432	4730	27
10	2650	3129	3607	4088	4570	4872	44
11	2380	2836	3294	3754	4270	4573	24
12	2580	3038	3506	3973	4441	4734	43
13	2493	2957	3420	3874	4341	4625	24
14	3525	4146	4778	5441	6123	6504	100
15	2355	2797	3164	3604	4042	4307	20
18	3196	3775	4365	4976	5639	6008	77
19	785	891	1017	1113	1151	1151	+175
20	2165	2563	2963	3359	3787	4031	4

TABLE 1.58

(8- BY 20-INCH) PANEL LA1-3-2 GAGE READINGS (CONT.)

STRAIN GAGE NO.	LOAD (LBS) 10,000	20,000	30,000	45,000	50,000	55,000	60,000	65,000
			STRAIN IN MICRO IN./IN.					
1	893	1944	2946	4342	4962	5446	5943	6482
2	1771	3001	4382	6157	7020	7690	8403	9321
3	944	1977	2974	4363	5031	5555	6107	6685
4	1337	2347	3303	4511	5229	5718	6302	6871
5	1032	2028	3059	4381	5058	5537	6049	6582
6	1623	3100	4617	6745	7774	8677	9281	10984
7	954	1924	2892	4326	4822	5321	5874	6407
8	1132	2096	3047	4481	4976	5474	5946	6444
9	936	1886	2831	4258	4742	5247	5800	6346
10	1082	2042	2991	4417	4907	5397	5881	6371
11	877	1802	2778	4108	4595	5085	5609	6114
12	1036	1968	2894	4280	4760	5236	5718	6214
13	1001	1941	2864	4236	4705	5163	5680	6186
14	1401	2646	3878	5733	6368	7048	7704	8423
15	957	1861	2736	4041	4490	4931	5380	5824
16	1126	2018	2895	4201	4647	5112	5623	6142
17	917	1790	2657	3960	4405	4845	5290	5705
18	1225	2340	3478	5247	5865	6513	7244	8051
19	310	530	725	966	985	1010	1011	1034
20	829	1638	2437	3636	4045	4434	4810	5124

TABLE 1.59

SHORT COMPRESSION (3- BY 3-INCH) TESTS AT +160°F AND -65°F

SPECIMEN GEOMETRY

ID	W (IN.)	T (IN.)	H (IN.)
A1-5 (+160°F)	3.236	.767	2.937
A1-6 (+160°F)	3.138	.778	2.593
A1-7 (-65°F)	3.238	.772	3.026
A1-8 (-65°F)	3.107	.781	2.942

ID=IDENTIFICATION, W=WIDTH, T=DEPTH, H=LENGTH

SPECIMEN A1-5

LOAD (LBS)	COMP. STRAIN (MICRO IN./IN.) GAGE 1	Ti GAGE 2
2000	- 9	- 657
4000	- 333	-1459
6000	- 834	-2144
8000	-1285	-2708
10000	-1804	-3321
12000	-2322	-3915
14000	-2794	-4432
16000	-3330	-5013
17000	-3605	-5210
ULTIMATE LOAD 17200 LBS		

SPECIMEN A1-6

LOAD (LBS)	COMP. STRAIN (MICRO IN./IN.) GAGE 1	Ti GAGE 2
2000	- 651	- 310
4000	-1576	- 821
6000	-2414	-1270
8000	-3251	-1696
10000	-4139	-2105
12000	-5071	-2548
14000	-5874	-2970
16000	5286	-3734
17000	5286	-4182
ULTIMATE LOAD 17300 LBS		

SPECIMEN A1-7

LOAD (LBS)	COMP. STRAIN (MICRO IN./IN.) GAGE 1	Ti GAGE 2
2000	- 358	- 422
4000	- 634	-1113
6000	- 845	-1716
8000	-1060	-2346
10000	-1271	-3021
ULTIMATE LOAD 12000 LBS		

SPECIMEN A1-8

LOAD (LBS)	COMP. STRAIN (MICRO IN./IN.) GAGE 1	Ti GAGE 2
2000	- 424	- 468
4000	- 830	-1109
6000	-1218	-1755
8000	-1529	-2302
10000	-1910	-2455
11000	-2072	-3266
12000	-2244	-3546
13000	-2413	-3832
14000	-2580	-4097
15000	-2762	-4435
16000	-2952	-4770
17000	-3138	-5099
ULTIMATE LOAD 18000 LBS		

TABLE 1.60

LOAD VERSUS STRAIN FOR PANELS AA7 AND AA8

PANEL AA7

SPECIMEN IDENTIFICATION	WIDTH (IN.)	THICKNESS (IN.)	HEIGHT (IN.)
-65°F AA7	3.101	.7931	3.215
	TITANIUM STRAIN (MICRO IN./IN.)	COMPOSITES STRAIN (MICRO IN./IN.)	
LOAD	GAGE 1	GAGE 2	
2K	− 709	− 150	
4	−1,223	− 695	
6	−1,644	−1,212	
8	−2,050	−1,718	
10	−2,445	−2,203	
12	−2,850	−2,703	
14	−3,235	−3,190	
16	−3,625	−3,690	
18	−4,019	−4,209	
20	−4,410	−4,700	
22	−4,815	−5,204	
24	−2,286	−6,982	
26	−2,374	−7,343	
28	−2,551	−7,103	

PANEL AA8

SPECIMEN IDENTIFICATION	WIDTH (IN.)	THICKNESS (IN.)	HEIGHT (IN.)
-65°F AA8	3.049	.7892	3.186
	TITANIUM STRAIN (MICRO IN./IN.)	COMPOSITES STRAIN (MICRO IN./IN.)	
LOAD	GAGE 1	GAGE 2	
2K	− 760	− 160	
4	−1,300	− 530	
6	−1,720	−1,015	
8	−2,112	−1,530	
10	−2,510	−2,060	
12	−2,885	−2,566	
14	−3,276	−3,105	
16	−3,675	−3,624	
18	−4,070	−4,136	
20	−4,463	−4,647	
22	−4,842	−5,160	
24	−3,236	−7,310	

230

TABLE 1.61

LOAD VERSUS STRAIN FOR PANELS AA9 AND AA14

PANEL AA9

SPECIMEN IDENTIFICATION	WIDTH (IN.)	THICKNESS (IN.)	HEIGHT (IN.)
−65°F AA9∗	3.079	.7896	3.166
	TITANIUM STRAIN (MICRO IN./IN.)	COMPOSITES STRAIN (MICRO IN./IN.)	
LOAD	GAGE 1	GAGE 2	
2K	− 940	+ 6	
4	− 1,716	− 51	
6	− 2,330	− 356	
8	− 2,820	− 760	
10	− 3,292	−1,203	
12	− 3,750	−1,640	
14	− 4,192	−2,083	
16	− 4,645	−2,534	
18	− 5,086	−2,990	
20	− 5,545	−3,440	
22	− 5,995	−3,895	
24	− 6,452	−4,338	
26	− 6,905	−4,810	
28	− 7,344	−5,273	
30	− 7,805	−5,754	
32	− 8,264	−6,237	
34	− 8,725	−6,723	
36	− 9,202	−7,216	
38	− 9,727	−7,725	
40	−10,291	−8,235	
42	−10,919	−8,788	
44	−11,535	−9,342	
46	−12,195	−9,912	

FAILURE LOAD AT 47,700 POUNDS

∗ SPECIMEN AA9 WAS SOAKED IN WATER FOR 24 HOURS
PRIOR TO TEST

PANEL AA14

SPECIMEN IDENTIFICATION	WIDTH (IN.)	THICKNESS (IN.)	HEIGHT (IN.)
−65°F AA14	2.479	.7756	2.985
	TITANIUM STRAIN (MICRO IN./IN.)	COMPOSITES STRAIN (MICRO IN./IN.)	
LOAD	GAGE 1	GAGE 2	
2K	−1,046	− 2	
4	−1,841	− 355	
6	−2,443	− 918	
8	−2,996	−1,508	
10	−3,540	−2,115	
12	−4,092	−2,745	
14	−4,617	−3,350	
16	+ 209	−5,595	
18	+ 207	−6,415	
20	+ 207	−7,252	
22	+ 205	−8,051	
24	+ 207	−8,920	

PREMATURE FAILURE AT 14,000 POUNDS

FINAL FAILURE AT 24,000 POUNDS

TABLE 1.62

TEST SUMMARY OF LARGE PANEL RESULTS AT ROOM TEMPERATURE, +160°F, AND -65°F

RATIO TO ROOM TEMPERATURE	PANEL SIZE AND NUMBER	MAXIMUM FAILURE LOADING (LB)	MAXIMUM LOADING (LB/IN.)	CURE CYCLE	AVERAGE STRAIN (MICRO IN./IN.) TITANIUM	AVERAGE STRAIN (MICRO IN./IN.) COMPOSITE	EQUIVALENT LENGTH IF C = 2.0 *
-	10 x 27 IN. (LA1-14P)	93,830 ROOM TEMPERATURE	9,383	F & G	5,405	7,034	20.3
1.0	8 x 20 IN. (LA1-3-2)	70,000 ROOM TEMPERATURE	8,750	A	6,259	7,647	15.01
0.724	10 x 20 IN. (LA1-11-2P) (ALUMINUM POWDER FILLER ON ENDS)	63,360 160°F	6,336	F & G	4,165	4,835	15.01
0.76	7 x 15 IN. (LA1-12-1P) (SAUEREISEN ON ENDS)	46,640 160°F	6,663	F & G	4,982	5,654	11.3
1.476	7 x 15 IN. (LA1-12-2P)	90,420 -65°F	12,917	F & G	8,459	8,626	11.3

* C = DEGREE OF FIXITY
  C=2.0 IS A CONTINUOUS BEAM PIN SUPPORTED BY RIB

1. Report No. NASA CR-178166	2. Government Accession No.	3. Recipient's Catalog No.
4. Title and Subtitle Laminar Flow Control Perforated Wing Panel Development		5. Report Date OCT 1986
		6. Performing Organization Code
7. Author(s) J. E. Fischler et. al.		8. Performing Organization Report No.
9. Performing Organization Name and Address DOUGLAS AIRCRAFT COMPANY McDONNELL DOUGLAS CORPORATION LONG BEACH, CALIFORNIA, 90846		10. Work Unit No.
		11. Contract or Grant No. NAS1-17506
12. Sponsoring Agency Name and Address NATIONAL AERONAUTICS AND SPACE ADMINISTRATION WASHINGTON, DC 20546		13. Type of Report and Period Covered CONTRACTOR REPORT
		14. Sponsoring Agency Code 505-60-31-01

15. Supplementary Notes

LANGLEY TECHNICAL MONITOR: MR. D. V. MADDALON

16. Abstract

Many structural concepts for a wing leading edge laminar flow control hybrid panel were analytically investigated. After many small, medium, and large tests, the selected design was verified.

New analytic methods were developed to combine porous titanium sheet bonded to a substructure of fiberglass and carbon/epoxy cloth. At $-65^\circ F$ and $+160^\circ F$ test conditions, the critical bond of the porous titanium to the composites failed at lower than anticipated test loads.

New cure cycles, design improvements, and test improvements significantly improved the strength and reduced the deflections from thermal and lateral loadings.

The wave tolerance limits for turbulence were not exceeded. Consideration of the beam-column mid-bay deflections from the combinations of the axial and lateral loadings and thermal bowing at $-65^\circ F$, room temperature, and $+160^\circ F$ were included.

The tests performed were very many lap shear tests for seven cure cycles, very many 3- by 3-inch panels, several 4- by 8-inch wide by 10-inch long panels, some 7- by 15-inch panels, some 8- by 20-inch panels, and one two-bay 10- by 27-inch panel.

The results of this task indicated that sufficient verification has been obtained to fabricate a demonstration vehicle.

17. Key Words (Suggested by Authors(s)) LAMINATED FLOW CONTROL, PERFORATED SURFACES, SURFACE WAVINESS, FLUTE WAVINESS, BEAM-COLUMN, AXIAL STRAIN, LATERAL LOAD, COHESIVE FAILURE, ADHESIVE FAILURE, THERMAL BOWING CRITICAL FAILURE MODE, LAP SHEAR	18. Distribution Statement SUBJECT CATEGORY 24

19. Security Classif.(of this report) UNCLASSIFIED	20. Security Classif.(of this page) UNCLASSIFIED	21. No. of Pages 240	22. Price